ЖУРНАЛ
ЭКСПЕРИМЕНТАЛЬНОЙ И ТЕОРЕТИЧЕСКОЙ
ФИЗИКИ
Zhurnal Eksperimental'noi i Teoreticheskoi Fiziki

SOVIET PHYSICS

JETP

VOL. 13, NO. 4 OCTOBER, 1961

A Translation

of the

Journal of Experimental and Theoretical Physics

of the

Academy of Sciences of the USSR

(Russian Original Vol. 40, No. 4, April, 1961)

Published by the
AMERICAN INSTITUTE OF PHYSICS
INCORPORATED

SOVIET PHYSICS
JETP

A translation of the Journal of Experimental and Theoretical Physics of the USSR.

A publication of the

AMERICAN INSTITUTE OF PHYSICS

Governing Board

Ralph A. Sawyer, *Chairman*
James G. Baker
R. H. Bolt
Wallace R. Brode
Harvey Brooks
Dirk Brouwer
J. H. Elliott
Herbert A. Erf
N. S. Gingrich
S. A. Goudsmit
W. W. Havens, Jr.
W. V. Houston
Winston E. Kock
R. Bruce Lindsay
David L. MacAdam
H. Victor Neher
Leonard O. Olsen
C. J. Overbeck
Ray Pepinsky
S. L. Quimby
Francis W. Sears
Frederick Seitz
C. G. Suits
Mary E. Warga
William R. Willets

Administration

Elmer Hutchisson
Director
Wallace Waterfall
Secretary and Treasurer
Henry A. Barton
Administrative Consultant
W. C. Kelly
Director of Education
Eugene H. Kone
Director of Public Relations
Hugh C. Wolfe
Director of Publications
Kathryn Setze
Assistant Treasurer
James E. Mills
Supervisor, Editorial Department
Sistina Greco
Circulation Manager
Edward Tober
Manager, Production and Distribution
Theodore Vorburger
Advertising Manager
Emily Wolf
Manager, Special Services

American Institute of Physics Advisory Board on Russian Translations

Robert T. Beyer, *Chairman*
J. George Adashko, Freeman Dyson, Dwight Gray,
Morton Hamermesh, David Harker, Harold F. Weaver

Editor of Soviet Physics—JETP

J. George Adashko, 25 West 81st St., New York 24, New York

Soviet Physics—JETP is a monthly journal published by the American Institute of Physics and contains a complete translation of the Journal of Experimental and Theoretical Physics of the U.S.S.R. Academy of Sciences.

This translating and publishing project was undertaken by the institute in the conviction that dissemination of the results of researches everywhere in the world is invaluable to the advancement of science. The National Science Foundation of the United States has encouraged the project initially and is supporting it in large part by a grant.

The American Institute of Physics and its translators propose to translate faithfully all the material appearing in the original articles. The views expressed in the translations are therefore those of the original authors, and not those of the translators nor of the American Institute of Physics.

Volume 1 of Soviet Physics—JETP corresponds to Russian Volume 28 (1955). Two volumes are published annually, each of six issues. Each volume contains the translation of one volume of the Journal of Experimental and Theoretical Physics.

Beginning with Vol. 9 (36), the transliteration of the names of Russian authors follows British Standard 2979, which is being adopted by a large number of scientific journals in the United States. The Library of Congress transliteration is followed in the earlier volumes.

Subscription Prices

Per Year (12 issues), starting with Vol. 13, No. 1

General:	
United States and Canada	$75.00
Elsewhere	79.00
Libraries of non-profit degree-granting Institutions:	
United States and Canada	$50.00
Elsewhere	54.00
Single Copies	$ 8.00

Subscriptions should be addressed to the American Institute of Physics, 335 East 45th Street, New York 17, New York.

SOVIET PHYSICS, JETP is published monthly by the American Institute of Physics, Inc. Second Class postage paid at New York, N. Y. and Ann Arbor, Michigan.

Copyright by American Institute of Physics 1961

SOVIET PHYSICS

JETP

A translation of Zhurnal Éksperimental'noĭ i Teoreticheskoĭ Fiziki.

Vol. 13, No. 4, pp 695-869 (Russ. orig. Vol. 40, No. 4, pp 989-1236, April, 1961) October, 1961

EXPERIMENTAL INVESTIGATION OF ELECTRON CAPTURE BY MULTIPLY CHARGED IONS

V. S. NIKOLAEV, I. S. DMITRIEV, L. N. FATEEVA, and Ya. A. TEPLOVA

Institute of Nuclear Physics, Moscow State University

Submitted to JETP editor June 3, 1960; resubmitted December 27, 1960

J. Exptl. Theoret. Phys. (U.S.S.R.) 40, 989-1000 (April, 1961)

The electron capture cross sections $\sigma_{i,i-1}$ of multiply charged light ions having charge i and atomic numbers Z from 2 to 18 were determined for ions moving with velocities $v = (2.6-12) \times 10^8$ cm/sec in helium, nitrogen, argon, and krypton. Approximately the same dependence of $\sigma_{i,i-1}$ on v was found for all ions in a given gas. A correlation was found between the cross sections in different gases and the numbers of electrons in specified shells of the gas atoms. Minima in the dependence of $\sigma_{i,i-1}$ on Z were found for low-charge ions.

1. INTRODUCTION

ELECTRON capture by fast ions passing through matter has so far been studied mainly for protons and helium ions.[1] Heavier ions have been studied principally at velocities under 10^8 cm/sec.[2,3] Data obtained at higher velocities were available only for nitrogen[4] and oxygen ions.[5] The theoretical papers are also concerned with the passage of hydrogen and helium ions through matter;[6,7] only estimates of the cross sections are available for other ions.[5,8,9]

The present paper reports an experimental investigation of single-electron capture by ions of light elements with $Z \geq 2$ passing through helium, nitrogen, argon, and krypton. Measurements for He, Li, B, and N ions were obtained in the velocity range $(2.6-4) \times 10^8$ to $\sim 12 \times 10^8$ cm/sec, for Ne ions at $(2.6-6) \times 10^8$ cm/sec, and for P and Ar ions at 2.6 and 4.1×10^8 cm/sec. For the purpose of determining the dependence of the cross sections on Z, measurements were also obtained for Be, C, and O ions in helium and nitrogen at $v = 8 \times 10^8$ cm/sec, and for Na, Mg, Al, and Kr ions in helium, nitrogen, and krypton at $v = 2.6 \times 10^8$ cm/sec.

2. PROCEDURE

Cross sections for the capture of a single electron were measured along with cross sections for other electron capture and loss processes, using the experimental setup represented in Fig. 1. Multiply charged ions were accelerated in the 72-cm cyclotron and were focused at a point 8 m from the cyclotron chamber.[10] Near the focus the beam was defined by two 1-cm slits (1 and 3). A thin ($\sim 2\mu g/cm^2$) celluloid film 2 was placed behind slit 1; after traversing this film the beam contained ions with different charges. The first analyzing magnet H_1 directed ions with a specified charge i into the charge-exchange (collision) chamber B, consisting of a cylinder 8 cm in diameter and 38 cm long with inlet and exit channels (4 and 5) 0.5 cm high, 0.2 cm wide, and 2.6 cm long. Gas was admitted to the chamber continuously; the pressure was measured with 3 – 5% accuracy by ionization gauges calibrated for the different gases against an oil compression gauge.

The helium, nitrogen, and argon target gases contained less than 0.5% impurities; the krypton contained 7% xenon. The pressure in the collision chamber varied from $(1-2) \times 10^{-5}$ mm Hg (re-

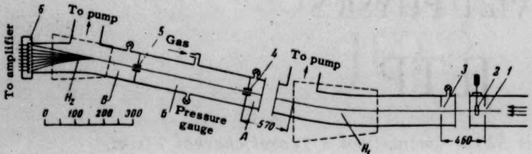

FIG. 1. Diagram of apparatus. Scale in mm.

sidual pressure) to 7×10^{-3} mm for helium and 10^{-3} mm for the other gases. The pressure was $(0.5-2) \times 10^{-5}$ mm in the chambers traversed by the ions before (A) and after (C) the collision chamber.

When a beam of ions with the initial charge i traversed a gas, ions with charges $k \neq i$ resulted from electron capture or loss. The charge distribution in the beam was determined by a second analyzing magnet H_2 and a system (6) of eight proportional counters, each of which registered ions with a single specified charge. The first counter registered neutral particles, while the last counter registered septuply charged ions. The counters were separated from the high-vacuum portion of the apparatus by a slit 0.08 mm high and 100 mm long, sealed with a $\sim 20 \mu g/cm^2$ celluloid film. The entrance window of each counter was 10 mm wide. The field of the second analyzing magnet was adjusted to cause most ions to impinge on the middle of each appropriate counter. This adjustment was monitored by placing before each counter a screen, with a 2-mm slit, which could be moved across the counter entrance window. The counters exhibited practically 100% efficiency in registering particles that passed through their entrance windows.

The fraction Φ_{ik} of ions with a given charge k ($\Sigma_k \Phi_{ik} = 1$) was calculated from the simultaneous readings of all counters. Φ_{ik} was determined for different initial ion charges i at several gas pressures in the target chamber including the residual pressure. The maximum pressures at which Φ_{ik} was measured were such that the intensity reduction of the primary beam as a result of charge exchange amounted to about 20 to 30%, i.e. $\Phi_{ii} \approx 0.7-0.8$. The charge distribution at each pressure was measured three to six times; in each instance the counters registered a total of at least 10^4 particles. The individual measurements usually did not differ by more than the statistical error, which was of the order $2-3\%$ for the most intense ion groups produced by charge exchange. The possible error in Φ_{ik} resulting from varying height of the counter entrance slits did not exceed $2-3\%$.

Since the charge distribution of the beam was measured at relatively low pressures, with most ion charges remaining unchanged after traversal of the gas, the ratio of ions with charges i + 1 and i − 1 was determined mainly by the cross sections for single-electron capture and loss. The experimental values of $\Phi_{i,i\pm 2}$ made it possible to determine the cross sections for two-electron capture and loss, values of $\Phi_{i,i\pm 3}$ led to the cross sections for three-electron capture and loss etc. The cross sections were calculated by solving the charge exchange equation

$$d\Phi_{ik}(t)/dt = \sum_j \Phi_{ij}(t)\sigma_{jk}, \qquad (1)$$

where t is the number of gas atoms in a volume with 1-cm² cross section along the ion path ($t = \int N dl$, where N is the number of gas atoms per cm³ and dl is an ion path element in the gas), σ_{jk} with $j \neq k$ is the cross section for the process which changes the ion charge from the initial value j to k, and

$$\sigma_{kk} = -\sum_l{}' \sigma_{kl}$$

(the primed summation indicating $j \neq k$).

The calculation of cross sections from experimental results was usually confined to the first approximation

$$\Phi_{ik} = \sigma_{ik} t \qquad (k \neq i) \qquad (2)$$

at pressures where Φ_{ik} is proportional to t (i.e. to the pressure). However, for $\Phi_{ii} \sim 0.7-0.8$ the single-electron capture and loss cross sections, $\sigma_{i,i+1}$ and $\sigma_{i,i-1}$, calculated from this formula incur an error of $20-30\%$, which could only be reduced by higher approximations. A more exact relationship between Φ_{ik} and σ_{ik} is also required in calculating cross sections for the capture and loss of two or more electrons; the possibility must be allowed that even at the residual pressure a considerable fraction of the ions would be formed by successive single-electron captures or losses. We know that in this case the cross section cannot be determined from the slope of the curve representing Φ_{ik} as a function of the admitted target gas pressure. In the present work we used a practically exact solution of Eq. (1) (for $\Phi_{ii} \sim 0.6-0.7$) in order to achieve complete elimination of errors in calculating cross sections from the experimental values Φ_{ik}.

Since charge exchange took place in a mixture of admitted and residual gases, the cross sections σ_{jk} were replaced in (1) by $\sigma_{jk}\alpha + \sigma'_{jk}\alpha'$, where σ_{jk} pertains to the admitted gas and σ'_{jk} to the residual gas, and α and α' are the relative concentrations ($\alpha + \alpha' = 1$). In the solution α was taken as constant for each of the chambers A, B, and C along the ion path (Fig. 1). The initial conditions for A were $\Phi_{ik} = \delta_{ik}$, where $\delta_{ik} = 0$ for $k \neq i$ and $\delta_{ii} = 1$. The values of Φ_{ik} at the boundary between chambers A and B, obtained by solving (1), were taken as initial conditions in solving the equation for chamber B etc. The final expression for Φ_{ik}, obtained after integrating (1) and used to calculate cross sections, is

$$\Phi_{ik} = \delta_{ik} + g_{ik} + \tfrac{1}{2}\sum_{p}(g_{ip}g_{pk} + \gamma g'_{ip}g_{pk} - \gamma g_{ip}g'_{pk})$$
$$+ \tfrac{1}{6}\sum_{p,q}(g_{ip}g_{pq}g_{qk} + 2\gamma g'_{ip}g_{pq}g_{qk} - \gamma g_{ip}g'_{pq}g_{qk}$$
$$- \gamma g_{ip}g_{pq}g_{qk}) + \tfrac{1}{24}\sum_{p,q,r} g_{ip}g_{pq}g_{qr}g_{rk}$$
$$+ \tfrac{1}{120}\sum_{p,q,r,s} g_{ip}g_{pq}g_{qr}g_{rs}g_{sk}, \qquad (3)$$

where

$$g_{js} = \sigma_{js}t + \sigma'_{js}t', \quad g'_{js} = \sigma'_{js}t', \quad \gamma = (\beta'_1 - \beta'_3) - (\beta_1 - \beta_3),$$

and β_m is the fraction of gas molecules in the m-th chamber along the ion path ($\beta_1 + \beta_2 + \beta_3 = 1$); σ, t, and β pertain to the admitted gas and σ', t′, and β' to the residual gas.

β_1 and β_3 were determined experimentally from the ratios between pressures in different portions of the apparatus, taking into account the ion path length in each portion; the values were small for the admitted gas. The largest values were found in the work with helium ($\beta_1 = 0.05$ and $\beta_3 = 0.035$), and were 2.5 – 3 times larger than for the other gases. For the residual gas $\beta'_1 = 0.45$ and $\beta'_3 \approx 0.07$, so that γ was close to 0.4.

Φ'_{ik} for the residual gas and Φ_{ik} for specified pressures of the admitted gas were known experimentally. Solving the system (3) of algebraic equations with these data, we first obtained g'_{ik} for the residual gas and then σ_{ik}, the charge-exchange cross section for the investigated gas. The equations were solved on the "Strela" computer of Moscow State University.

The accuracy of the cross sections depended on the errors in the largest terms of Eq. (3). The errors in the cross sections for capture and loss of a single electron depended on the errors of $\Phi_{i,i\pm1}$ and pressure in the first-approximation formula. In calculating the cross sections for capture or loss of several electrons the terms representing successive captures or losses were sometimes large; the errors in the cross sections then depended on errors in $\Phi_{i,i\pm1}$, $\Phi_{i\pm1,i\pm2}$ etc. as well as errors in $\Phi_{i,i\pm2}$ or $\Phi_{i,i\pm3}$. The cross sections calculated from experimental values Φ_{ik} obtained at different pressures agreed within the limits of error.

In collisions between ions and gas atoms, besides electron captures and losses, ion scattering took place with the result that some ions with changed charge did not emerge from the collision chamber. Therefore from a rigorous point of view the cross sections obtained in the described experiments represent only electron capture or loss accompanied by ion scattering at angles $\theta \leq \theta_m$, where θ_m is the maximum scattering angle of particles emerging from the collision chamber. The mean value of θ_m was $\sim \Delta/l = 0.005$ rad (l is the length of the collision chamber B and Δ is the width of the entrance channel 5). However, there are grounds for believing that at the given ion energies only a small fraction of each cross section, not exceeding the limits of error, is associated with scattering at larger angles.

In all our cases, the scattering at angles $\theta \geq \theta_m$ can be treated classically. For the total scattering cross section at angles $\theta \geq \theta_m$ we can therefore take $\sigma_p(\theta_m) = \pi p^2(\theta_m)$, where $p(\theta)$ is the impact parameter for scattering at the angle θ. If we obtain $p(\theta)$ by using the calculations of Everhart et al.,[11] which agree well with experiment[12] in our required region of p values, then $\sigma_p(\Delta/l)$ is not greater than 1 – 3% of the total value obtained for the charge-exchange cross section $\sigma_i = \Sigma'_k\sigma_{jk}$, and reaches 5 – 10% only for singly charged ions with minimum velocity in argon and krypton.

From experiments[12] on the charge distribution of scattered particles, at somewhat lower velocities than in the present work, it is known that the largest fraction of scattered ions having a specified charge does not exceed one-half the total number of scattered particles and is practically independent of the velocity. Since there is no reason to assume that this fraction can be larger in our velocity range, for each given process of electron capture or loss we can take $\frac{1}{2}\sigma_p(\theta_m)$ as the maximum possible cross section for scattering at $\theta > \theta_m$. In most instances $\frac{1}{2}\sigma_p(\Delta/l)$ did not exceed the random errors of the derived cross sections.

There is experimental confirmation of the conclusion that the fraction of the cross section associated with scattering at angles $\theta > \theta_m$ is within the limits of the indicated random errors. Particles scattered at angles from 1.5 to 2.5 Δ/l in the last third of the ion path within the target chamber entered the counters close to the edges of the entrance windows. The number of these particles was measured by means of a slotted screen placed in front of the counter entrance window. It was found that the few particles scattered at the given angles, did not exceed the background of accidental pulses (~ 1 pulse per minute in each counter) while the usual registered beam intensity was $(1-2) \times 10^2$ particles per sec.

3. EXPERIMENTAL RESULTS

Figure 2 shows the cross sections for single-electron capture by He, Li, B, and N ions. Figures 3, 4, and 5 show the cross sections for the other ions. The cross sections were calculated per atom. In order to give an idea of the maximum possible cross sections for scattering at $\theta > \theta_m$, Figure 2 shows $\frac{1}{2}\sigma_p(\Delta/l)$ for singly charged nitrogen ions. The scattering cross section depends only slightly on the ionic nuclear charge Z. For helium ions $\sigma_p(\Delta/l)$ is about 5% larger than for nitrogen ions, while for argon ions in nitrogen, argon, and krypton it is 5 — 12% smaller, and in helium it is 30% smaller, than for nitrogen ions. For ions with charge $i = Z$ the scattering cross section exceeds $\sigma_p(\Delta/l)$ for singly charged nitrogen ions by not more than 40% at $v = 2.6 \times 10^8$ cm/sec and by not more than 25% at $v \geq 6 \times 10^8$ cm/sec.

Figure 2 also shows the values of σ_{10} and σ_{21} for helium ions, taken from Allison's review article.[1] In helium at $v \approx 4 \times 10^8$ cm/sec the values of σ_{10} from reference 1 agree with our work, but the values of σ_{21} are 40% under ours. A reasonable interpolation can be made between our values of σ_{10} in nitrogen and argon for $v \gtrsim 4 \times 10^8$ cm/sec and those in reference 1 for $v \lesssim 3 \times 10^8$ cm/sec. It should be noted that the values of σ_{10} given in reference 1 for helium ions in air are about 30% larger than in nitrogen, according to both our own data and reference 1. σ_{21} in air as given in reference 1 agrees with our results in nitrogen at $v \sim (4-5) \times 10^8$ cm/sec, but at $v \approx (6-8) \times 10^8$ cm/sec it is smaller by the factor 1.5 than the results given below.

Our earlier[4] cross sections for electron capture by nitrogen ions in nitrogen and argon, with θ_m larger by the factor 1.5, agree with the present measurements within the limits of error.

The experimental values of σ_{43} and σ_{54}, given in reference 5, for oxygen ions in argon at $v \sim 10^9$ cm/sec agree well with our present results, since the ratios of these cross sections to the corresponding cross sections for nitrogen ions in the present work agree with our ratios of these cross sections at $v = 8 \times 10^8$ cm/sec. σ_{65} in reference 5 is 1.5 times larger than could be expected from our present results.

The following regularities are derived from the experimental results.

a) Dependence of $\sigma_{i,i-1}$ on v. Figure 2 (a — d) shows that the relationship between cross sections and velocity, which can be represented by $q = -d \log \sigma_{i,i-1}/d \log v$, depends mainly on ion velocity and the medium, while depending only slightly on the charge i of the ion and Z of its nucleus. As v increases in helium and nitrogen, q increases monotonically from ~ 1 — 2 at $v = (2.6-4) \times 10^8$ cm/sec to ~ 5 — 7 at $v \sim 10^9$ cm/sec. A decrease of q is observed in argon and krypton for $v > 8 \times 10^8$ cm/sec. The maximum of q, at $v = (6-8) \times 10^8$ cm/sec, is ~ 6 in argon and ~ 7 in krypton. At $v \sim 10^9$ cm/sec we have $q \sim 4$ in argon and $q \sim 3$ in krypton.

The general character of the dependence of $\sigma_{i,i-1}$ on v for the investigated ions agrees with that of σ_{10} for protons.[13] However, q for protons is larger by ~ 2 than for the other ions.

b) Dependence of $\sigma_{i,i-1}$ on Z. Figures 3 and 4 show that this is determined by the ion charge i. For ions with small i minima are observed in the region of Z where a transition occurs from the filling of one electron shell to another. As i increases the minima become shallower, and at sufficiently large values of i the cross section depends only slightly on Z. In all cases the cross section minimum corresponds to the capture of the first L or M electron. The minimum is found at larger Z only for σ_{10} in helium and nitrogen.

c) Dependence of $\sigma_{i,i-1}$ on i. For ions of a given element $\sigma_{i,i-1}$ can be represented approximately by the power function i^m. As a rule, m is somewhat smaller in helium than in other gases. There appears to be a general tendency toward stronger dependence of $\sigma_{i,i-1}$ on i as v increases. For example, as the velocity of nitrogen ions increases within the range $(2.6 - 8) \times 10^8$ cm/sec, m increases from ~ 1.5 to ~ 3.

In accordance with the foregoing properties of $\sigma_{i,i-1}$ as a function of Z, m varies greatly for different ions and attains maximum values for Z = 3, 11, and 12 (Fig. 6). A similar dependence

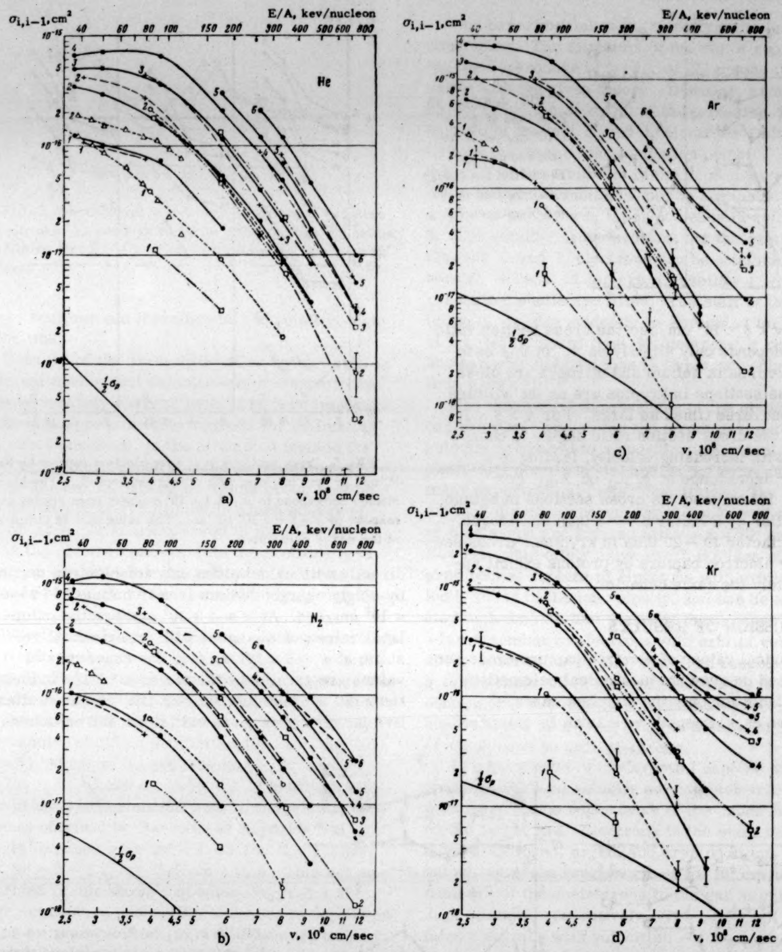

FIG. 2. Cross sections $\sigma_{i,i-1}$ vs ion velocity v and ion energy per nucleon E/A in (a) helium, (b) nitrogen, (c) argon, and (d) krypton, for ions of: ○ – He, □ – Li, + – B and ● – N. Δ represents cross sections for He ions taken from Allison's review article.[1] The value of i is indicated at the ends of the curves. Only errors above 10% are indicated.

on Z − i (the number of electrons) is exhibited by the exponent m′ in the dependence of $\sigma_{i,i-1}$ on i for different ions with identical values of Z − i.

d) Dependence of $\sigma_{i,i-1}$ on the medium. The cross section for electron capture by a given ion usually increases with the atomic number Z_m of the gaseous medium (Fig. 5). The ratios of cross sections in different gases depend generally on all the parameters (i, v, Z, and Z_m). However, as Z_m increases the dependence of the ratios on i and Z becomes weaker. For example, the ratios of the cross sections in argon and krypton differ on the whole by not more than 20% for ions with different i and Z.

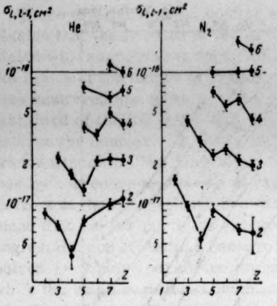

FIG. 3. $\sigma_{i,\,i-1}$ vs Z of ions at v = 8 × 10⁸ cm/sec in helium and nitrogen. The initial ion charge i is indicated at the end of each curve.

For $v < 8 \times 10^8$ cm/sec the cross section ratio usually depends only slightly on v. In this case cross sections in helium and nitrogen are close, and cross sections in krypton are on the average only about three times as large. For $v > 8 \times 10^8$ cm/sec the cross section ratio begins to change rapidly with increasing velocity, leading to a stronger dependence of $\sigma_{i,i-1}$ on Z_m. For $v \sim 12 \times 10^8$ cm/sec the cross sections in helium are smaller by a factor 2.5 — 4 than in nitrogen, and by a factor 10 — 20 than in krypton. Cross sections for electron capture by protons exhibit approximately the same behavior.[13]

4. DISCUSSION OF RESULTS

Numerical values of electron capture cross sections based on quantum mechanical calculations are available for only the simplest cases.[5,6] Therefore experimental values can be compared directly with calculations only for electron capture by singly charged helium ions in helium at (4 — 6) × 10⁸ cm/sec. At $v \approx 4 \times 10^8$ cm/sec the calculated values of σ_{10} agree with experimental results; at $v \approx 6 \times 10^8$ cm/sec the experimental values are greater by the factor 1.7. The calculations did not take into account the increased effective ion charge in close collisions; the calculated

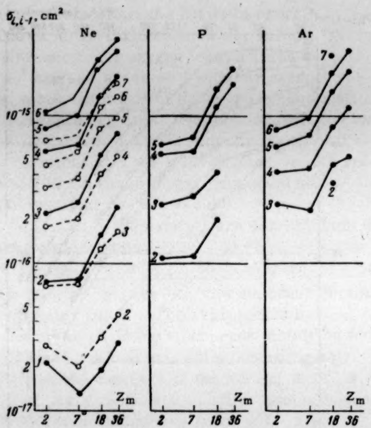

FIG. 5. Cross sections $\sigma_{i,i-1}$ for electron capture by Ne, P, and Ar ions in gases with atomic numbers Z_m. The black circles correspond to v = 4.1 × 10⁸ cm/sec; open circles correspond to v = 5.6 × 10⁸ cm/sec. The value of i is indicated at the end of each curve.

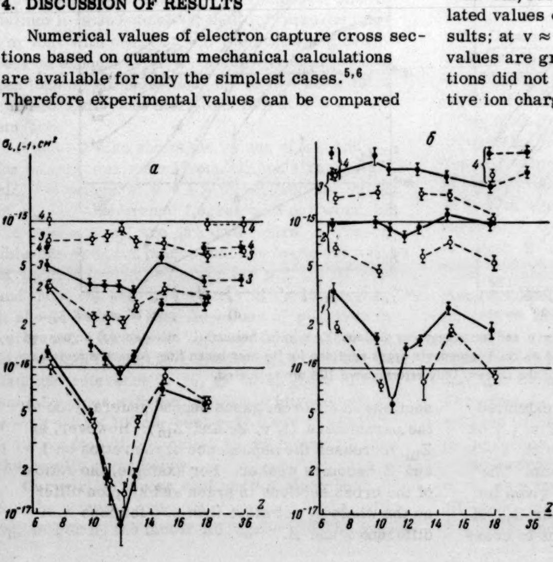

FIG. 4. $\sigma_{i,i-1}$ vs Z of ions at v = 2.6 × 10⁸ cm/sec in: a – helium (●) and nitrogen (○), b – krypton (●) and argon (○). The ion charge i is indicated at the end of each curve.

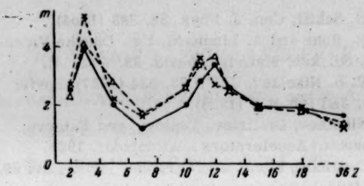

FIG. 6. The exponent $m = \Delta \log \sigma_{i,i-1}/\Delta \log i$ in helium (●), nitrogen (Δ), and krypton (×) for different ions. For helium and lithium ions $v = 4 \times 10^8$ cm/sec; otherwise, $v = 2.6 \times 10^8$ cm/sec.

cross sections can therefore be too small at high velocities.

Because of the great difficulties encountered in quantum mechanical calculations of electron capture by multiply charged ions, it is very important to develop approximation methods for estimating the cross sections. In the attempted method the electron capture cross section is represented by the product σ'fn, where σ' is the cross section for an ion-electron collision in which energy of the order $\mu v^2/2$ is transferred to the electron (μ is the electron mass), f is the probability of electron capture after the collision, and n is the number of gas-atom electrons effectively participating in the capture.

When this method was first used to obtain cross sections for the capture of an electron by a fast α particle, Bohr[14] obtained values of σ_{21} close to the experimental values. According to Bohr's formula the cross section $\sigma_{Z,Z-1}$ for electron capture by bare nuclei would be proportional to Z^5 (that is, $m' = 5$), since σ' is proportional to Z^2 and $f \approx (Zv_0/v)^3$, where $v_0 = e^2/\hbar = 2.19 \times 10^8$ cm/sec. Our present experimental data in conjunction with results obtained by Barnett and Reynolds[13] at $v \sim 10^9$ cm/sec give $m' = 4 - 5$ for $Z = 1$ and 2 and $m' = 2 - 2.5$ for Z from 3 to 5. This not unexpected result shows that when $Zv_0/v \gtrsim 1$ the electron capture probability f ceases to depend on Z, as a result of which m' is determined only by the dependence of σ' on Z and approaches the value 2.

Satisfactory agreement with the available experimental data was obtained when this method was used to evaluate cross sections for electron capture by nitrogen ions.[9] It was shown that when i is small $\sigma_{i,i-1}$ must depend on ion size and the electron binding energy after capture, which fluctuate considerably with Z, while for sufficiently large values of i the cross section is dependent only on i and v, but is independent of Z.

Our experimental results confirm the foregoing conclusion. The minimum of the curve representing the dependence of $\sigma_{i,i-1}$ on Z agrees in most cases with the given theory. However, such effects as the reduction of $\sigma_{i,i-1}$ with increasing Z in the capture of the last K and L electrons (with continuous increase of the ionization potential) and the shift of the minimum in the dependence of σ_{10} on Z in light elements cannot be accounted for solely on the basis of the hypotheses in reference 9. The smaller cross sections for the capture of the last K and L electrons can be attributed reasonably to reduced capture probability f when the respective shells are filled. The shift of the minimum of σ_{10} can evidently be accounted for by loss of the weakly bound first M electron. It remains unclear why electron loss is important only in light gases.

The theoretical dependences of the electron capture cross section on the target gas and ion velocity are based to a considerable extent on a statistical atomic model and do not represent many experimental facts. Specifically, the statistical model cannot account for the observed decrease of q in argon and krypton for $v > 8 \times 10^8$ cm/sec. However, this effect agrees with the idea of the preferential capture of electrons with orbital velocity close to the ion velocity, and can be associated with the fact that atoms of these gases contain a large number of electrons with orbital velocities of the order 1.5×10^9 cm/sec. The reduction of q is not observed in nitrogen, the atoms of which contain only two electrons with this velocity. The highest value of q is reached in helium, the atoms of which have no such electrons.

The hypothesis of preferential capture of electrons with orbital velocity near the ion velocity is confirmed by the dependence of the cross sections on the target gas. Electrons in the outer shells of helium, nitrogen, argon, and krypton atoms have velocities in the range $\sim (3-6) \times 10^8$ cm/sec, the numbers of these electrons in the gas atoms being 2, 5, 8, and 8, respectively. The next shell contains electrons with velocities $\sim (1-2) \times 10^9$ cm/sec, the numbers of electrons being 0, 2, 8, and 18, respectively. The cross section ratio in these gases averaged over all ions at $v = (4-8) \times 10^8$ cm/sec is 4:5:8:10; at $v \sim 12 \times 10^8$ cm/sec the ratio is 1:4:8:20. These ratios are approximately the same as the ratios of the numbers of electrons in the corresponding shells of the gas atoms. The cross sections are twice as large only in the case of electron capture from the K shell, at $v = (4-8) \times 10^8$ cm/sec in helium and $v \sim 1.2 \times 10^9$ cm/sec in nitrogen.

In conclusion we wish to thank the cyclotron crew, A. A. Danilov, G. V. Koshelyaev, M. Kh. Listov, A. P. Ozyabkin, and V. P. Khlapov, for assistance, and also M. K. Akimova for programming and operating the computer.

---

[1] S. K. Allison, Revs. Modern Phys. **30**, 1137 (1958).

[2] Jones, Ziemba, Moses, and Everhart, Phys. Rev. **113**, 182 (1959).

[3] I. P. Flaks and E. S. Solov'ev, J. Tech. Phys. (U.S.S.R.) **28**, 599, 612 (1958), Soviet Phys.-Tech. Phys. **3**, 564, 577 (1958).

[4] Nikolaev, Fateeva, Dmitriev, and Teplova, JETP **33**, 306 (1957), Soviet Phys. JETP **6**, 239 (1958).

[5] R. L. Gluckstern, Phys. Rev. **98**, 1817 (1955).

[6] T. Pradhan, Phys. Rev. **105**, 1250 (1957).

[7] H. Schiff, Can. J. Phys. **32**, 393 (1954).

[8] N. Bohr and A. Lindhard, Kgl. Danske Videnskab. Selskab, Mat.-fys. Medd. **28**, 7 (1954).

[9] V. S. Nikolaev, JETP **33**, 534 (1957), Soviet Phys. JETP **6**, 417 (1958).

[10] Nikolaev, Dmitriev, Teplova, and Fateeva, Ускорители, (Accelerators), Atomizdat, 1960.

[11] Everhart, Stone, and Carbone, Phys. Rev. **99**, 1287 (1955).

[12] Fuls, Jones, Ziemba, and Everhart, Phys. Rev. **107**, 704 (1957).

[13] C. F. Barnett and H. K. Reynolds, Phys. Rev. **109**, 355 (1958).

[14] N. Bohr, Kgl. Danske Videnskab. Selskab, Mat.-fys. Medd. **18**, 8 (1948).

Translated by I. Emin
163

SOVIET PHYSICS JETP VOLUME 13, NUMBER 4 OCTOBER, 1961

POSITRON ANNIHILATION IN SULPHUR, SELENIUM, AND SILICON

K. A. BASKOVA, B. S. DZHELEPOV, and Z. A. KOMISSAROVA

Leningrad State University

Submitted to JETP editor July 1, 1960

J. Exptl. Theoret. Phys. (U.S.S.R.) 40, 1001-1003 (April, 1961)

The angular distribution of annihilation γ rays is measured for crystalline and amorphous sulphur, selenium, and silicon.

MEASUREMENTS have shown[1,2] that the difference in the positron-annihilation process for crystalline and for amorphous substances affects the angular distribution of the annihilation γ rays. The angular distribution in a two-quanta annihilation usually has a bell-shaped form. In crystalline substances, as compared to amorphous ones, there is a narrower maximum and a relatively wide base. The narrow maximum is thought to be due to the production of positronium.[3]

In the present experiment, the annihilation of positrons was investigated in crystalline and amorphous sulphur, selenium, and silicon.

The measurements were carried out with the setup described in detail by Baskova and Dzhelepov.[4]

The results of the measurements are presented in Fig. 1 — 3, where the curves of the angular distribution of γ rays produced in the annihilation of positrons in sulphur, selenium, and silicon are shown.

The angular distribution curves for crystalline and amorphous sulfur coincide within the limits of error of the experiment. This result is in agreement with the data of Ferguson and Lewis.[5] It follows from this that, for sulphur, there is no second component in the distribution due to a different lifetime.

As can be seen from Fig. 2, the angular distributions for crystalline and amorphous silicon differ greatly only for large angles. The angular distribution for crystalline silicon is in agreement with that measured by Page and Heinberg.[1] However, the amplitude of the narrow maximum for the amorphous silicon is, according to our data, considerably smaller. This is evidently due to the admixture of about 25% of crystalline silicon in our samples of amorphous silicon.

The angular distribution curves for crystalline selenium and amorphous (vitreous, red, and black) selenium are shown in Fig. 3. It can be seen that the different forms of selenium have angular distribution curves of different width. From a comparison of the half-widths of the curves, it can be seen that the widest curve is that for crystalline selenium. A narrower maximum is observed for amorphous selenium.

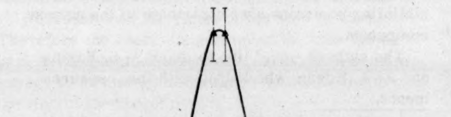

FIG. 1. Angular distribution of γ rays produced in positron annihilation in sulfur: ● – crystalline, Δ – amorphous.

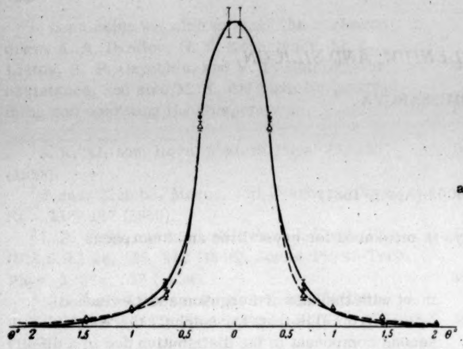

FIG. 2. Angular distribution of γ rays produced in positron annihilation in silicon: ● – crystalline, Δ – amorphous.

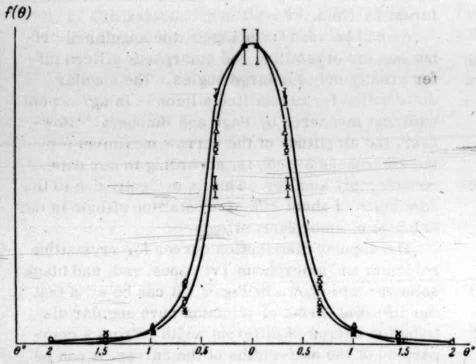

FIG. 3. Angular distribution of γ rays produced in positron annihilation in selenium: ● – crystalline, Δ – amorphous, ○ – amorphous red, and × – amorphous black.

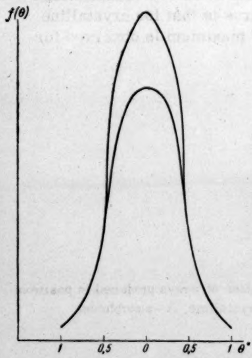

FIG. 4. Narrow component of the angular distribution of γ rays produced in positron annihilation in amorphous selenium.

The narrow component of the angular distribution for black and red selenium is represented in Fig. 4 (as was also done by Page and Heinberg[1]). An estimate carried out permits us to conclude that the intensity of the narrow component amounts to 18 ± 8%. In its order of magnitude, the intensity of the narrow component is in agreement with the values obtained for other amorphous substances.

The value obtained cannot be solely due to the fraction of positronium produced, since freely annihilating positrons also contribute to the narrow component.

The authors would like to thank A. S. Basina and A. A. Koran, who helped with the measurements.

---

[1] L. Page and M. Heinberg, Phys. Rev. **98**, 206 (1955); **102**, 1545 (1956).

[2] A. Stewart, Phys. Rev. **99**, 308 (1955); Canad. J. Phys. **35**, 168 (1957).

[3] R. Ferrell, Rev. Mod. Phys. **28**, 511 (1956).

[4] K. A. Baskova and B. S. Dzhelepov, Izv. Akad. Nauk SSSR, Ser. Fiz. **20**, 951 (1956), Columbia Tech. Transl. p. 860.

[5] A. Ferguson and J. Lewis, Phil. Mag **44**, 1332 (1953).

Translated by H. Kasha
164

SOVIET PHYSICS JETP VOLUME 13, NUMBER 4 OCTOBER, 1961

NEUTRON EMISSION FROM STRONGLY EXCITED NUCLEI

A. S. KARAMYAN,* G. A. DOROFEEV, and D. S. KLOCHKOV

Submitted to JETP editor October 6, 1960

J. Exptl. Theoret. Phys. (U.S.S.R.) 40, 1004-1006 (April, 1961)

The relative intensities and angular distributions of neutrons with effective energies of 10, 15, and 25 Mev produced by multiply charged ions in (C^{12}, xn, xp) and (O^{16}, xn, xp) reactions were investigated. The results are in satisfactory agreement with the predictions of the statistical model of nuclear reactions.

KARAMYAN and Pleve[1] observed that at large excitation energies the cross sections of the reactions (C^{12}, 2n) and (O^{16}, 2n) for vanadium and niobium are quite large. This effect was attributed to the direct interaction of the incident ions with nucleons of the target nucleus. If the main part of the excitation is then taken away by the emitted neutrons, it is natural to assume that the mean energy of these neutrons is approximately equal to half the excitation energy. In the overall energy distribution of neutrons produced as a result of all possible reactions, a group of neutrons in the high-energy region should then be quite distinct. The present work was undertaken to test this hypothesis.

The experimental arrangement is shown in the figure. The target and detectors, which were made of copper, iron, and graphite of natural isotopic composition, were bombarded by the internal beam of a cyclotron. The C^{12} and O^{16} ion current at an orbit radius of 69 cm was $\sim 0.5\ \mu a$. The maximum energies of the C^{12} and O^{16} ions were then 80 Mev and 108 Mev, respectively. The thickness of the bombarded targets was considerably greater than the range of the ions in them. Therefore the energy spectrum of the ions taking part in the reaction extended from their maximum energy to an energy determined by the Coulomb barrier of the target nuclei.

In the experiment for which the data are shown in the first line of Table I, a uranium plate was placed behind a vanadium target $\sim 10\ \text{mg/cm}^2$ thick. Since the ions traveling through the vanadium were of insufficient energy to overcome the Coulomb barrier of the uranium, they stopped in the uranium without evoking nuclear reactions. Hence the energy interval of the ions taking part in the reaction was appreciably reduced.

To record the fast neutrons, we used the reactions $Fe^{56}(n, p)Mn^{56}$, $Cu^{63}(n, 2n)Cu^{62}$, and $C^{12}(n, 2n)C^{11}$ with energy thresholds of about 5, 12, and 22 Mev, respectively.[2] The exposure time was 20 min. The absolute β activity of the fast-neutron detectors was measured by a 4π counter. Iron and copper foil cut into four equal strips were used for the measurement of the neutron angular distribution. Their β activity was measured with end-window counters. The detector activity corresponding to the chosen threshold reaction was identified by the half-lives and the absorption curve for

Table I.

Reaction	$R = A_{Cu}/A_{Fe}$	$\overline{T}_0$, Mev exptl. (c.m.s.)	T_0, Mev theoret.	$E_{min}-E_{max}$, Mev
$V + C^{12}$	2.64±0.25	3.5	3.0—3.5	64—79
$V + C^{12}$	1.84±0.20	3.2	2.4—3.5	35—79
$V + O^{16}$	2.16±0.20	3.3	2.4—3.6	38—90
$Nb + C^{12}$	1.36±0.14	2,5	2.2—2.6	52—72
$Nb + O^{16}$	1.47			
$Ta + C^{12}$	1,45			
$Ta + O^{16}$	1,27			
$U + O^{16}$	1.57			

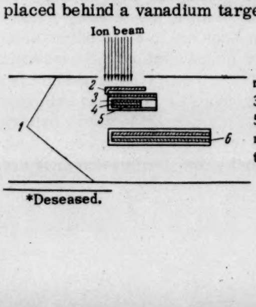

Experimental arrangement: 1 – dee; 2 – target; 3 – copper; 4 – graphite; 5 – iron; 6 – detector for measurement of the neutron angular distribution.

Table II. Neutron Angular Distributions*

Reaction	C.m.s. angle, deg				Effective neutron energy, Mev
	0±12	27±10	45±7	55±5	
$V + C^{12}$	1	0.93	0.80	0.70	10
$V + C^{12}$	1	0.82	0.60	0,50	15
$Nb + C^{12}$	1	0.90	0.80	0.70	10
$Nb + C^{12}$	1	0.85	0.70	0,65	15
$Ta + C^{12}$	1	0,93	0,90	0.86	10
$Ta + C^{12}$	1	0.88	0,85	0.75	15

*The error in the relative values is ≤ ± 3%.

---

*Deseased.

β particles. The investigated reactions and ratio R of the activity induced in the copper (A_{Cu}) and iron (A_{Fe}) detectors are given in Table I, and the angular distributions of the neutrons produced by the C^{12} ions are given in Table II.

The results were compared with the predictions of the statistical model of nuclear reactions. According to this theory, the energy spectrum of the neutrons emitted from excited nuclei is approximately of the form

$$W(\varepsilon) \sim \varepsilon \int\limits_{\varepsilon/T_0}^{\infty} dx e^x / x,$$

where ϵ is the c.m.s. neutron energy, $T_0 = \sqrt{10E^*/A}$ is the initial temperature of the compound nucleus at an excitation energy of E^*.[3]

To calculate the values of R theoretically, this spectrum was transformed into the laboratory system spectrum. Then, for different values of T_0 we took the numerical product of the functions representing the neutron spectrum in the laboratory system and the dependence of the effective cross section of the threshold reaction on the neutron energy for Fe^{56}, Cu^{63}, and C^{12}. The effective energy of the neutrons recorded by the detectors was determined by the maximum of this product and turned out to be ~ 10, 15, and 25 Mev, respectively; the value was almost the same for all reactions. In the calculation of the values of R, we took into account the weight of the targets and their isotopic composition. The final value of R also contained a correction taking into account the self-absorption of β particles in the detectors. This correction, no greater than 10%, was determined experimentally.

Table I gives the values of $\overline{T}_0$ at which the theoretical value of R is the same as the experimental value. The averaging signifies that ions of energy varying over a wide range of values take part in the reactions.

As seen from Table I, the values of $\overline{T}_0$ are in satisfactory agreement with the theoretical values of T_0. The reason for the closeness of the values of T_0 to the maximum values of T_0 is that the reaction cross section increases with increasing energy of the incident ions. We note that for the $V + C^{12}$ and $V + O^{16}$ reactions the intensity of neutrons of energy greater than 22 Mev (in the case of a graphite detector) also corresponds to the above-mentioned shape of the neutron spectrum. It should be kept in mind, however, that the angular momenta of the compound nucleus are not taken into account in the theoretical calculation of the spectrum.

The data of Table II on the neutron angular distributions have two interesting characteristics: a) neutrons of high energy have a more peaked angular distribution; b) as the mass of the target nucleus increases, the anisotropy in the angular distributions becomes less marked. However, for a detailed comparison with the theory, it would be desirable to measure the angular distribution of neutrons emitted in the forward and backward directions in reactions produced by monoenergetic ions. Unfortunately, since we worked with the internal beam of the cyclotron, we were not able to do this.

Nevertheless, since our results are not in contradiction with Strutinskii's calculations[4] based on the statistical model of nuclear reactions, it can be concluded qualitatively that the neutrons are emitted by a compound nucleus.

In conclusion, we consider it our duty to thank G. N. Flerov for his interest in the work and for his day-to-day guidance, and also V. M. Strutinskii for helpful discussions on the problem under study.

---

[1] A. S. Karamyan and A. A. Pleve, JETP **37**, 654 (1959), Soviet Phys. JETP **10**, 467 (1960).

[2] D. Hughes, Neutron Cross Sections, Pergamon Press, London, 1957.

[3] Yu. V. Adamchuk and V. M. Strutinskii, (Theory of Nuclear Level Density and Radiation Widths), Preprint, Inst. Atom. Energy U.S.S.R. Acad. Sci., 1960.

[4] V. M. Strutinskii, Труды Всесоюзной конференциик по ядерным реакциям при малых и средних энергиях, (Proceedings of the All-Union Conference on Nuclear Reactions at Low and Medium Energies, November, 1957), U.S.S.R. Acad. Sci., 1958, p. 576.

Translated by E. Marquit
165

SOVIET PHYSICS JETP VOLUME 13, NUMBER 4 OCTOBER, 1961

ALPHA DECAY OF THE Bi^{210m} *ISOMER*

L. I. RUSINOV,* Yu. N. ANDREEV, S. V. GOLENETSKII, M. I. KISLOV, and Yu. I. FILIMONOV

Leningrad Physico-Technical Institute, Academy of Sciences, U.S.S.R.

Submitted to JETP editor October 11, 1960

J. Exptl. Theoret. Phys. (U.S.S.R.) 40, 1007-1015 (April, 1961)

The long-lived α active isomer Bi^{210m} has been studied. Lines with energies of 4930 ± 10 kev (60%), 4890 ± 10 kev (34%), 4590 ± 10 kev (5%), and 4480 ± 15 kev (~ 0.5%) have been detected in the α spectrum. Gamma radiation from the daughter nucleus Tl^{206} has been detected and studied. Gamma rays of energies 262, 301, 340, and 610 kev have been found. The existence of the coincidences $\alpha 4930 - \gamma 262$, $\alpha 4890 - \gamma 301$, $\alpha 4590 - \gamma 610$, and $\alpha 4590 - \gamma 340$ kev has been established. The γ-transition multipolarities were determined from the internal-conversion electron spectrum and were found to be E2 for 262 kev and M1 for 301 kev. The measured lifetimes of the Tl^{206} levels are $\tau(262 \text{ kev}) = 1.7 \times 10^{-9}$ sec and $\tau(301 \text{ kev}) = 4.6 \times 10^{-9}$ sec. A decay scheme for Bi^{210m} is constructed on the basis of the experimental data. It is shown that RaE is the ground state of Bi^{210} and the long-lived Bi^{210m} is its excited state (250 kev) with a partial half-life of $\sim 5 \times 10^{10}$ years relative to the isomeric transition. The experimental data are compared with the theoretical calculations of the energy states of the Tl^{206} and Bi^{210} nuclei.

1. INTRODUCTION

THE long-lived α active isomer Bi^{210} was first detected in 1950.[1] Hughes and Palevsky[2] estimated its half-life to be $T_{1/2} = (2.6 \pm 0.8) \times 10^6$ years from the difference in the thermal neutron absorption cross section of the Bi^{209} nucleus and the Bi^{210} (RaE) production cross section. Levy and Perlman[3] confirmed the correctness of assigning the mass number 210 to the α-active bismuth nucleus by means of electromagnetic separation of the isotopes and determined the α-particle energy as $E_\alpha = 4935 \pm 20$ kev. In their measurements, Levy and Perlman used a pulse ionization chamber and a long-lived Bi^{210} sample with a specific α activity of 140 min^{-1} mg^{-1}.

The study of the energy levels in the odd-odd nuclei ${}_{83}Bi^{210}_{127}$ and ${}_{81}Tl^{206}_{125}$ is of considerable interest. In addition to the filled shells, the Bi^{210} nucleus has one proton and one neutron and the Tl^{206} nucleus has one proton and one neutron "hole." The levels of these nuclei can be calculated on the basis of the nuclear shell model with allowance for the interaction with the core and the pair interaction. Up to the present time, however, there is practically no experimental data on the excited states of these nuclei. Thus, for the Bi^{210} nucleus, only the 47-kev level (from RaD β decay) has been determined, while the position of the isomeric level remained unknown; excited states of the Tl^{206} nucleus have not been observed in general.

The aim of the present work was to establish the successive levels in the Bi^{210} and Tl^{206} nuclei and to determine their quantum characteristics. Preliminary results have been published earlier.[4,5]

2. EXPERIMENTAL METHOD

The Bi^{210m} decay was studied with the aid of a pulse ionization chamber with a grid, scintillation γ spectrometer, multi-channel time analyzer, and a thin line magnetic β spectrometer.

The Bi^{210m} sample was obtained from the (n, γ) reaction by lengthy irradiation of Bi^{209} in a reactor. Produced alongside with the long-lived Bi^{210m} ($\sigma = 14 \pm 3$ mb) is the five-day Bi^{210} (RaE), with approximately the same cross section ($\sigma = 19 \pm 2$ mb); the Bi^{210} decays into Po^{210}. Since Po^{210} has a half-life of 138 days, and Bi^{210m} has a half-life of 2.6×10^6 years, the α radiation of the polonium will be considerably more intense ($10^5 - 10^6$ times as great) than the Bi^{210m} α radiation. Therefore the sample underwent careful chemical treatment to remove the Po^{210} and other radioactive contamination.[6] Moreover, the sample was enriched with the Bi^{210} isotope by the electromagnetic method. As a result, we obtained a source with a specific α activity of ~ 14 000 min^{-1} mg^{-1}.

---

*Deceased.

For the study of the Bi^{210m} α radiation, we used a pulse ionization chamber with a grid and a geometry of $\sim 2\pi$. The geometrical and electric parameters of the chamber were calculated by the method of Bunemann and Cranshaw.[7] The source was deposited on a stainless steel disk; its area was 25 cm^2 and active layer thickness 10 $\mu g/cm^2$. The chamber was filled with a mixture of Ar (90%) + CH_4 (10%) at atmospheric pressure. The addition of methane decreased the collection time of the electrons on the collector. We chose the differentiation and integration constants of the amplifier to correspond to the minimum noise and weakest dependence of the pulse amplitudes on the α-particle angle of flight: $\tau_{dif} = \tau_{int} = 5\ \mu sec$. During operation, the gas mixture was continuously purified to remove electro-negative impurities, chiefly oxygen, by heated calcium chips. The chamber design allowed the rapid replacement of the samples without disturbance of the mixture composition.

The amplitude of the pulses from the electrode on which the sample was placed depends on the angle of flight of the α particle with respect to the chamber axis. These pulses were used to control the gating circuit for the analyzed pulses from the collector. In this way, we achieved the electron collimation described by Bochagov et al.[8]

The resolving power of the chamber was 28 kev for the U^{233} 4816-kev α line. A NaI(Tl) crystal with an FÉU-S photomultiplier was used as the detector. The spectrometer resolving power for the Cs^{137} (661-kev) line was 8%.

We studied the $\alpha\gamma$ coincidences with this spectrometer and the ionization chamber described above. The chamber design made it possible to place the scintillation detector in the direct vicinity of the chamber source.

The lifetimes of the excited states of the Tl^{206} nucleus were measured on a multi-channel time analyzer of 10^{-9}-sec range whose operation was based on the principle of transformation of the delay time between two pulses into an amplitude.[9]

The γ rays were recorded by a stilbene crystal and the α particles, by a thin plastic scintillator (a solution of terphenyl and polystyrene). An FÉU-33 photomultiplier was used. The half-width of the prompt coincidence curve (resolving time of the circuit), measured with a Co^{60} source, was $2\tau = 10^{-9}$ sec.

The study of the internal conversion electron spectrum was made on an air-core magnetic β spectrometer with a thin lens and ring focus.[10] The Bi^{210m} sample was deposited on a platinum foil 50 μ thick (platinum was used as a base because of the special nature of a deposit of an active substance). The source had a diameter of 10 mm and an active layer thickness of about 1 mg/cm^2. The spectrometer resolving power with such a source was $\Delta H\rho/H\rho = 6\%$ and the transmission was 1%.

With the source activity of $4000\ (2\pi)^{-1}\ min^{-1}$, the detector background (G-M end-window counter) was greater than the number of recorded electrons on the most intense conversion line. Since all conversion electrons are in coincidence

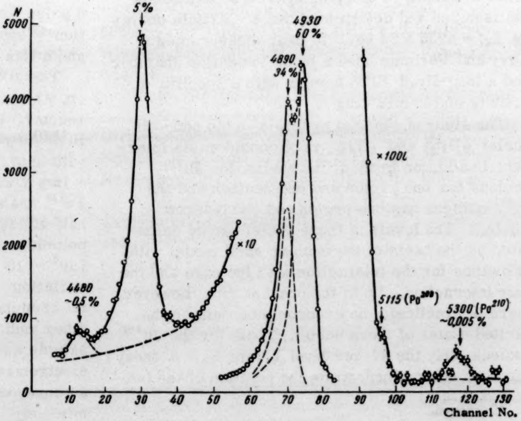

FIG. 1. α spectrum of Bi^{210m} (the resolved components of the spectrum are shown dotted).

with α particles of bismuth, we used the method of αe^- coincidences to reduce the background. We placed a scintillation counter, which recorded α particles, close to the source in the spectrometer. This counter consisted of a plastic scintillator (made in the shape of a thin hollow cone and placed on the side of the active layer), a light pipe, and an FÉU-1B photomultiplier shielded from the magnetic field of the spectrometer. The pulses from this counter and the pulses from the electron detector were applied to a coincidence circuit with a resolving time of 10^{-6} sec. In this case, the random-coincidence background due to cosmic radiation and radioactive contamination of the spectrometer material was approximately 10 pulses per 30 hours, and the number of αe^- coincidences on the most intense line was 400 pulses during the same time.

RESULTS OF THE MEASUREMENTS

α spectrum. The Bi^{210m} sample available to us had a specific activity 100 times that of the sample used by Levy and Perlman.[3] This made it possible to observe weak α groups with a comparatively high energy resolution.

Two well-separated intense lines 4930 ± 10 kev (60%) and 4890 ± 10 kev (34%) stand out in the α spectrum (Fig. 1). Also seen are α lines of 4590 ± 10 kev (5%) and 4480 ± 15 kev (~ 0.5%). These four lines should be assigned to the Bi^{210m} nucleus for the following reasons: 1) the sample emits β particles with $E_{max} = 1500 \pm 30$ kev, which corresponds to the known[11] limiting energy of the β spectrum of the daughter nucleus Tl^{206} (the β particles were recorded by a scintillation counter); 2) the probability of an impurity is small, since the sample underwent careful chemical purification, and the isotope was separated by the electromagnetic method; 3) no lines with such (or close) energies are observed among the known α emitters.

Apart from the transitions already cited, two α transitions of low intensity and energies of 5115 ± 15 and 5300 ± 15 kev (~ 0.005%) were also observed. As will be shown below, an α transition to the Tl^{206} ground state would have an energy of 5185 kev. If it is assumed that the 5115-kev α transition belongs to Bi^{210m}, then there should exist in the Tl^{206} nucleus a 70-kev level from which the γ transition to the ground state is strongly converted. The range of the conversion electrons (of energy ~ 60 kev) would lie entirely in the gap between the high-voltage electrode and the grid of the ionization chamber. One would then observe in the α spectrum two maxima of approximately equal intensity: one at an energy of ~ 5180 kev, when the α particle and the conversion electron in coincidence with it produce the ionization in the chamber; the second at an energy of 5115 kev, when the conversion electron stops in the base. However, there are no maxima on the α-spectrum curve in the energy interval 5140 — 5260 kev, within the limits of experimental error (10^{-3}% in intensity). Consequently, the 5115 ± 15 kev transition should be attributed to some impurity. Calculations indicate that the observed intensity of the 5115-kev line can be explained by the presence of a contamination of 10^{-16} g of Po^{208} ($T_{1/2} = 2.93$ years).

The 5300-kev line belongs to Po^{210}. Its intensity was checked over three half-life periods of polonium ($T_{1/2} = 138$ days) and proved to be constant at ~ 0.005%. Hence, the presence of Po^{210} in the sample is due not to a contamination, but to the isomeric transition $Bi^{210m} \xrightarrow{\gamma, e^-} Bi^{210}$ (RaE) with a subsequent β decay RaE $\xrightarrow{\beta^-}$ Po^{210}. Knowing the half-life of Bi^{210m} (2.6×10^6 years) and the amount of Po^{210} in equilibrium, we can calculate that the partial half-life of the isomeric state relative to the $Bi^{210m} \xrightarrow{\gamma, e^-}$ RaE transition is ~ 5×10^{10} years.

In the measurement of the α-transition energies, we used as references: Th^{230} ($E_\alpha = 4682$ kev), U^{233} ($E_\alpha = 4816$ kev), Pu^{239} ($E_\alpha = 5147$ kev), and Am^{241} ($E_\alpha = 5480$ kev).

γ spectrum and $\alpha\gamma$ coincidences. The present experiment was the first in which the γ radiation of the Tl^{206} nucleus following the α decay of Bi^{210m} was detected and studied. Lines corresponding to transitions of 262 ± 10 and 301 ± 10 kev, whose intensities are in the ratio 1 : 0.45, can be seen clearly in the γ spectrum. Also observed are the characteristic 72-kev x-ray line of Tl.

In order to establish the decay scheme of Bi^{210m}, we investigated the $\alpha\gamma$ coincidences. Gamma lines of 262 and 301 kev are observed in the spectrum of coincidences with the two most intense α groups 4890 and 4930 kev. Only the 262-kev γ line appears in the spectrum of coincidences with the 4930-kev group; the 310-kev line is not present. Consequently, the 301-kev γ transition is in coincidence with the 4890-kev α group, and the 262-kev γ transition, with the 4930-kev α group, i.e., the 4930-kev α transition goes to an excited state of Tl^{206} and not to the ground state, as had been suggested earlier.[3]

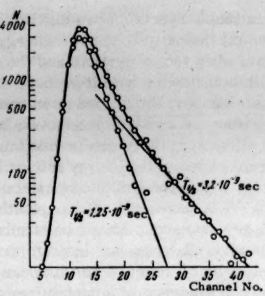

FIG. 2. αγ delayed coincidence curve for Bi^{210m}.

Observed in coincidence with the 4590-kev α group are 340 ± 15 and 610 ± 20 kev γ transitions, which were not noted in the singles γ spectrum, owing to the considerable background from the scintillation counter (α-source activity of $7000\,(4\pi)^{-1}$ min^{-1}). The presence of the 610-kev peak in the spectrum cannot be explained by the simultaneous recording in the scintillator of 262-kev and 340-kev γ quanta in cascade, in view of the small solid angle of the γ counter (~ 0.05 of 4π).

Lifetimes of excited states of the Tl^{206} nucleus. We carried out measurements of the lifetimes of the excited states of the Tl^{206} nucleus in the range of 5×10^{-10} to 2×10^{-8} sec by the delayed αγ-coincidence method by means of a multichannel time analyzer. The obtained curve is shown in Fig. 2. It corresponds to coincidences between the most intense α transitions, i.e., 4930 and 4890 kev, with 262- and 301-kev γ quanta; the contribution from the 4480- and 4590-kev α transitions was slight, owing to their low intensity. In this case, there was no energy selection in the α channel or in the γ channel.

The experimental curve was resolved into two components, one with $T_{1/2} = (1.25 \pm 0.2)\times10^{-9}$ sec (mean lifetime $\tau_1 = 1.7\times10^{-9}$ sec) and the other with $T_{1/2} = (3.2 \pm 0.3)\times10^{-9}$ sec ($\tau_2 = 4.6\times10^{-9}$ sec). They were identified from the ratio of intensities. The relative intensity of the prompt component was 60 — 70% and of the delayed component, 30 — 40%. Such an intensity ratio also occurs for the 4930- and 4890-kev α transitions and for the 262- and 301-kev β transitions in coincidence with them. Therefore the lifetime $\tau_1 = 1.7\times10^{-9}$ sec should be assigned to the level to which the 4930-kev α transition goes, and the lifetime $\tau_2 = 4.6\times10^{-9}$ sec, to the level to which the 4890-kev α transitions goes.

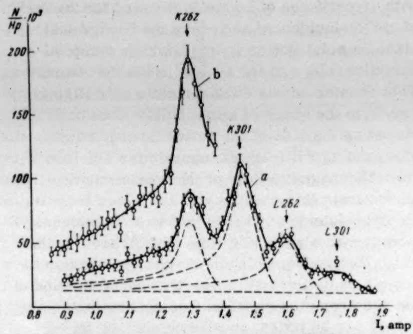

FIG. 3, Conversion electron spectrum of Tl^{206} (I is the spectrometer coil current in amperes). The resolved components of the spectrum are shown dotted.

Conversion electron spectrum of Tl^{206}. We investigated the internal conversion electron spectrum of the daughter nucleus Tl^{206} in the region between 80 and 330 kev. The lower limit of the measured energies was set by the source thickness ~ 1 gm/cm^2; a thinner source could not be used since its activity would be too low.

The conversion electron spectrum measured with a thin line magnetic β spectrometer is shown in Fig. 3. The background was reduced by the αe^- coincidence method (see Sec. 2).

Four internal conversion electron lines with energies of 176 ± 5, 215 ± 5, 250 ± 5, and 292 ± 5 kev were observed in the spectrum (curve a was measured over a time of 700 hours). Their intensity ratio was 0.6 : 1.0 : 0.4 : 0.16. The first two lines were identified as K lines of γ transitions at 262 ± 5 and 301 ± 5 kev; the last two lines were identified as the L lines of the same transitions. Curve b of Fig. 3 represents part of the same spectrum between 80 and 200 kev measured with larger statistics.

The spectrometer was calibrated with the ThB conversion line of energy 148.05 kev. The shape of this line was used to resolve the spectrum into the individual components. In order to take into account the distortion of the line shape due to backscattering of the electrons, the ThB source, as well as the Bi^{210} source, were deposited on a platinum foil.

4. DISCUSSION OF THE RESULTS

On the basis of the obtained data, we constructed the Bi^{210} decay scheme (Fig. 4).

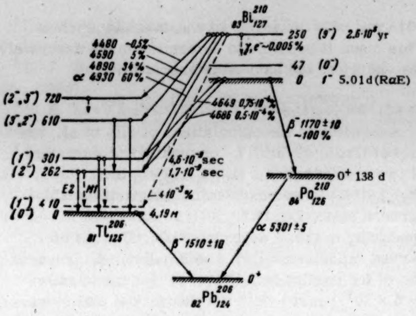

FIG. 4. Decay scheme of Bi^{210m}.

The levels of the Tl^{206} nucleus are determined from the α spectrum and the αγ coincidences. It is improbable that the 262- and 301-kev transitions do not go to the Tl^{206} ground state, since no γ lines of large energy (direct transitions) or γ lines corresponding to cascade transitions are observed. From the presence of the coincidences α4930 — γ262 and α4890 — γ301 kev, it therefore follows that the Tl^{206} nucleus has levels of 262 and 301 kev. Then the 4590- and 4480-kev α transitions go to the 610- and 720-kev levels, respectively. The existence of the 610-kev level is also confirmed by the coincidences α4590 — γ610 kev. The existence of a Tl^{206} level of about 60 kev, which was proposed by us earlier,[5] was not confirmed.

The multipolarities of the 262- and 301-kev γ transitions were established by comparison of the experimental values of the internal conversion coefficients α_K and the ratios K/L with their theoretical values (Table I). The internal conversion coefficients α_K were determined from the spectra of αγ coincidences by the ratio of the number of x-ray quanta accompanying the conversion to the number of nonconversion γ quanta. The large error was due to the approximate character of the corrections for the dependence of the γ spectrometer efficiency on the quantum energy and the error in the graphical resolution of the γ spectrum. The ratio K/L for the 262- and 301-kev transitions was determined from the internal conversion electron spectrum (Fig. 3).

From the data of Table I it is possible to conclude that the 262-kev transition is of the E2 type and the 301-kev transition is of the M1 type. Analysis of the Tl^{206} β spectrum leads to the value 0⁻ for the spin and parity of the ground state of thallium.[11] Then, from our determinations of the multipolarities of the γ transitions, we can fix the spins and parities as 2⁻ for the 262-kev level and 1⁻ for the 301-kev level.

According to the nuclear shell model, the ground and first excited state of the Tl^{206} nucleus should correspond to the configurations $(s_{1/2})_p^{-1}(p_{1/2})_n^{-1}$, $(d_{3/2})_p^{-1}(p_{1/2})_n^{-1}$, and $(s_{1/2})_p^{-1}(f_{5/2})_n^{-1}$. For each of these configurations, the residual interaction of the nucleons leads to doublet splitting and a level shift. Sliv et al.[13] calculated the splitting and level shift arising as a result of pair interactions of the outer nucleons and the interaction with the core surface. The results of the calculations are in good agreement with experiment. The 262-kev (2⁻) and 301-kev (1⁻) levels correspond primarily to the configuration $(d_{3/2})_p^{-1}(p_{1/2})_n^{-1}$. The 610- and 720-kev levels apparently belong to the configuration $(s_{1/2})_p^{-1}(f_{5/2})_n^{-1}$, where one of these levels (although this does not follow from the calculations) has a spin and parity of 2⁻ and the other 3⁻.

The amount of splitting calculated for the configuration $(s_{1/2})_p^{-1}(p_{1/2})_n^{-1}$ proved to be small, only 5 — 10 kev. Hence, it is suggested that there is an excited level of energy 5 — 10 kev, spin and parity 1⁻ close to the Tl^{206} ground state, and the γ transitions from the 262- and 301-kev levels should go not only to the ground state, but also to this level. However, there is still no direct experimental proof of the existence of the 5 — 10 kev level. On the basis of the resolving power of our β spec-

TABLE I. Determination of the Nature of the 262- and 301-kev Transitions

Transition energy, kev	Compared quantities	Exptl. value	Theoretical values[12]						Possible type of transition
			*E*1	*E*2	*E*3	*M*1	*M*2	*M*3	
262	*K/L*	1.5±0.3	5.8	1.37	0.35	5,7	3.8	2.0	*E*2, *M*3
	α_K	0.15±0.06	0.0345	0.094	0.25	0.5	1.9	5.52	*E*2, *E*3
301	*K/L*	6,3±1.0	5.5	1.8	0.59	5.6	4.2	1.8	*E*1, *M*1
	α_K	0.26±0.1	0.023	0,06	0.165	0.30	1.05	2.90	*E*3, *M*1

trometer, we can only say that the energy of the low-lying excited level (if it exists) is not more than 10 kev. From the size of the experimental error in the determination of K/L, it follows that the possible mixture of M1 radiation in the transition from the 262-kev level does not exceed 7% and the mixture of E2 radiation in the transition from the 301-kev level does not exceed 20%. Such mixtures could be the result of transitions from these levels to the level at 5 — 10 kev.

The transition from the 301-kev level (M1, $1 \rightarrow 0$) should be l-forbidden ($d_{3/2} \rightarrow s_{1/2}$, $\Delta l = 2$). In fact, $\tau_{\text{exptl}}(301\ \text{kev})/\tau_{\text{theoret}}(301\ \text{kev}) \approx 10^4$, where τ_{theoret} is the lifetime calculated from Moszkowski's formula.[14] The large value of l-forbiddenness is, perhaps, evidence of the fact that the mixture of neighboring configurations with $(d_{3/2})_p^{-1}(p_{1/2})_n^{-1}$ is small. As regards the 262-kev transition (E2, $2 \rightarrow 0$), we find $\tau_{\text{exptl}}/\tau_{\text{theoret}} \approx 0.5$.

If no assumption is made as to the existence of the 1^- level close to the Tl^{206} ground state, then the ground state 0^- and the 301-kev (2^-) level should be assigned to the configuration $(s_{1/2})_p^{-1}(p_{1/2})_n^{-1}$ and the 262-kev (2^-) level, to the configuration $(d_{3/2})_p^{-1}(p_{1/2})_n^{-1}$. The transition from 301 kev (M1, $1 \rightarrow 0$) will take place between the levels of one doublet. In this case, its experimental probability is approximately 10^{-3} times the theoretical value calculated by Varshalovich's method.[15] This strong forbiddenness cannot be satisfactorily explained. Therefore the variant of the Tl^{206} level scheme with the introduction of the low-lying 5 — 10 kev level is preferable, since it attributes the disparity between the experimental and theoretical probabilities for the 301-kev transition to l-forbiddenness.

The position of the isomeric level of Bi^{210} with $T_{1/2} = 2.6 \times 10^6$ years can be established from the energy balance of the decay branches:

$$Bi^{210m} \xrightarrow{\alpha} Tl^{206} \xrightarrow{\beta^-} Pb^{206}, \quad Bi^{210}(RaE) \xrightarrow{\beta^-} Po^{210} \xrightarrow{\alpha} Pb^{206}.$$

For the first branch

$$Q_\alpha(Bi^{210m}) + E_\beta(Tl^{206}) = 6796 \pm 15\ \text{kev};$$

for the second branch

$$E_\beta(RaE) + Q_\alpha(Po^{210}) = 6574 \pm 15\ \text{kev}.$$

The energy of the isomeric state Bi^{210m} is determined from the equality of these quantities and is equal to 222 ± 20 kev. Walen and Bastin-Scoffier[16] studied the decay $RaE \xrightarrow{\alpha} Tl^{206}$ on a magnetic α spectrometer. They observed α transitions of energies 4649 and 4686 kev going to the 301- and 262-kev levels of the daughter nucleus. This made it possible to determine more accurately the energy of the excited isomeric level:

$$Q_\alpha(Bi^{210m}) - Q_\alpha(RaE) = 250 \pm 10\ \text{kev}$$

According to the calculations of Sliv et al., the lowest levels of Bi^{210} belong mainly to a mixture of two configurations $(h_{9/2})_p(g_{9/2})_n$ and $(h_{9/2})_p(i_{11/2})_n$ and have spins and parities 1^- (ground state, i.e. RaE), 0^- (47-kev level[17] appearing in the β decay of RaD), 1^- (not observed experimentally), and 9^-. From a comparison of the partial half-life of the isomeric state ($\sim 5 \times 10^{10}$ years) with the theoretical estimates from Weisskopf's formula,[18] it follows that the spin of the isomer Bi^{210m} is not less than 7. The theoretical value of the spin and parity 9^- is shown on the decay scheme.

TABLE II. Reduced Forbiddenness Factors for α Transitions of the Bi^{210} Nucleus

	E_α, kev	ΔL	Reduced forbiddenness factors
Bi^{210m}	4930	8	$5,5 \cdot 10^3$
	4890	8	$6.1 \cdot 10^3$
	4590	8	$5.3 \cdot 10^2$
		or 6	$7 \cdot 10^3$
	4480	6	$1.4 \cdot 10^4$
		or 8	$1 \cdot 10^3$
	5180	8	$4 \cdot 10^9$
RaE	4686	2	$3 \cdot 10^2$
	4649	0	$2.1 \cdot 10^2$

The isomer decays mainly by the emission of α particles. Table II gives the reduced forbiddenness factors for the α transitions to the Tl^{206} levels. It is of interest that the forbiddenness coefficients for the α transitions going to the levels of a single doublet (262 and 301 kev) are close to each other in the case of Bi^{210m} ($E_\alpha = 4930$ and 4890 kev) and in the case of RaE ($E_\alpha = 4686$ and 4649 kev). The strong forbiddenness for the α transitions of Bi^{210} are connected with the difficulty of forming α particles in the nucleus from nucleons in different shells. The forbiddenness coefficient for the 5180-kev transition to the proposed 5 — 10 kev level (1^-) is not less than 10^9.

In conclusion, the authors consider it their duty to express their gratitude to L. A. Sliv and D. A. Varshalovich for discussions of the results, to N. B. Abel'skaya, E. G. Gracheva, V. V. Maslovskaya, and L. Ya. Rudaya for chemical purification of the samples to remove radioactive contamination and for the preparation of the samples, to V. S. Eletskii and A. E. Nevskii who took part in the construction and setting up of the equipment.

[1] Neumann, Howland, and Perlman, Phys. Rev. 77, 720 (1960).

[2] D. J. Hughes and H. Palevsky, Phys. Rev. **92**, 1206 (1953).

[3] H. B. Levy and I. Perlman, Phys. Rev. **94**, 152 (1954).

[4] Golenetskii, Rusinov, and Filimonov, JETP **35**, 1313 (1958), Soviet Phys. JETP **8**, 917 (1959).

[5] Golenetskii, Rusinov, and Filimonov, JETP **37**, 560 (1959), Soviet Phys. JETP 10, 395 (1960).

[6] Abel'skaya, Gracheva, Ershova et al., Радиохимия (Radiochemistry), in press.

[7] O. Bunemann and T. E. Cranshaw, Can. J. Research **A27**, 191 (1949).

[8] Bochagov, Vorob'ev, and Komar, Izv. Akad. Nauk SSSR, Ser. Fiz. **20**, 1455 (1956), Columbia Tech. Transl. p. 1331.

[9] R. E. Green and R. E. Bell, Nuclear Instr. **3**, 127 (1958).

[10] Keller, Koenigsberg, and Paskin, Rev. Sci. Instr. **21**, 713 (1950).

[11] D. E. Alburger and G. Friedlander, Phys. Rev. **82**, 977 (1951).

[12] L. A. Sliv and I. M. Band, Таблицы коэффициентов внутренней конверсии, (Tables of Internal Conversion Coefficients), U.S.S.R. Acad. Sci., Parts 1 and 2, 1956-1958.

[13] Sliv, Sogomonova, and Kharitonov, JETP **40**, 946 (1961), Soviet Phys. JETP **13**, 661 (1961).

[14] S. A. Moszkowski, Phys. Rev. **89**, 474 (1953).

[15] D. A. Varshalovich, JETP **38**, 172 (1960), Soviet Phys. JETP **11**, 125 (1960).

[16] R. J. Walen and G. Bastin-Scoffier, J. phys. radium **20**, 589 (1959).

[17] Bashilov, Dzhelepov, and Chervinskaya, Izv. Akad. Nauk SSSR, Ser. Fiz. **17**, 428 (1953).

[18] V. F. Weisskopf, Phys. Rev. **83**, 1073 (1951).

Translated by E. Marquit
166

ELECTRONIC PARAMAGNETIC RESONANCE IN THE V^{3+} ION IN CORUNDUM

G. M. ZVEREV and A. M. PROKHOROV

Institute for Nuclear Physics, Moscow State University

Submitted to JETP editor October 14, 1960

J. Exptl. Theoret. Phys. (U.S.S.R.) 40, 1016-1018 (April, 1961)

The spin Hamiltonian constant $g_\perp$ has been determined experimentally. A theoretical interpretation of the spin Hamiltonian constants D, $g_{||}$ and $g_\perp$ is presented. The value of the trigonal crystal field parameter is found to be $\Delta = -280\ \text{cm}^{-1}$ and the spin-orbit coupling constant $\lambda = +38\ \text{cm}^{-1}$.

We published earlier[1,2] the main results of a study of the electron paramagnetic resonance spectrum of the V^{3+} ion in corundum. The aim of the present work is the determination of $g_\perp$ and a theoretical analysis of the values of the constants of the spin Hamiltonian.

1. We expressed the positions of the lines of the spectrum by the formula[2]

$$h\nu = \left[2 - \frac{(g_\perp \beta H \sin\theta)^2}{D^2}\right](g_{||}\beta H \cos\theta + Am) + \frac{E^2}{g_{||}\beta H \cos\theta}, \quad (1)$$

derived on the assumption that $D \gg g_{||}\beta H$, $g_\perp\beta H$; $g_{||}\beta H \gg E, A, B$. When the trigonal crystal axis lies perpendicular to the direction of the external magnetic field ($\theta = 90°$), the line position corresponds, according to (1), to an effective field $H = \infty$. However, (1) does not apply for large fields since the assumption $D \gg g_{||}\beta H$, $g_\perp\beta H$ is no longer valid.

We calculate the spin energy levels of the V^{3+} ion for $\theta = 90°$ on the assumption that D and $g_\perp\beta H$ are of the same order of magnitude. For $\theta = 90°$ the spin Hamiltonian takes the form

$$\hat{\mathcal{H}} = D\hat{S}_z'^2 + g_\perp\beta H\hat{S}_x' + E(\hat{S}_x'^2 - \hat{S}_y'^2) + A\hat{S}_z'\hat{I}_z + B(\hat{S}_x'\hat{I}_x + \hat{S}_y'\hat{I}_y). \quad (2)$$

The terms describing the hyperfine structure will be accounted for later by perturbation theory.

Solution of the secular equation gives the following expressions for the energy levels

$$\varepsilon_1 = \tfrac{1}{2}(D+E) - \left[\tfrac{1}{4}(D+E)^2 + (g_\perp\beta H)^2\right]^{1/2}, \quad \varepsilon_2 = D - E,$$

$$\varepsilon_3 = \tfrac{1}{2}(D+E) + \left[\tfrac{1}{4}(D+E)^2 + (g_\perp\beta H)^2\right]^{1/2}. \quad (3)$$

The dependence of the positions of the energy levels on the magnitude of the applied magnetic field is shown in Fig. 1.

The energy of the transition $\epsilon_3 \longleftrightarrow \epsilon_2$ is equal to

$$h\nu = \tfrac{1}{2}(3E - D) + \left[\tfrac{1}{4}(D+E)^2 + (g_\perp\beta H)^2\right]^{1/2} \approx (g_\perp\beta H)^2 D^{-1}. \quad (4)$$

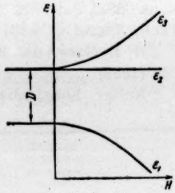

FIG. 1. Energy levels of the V^{3+} ion as a function of magnetic field perpendicular to the trigonal crystal axis.

The approximate equality applies for small $g_\perp\beta H/D$ and for E neglected. We can estimate for what value of the magnetic field the resonance line for $\theta = 90°$ can be observed. Taking $g_\perp \sim 1.6$, as predicted by theory, the field H should be ~ 40 koe in an experiment at a frequency of 37 500 Mc/sec. The line would be observed in a field ~ 20 koe at 9000 Mc/sec. Calculation of the matrix elements of the transition $\epsilon_2 \longleftrightarrow \epsilon_3$ leads to the following result:

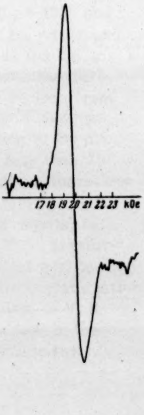

FIG. 2. Electronic paramagnetic resonance line of the V^{3+} ion in corundum with magnetic field perpendicular to the trigonal axis

$$\langle \varepsilon_2 | \hat{S}'_x | \varepsilon_3 \rangle = 0,$$

$$\langle \varepsilon_2 | \hat{S}'_y | \varepsilon_3 \rangle = - ih\nu \, [(h\nu)^2 + (g_\perp \beta H)^2]^{-1/2} \approx - i \, (g_\perp \beta H) \, D^{-1},$$

$$\langle \varepsilon_2 | \hat{S}'_z | \varepsilon_3 \rangle = - (g_\perp \beta H) \, [(h\nu)^2 + (g_\perp \beta H)^2]^{-1/2} \approx - 1. \quad (5)$$

Since the matrix element $\hat{S}'_Z$ has the largest value, the high frequency field must be in the direction of the trigonal crystal axis in order to observe the resonance line.

The line in the perpendicular orientation should show a hyperfine structure with eight equidistant components, differing in energy by an amount

$$\Delta\varepsilon = 2h\nu g_\perp \beta HB \, / \, [(h\nu)^2 + (g_\perp \beta H)^2]. \quad (6)$$

2. The experimental determination of $g_\perp$ was made at 9300 Mc/sec at a temperature of 4.2° K. The corundum crystal, containing 0.13% vanadium impurity, was oriented so that its trigonal axis was perpendicular to the steady magnetic field and parallel to the high frequency magnetic field in the resonator. A very broad line was found with its peak at 19 800 oe. The value of the field strength was measured with a magnetometer using a Hall probe. Using the value[2] $D = 7.0 \pm 0.3 \text{ cm}^{-1}$ and putting $E = 0$, the value derived from (4) is $g_\perp = 1.63 \pm 0.05$.

Using (4), the constants D and $g_\perp$ can in principle be determined from the position of the line in the perpendicular orientation for various frequencies. However, the position of its peak cannot be determined with sufficient accuracy because of the large line width, and the error in determining D by this method would be extremely large.

The line width is associated mainly with the unresolved hyperfine structure. Besides, since in the accessible range of fields the energy of the ϵ_3 level depends weakly on magnetic field, while the energy of level ϵ_2 does not change, the line for the transition $\epsilon_2 \longleftrightarrow \epsilon_3$ is appreciably field broadened. The effect of scatter in the directions of the trigonal axis also contributes a certain amount to the line width.[2] Calculation shows that hyperfine structure should contribute ~ 1000 oe to the line width (if we put $B \approx A$).

3. The constants D, $g_{||}$ and $g_\perp$ of the spin Hamiltonian can be derived theoretically. In a crystal field of cubic symmetry, the sevenfold degeneracy of the F ground level of the V^{3+} ion is partly lifted. The lowest level becomes an orbital triplet. Further splitting of this level takes place under the influence of spin-orbit coupling and the crystalline field of trigonal symmetry. This splitting is described by the fine structure Hamiltonian:[3]

$$\hat{W} = \Delta \, (1 - \hat{l}'^2_z) - \alpha\lambda \hat{l}'_z \hat{S}_z - \alpha'\lambda \, (\hat{l}'_x \hat{S}_x + \hat{l}'_y \hat{S}_y), \quad (7)$$

where $\hat{\mathbf{l}}'$ is the effective orbital momentum operator $l' = 1$, $\hat{\mathbf{S}}$ is the spin operator $S = 1$, Δ is the parameter of the crystal field of trigonal symmetry, λ is the spin-orbit coupling constant and α and α' are constants close to $3/2$. We have here neglected the contribution of spin-spin interaction between the electrons of the paramagnetic ions, since this is insignificant.

We can find the energy level scheme by solving the secular equation. In order to obtain two closely spaced levels (singlet and doublet) at the bottom, we have had to put $\Delta < 0$. The distance between the singlet and doublet, corresponding to the constant D of the spin Hamiltonian is equal to

$$D = \tfrac{1}{2} \{ [(\Delta + \alpha\lambda)^2 + 8\alpha'^2\lambda^2]^{1/2} - [\Delta^2 + 4\alpha'^2\lambda^2]^{1/2} - \alpha\lambda \} \approx \alpha'^2\lambda^2 / |\Delta|. \quad (8)$$

This approximate expression is valid for small λ/Δ.

In order to find the g-factors one must find the wave functions of the lowest energy states, and calculate the matrix elements of the interaction operator of the ion with the external magnetic field. We obtain the result[3,5]

$$g_{\parallel} \approx 2 - (\alpha + 2) \, \alpha'^2\lambda^2/\Delta^2, \qquad g_\perp \approx 2 - 2\alpha'^2\lambda \, / \, |\Delta|. \quad (9)$$

Expressions (8) and (9) enable us to determine from the constants of the spin Hamiltonian ($D = 7.0$ cm^{-1}, $g_{||} = 1.915$, $g_\perp = 1.63$) the values $\Delta = -280$ cm^{-1}, $\lambda = 38$ cm^{-1}, $\alpha = 1.40$ and $\alpha' = 1.17$.

Pryce and Runciman[6] studied corundum with vanadium optically and calculated the energy level scheme for this ion. The values $\Delta = -1200$ cm^{-1} and $\lambda \approx 70$ cm^{-1} which they chose could not explain the experimental g-factor values. We obtained considerably smaller values of the spin-orbit coupling constant than for the free ion ($\lambda = 104$ cm^{-1}). The reduction in λ indicates the presence of covalent binding between the d-electrons of the paramagnetic ion and the electrons of the surrounding oxygen ions.

The authors express their thanks to A. I. Smirnov for help in carrying out the experiment.

---

[1] G. M. Zverev and A. M. Prokhorov, JETP **34**, 1023 (1958), Soviet Phys. JETP **7**, 706 (1958).

[2] G. M. Zverev and A. M. Prokhorov, JETP **38**, 449 (1960), Soviet Phys. JETP **11**, 330 (1960).

[3] A. Abragam and M. H. L. Pryce, Proc. Roy. Soc. **A205**, 135 (1951).

[4] M. H. L. Pryce, Phys. Rev. **80**, 1107 (1950).

[5] A. S. Chakravarty, Proc. Phys. Soc. **74**, 711 (1959).

[6] M. H. L. Pryce and W. A. Runciman, Disc. Faraday Soc. **26**, 34 (1958).

Translated by R. Berman
167

SOVIET PHYSICS JETP VOLUME 13, NUMBER 4 OCTOBER, 1961

STRIPPING REACTIONS ON THE Zr^{90} *AND* Zr^{91} *NUCLEI*

N. I. ZAIKA and O. F. NEMETS

Institute of Physics, Academy of Sciences, Ukr. S.S.R.

Submitted to JETP editor October 31, 1960

J. Exptl. Theoret. Phys. (U.S.S.R.) 40, 1019-1021 (April, 1961)

The values of the transferred angular momenta, parities, and possible spins of the ground and excited states of the Zr^{90} and Zr^{91} nuclei are determined by comparing the experimental proton angular distributions in stripping reactions with the theory.

THE angular distributions of protons in the reactions $\mathrm{Zr}^{90,91}$ (d, p) $\mathrm{Zr}^{91,92}$ were investigated using the extracted beam of 13.6-Mev deuterons from the cyclotron of the Physics Institute of the Ukrainian Academy of Sciences.

The geometry and experimental procedure were described earlier.[1] The present experiment differed in that a polystyrene absorber was placed ahead of the chamber to cut off the deuteron. The Zr^{90} target was a polystyrene film containing finely powdered enriched $\mathrm{Zr}^{90}\mathrm{O}_2$.

The angular distributions obtained are shown in the figure. The solid curves are calculated by the Butler theory.[2]

The spin, orbital-momentum, and energy-level data obtained by comparison with experiment, and also the radii r_0 used in the calculations, are listed in the table.

The values of Q, 5 Mev for Zr^{90} (d, p) Zr^{91} and 6.5 Mev for Zr^{91} (d, p) Zr^{92}, agree with the data of reference 3.

According to the level scheme proposed by Klinkenberg, when the number of neutrons exceeds 50 the states $d_{5/2}$, $g_{7/2}$, $h_{11/2}$, $d_{3/2}$, and $s_{1/2}$ begin to be filled. Nilsson's calculations give for the spherical case a somewhat different filling order, namely $d_{5/2}$, $g_{7/2}$, $s_{1/2}$, $d_{3/2}$, and $h_{11/2}$. The spin and parity $5/2^+$ which our experiments yield for

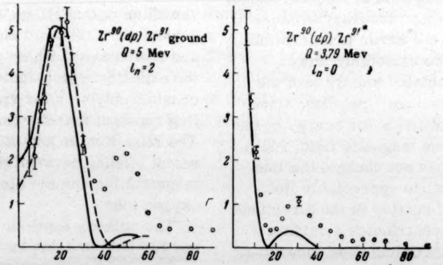

Reaction	J_{init}	Energy of the level of the final nucleus, Mev	l_n	J^{π}_{fin}	r_0, Fermi units
Zr^{90} (*d*, *p*) Zr^{91}	0	0	2	$^3/_2{}^+$, $^5/_2{}^+$	7.16 (6.15)*
		1.21	0	$^1/_2{}^+$	7.16
Zr^{91} (*d*, *p*) Zr^{92}	$^5/_2$	0	2	$\underline{0}^+$, 1^+—5^+	7.19
		0.93	2	$0^+, 1^+, \underline{2}^+, 3^+, 4^+, 5^+$	7.19

*The number in the parentheses is the radius for the dotted curve, Fig. 1a.

the ground[6] state of Zr^{91} agree with the data that Brun et al. obtained by measuring the spin directly, and with the values of the spin predicted by the shell model ($d_{5/2}$). The spin and parity $^1/_2{}^+$ of the first-excited state (with energy 1.21 Mev) does not fit in any of the schemes referred to above. To explain the obtained value of the spin within the framework of Nilsson's calculations for the spherical case,[5] it is necessary to assume that the state $g_{7/2}$, which should lie between $d_{5/2}$ and $s_{1/2}$, either was not registered by us or does not exist at all. In Klinkenberg's scheme even the states $g_{7/2}$, $h_{11/2}$ and $d_{3/2}$ would have to be regarded as unregistered or nonexistent.

On the other hand, Dzhelepov and Peker[7] give for the 1.21-Mev level of Zr^{91} a value $J^{\pi} = {}^5/_2{}^+$, which is also difficult to interpret from the point of view of the shell model. We note that in the case of the reaction Sr^{88} (d, p) Sr^{89} it was observed[8] that for the first excited state of Sr^{88} the 51-st neutron is also captured in the $s_{1/2}$ state. Such a coincidence can hardly be accidental.

According to Dzhelepov and Peker,[7] $J^{\pi} = 2^+$ for the 0.93-Mev level of Zr^{92}. If the spin and parity of the ground state of Zr^{91} are $^5/_2{}^+$, then according to the selection rules this state can be formed in stripping reactions[2] by transfer of angular momenta 0, 2, and 4. The fact that only the momentum $l_n = 2$ is observed signifies that $l_n = 0$ is forbidden by the selection rules of the shell model. The possibility that the transitions to the ground states of the final nuclei are forbidden was pointed out by Bethe and Butler.[9] We know of no other examples for transitions into excited states.

In conclusion, the authors take this opportunity to thank A. P. Klyucharev for providing the metal target of enriched Zr^{91} and to the cyclotron crew for ensuring uninterrupted operation of the apparatus.

---

[1] N. I. Zaika and O. F. Nemets, Izv. AN SSSR, Ser. Fiz. **23**, 1460 (1959), Columbia Tech. Transl. p. 1447.

[2] S. T. Butler, Proc. Roy. Soc. **A208**, 559 (1951).

[3] F. B. Shull and C. E. McFarland, Phys. Rev. **87**, 216 (1952). J. A. Harvey, Phys. Rev. **81**, 353 (1951).

[4] P. F. A. Klinkenberg, Revs. Modern Phys. **24**, 63 (1952).

[5] S. G. Nilsson, Kgl. Dan. Vid. Selsk. Mat.-Fys. Medd. **29**, No. 16 (1955).

[6] Brun, Oeser, and Staub, Phys. Rev. **105**, 1929 (1957).

[7] B. S. Dzhelepov and L. K. Peker, Схемы распада радиоактивных ядер (Decay Schemes of Radioactive Nuclei), Academy of Sciences USSR, 1958.

[8] N. I. Zaika and O. F. Nemets. Izv. AN SSSR, Ser. Fiz. **24**, 865 (1960), Columbia Tech. Transl. in press.

[9] H. A. Bethe and S. T. Butler, Phys. Rev. **85**, 1045 (1952).

Translated by J. G. Adashko
168

SOVIET PHYSICS JETP VOLUME 13, NUMBER 4 OCTOBER, 1961

NEUTRON DIFFRACTION STUDY OF THE CRYSTALLINE STRUCTURE OF SOLID HYDROGEN AND DEUTERIUM

V. S. KOGAN, B. G. LAZAREV, R. P. OZEROV and G. S. ZHDANOV

Physico-Technical Institute, Academy of Sciences, Ukr. SSR; L. Ya. Karpov Physico-Chemical Institute

Submitted to JETP editor November 5, 1960

J. Exptl. Theoret. Phys. (U.S.S.R.) **40**, 1022-1026 (April, 1961)

Neutron diffraction analysis at 12°K has confirmed the structure of deuterium and the tetragonal variant of the hydrogen structure, as found by x-ray diffraction methods. For neutrons, the diffraction patterns were found to be considerably richer than for x-rays, for both hydrogen and deuterium. This is due, in the first place, to the appearance of interferences at angles greater than those for which the intensity of the x-ray interferences, which falls rapidly with increasing scattering angle, decreases to zero, and, in the second place, to the occurrence in the neutron diffraction patterns of interferences having odd index sums, which are forbidden for body-centered structures made up of identical particles. The latter may be accounted for, if it is assumed that the ortho- and para-molecules are distributed through the lattice in an ordered manner, and have different neutron scattering cross-sections. In certain cases interferences were observed at small angles, to which indices may be assigned by proceeding from the assumption that the ortho- and para-molecules are ordered within a volume containing eight cells.

X-RAY structural analysis of polycrystalline samples of hydrogen and deuterium has shown that at 4.2°K these two isotopes possess different lattice structures.[1] This conclusion regarding the structure of hydrogen and deuterium was based, however, upon the analysis of x-ray diffraction patterns having an extremely small number of lines, and those only at small angles. The sparseness of the interference patterns was due to the rapid fall in the intensity of the x-ray interferences with increasing scattering angle, characteristic of diffraction by light elements. The lines in the x-ray patterns for solid hydrogen could not be indexed uniquely, and as a result of their analysis this isotope could be assigned, with equal probability, either a hexagonal (with axis ratio $c/a = 1.73$) or a tetragonal (with axis ratio $c/a = 0.82$) structure. The structure of deuterium was determined to be tetragonal (with axis ratio $c/a = 1.73$).

With the object of securing more complete information on the crystalline structures of hydrogen and deuterium, a neutron diffraction study of these isotopes was undertaken. The coherent scattering amplitude for neutrons does not depend upon the angle of scattering. This led to the expectation that neutron diffraction patterns could be obtained for the hydrogen isotopes which would have a greater number of interferences at large angles than the x-ray patterns. Such neutron diffraction patterns could be accurately indexed, and a more certain solution could be found to the problem of the crystalline structure of hydrogen and deuterium.

EXPERIMENTAL METHOD

The investigation was carried out using the apparatus previously described.[2,3] The absence of any need for a magnetic field allowed a modification to be introduced in the construction of the cryostat: the outer jacket and screen (both of copper) were removed to a distance of 100 mm from the central container holding the object under study. In addition, the copper container was replaced by one made from a titanium-zirconium alloy (32 atomic percent zirconium), clamped with an indium gasket to the bottom of the reservoir containing the cooling agent. These changes made it possible to avoid completely the effects of coherent scattering of the neutrons by the jacket and screen (through collimation) and also by the container (since a titanium-zirconium alloy containing 32% zirconium does not yield coherent scattering).

Liquid hydrogen was employed as the cooling agent, being pumped on with a forevacuum pump.

The samples had a temperature of 11 - 12° K, as determined from the vapor pressure at their surfaces. One filling of the cryostat with the coolant liquids (nitrogen and hydrogen) sufficed for more than 24 hours of operation.

Under the conditions of crystallization prevailing in the experiment, the hydrogen and deuterium samples took the form of aggregates of coarse crystals. The orientation of these crystals varied in an uncontrollable fashion from sample to sample; in all probability, they did not remain constant even in a given sample over the duration of a run, due to the intensive recrystallization and self-diffusion processes taking place at the temperatures of the experiment. The following measures were taken to reduce the effect of the coarse crystalline structure of the samples:

1. The sample was made to oscillate, together with the entire cryostat, through 120°, at a period such that an integral number of oscillations took place during a single measurement.

2. The neutron diffraction patterns obtained on different days from separate samples, under varying experimental conditions (i.e., statistics, collimation, etc.), were averaged, with these differing conditions taken into consideration.

These measures, however, could not insure the provision of unique data on the intensities of the interference maxima, which would have permitted determination of the orientations of the molecules in the unit cell. The neutron diffraction patterns yielded information only on the absence or presence of the maxima, and on their positions.

RESULTS

A. Deuterium. Figure 1 presents some of the neutron diffraction patterns obtained for deuterium samples having an ortho-molecule concentration equal to or somewhat smaller than the equilibrium value for room temperature. As noted above, the relative intensities of reflections having the same indices vary among the diffraction patterns obtained from different samples. The positions of the reflections, however, can be established with a sufficient degree of precision, especially if through a particular choice of the cryostat position it is possible to find one peak of such intensity as to correspond to reflection from a monocrystal oriented at the Bragg angle. Indexing, using the Hull-Davey curves, and appropriate elementary calculations permitted establishment of the fact that the crystalline lattice of deuterium belongs to the tetragonal system. The dimensions of the unit cell are a = 3.38 A and c = 5.60 A (c/a = 1.66). Positions of the maxima as computed from these parameters are indicated in Fig. 1 by the small arrows. The slight deviations of some of the maxima from their calculated positions may be explained by the fact that the monocrystals giving rise to the corresponding reflections are displaced relative to one another within the container, the diameter of which is 10 mm. The incoherent scattering background for deuterium (after subtracting out the instrumental background) is essentially zero.

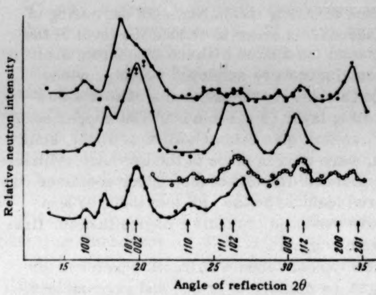

FIG. 1. Neutron diffraction patterns for deuterium at T ~ 12°K (upper curve obtained by averaging four neutron patterns taken without oscillation of the sample).

B. Hydrogen. The investigation of hydrogen by neutron diffraction is greatly hampered by the

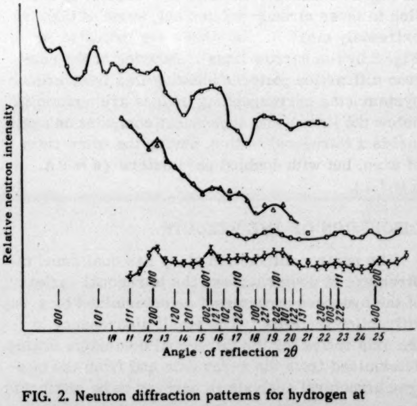

FIG. 2. Neutron diffraction patterns for hydrogen at T ~ 12°K (two lower patterns obtained with the aid of the flat container; upper pattern with the ordinary cylindrical container; second from the top, obtained with a cylindrical container empty at the center).

presence of strong incoherent spin scattering of the neutrons. In order to reduce the level of the background associated with the incoherent scattering, containers were employed which provided sample thicknesses not exceeding that of a 50%-attenuating layer (3 - 4 mm). A flat copper container, as well as a double-walled cylinder, empty within, were used in place of the ordinary cylindrical container. The use of the copper container was rendered feasible by the fact that the hydrogen lines are produced at smaller angles than the first line from copper.

A few typical neutron diffraction patterns for hydrogen (a mixture of ortho- and para-molecules having nearly the equilibrium distribution for room temperature) are presented in Fig. 2. The coherent scattering maxima in these patterns are only weakly evident above the incoherent scattering background; however, analysis of a large number of the diffraction patterns (more than 20) permitted determination of the positions of the maxima with adequate precision. Indexing, with the aid of the Hull-Davey curves, and subsequent computation permitted assignment of the hydrogen structure to the tetragonal system. The unit-cell dimensions are $a = 4.5\,A$, $c = 3.6\,A$ ($c/a = 0.81$). The positions of the interference maxima corresponding to this structure are indicated in Fig. 2 by the heavy lines; the indices of these maxima are written in above the corresponding lines. In a few cases (see, for example, the upper neutron diffraction pattern in Fig. 2) still other maxima are visible, in addition to those already pointed out, some of them at extremely small angles (these are indicated in Fig. 2 by the narrow lines). Indexing of the neutron diffraction patterns showing this interference system (the corresponding indices are written in below the lines) and subsequent computation again yields a tetragonal lattice, having the same ratio of axes, but with doubled parameters ($a \approx 9\,A$, $c \approx 7\,A$).

DISCUSSION OF THE RESULTS

The neutron diffraction study has confirmed the structure of deuterium and the tetragonal variant of the hydrogen structure,* as determined by x-ray diffraction methods.[1] The small discrepancy in the axis ratios for the tetragonal deuterium lattice determined from the x-ray data and from the neutron structural analysis is perhaps to be attributed to the difference in the temperatures at which these investigations were carried out (4.2 and 12°K, respectively). However, the agreement of the results from the x-ray and neutron structural analyses is confined to the symmetry, the parameters, and the axis ratio of the unit cell. In the x-ray diffraction patterns only those reflections having even index sums were present as is characteristic for body-centered structures. In the neutron diffraction patterns, in addition to further maxima with even sums of indices, appearing at relatively large angles, lines are also present which have odd index sums; this corresponds to a primitive unit cell rather than the body-centered one inferred from the x-ray structural analysis data. This discrepancy might be explained in the following manner:

1. The amplitudes for coherent scattering of neutrons by the ortho- and para-molecules in hydrogen and deuterium are unequal.
2. The distribution of the ortho- and para-molecules within the lattice is not purely statistical. In this event the lines having odd sums of indices could be regarded as coming from the superstructure. With respect to x-rays the ortho- and para-molecules are completely equivalent, and the superstructure has no effect.

Published data on the properties of hydrogen and deuterium in the ortho- and para-states do not as yet permit a definite answer to the question of the validity of the hypothesis, advanced above, that the interference patterns observed in neutron diffraction by these isotopes are to be attributed to an ordered arrangement of ortho- and para-molecules in their lattices.

The ortho- and para-molecules of one and the same isotope are so similar in all their properties that until fairly recently it was thought that they constitute ideal mixtures. Vapor pressure data,[6] however, have shown that, for hydrogen as well as deuterium, the ortho - para mixtures fail to obey Raoult's law for ideal solutions. Through the use of Clapeyron's equation it has been established that the latent heat of vaporization and the internal energy in the liquid and solid phases are quadratic, rather than linear, functions of the composition. This suggests a difference in the mutual energies of the various types of molecular pairs, and the possibility, in principle, of an energetic advantage in the ordering of the ortho- and para-molecules in the hydrogen and deuterium lattices. Further, this hypothetical ordering is not contradicted by the data on the specific heats of ortho - para hydrogen mixtures (a departure, beginning at 12°K, of the temperature dependence of the mixture specific heats from the analogous curve for pure parahydrogen[7]), nor by the results of a study of nuclear magnetic resonance in solid hydrogen (a rapid broadening of the resonance line, from 0.1 oersted at 12°K to ~ 8 oersteds at 10°K and below, which implies a sharp change in the rates of the diffusion processes within this temperature interval[8]).

---

*This variant is also confirmed by measurements of the specific heat and the nuclear magnetic moment, as is shown in a theoretical paper by Dukhin[4] and in the experiments of Galkin and Matyash.[5]

A direct experimental test of the validity of the hypothesis concerning the existence of a superstructure in the lattices of solid ortho - para mixtures of hydrogen and deuterium would, it appears, be provided by the investigation of mixtures of controlled composition, ranging down to pure parahydrogen and ortho-deuterium.

The authors wish to express their gratitude to B. N. Samoilov, who made possible the work with liquefied gases, as well as to N. E. Yukovich for supplying the liquid hydrogen, and to S. V. Kiselev and A. L. Donde for their participation in the experiments.

---

[1] Kogan, Lazarev and Bulatova, JETP **37**, 678 (1959), Sov. Phys. JETP **37**, 485 (1960).

[2] Ozerov, Kiselev, Karpovich, Goman'kov and Loshmanov, Кристаллография, **5**, 317 (1960), Sov. Phys. Crystallography **5**, 294 (1960).

[3] Kogan, Lazarev, Zhdanov and Ozerov, Кристаллография, **5**, 320 (1960), Sov. Phys. Crystallography **5**, 297 (1960).

[4] S. S. Dukhin, JETP **37**, 1486 (1959), Sov. Phys. JETP **37**, 1054 (1960).

[5] A. A. Galkin and I. V. Matyash, JETP **37**, 1831 (1959), Sov. Phys. JETP **37**, 1292 (1960).

[6] Wooley, Scott and Brickwedde, J. Research Natl. Bur. Standards **41**, 379 (1948).

[7] R. B. Hill and B. W. Ricketson, Phil. Mag. **45**, 277 (1954).

[8] J. Hatton and B. V. Rollin, Proc. Roy. Soc. **199**, 222 (1949).

Translated by S. D. Elliott
169

SOVIET PHYSICS JETP VOLUME 13, NUMBER 4 OCTOBER, 1961

ESTIMATE OF THE UPPER LIMIT OF THE CHARGE-EXCHANGE CROSS SECTION FOR THE pn INTERACTION AT 8.5 Bev

V. A. NIKITIN and É. N. TSYGANOV

Joint Institute for Nuclear Research

Submitted to JETP editor November 11, 1960

J. Exptl. Theoret. Phys. (U.S.S.R.) 40, 1027-1030 (April, 1961)

The upper limit of the cross section for elastic scattering of 8.5 Bev protons on neutrons accompanied by charge exchange was studied by the photographic emulsion technique and was found to be 0.46 ± 0.15 mb.

ACCORDING to statistical theory, the pn charge-exchange scattering cross section σ_{ex} should be small at high energies (as is the case for the cross section of any possible reaction involving the inelastic interaction of nucleons); at 10 Bev, $\sigma_{ex} \sim 2 \times 10^{-4}\,\sigma_{in}$ (see reference 1), where σ_{in} is the cross section for all inelastic processes. It is not impossible, however, that charge exchange stands apart from all the remaining reactions.

Another circumstance which makes charge-exchange scattering of interest is the fact that the ratio $\sigma_{ex}/\sigma_{el\,pp}$ ($\sigma_{el\,pp}$ is the pp elastic scattering cross section), under the condition of isotopic invariance, depends on the contribution of the one-meson interaction scheme to the process of elastic scattering of nucleons. Thus, if NN elastic scattering takes place only as a result of the exchange of a single π meson, then the above-mentioned ratio is equal to 4.

Under certain assumptions, it is possible to estimate the maximum difference of the pp and pn total interaction cross sections $\Delta_{tot} = \sigma_{pp} - \sigma_{pn}$. Indeed, owing to isotopic invariance, we have the following relation between the amplitudes of the corresponding elastic processes:

$$A_{pp}^{(3)(0)} - A_{pn}^{(3)(0)} = A_{ex}^{(3)(0)}. \qquad (1)$$

The indices 3, 0 indicate that this relation holds separately for the triplet and singlet states of the nucleons (for ordinary spin). Using also the relations

$$\frac{k}{4\pi}\,\mathrm{Im}\,A(0) = \sigma_{tot}, \qquad \sigma_{ex}(\theta) \geqslant [\mathrm{Im}\,A_{ex}(\theta)]^2$$

(here k is the wave vector of the incident particle and σ_{tot} is the total interaction cross section), we obtain

$$\Delta_{tot} \leqslant \frac{4\pi}{k}\left[\frac{3}{4}\sqrt{\sigma_{ex}^{(3)}(0)} + \frac{1}{4}\sqrt{\sigma_{ex}^{(0)}(0)}\right]. \qquad (2)$$

Here $\sigma_{ex}^{(3)}(0)$ and $\sigma_{ex}^{(0)}(0)$ are the differential charge-exchange cross sections for $\theta = 0°$ in the triplet and singlet states of the nucleons, respectively. These cross sections are related to the cross section $\sigma_{ex}(0)$ measured with an unpolarized target and an unpolarized beam in the following way:

$$\tfrac{3}{4}\,\sigma_{ex}^{(3)}(0) + \tfrac{1}{4}\,\sigma_{ex}^{(0)}(0) = \sigma_{ex}(0).$$

Hence the bracketed expression in formula (2) takes on a maximum value $\sqrt{\sigma_{ex}(0)}$ when $\sigma_{ex}^{(3)}(0) = \sigma_{ex}^{(0)}(0)$ and a minimum value $\frac{1}{2}\sqrt{\sigma_{ex}(0)}$ when $\sigma_{ex}^{(3)}(0) = 0$. Thus, a measurement of the difference Δ_{tot} and the differential charge-exchange cross section for $\theta = 0°$ gives some information on the role of the spin interaction.

Under the assumptions 1) that the cross sections are independent of the spin state of the nucleons and 2) that the angular dependences of the differential pp elastic scattering cross section and the differential pn charge-exchange scattering cross section are similar, formula (2) takes the form

$$\Delta_{tot} \leqslant (4\pi/k)\sqrt{\sigma_{ex}\sigma_{el\,pp}(0)/\sigma_{el\,pp}}, \qquad (3)$$

where $\sigma_{el\,pp}(0)$ is the differential pp elastic scattering cross section for $\theta = 0°$.

If it is assumed that the pp elastic scattering amplitude is purely imaginary, then inequality (3) can be simplified to

$$\Delta_{tot} \leqslant \sqrt{\sigma_{ex}\sigma_{pp\,tot}/\sigma_{el\,pp}}. \qquad (4)$$

In the present article we attempt to estimate the upper limit of the charge-exchange cross section in the scattering of 8.5-Bev protons on bound neutrons in emulsion nuclei.

EXPERIMENTAL METHOD AND RESULTS

A 10 × 10 × 2 cm emulsion stack was exposed to a beam of 8.5-Bev protons.

The beam was directed perpendicularly to the emulsion pellicles. The advantage of such a method for the observation of events such as pp elastic scattering and charge exchange $p + n \rightarrow n + p$ has been discussed previously.[2] Area scanning was employed.

We selected for analysis all two-prong and one-prong stars containing one black or gray prong (the latter corresponds to protons of energy ≤ 300 Mev). The two-prong stars included elastic scatterings of protons on hydrogen and quasi-elastic pp scatterings, i.e., scatterings of protons on bound protons of emulsion nuclei. The one-prong stars should include the charge-exchange reactions $p + n \rightarrow n + p$ (if such reactions occur).*

If the number of quasi-free protons and neutrons is the same, then the charge-exchange cross section is

$$\sigma_{ex} = (N_{ex} / N_{\text{quasi } pp})\, \sigma_{el\ pp} K, \tag{5}$$

where N_{ex} and $N_{\text{quasi pp}}$ are the numbers of cases of each type after analysis of the events and K is the ratio of the efficiencies of recording two- and one-prong stars.

This estimate will be increased or decreased, depending on the strictness of the criteria by which the cases of charge exchange and quasi-elastic scattering are selected.

The selection criteria were as follows:

1. Separation of charge-exchange events: a) we selected stars without recoil nuclei; b) the prong in a one-prong star was regarded as the recoil proton produced as a result of the charge exchange of a neutron. Therefore the relation between the angle of flight of the recoil proton θ and its momentum p should include the binding energy of the neutrons in the nucleus and their momentum distribution. To take this into account, we constructed on the (θ, p) plane the region in which points corresponding to charge-exchange reactions could lie. The density of points outside this region is a measure of the background.

2. Separation of pp quasi-elastic scattering. This separation reduced to the calculation (for two-prong stars without a recoil nucleus or a beta-decay electron) of the momentum of the target proton, i.e., of a proton bound in a nucleus. This momentum was calculated as the difference between the observed recoil-proton momentum and the momentum transfer. The first quantity was measured from the range (or ionization) in emulsion and the second was determined from the scattering angle of the primary proton. This angle was measured to an accuracy of 0.2°.

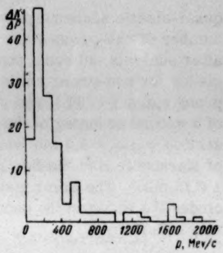

Distribution of two-prong stars without a recoil nucleus or a beta-decay electron as a function of the target-proton momentum.

We then constructed the distribution of the number of cases as a function of the momentum of the target proton dN(p)/dp (see the figure). This distribution has a maximum near the point p = 200 Mev, corresponding to the pp quasi-elastic scatterings. The width of the maximum depends on the value of the mean momentum of the target proton inside the nucleus and the measurement error. The dip in the curve close to the point p = 0 results from the errors in the measurements of the angles and momenta of the particles, which lead to an increased momentum p of the target proton. The value of the function dN(p)/dp at large p characterizes the background. In our case, it turned out to be ~ 10%. For the estimate of the background, we also attempted to separate similar "quasi-elastic" cases for three-prong stars by neglecting one of the prongs. It turned out that the probability of the separation of a "quasi-elastic" case for a three-prong star was one-tenth of that for a two-prong star. This indicates that the described method gives a sufficiently reliable separation of the quasi-elastic cases.

It is seen from the above that the two-prong stars are subjected to stricter selection criteria than the one-prong stars. Expression (5) therefore gives an upper limit for the charge-exchange cross section. One could attempt to obtain the cross section σ_{ex} from expression (5) by applying to the two-prong stars the same selection criteria that is applied to the one-prong stars. This could be done, however, only if it is known beforehand that the background-effect ratio in pp scattering and in pn charge-exchange scattering is the same.

A total of 8.08 cm^3 of emulsion was scanned. Of the 1859 recorded two-prong stars, 466 pp quasi-elastic scatterings were separated. The number of one-prong stars found was 55, and after analysis, 20 remained. The scanning efficiency for two-prong stars (~ 92%) and for one-prong stars (~ 75%) was found from the results of a second scanning of the entire area. The cross section $\sigma_{\text{el pp}} = 8.7$ mb was taken from the work of Markov et al.[2] We finally obtained $\sigma_{\text{ex}} \leq 0.46 \pm 0.15$ mb.* The error given is statistical and includes the error in the determination of the scanning efficiency.

---

*This reaction can also be regarded as elastic backward scattering of a proton on a neutron in the c.m.s.

CONCLUSIONS

a) The ratio of the cross sections $\sigma_{\text{ex}}/\sigma_{\text{el pp}} \leq 0.07$. This means that the contribution of one-meson scattering to the cross section for elastic interactions of nucleons does not exceed 2%.†

b) According to the data of Markov et al.,[2] $\sigma_{\text{el pp}}(0) \approx 160$ mb/sr. We therefore obtain from formula (3) $\Delta_{\text{tot}} \leq 11$ mb. From formula (4) we obtain $\Delta_{\text{tot}} \leq 9$ mb, which is also not in contradiction with the available experimental data.[3]

c) The obtained limit for the charge-exchange cross section is too high to check the predictions of the statistical theory.

We thank M. I. Podgoretskii, V. G. Grishin, and V. N. Strel'tsov for advice and discussions.

---

*It should be noted that we made the important assumption that the momentum transfer in the case of charge exchange is not much smaller than the momentum transfer in the case of elastic scattering. If this is not so, then charge exchange with a bound neutron cannot be observed at all.

†We did not take into account possible interference between the one-meson and multi-meson interactions.

[1] Blokhintsev, Barashenkov, and Barbashov, The Structure of the Nucleon, Joint Institute for Nuclear Research Preprint R-317.

[2] Markov, Tsyganov, Shafranova, and Shakhbazyan, JETP 38, 1471 (1960), Soviet Phys. JETP 11, 1063 (1960).

[3] Tenth Annual International Conference on High Energy Physics at Rochester, 1960.

Translated by E. Marquit
170

SOVIET PHYSICS JETP VOLUME 13, NUMBER 4 OCTOBER, 1961

RESONANCE SCATTERING OF GAMMA RAYS BY Te^{124} *NUCLEI*

A. F. AKKERMAN, D. K. KAIPOV and Yu. K. SHUBNYĬ

Nuclear Physics Institute, Academy of Sciences, Kazakh SSR

Submitted to JETP editor November 14, 1960; revised manuscript submitted January 6, 1961

J. Exptl. Theoret. Phys. (U.S.S.R.) 40, 1031-1032 (April, 1961).

The lifetime of the excited state at 608 kev in Te^{124} was determined from the experimental value of the cross section for resonance scattering of γ quanta. The value obtained is compared with the predictions of the single particle model.

We have studied the resonance scattering by Te^{124} of the 608-kev γ quanta which are emitted in the decay Sb^{124} → Te^{124}. The resonance condition was guaranteed by the Doppler broadening of the 608-kev line resulting from recoil in the preceding part of the cascades,[1] which are listed in the table.

To eliminate effects of slowing down of recoil nuclei on the shape of the spectrum, the main experiment was done with a gaseous source. A 3.4-mC source of highly volatile $SbCl_3$ was heated to 220° and converted completely to gas. The vapor pressure in the ampoule did not exceed atmospheric. The scatterers were cylinders of TeI_2 and CdO. Measurements were made with solid and gaseous sources. In the latter case, with a tellurium scatterer we observed an increase in counting rate (by 0.43 pulse/sec) over a cadmium scatterer.

The cross section $\bar{\sigma}$ for resonance scattering was computed using the standard formula,[2] and when the angular distribution of the scattered γ quanta and the self absorption in the scatterer were included we found the value $(3.5 \pm 1.1) \times 10^{-25}\,\mathrm{cm}^2$. The lifetime τ_γ for the 608-kev level of Te^{124} was found from the formula

$$\tau_\gamma = (\sigma_0 \pi \hbar / 2\bar{\sigma}) N(E_r)/N, \qquad (1)$$

where $N(E_r)/N$ is the fraction of the 608-kev γ quanta which fall in a 1-ev interval around the resonance energy. We computed the partial values of $N(E_r)/N$ by starting from the relative intensities of the cascades,[3,4] disregarding effects of chemical binding. However the latter do not essentially change the total value $N(E_r)/N = 0.058 \pm 0.006$. The error in $N(E_r)/N$ resulting from the inaccuracy in the determination of the relative

$\beta\gamma$-cascades in the Sb^{124} → Te^{124} decay

	End point of β spectrum, kev	Intensity of β component, %	Cascades preceding the 608-kev level	Relative intensity of cascade, %	Partial values $N(E_r)/N$, %
1	2312	28	β	28	1.44
2	1596	10	$\beta(\gamma-723)$	10	0.68
3	952	4	$\beta(\gamma-1370)$	4	0,24
4			$\beta(\gamma-646)(\gamma-646)$	$\leqslant 1$*	
5			$\beta(\gamma-724)(\gamma-646)$	$\leqslant 1$*	
6	610	49	$\beta(\gamma-1692)$	47	2.78
7			$\beta(\gamma-1047)(\gamma-646)$	~ 2*	
8			$\beta(\gamma-969)(\gamma-724)$		
9	219	9	$\beta(\gamma-2088)$	6,5	0.30
10			$\beta(\gamma-1450)(\gamma-646)$	~ 1*	
11			$\beta(\gamma-1361)(\gamma-723)$	$\leqslant 1$*	
12			$\beta(\gamma-714)(\gamma-1370)$	$\leqslant 3$*	
13			$\beta(\gamma-714)(\gamma-724)(\gamma-646)$		
14			$\beta(\gamma-714)(\gamma-646)(\gamma-723)$		
					$\Sigma=5.84$

*Inclusion of these cascades adds approximately 0.4% to $N(E_r)/N$.

intensities of the cascades is 8%, which is greater than the errors due to neglect of correlations[1] and the choice of the variant of β decay theory.[5]

According to Eq. (1), the lifetime of the 608-kev level was $(5.8 \pm 1.5) \times 10^{-12}$ sec. A value of $\tau_\gamma < 2 \times 10^{-11}$ sec was found[6] by using $\beta\gamma$ coincidences. By studying Coulomb excitation,[7] the reduced transition probability $B(E2, 0^+ \to 2^+)$ was found to be $0.39\ e^2 \cdot \text{barn}^2$, which gives $\tau_\gamma = 12.6 \times 10^{-12}$ sec. Computations using the Weisskopf[8] formula, which is based on the single particle model, give the value $\tau_\gamma = 1.2 \times 10^{-10}$ sec. Thus the E2 quadrupole transition at 608 kev in Te^{124} is enhanced, with an enhancement factor equal to 20, which shows the collective nature of the excitation.

The authors thank Yu. G. Kosyak for help in computing the spectra, and T. A. Zotov for preparing the source.

[1] F. R. Metzger, Phys. Rev. **101**, 286 (1956).

[2] C. P. Swann and F. R. Metzger, Phys. Rev. **108**, 982 (1957).

[3] Zolotavin, Grigor'ev and Abroyan, Izv. Akad. Nauk SSSR, ser. Fiz. **20**, 289 (1956), Columbia Tech. Transl. p. 271.

[4] Dzhelepov, Zhukovskii, and Predovskii, Izv. Akad. Nauk SSSR, ser Fiz. **21**, 1614 (1957), translation p. 1602.

[5] Akkerman, Kaipov and Shubnyĭ, Vestnik Akad. Nauk Kazakh SSR, 12 (1960).

[6] C. F. Coleman, Phil. Mag. **46**, 1135 (1955).

[7] G. M. Temmer and N. P. Heydenburg, Phys. Rev. **104**, 967 (1956).

[8] V. Weisskopf, Phys. Rev. **83**, 1073 (1951).

Translated by M. Hamermesh
171

SOVIET PHYSICS JETP VOLUME 13, NUMBER 4 OCTOBER, 1961

MASS OF THE Pu^{240} *ISOTOPE*

R. A. DEMIRKHANOV and V. V. DOROKHOV

Submitted to JETP editor November 19, 1960

J. Exptl. Theoret. Phys. (U.S.S.R.) 40, 1033-1034 (April, 1961)

Precision mass-spectrographic measurements of the mass of the Pu^{240} isotope have been made.

We measured the mass of the Pu^{240} isotope on a mass spectrograph with a resolving power of ~ 60,000.[1] The Pu^{240} ions were produced by the evaporation of plutonium enriched to approximately 10 — 12% Pu^{240}. The doublet used for the measurement was produced by the Pu^{240} ion and a fragment of the organic compound of perylene ($C_{20}H_{12}$, M = 252) containing $C_{18}C^{13}H_{11}$ (M = 240). The mass of the C^{12}, C^{13}, and H^1 isotopes were measured previously with sufficient accuracy.[1,2] The ions were produced in an arc ion-source in which the basic discharge was maintained in helium. The vapors of the plutonium and the organic compound were introduced into the discharge by the evaporation of these substances in crucibles of special design.

The analysis of the doublet $C_{18}C^{13}H_{11} - Pu^{240}$ was carried out in the standard way.[1] To determine the dispersion constant, we used perylene fragments with a mass difference of one mass of hydrogen (M = 239, M = 240, and M = 241). The value of the doublet and the value of the mass of the Pu^{240} isotope corresponding to it were found to be the following:

$C^{12}_{18}C^{13}H_{11} - Pu^{240}$ doublet:	$\Delta M = 35.497 \pm 0.126$ mmu
Pu^{240} mass:	240.130316 ± 130 amu
Pu^{240} mass from reference 3	240.129105 ± 100 amu

For comparison, we have given here the Pu^{240} mass from the work of Huizenga.[3]

The mass-spectrographic mass of Pu^{240} has not been measured until now. The difference in the value obtained in the present experiment from Huizenga's value is 1.211 ± 0.170 mmu, i.e., about seven times the total error of measurement. This difference, however, can be accounted for by the difference in the values for the reference element used by Huizenga, namely, the mass of the Pb^{208} isotope. The value of 208.041640 ± 1000 amu for this mass, which he used as the standard in the calculations, was taken from the measurements of Stanford et al.[4] This value differs by approximately 10^{-3} amu from the data of later measurements made independently in two different experiments, according to which M (Pb^{208}) = 208.042658 ± 35 amu[5] and M (Pb^{208}) = 208.042779 ± 6 amu.[6] The mean difference between these values, which are in satisfactory agreement with each other, and the standard mass of the Pb^{208} isotope used by Huizenga is 1.073 ± 0.050 mmu. If this difference is taken into account, then the mass of the Pu^{240} isotope calculated from the measurements of Huizenga will be M (Pu^{240}) = 240.130178 ± 120 amu, which is in good agreement with the value obtained in the present experiment.

Moreover, the data of Everling, König, Mattauch and Wapstra[9] were available to us. These authors made a statistical analysis of the data on the masses of isotopes in the range $1 \leq A \leq 254$ with the aid of an electronic computer by the method of least squares. According to their data, the value of the mass of the Pu^{240} isotope is equal to M (Pu^{240}) = 240.130292 ± 40, which is in very good agreement with the value obtained in the present experiment.

It is known that the Pu^{240} isotope and the Th^{232} isotope are members of the natural radioactive 4n series. The mass of the Th^{232} isotope has been measured previously.[7] To check the accuracy of the measurements and the consistency of the results, it is of interest to compare the difference in the masses of Pu^{240} and Th^{232} obtained by the mass-spectrographic method and the difference calculated from the energies of the α decays by which the isotope Pu^{240} is converted into Th^{232}, i.e., of the decays

$${}_{94}Pu^{240} \rightarrow {}_{92}U^{236} \rightarrow {}_{90}Th^{232}.$$

The total values of the decay energies Q and the value of the α-particle mass have been measured with sufficient reliability.[8,1] The values of the Pu^{240} and Th^{232} masses obtained by the mass-spectrographic method are completely unrelated to each other. They were measured from different doublets at different times. The value of the difference obtained by the mass-spectrographic method is $\Delta M\ (Pu^{240} - Th^{232}) = 8.018448 \pm 270$ amu. The analogous difference obtained with the aid of the Q-values for the α decays is $\Delta M = 8.018324 \pm 150$ amu. The difference between these two values is $\delta = 0.124 \pm 0.310$ mmu, i.e., almost one-third the error of measurement. This agreement in the results obtained by completely different methods indicates that the value found for the mass of the Pu^{240} isotope is sufficiently reliable.

---

[1] Demirkhanov, Gutkin, Dorokhov, and Rudenko, Атомная энергия (Atomic Energy) **2**, 21 (1956), Transl. J. Nuclear Energy **3**, 251 (1956).

[2] Demirkhanov, Gutkin, and Dorokhov, Атомная энергия (Atomic Energy) **6**, 544 (1957).

[3] J. R. Huizenga, Physica **21**, 410 (1955).

[4] Stanford, Duckworth, Hogg, and Geiger, Phys. Rev. **85**, 1039 (1052).

[5] Demirkhanov, Gutkin, and Dorokhov, Doklady Akad. Nauk SSSR **118**, 1103 (1958), Soviet Phys.-Doklady **3**, 141 (1958).

[6] Benson, Damerow, and Ries, Phys. Rev. **113**, 1105 (1958).

[7] Demirkhanov, Gutkin, and Dorokhov, Doklady Akad. Nauk SSSR **124**, 301 (1959), Soviet Phys.-Doklady **4**, 105 (1959).

[8] B. M. Foreman, Jr. and G. T. Seaborg, J. Inorg. Nuclear Chem. **7**, 305 (1958).

[9] Everling, König, Mattauch, and Wapstra, Preprint.

Translated by E. Marquit
172

SOVIET PHYSICS JETP VOLUME 13, NUMBER 4 OCTOBER, 1961

MAGNETOELECTRIC EFFECT IN CHROMIUM OXIDE

D. N. ASTROV

All-Union Institute for Physico-Technical and Radio-Engineering Measurements

Submitted to JETP editor November 29, 1960

J. Exptl. Theoret. Phys. (U.S.S.R.) 40, 1035-1041 (April, 1961)

The magnetization produced by an electric field in a Cr_2O_3 single crystal was investigated. The magnetization is proportional to the field, as predicted by theory.[2,3] The proportionality coefficient was measured to be 4.3×10^{-4} at 20° C. The magnetic moment along the threefold axis and the magnetic moment in the basal plane have opposite signs in the temperature range from 310° K to 80° K. Near the transition temperature the magnetic moment in the basal plane is well fitted by $\alpha_\perp \propto (T_N - T)^{1/2}$, in agreement with the theory of second-order phase transitions. The temperature dependence of the magnetic moment along the threefold axis is very complicated. Possible causes of the observed temperature dependence are discussed. A connection is established between the sign of the magnetic moment and the magnetic structure.

AN earlier communication[1] reported preliminary results of a study of the magnetoelectric effect in antiferromagnetic materials. It was established that when a single crystal of chromium oxide is placed in an electric field, it exhibits a magnetic moment proportional to the field. The possibility, in principle, of the occurrence of such an effect in substances with magnetic structure was first pointed out by Landau and Lifshitz.[2] Dzyaloshinskii, in a more detailed examination of this question, showed that at least one of the substances with known magnetic structure, namely, chromium oxide, ought to exhibit a magnetoelectric effect.

This conclusion was the result of an analysis of the behavior of the thermodynamic potential under all the symmetry transformations of the chromium oxide magnetic class. Dzyaloshinskii showed that the transformations of this class leave two expressions in the thermodynamic potential invariant; each is linear in **E** and **H** and the invariance corresponds to a linear relation between the inductions and field intensities in the substance:

$$D_{\|} = \varepsilon_{\|} E_{\|} + \alpha_{\|} H_{\|}, \qquad \mathbf{D}_\perp = \varepsilon_\perp \mathbf{E}_\perp + \alpha_\perp \mathbf{H}_\perp;$$

$$B_{\|} = \mu_{\|} H_{\|} + \alpha_{\|} E_{\|}, \qquad \mathbf{B}_\perp = \mu_\perp \mathbf{H}_\perp + \alpha_\perp \mathbf{E}_\perp. \tag{1}$$

The components marked $\|$ are directed along the crystal axis, those marked $\perp$ lie in the basal plane.

The present work gives the results of a more detailed investigation of the magnetoelectric effect in chromium oxide.

In reference 1, measurements were made on an irregularly shaped single crystal oriented arbitrarily relative to a highly inhomogeneous applied electric field. In order to show up the anistropy of the magnetoelectric effect and simplify the calculation of the internal field in the sample, the chromium oxide single crystal, grown by the Verneuil process,* was made spherical. The shaping of the single crystal was carried out with silicon carbide. A sample 6.4 ± 0.1 mm in diameter was oriented by means of an x-ray Laue pattern and was then attached to an appropriate holder with BF glue. The accuracy of orientation of the sample was 3 or 4 degrees.

Figure 1 shows the apparatus used to measure the exact value of $\alpha_{\|}$, the constant of proportionality between the magnetic moment and the electric field applied along the C_3 axis of the sample, 1. The magnetic moment thus produced was detected by an astatic pair of coils, 4; the output of the coils was fed through a symmetrizing transformer into an amplifier. The noise at the input of the circuit did not exceed 2×10^{-7}v. The measurements were carried out at 10^4 cps.

The special feature of the apparatus is that it makes possible a sufficiently uniform field in the sample. With this purpose, the diameter of the electrodes, 2, was made three times the diameter of the sample; the electrodes and the sample were placed in a teflon container, 3, filled with a liquid with dielectric constant as close as possible to 12,

---

*The author takes this opportunity to convey his gratitude to A. A. Popova of the Institute of Crystallography, who grew the single crystal.

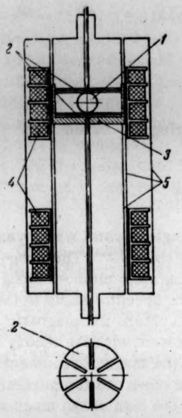

FIG. 1

the dielectric constant of chromium oxide,[4] in order that the electric field in the sample be uniform.

The majority of organic liquids with sufficiently high values of ϵ either strongly absorb moisture from the air (alcohols, acetone) and acquire an observable conductivity ($\geq 10^{-7}$) which makes them difficult to work with, or have a significantly frequency-dependent dielectric constant at room temperature (cresols), or, finally, mix poorly with nonpolar liquids with small ϵ (carbon tetrachloride, xylylols), thus making difficult the preparation of a mixture with the necessary value of the dielectric constant. The most suitable liquid proved to be dichlorethane, with a dielectric constant of 10.4 at 25° C.[5] Dichlorethane absorbs practically no moisture from the air and has a conductivity $\leq 5 \times 10^{-9}$ after double distillation. Because of the difference between the dielectric constants of chromium oxide and dichlorethane, the field in the sample is not perfectly uniform; its intensity is somewhat less than the field intensity between the electrodes.

Estimating the magnitude of the actual field in the sample is very complicated; a solution to the problem of the field distribution in a dielectric sphere pressed between two conducting planes has not been attained. One can only calculate that if the difference between the dielectric constants of the sphere, ϵ_i, and the medium, ϵ_e, is not large, the field inside the sphere will differ from a uniform field by a factor of order $(\epsilon_i - \epsilon_e)/\epsilon_i$.

In preparing the apparatus for determining an accurate value of $\alpha_{\parallel}$, steps were taken to avoid short-circuited loops in the electrostatic screens, 5, and to lessen the losses in the electrodes; the latter were two slit discs, one rotated through a small angle relative to the other, with electrical connections only at their centers.

In calculating the magnetic flux, one must take into account the fact that a significant fraction of the lines of magnetic induction from the sphere magnetized by the electric field are closed inside the detecting coil and give no contribution to the voltage produced on the coil. The magnetic flux outside the coil which contributes to the measured voltage is given by the formula

$$\Phi = 4\pi\nu \int_0^{l/2} \int_R^{\infty} H(\rho,\ z)\, \rho\, d\rho\, dz, \tag{2}$$

where $H(\rho, z)$ is the projection on the z axis (axis of the coil) of the magnetic field intensity at any point due to the magnetized sphere, and R, l, and ν are the radius, length, and number of turns per unit length of the detecting coil, respectively.

After evaluating the integral, we have

$$\Phi = (2\pi l \nu m/R)\,(1 + l^2/4R^2)^{-1/2}; \tag{3}$$

here m is the magnetic moment produced by the magnetoelectric effect in the sample.

The value of m can be calculated as follows. The connection between the field inductions and intensities in the magnetoelectric substance is given by Eqs. (1). For a dielectric sphere in an external electric field $\mathscr{E}_i$ and no external magnetic field, we have[2]

$$E_i = \frac{3\varepsilon_e}{2\varepsilon_e + \varepsilon_i}\mathscr{E}_i, \tag{4}$$

$$2H_i + B_i = 0. \tag{5}$$

By using Eq. (1), we obtain (for Cr_2O_3, $\mu_i \approx 1$)

$$B_i = \frac{2}{3}\alpha_i E_i = \frac{2\varepsilon_e \alpha_i}{2\varepsilon_e + \varepsilon_i}\mathscr{E}_i. \tag{6}$$

The magnetic moment of a sphere of radius a is

$$m = \frac{1}{4\pi}(B_i - H_i)\frac{4}{3}\pi a^3 = \alpha_i a^3 \frac{\varepsilon_e}{2\varepsilon_e + \varepsilon_i}\mathscr{E}_i. \tag{7}$$

Finally, for the induced flux we obtain

$$\Phi = 2\pi n \frac{\alpha_i \varepsilon_e}{2\varepsilon_e + \varepsilon_i}\frac{a^3}{R}\left(1 + \frac{l^2}{4R^2}\right)^{-1/2}\mathscr{E}_i, \tag{8}$$

where n is the number of turns on the detecting coil.

Since the amplification of the amplifier, the impedance and mutual inductance of the detecting coils, and the impedance of the symmetrizing transformer were all known, it was easy to compute the voltage produced on the detecting coil as a result of the magnetoelectric effect due to an applied field of known intensity, and from this the

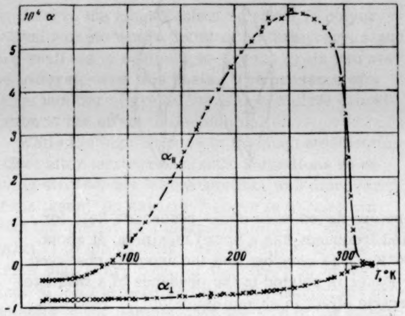

FIG. 2

constant $\alpha_\parallel$ characterizing the effect along the C_3 axis. The electric field intensity varied within the limits 1700 and 90 v/cm; $\alpha_\parallel$ did not vary within the experimental accuracy. The corresponding voltages on the detecting coil were about 6.6 and 0.35 μv.

The constant $\alpha_\parallel$ was measured to be 4.3×10^{-4} at 20° C. Curves giving the temperature dependence of $\alpha_\parallel$ and $\alpha_\perp$ were normalized to this value. These curves were measured in a separate apparatus which allowed the dependence of the coefficient α on the angle of rotation of the sample to be determined throughout the temperature interval from the antiferromagnetic transition point (310° K) to hydrogen temperature. This apparatus differed from that shown in Fig. 1 in that its basic detecting coil consisted of two identical parts separated by a distance of 10 mm. The sample was oriented perpendicular to the axis of these coils and placed in the electric field in such a way that it was possible to rotate it about any direction lying in the basal plane of the crystal. The apparatus was placed in a vacuum chamber in a Dewar flask with liquid nitrogen or hydrogen. The temperature was measured with a copper-constantan thermocouple and regulated with a heater. The electrical circuits were the same as those described above.

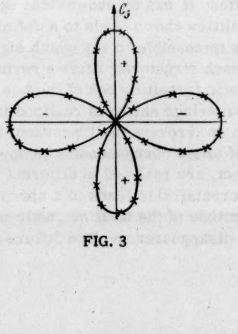

FIG. 3

Figure 2 shows the temperature dependence of the coefficients $\alpha_\parallel$ and $\alpha_\perp$. A preliminary measurement at room temperature established that the coefficient $\alpha_\perp$ is the same, within the experimental accuracy, for all directions lying in the basal plane of the crystal; the corresponding rotation curves were circles.

It should be noted that the curves given for the temperature dependence were obtained with the sample placed in a very nonuniform electric field. With the special apparatus we obtained rotation curves with the sample placed between electrodes whose dimensions were three times the diameter of the sample (and with the space between filled with dichlorethane) and established that at room temperature the rotation curves are the same in the uniform and in the nonuniform field. Figure 3 shows a typical rotation curve taken in the nonuniform field at the arbitrarily chosen temperature 103° K; the axis of rotation is perpendicular to the plane of the figure.

$\alpha_\perp$ has the temperature dependence characteristic of ferromagnetic susceptibilities near the Curie point. Near the transition the temperature dependence of $\alpha_\perp$ is well fitted by $\alpha_\perp \propto (T_N - T)^{1/2}$ with T_N the transition temperature. This is in agreement with the theory of second-order phase transitions (if we assume that the anisotropy constant is independent of temperature). The fit is shown graphically in Fig. 4, which shows the dependence of $\alpha_\perp^2$ on $T_N - T$. It is clear that $\alpha_\perp \propto (T_N - T)^{1/2}$ up to values of $T_N - T$ of about 80°.

The temperature dependence of $\alpha_\parallel$ is much more complex. $\alpha_\parallel$ has a broad maximum at about 250° K and then decreases with decreasing temperature; at 80° K it changes sign and then tends to a constant value. Near the transition temperature $\alpha_\parallel$ varies in a very complicated way, and we could not find a simple formula to fit its temperature dependence.

The causes of this temperature dependence of $\alpha_\parallel$ are still not clear. A possible hypothesis would be that the magnetic structure of chromium

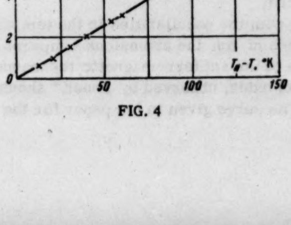

FIG. 4

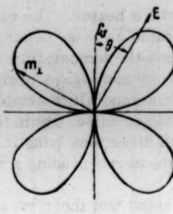

FIG. 5

oxide, determined by the measurements of Brockhouse[6] and McGuire et al.,[7,8] somehow changes with temperature and as a result of this change the spins of the magnetic ions have a non-zero projection on the basal plane. Then terms of the type $\alpha_1 E_X H_Y$, $\alpha_2 E_X H_Z$, etc. appear in the thermodynamic potential and Eq. (1), which describes the magnetoelectric effect when the spins are along the threefold axis, must be materially changed. For example, a component of the magnetic moment along one of the axes in the basal plane will arise from electric field components along the other two axes. Therefore, one should observe a magnetic moment in a direction perpendicular to the applied electric field, and the temperature dependence of the effect can be very complex.

An attempt was made to measure this "perpendicular" effect. Figure 5 shows the rotation curve obtained; the axis of rotation is perpendicular to the plane of the figure. It is clear that when the electric field vector lies in the basal plane the magnetic moment along the C_3 axis is zero. Correspondingly, when the field is along C_3, there is no moment in the basal plane. It is easy to see that such a diagram is obtained by using Eq. (1) for the component of the magnetic moment perpendicular to the applied electric field; this component is $\frac{1}{2}(\alpha_\perp - \alpha_\parallel)\sin 2\theta$, where θ is the angle between the electric field direction and the crystal axis. If the hypothesis about the change in magnetic structure were correct, then a non-zero magnetic moment in the basal plane should have been observed with the field applied along the crystal axis. Thus, the hypothesis that the magnetic structure of chromium oxide is incorrectly determined by the measurements of Brockhouse[6] and McGuire et al.[7,8] is not supported by the experiment and must be rejected.

Along with the peculiarities in the temperature dependence of $\alpha_\parallel$, the anomalous temperature dependence of the antiferromagnetic resonance in chromium oxide, observed by Foner,[9] should be noted. The curve given in his paper for the temperature dependence of the resonance field for fixed frequency has a broad maximum at about 250° K. It is possible that the anomaly observed by Foner is related to the presence of a magnetoelectric effect in chromium oxide.

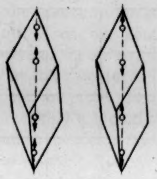

FIG. 6

From the curves, it is also clear that the signs of $\alpha_\parallel$ and $\alpha_\perp$ are different in the temperature range from 80° K to the antiferromagnetic transition. The signs of $\alpha_\parallel$ and $\alpha_\perp$ were fixed by measuring the phase difference between the voltage on the electrodes and the voltage at the output of the detecting amplifier. Moreover, it turned out that the sign of $\alpha_\parallel$, for example, can be negative as well as positive, i.e., the magnetic moment produced can be parallel or antiparallel to the applied field, while the magnitude of $\alpha_\parallel$ does not change, but, as mentioned above, the signs of $\alpha_\parallel$ and $\alpha_\perp$ always remain opposite. The sign of $\alpha_\parallel$ observed in any particular case depends on the history of the sample. If the sample is heated to a temperature above the transition point and then cooled slowly, the sign of $\alpha_\parallel$ can be positive or negative, and is independent of its value before the sample was heated. If the sample is cooled rapidly, so that the transition occurs as irreversibly as possible, the sign of $\alpha_\parallel$ is again arbitrary, but its magnitude is sharply decreased. The different signs of the magnetoelectric effect can be most naturally explained by the existence of two electrically equivalent possibilities for the spin orientations in the magnetic unit cell of chromium oxide, as shown in Fig. 6.

From the thermodynamic theory of the magnetoelectric effect it can be shown[2] that each of the two possibilities shown leads to a definite sign for α, but it is impossible to say which sign corresponds to each structure. After a reversible antiferromagnetic transition one of the two types of magnetic orderings shown is realized in the single crystal. In an irreversible transition, the different types of order corresponding to opposite signs for the effect, are realized in different regions of the single crystal; this leads to a sharp decrease in the magnitude of the total magnetic moment and even to its disappearance. The failure of attempts to observe the magnetoelectric effect in polycrystalline sample where definite, but arbitrary, signs are realized in each single-crystal grain can also be understood on this basis. The presence of a large number of grains leads to complete cancellation of the effect in the sample.

While the sign changes in the magnetoelectric effect after antiferromagnetic transitions were being studied, the following effect was discovered. If the transition described above is carried out with the sample in a magnetic field of about 500 oe parallel to the C_3 axis, then the effect has the same sign every time. If the direction of the applied field is reversed without changing the orientation of the sample, then the sign of the effect also reverses, and this same sign is obtained every time the sample is cooled below the transition point. At the same time, it is easy to see that both structures shown in Fig. 6 remain energetically equivalent in an external magnetic field. The above effect of the magnetic field on the magnetoelectric effect was verified in twenty trials with transitions in the sample.

In conclusion, the author takes this opportunity to convey his profound gratitude to Academician P. L. Kapitza and I. E. Dzyaloshinskii for their constant interest in this work and valuable direction, and also to A. S. Borovik-Romanov for appraising the results.

---

[1] D. N. Astrov, JETP **38**, 984 (1960), Soviet Phys. JETP **11**, 708 (1960).

[2] L. D. Landau and E. M. Lifshitz, Электродинамика сплошных сред, (Electrodynamics of Continuous Media), Gostekhizdat 1957.

[3] I. E. Dzyaloshinskii, JETP **37**, 881 (1959), Soviet Phys. JETP **10**, 628 (1960).

[4] A. Güntherschulze and F. Keller, Z. Physik **75**, 78 (1932).

[5] Weissberger, Proskauer, Riddik, and Tups, Organic Solvents, (Russian translation) IIL 1958.

[6] B. N. Brockhouse, J. Chem. Phys. **21**, 961 (1953).

[7] McGuire, Scott, and Gronmis, Phys. Rev. **98**, 1562 (1955).

[8] T. R. McGuire, Phys. Rev. **102**, 1000 (1956).

[9] S. Foner, J. Phys. radium **20**, 336 (1959).

Translated by M. Bolsterli
173

SOVIET PHYSICS JETP VOLUME 13, NUMBER 4 OCTOBER, 1961

INVESTIGATION OF THE SPECTRUM AND ASYMMETRY OF ELECTRONS FROM THE $\pi - \mu - e$ DECAY IN NUCLEAR EMULSION

A. O. VAĬSENBERG, V. A. SMIRNIT-SKIĬ, and É. D. KOLGANOVA

Submitted to JETP editor December 1, 1960

J. Exptl. Theoret. Phys. (U.S.S.R.) 40, 1042-1049 (April, 1961)

The energy spectrum and spatial asymmetry of positrons from the π^+-μ-e decay in nuclear emulsion placed in a magnetic field have been measured. The values obtained for the Michel parameter $\rho = 0.66 \pm 0.07$ and the asymmetry parameter $\delta = 0.63 \pm 0.12$ are in agreement with the theory of the two-component neutrino.

1. EXPERIMENTAL METHOD AND DATA

In this article, we present the results of the study of the energy spectrum of electrons produced in the π^+-μ-e decay in nuclear emulsion and the dependence of the spatial asymmetry of the electrons on their energy. Part of the data has been published earlier.[1,2]

The basic measurements were carried out on μ^+ mesons from π-μ-e decays occurring in emulsion. A small part of the measurements were made for μ^--e^- decays. The experiment was performed with stacks of 50 — 100 NIKFI-R emulsion pellicles $10 \times 10 \times 0.04$ cm or $10 \times 15 \times 0.04$ cm. The stacks were exposed to beams of π^+ or μ^- mesons from the Joint Institute for Nuclear Research proton synchrotron in Dubna. For the study of the decay asymmetry, the emulsion stacks were placed between the poles of an electromagnet in a field of 15 koe parallel to the plane of the pellicles. In the measurements without a magnetic field, the stacks were placed in a double magnetic shield in which the field was $<10^{-2}$ oe.[3] The stacks were developed with semi-automatic equipment described by Samoĭlovich et al.[4]

The decay-electron spectrum was measured by the multiple scattering method. The selection criteria for the electron tracks required that the track length be at least 1 mm and that the point of the $\mu - e$ decay occur at least 50 μ from the surface of the pellicle. Moreover, all the analyzed decays had to be at least 1 cm from the edge of the pellicle.

During the first phase of the experiment, the measurements were made on a practically "noiseless" microscope stage which had glass guides,[5] a turntable for rapid orientation of the track, and a microscope stage-feed screw with an electronic device for the automatic displacement of the track by an arbitrary cell length. This "noiseless" stage was coupled to a Lumipan microscope. During the second phase of the experiment, the measurements were carried out on a Koristka MS-2 microscope.

We determined the energy of the decay electrons with the aid of a semi-automatic device for scattering measurements, a description of which will be given below. The parameter by which we determined the electron energy with this device was the mean value of the absolute magnitude of the second (D_2) and third (D_3) differences of the track coordinates perpendicular to the direction of displacement of the measuring stage of the microscope. The semi-automatic measuring device "excluded without replacement" second differences whose absolute value exceeded $4\bar{D}_2$ and the related third differences independently of their magnitude.

The measurements were made twice by two observers. The data of both measurements were averaged. We eliminated the noise by means of the formula $D^2_{2\text{true}} = D^2_2 - \Delta^2_2$, where Δ_2 is the mean value of the second differences of the noise measured with great accuracy on electron tracks whose over-all length was ~ 4 cm. The values of the noise for the second differences were 0.19 and 0.24 μ for the measurements on the Koristka and Lumipan microscopes, respectively. The cell length for the measurements was chosen so that the signal-to-noise ratio for the third differences was within the limits of 2.4 — 4.5.

The transition from the second differences to the energy was effected by means of the formula

$$E\,[\text{Mev}] = K/\alpha\,[\text{deg}],$$

where α is the scattering angle, which is equal to $(D_2/t)(180/\pi)$, and K is the scattering constant. This constant depends on the cell length t (in microns) in the following way:[6]

Table I

	Experiment No.			
	1	2	3	4
Sign of μ meson	+	—	—	+
Magnetic field, oe	0	0	11000	17000
Number of particles in the spectrum	1102	302	302	1867

$$K = K_0 (0.272 \log 6.31\, t + 0.090)^{1/2}. \qquad (1)$$

We took $K_0 = 26.3 \pm 0.5$ deg-Mev-$(100\,\mu)^{-1}$ (see discussion below as regards the choice of the value of this constant). For steep tracks with a dip angle greater than 6° with respect to the plane of the emulsion, we introduced a correction for the track dip. For a comparison of the measured spectra with the theoretical spectra, the electron energy ϵ was expressed in fractions of the maximum energy which the electron could attain in the $\mu^+ - e^+$ decay: $\epsilon = E/52.8$ (E in Mev).

For the study of the decay asymmetry, it was necessary to measure the electron angular distributions in addition to their energy. This task was simplified by the fact that we measured the energy only for decay electrons emitted "forward" or "backward."[3] In the first case, the μ^+-meson and electron tracks made angles of $\gamma = 0 \pm 45°$ and $\beta = 0 \pm 45°$ or $\gamma = 180 \pm 45°$ and $\beta = 180 \pm 45°$, respectively, relative to the magnetic field direction. In the second case, the directions of flight of the μ^+ meson and electron were opposite to each other, i.e., $\gamma = 0 \pm 45°$ and $\beta = 180 \pm 45°$ or $\gamma = 180 \pm 45°$ and $\beta = 0 \pm 45°$. Such a choice of angles made it possible to use for the analysis of the dependence of the asymmetry on the energy the statistically most significant part of the angular distribution.

A summary of the experiments and the statistics is given in Table I. Experiments 3 and 4 were set up to observe the asymmetry for μ^- decays in emulsion and the possible effect of the magnetic field on the magnitude of this asymmetry.[7] Since the electron spectrum from μ^- decays in emulsion does not differ from the positron spectrum, these data were included in the total statistics.

Table II

Interval ϵ	Spectra		
	1	3+4	2
0—0.1	1	2	5(2)
0.1—0.2	14	10	28(19)
0.2—0.3	44	27	93(46)
0.3—0.4	76	45	142(72)
0.4—0.5	124	69	201(117)
0.5—0.6	150	76	261(144)
0.6—0.7	146	84	293(171)
0.7—0.8	178	114	251(156)
0.8—0.9	132	73	203(139)
0.9—1.0	93	35	152(99)
1.0—1.1	60	37	95(64)
1.1—1.2	37	13	62(48)
1.2—1.3	20	9	35(24)
1.3—1.4	10	6	19(15)
1.4—1.5	10	2	10(8)
1.5	7	2	17(15)
Number of particles	1102	604	1867(1139)

The obtained data are collected in Table II, where the spectra measured in experiments 1, 2 + 3, and 4 are given for the energy intervals $\Delta\epsilon = 0.1$. The last spectrum was obtained for positrons from 1867 decays in a strong magnetic field of 17 000 oe. The same spectrum was used for the measurement of the asymmetry parameter δ. For this spectrum, the number of positrons emitted "backward" are shown in the parentheses.

Figure 1 shows a histogram for the spectrum of positrons emitted "backward" and "forward."

2. COMPARISON OF THE RESULTS WITH THE THEORY

The theory of β decay with account of parity nonconservation gives the following expression for the spectrum and angular distribution of the electrons produced in the decay $\mu \rightarrow e + \nu + \bar{\nu}$:[8]

$$N(\varepsilon, \vartheta)\, d\varepsilon d\Omega = \{3(1-\varepsilon) + 2\rho\left(\tfrac{4}{3}\varepsilon - 1\right)$$
$$\pm \xi \cos\vartheta\,[(1-\varepsilon) + 2\delta\left(\tfrac{4}{3}\varepsilon - 1\right)]\}\, \varepsilon^2\, d\varepsilon\, d\Omega. \qquad (2)$$

This expression was obtained by neglecting the radiation effects and the electron mass in comparison with its momentum. The constants ξ, ρ, and δ are related to the interaction constants in a definite way. In particular, it is known from two-component theory that $\rho = \delta = 3/4$ and $|\xi| = |C_V C_A^* + C_A C_V^*| \times (|C_V^2| + |C_A^2|)^{-1}$, while in the theory of the universal Fermi interaction with coupling constants of equal absolute magnitude and opposite sign ($C_V = -C_A$) we have $\rho = \delta = 3/4$ and $|\xi| = 1$.

The aim of the measurements was to determine the parameters ξ, ρ, and δ. The value of the

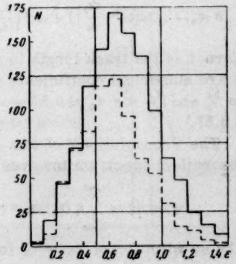

FIG. 1. Energy spectrum of positrons emitted backward (solid line) and forward (dotted line) in $\pi-\mu-e$ decays.

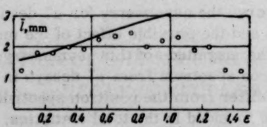

FIG. 2. Dependence of the mean track length in emulsion on the positron energy in the $\mu^+ - e^+$ decay. The solid curve is the calculated distribution of mean lengths; the circles represent the experimental data

parameter ξ for nuclear emulsion and its dependence on the magnetic field has been discussed previously.[3] It was shown that, for the NIKFI-R emulsion employed by us, the limiting value of the coefficient ξ obtained in a field of 17 000 oe is equal to $|\xi| = 0.85 \pm 0.05$.

In the present work, we determined the parameters ρ and δ. For a statistical estimate of these parameters by the χ^2 method, it is necessary to calculate the integrals

$$\Phi(\varepsilon)\,d\varepsilon = d\varepsilon \int \varphi(\varepsilon')\,\Gamma(\varepsilon', \varepsilon)\,d\varepsilon', \tag{3}$$

which result from "convolution" of the initial theoretical function with the "instrument function" $\Gamma(\epsilon', \epsilon)$ giving the probability of obtaining an energy ϵ from a measurement of a true energy ϵ'.

A similar "spreading" of the initial spectra in our measurements resulted from two basic factors: radiative slowing down of electrons in emulsion and dispersion of the scattering measurements.[9] The radiation length in emulsion is close to 29 mm, and although the lengths of a large part of the electron tracks lay within the limits of 1 — 3 mm, the distortion of the spectral shape due to bremsstrahlung proved to be important in the high-energy region, at the end of the electron spectrum. The loss of energy by the electrons due to bremsstrahlung in emulsion is described by the Bethe-Heitler formula[10] giving the probability that an electron with an initial energy ϵ_0 has, after traversing a layer t, an energy in the interval ϵ_t, $\epsilon_t + d\epsilon_t$:

$$\pi(\varepsilon_0, \varepsilon_t, t)\,d\varepsilon_t = \frac{d\varepsilon_t}{\varepsilon_0}(1+a)^{bt}\left(\frac{\varepsilon_t}{\varepsilon_0}\right)^a \frac{[\ln(\varepsilon_0/\varepsilon_t)]^{bt-1}}{(bt-1)!}. \tag{4}$$

Here t is the track length in radiation units; a and b are numerical coefficients equal, respectively, to $\frac{2}{5}$ and $\frac{4}{3}$ for $\epsilon_0 \leq 0.57$ and $\frac{1}{4}$ and $\frac{4}{3}$ for $\epsilon_0 > 0.57$.

The "convolution" of this expression with the theoretical spectrum involves finding the function

$$\varphi^*(\varepsilon)\,d\varepsilon = \int_{\varepsilon_0=\varepsilon}^{\varepsilon_0=1} \varphi(\varepsilon_0)\,d\varepsilon_0\,\pi(\varepsilon_0, 2\varepsilon - \varepsilon_0, t). \tag{5}$$

The substitution of $2\epsilon - \epsilon_0$ for ϵ_t in the integration is connected with that fact that in the measurements by the multiple scattering method, we actually measure the mean energy $\epsilon = (\epsilon_t + \epsilon_0)/2$.

In "convolution" of the theoretical spectrum with this expression for the energy of an electron traversing a layer of substance t, one should keep in mind the fact that the mean track length of the electrons, owing to what is known as the "flat stack effect" is different for different parts of the spectrum. This is illustrated in Fig. 2, where the mean length of the electron tracks is laid off along the ordinate axis and the measured value of the energy, along the abscissa axis. On the basis of these data, we divided the region of integration into five intervals ($\Delta\epsilon$ = 0—0.2, 0.2—0.4, 0.4—0.6, 0.6—0.8, and 0.8—1.0) taking the mean value of t for each interval from Fig. 2.

The functions obtained for $\varphi^*(\epsilon)$ are subject to a second "convolution" with distributions characterizing the scattering measurements. It is well known that the second differences in scattering measurements have a Gaussian distribution.[6] The necessity of measuring the entire spectrum with a constant signal-to-noise ratio leads to an increase in the dispersion of the scattering measurements as one goes from the beginning of the spectrum to the end. In this connection, we divided the spectrum into five intervals coinciding with those mentioned above, and we constructed the instrument function for each interval:

$$\Gamma_j(\varepsilon, \bar{\varepsilon}) = \sum w(n_i)\frac{\bar{\varepsilon}}{\varepsilon^2}\frac{\sqrt{n_i}}{\lambda\sqrt{2\pi}}\exp\left[-\frac{n_i}{2\lambda^2}\left(\frac{\varepsilon-\bar{\varepsilon}}{\varepsilon}\right)^2\right]. \tag{6}$$

Here $w(n_i)$ is the relative number of tracks measured with a division into n_i cells; λ is the dispersion parameter, which is equal to the coefficient of $1/\sqrt{n}$ in the expression for the relative error of the measurements: $\Delta D_2/D_2 = \lambda/\sqrt{n}$.

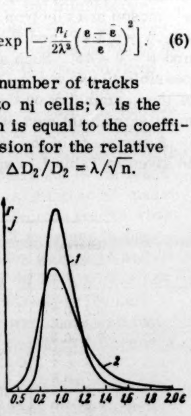

FIG. 3. The functions Γ_j for the beginning (1) and end (2) of the spectrum.

Figure 3 shows examples of the function Γ_j for the intervals $\Delta\epsilon$ = 0—0.2 and 0.8—1.0 with λ = 0.95.

The value of the parameter λ depends on the signal-to-noise ratio, and, under our conditions of measurement, its expected value[6] lies in the limits 0.8—1.0 for the second differences.

Constructing for each interval j the functions Γ_j, we carry out the second "convolution" according to the formula

$$\varphi^{**}(\varepsilon)=\int\limits_{0}^{\bar{\varepsilon}=1}\varphi_i^{*}(\bar{\varepsilon})\,d\bar{\varepsilon}\,\Gamma(\varepsilon,\ \bar{\varepsilon}), \qquad (7)$$

by using for each interval of integration over the limits $\bar{\epsilon}=0-1$ the corresponding function Γ_j. The bulk of these calculations was performed on an electronic computer.

As a result of the double "convolution" of the theoretical spectra and the instrument function, the obtained spectra $\varphi^{**}(\epsilon)$, with which the experimental data should be compared for the estimate of the parameters ρ and δ, proved to depend not only on the estimated parameters, but also on the parameters determining the measurements, especially on the quantity λ.

On the other hand, the form of the experimentally obtained spectrum depends on the choice of the scattering constant K. The parameters ρ and δ estimated from the minimum value of the χ^2 sum will therefore depend on the values chosen for λ and K.

In accordance with the general ideas underlying the statistical methods of estimating parameters, the "best fit" to the experimental data is the spectrum which gives the minimum value of χ^2 for the variation of the three parameters λ, K, and ρ. This means that we seek values of these parameters which satisfy the equation

$$\partial\chi^2/\partial K=\partial\chi^2/\partial\lambda=\partial\chi^2/\partial\rho=0.$$

We estimated the parameters ρ and δ by the following procedure. Considering a small change of the parameters K and λ and varying the parameter ρ in the interval 0.4—0.8 for each pair of values of K and λ, we found the values of K and λ for the absolute minimum $\chi^2_{\min}$. In the analysis, we considered the values $K=K_0(1+\eta)$, where $\eta=-0.03$, 0.00, 0.02, 0.04 and $\lambda=0.7$, 0.8, 0.9, 1.0, 1.1, 1.2. The exact values of $\chi^2_{\min}$ were found by quadratic extrapolation. Obtaining in this way the optimum values of K and λ, we determined ρ. For the analysis of the parameters K, λ, and ρ, we first used the spectrum for 3581 particles (Table II), where we divided it into nine intervals: $\Delta\epsilon=0.4-0.5$, $0.5-0.6$, $0.6-0.7$, $0.7-0.8$, $0.8-0.9$, $0.9-1.0$, $1.0-1.1$, $1.1-1.2$, $1.2-1.5$.

Figure 4 represents the dependence of the value of $\chi^2_{\min}$ on the value of K. In accordance with this estimate, we take for the quantity K_0 in formula (1) the value corresponding to the minimum of K_0, i.e., $K_0=26.3\pm0.4$, where the error corresponds to the deviation of the function χ^2 to a value exceeding that at the minimum by $\pm\sqrt{2p}$ (p is the number of degrees of freedom), i.e., to the value 9. The obtained value of K_0 is in agreement, within the limits of the measurement error, with the values of K_0 obtained in calibration measurements reported in the literature.[6]

In a similar way, we obtained for the quantity λ the value $\lambda=0.97\pm0.07$. This value is 5—10% higher than that following from the relations usually employed.[6] The difference can be accounted for by the additional dispersion due to the radiation losses and the device for the scattering measurements.

It should be noted that the choice of the quantity λ is not as important as the choice of K; for a given K, the quantity ρ is practically independent of λ, while the dependence of ρ on K is very strong: $\partial\rho/\partial K\approx0.18$.

Figure 5 shows the results of the statistical analysis of the values of the parameter ρ determined from the χ^2 test for the values of the parameters K and λ indicated above. The analysis was made for the total spectrum obtained with 3580 particles. Since radiative corrections to the spectrum[11,12] and the corrections for the "flat stack effect" are appreciable at the beginning of

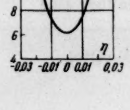

FIG. 4. Dependence of the value of $\chi^2_{\min}$ on the scattering constant $K=K_0(1+\eta)$.

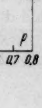

FIG. 5. Dependence of the value of χ^2 on the Michel parameter ρ for the positron spectrum.

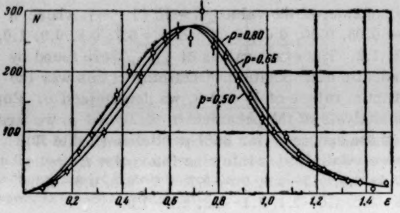

FIG. 6. Positron spectrum (3580 particles).

the spectrum, the analysis was begun with $\epsilon = 0.4$. The spectrum was split up into intervals of width $\Delta\epsilon = 0.05$ and extended to $\epsilon = 1.5$, which corresponds to twenty-two degrees of freedom. The minimum value of χ^2 in this figure corresponds to $\rho = 0.64$, which is also the estimate of this parameter from our data.

For the estimate of the error, we used the error formula

$$\sigma_\rho^2 = \sigma_{\text{st}}^2 + (\partial\rho/\partial K)\,\sigma_K^2 + (\partial\rho/\partial\lambda)^2\sigma_\lambda^2,$$

where the first term is the statistical error in the determination of ρ, and the second and third terms are the errors due to the uncertainty in the values of the constants K and λ. Our analysis indicates that the last error can be neglected in comparison with the first two. The statistical error in the determination of ρ was equal to 0.03. The basic error results from the uncertainty in the scattering constant. This was equal to $0.18 \times 0.4 = 0.07$. We finally obtain

$$\rho = 0.64 \pm 0.10.$$

This value of the parameter ρ is in agreement, within the limits of experimental error, with the values of ρ obtained by the emulsion technique[9] and by other methods.[13] The estimate given above of the parameter ρ was made without taking into account the radiative corrections. The introduction of the radiative corrections to the spectrum[11,12] in a manner similar to that used by Rosenson[14] and Dudziak et al.[15] shifts the effective value of ρ from 0.64 to 0.66, without affecting the error estimate.

Figure 6 shows the positron spectrum. The solid curves represent the theoretical spectrum for $\rho = 0.50$, 0.65, and 0.80 broadened by bremsstrahlung and the instrument error.

For an estimate of the parameter δ, we used the spectrum of the "forward-backward" difference shown in Fig. 1. As follows from formula (2), this difference is independent of the quantity ρ.

In order to obtain the theoretical spectral distribution of the difference, we should bear in mind the fact that in our case we have an almost "flat" geometry. If in (2) we replace $\cos\vartheta$ by $\cos\gamma\cos\beta$ and $d\Omega$ by $d\gamma\, d\beta$ and integrate over intervals of angles γ and β which were used [see formula (2)], we obtain

$$n(\varepsilon)\,d\varepsilon = \frac{32N\xi}{\pi^2}\left\{(1-\varepsilon) + 2\delta\left(\frac{4}{3}\varepsilon - 1\right)\right\}\varepsilon^2 d\varepsilon \cdot 0.975. \quad (8)$$

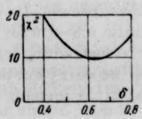

FIG. 7. Dependence of the quantity χ^2 on the parameter δ for the positron spectrum (from 1867 cases).

The coefficient 0.975 in this formula takes into account the deviation of our geometry from a "flat" geometry. The difference expected from this formula is 411 particles (for $|\xi| = 0.85$), while the number observed in the spectrum was 417.

Carrying out the above-described "convolution" operation for the spectrum (8), we obtain a family of curves with the parameter δ. The "best value" of the parameter δ was determined by the χ^2 test, where the quantity χ^2 was defined by the formula[16]

$$\chi^2 = \sum (N_{bi} - p_i N_i)^2 / N_i p_i (1 - p_i).$$

In this formula, N_i and N_{bi} are the total number of particles and the number of particles emitted backward, respectively, for the i-th interval and p_i and $(1 - p_i)$ are the theoretical probabilities of the emission of electrons "backward" and "forward," respectively, calculated from the "convolution" spectra for the value $\rho = 0.66$. Owing to the presence of the coefficients p_i and $(1 - p_i)$, the quantity ρ indirectly affects the value of δ.

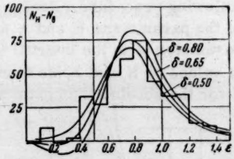

FIG. 8. Dependence of the asymmetry on the positron energy in the $\mu^+ - e^+$ decay.

A plot of the dependence of χ^2 on δ is shown in Fig. 7. It follows from this plot that the "best" value of δ is $\delta = 0.63$. In Fig. 8, the solid curves represent the energy dependence of the asymmetry corresponding to this value of δ and the values $\delta = 0.8$ and 0.5. To estimate the error in the value $\delta = 0.63$, we start from the formula

$$\sigma^2(\delta) = \sigma_{\text{st}}^2 + (\partial\delta/\partial K)^2\sigma_K^2 + (\partial\delta/\partial\rho)^2\sigma_\rho^2 + (\partial\delta/\partial\xi)^2\sigma_\xi^2.$$

The statistical error of this estimate is 0.08. The errors due to the uncertainty in the determination of the constants K and ρ are equal, respectively, to 0.07 and 0.08. The last term can be neglected. We finally obtain

$$\delta = 0.63 \pm 0.13.$$

This value is in agreement with the determinations of δ made by other methods.[13,17] The radiative corrections, which are important at the beginning of the spectrum, have practically no effect on this estimate.[18]

3. CONCLUSIONS

The measurements made in this and in the previous experiments give the following values for the parameters of $\mu - e$ decays in emulsion: $|\xi| = -0.85 \pm 0.05$, $\rho = 0.66 \pm 0.07$, $\delta = 0.63 \pm 0.12$. As was indicated earlier,[3] the deviation of $|\xi|$ from the value $|\xi| = 1$ predicted by the V-A variant of the theory is far beyond the limits of error, but can be attributed to the presence of an additional depolarization mechanism not eliminated by the magnetic field. The values of the Michel parameter ρ and of the asymmetry parameter δ proved to be less than the value 0.75 predicted by the two-component theory without the radiative corrections. It should be borne in mind, however, that the method of measuring the particle energy from its multiple scattering has, in general, a tendency to give a lowered value of the energy. This leads to a decrease in the values of ρ and δ obtained experimentally. Moreover, a source of a systematic shift in the values can be the incomplete correspondence between the "convolution" operations and the actual conditions of measurement. Therefore the results obtained by us should be considered to be in agreement with the two-component neutrino theory.

The authors thank A. I. Alikhanov for his interest in this work. The authors also thank the scanning staff for scanning a large number of pellicles and for making difficult measurements, and O. N. Vasil'ev for performing the calculations on the electronic computer.

---

[1] Vaĭsenberg, Smirnit-skii, Kolganova, and Rabin, JETP **37**, 326 (1959), Soviet Phys. JETP **10**, 231 (1960).

[2] A. O. Vaĭsenberg, JETP **37**, 566 (1959), Soviet Phys. JETP **10**, 401 (1960).

[3] A. O. Vaĭsenberg and V. A. Smirnit-skii, JETP **39**, 242 (1960), Soviet Phys. JETP **12**, 175 (1961).

[4] Samoĭlovich, Smirnit-skii, Sukhov, Ryabov, and Rulev, Приборы и техника эксперимента (Instruments and Measurement Techniques) No. 4, 58 (1959).

[5] Vaĭsenberg, Smirnit-skii, and Rabin, ibid. No. 2, 112 (1957).

[6] Bonetti, Dilworth, and Scarsi, Nuclear Emulsions, London, 1958.

[7] Vaĭsenberg, Kolganova, and Smirnit-skii, JETP 39, 1198 (1960), Soviet Phys. JETP **12**, 834 (1961).

[8] C. Bouchiat and L. Michel, Phys. Rev. **106**, 170 (1957).

[9] Bonetti, Levi-Setti, Panetti, and Rossi, Nuovo cimento **3**, 33 (1956).

[10] L. Eyges, Phys. Rev. **76**, 264 (1949).

[11] T. Kinoshita and A. Sirlin, Phys. Rev. **113**, 1652 (1959).

[12] S. M. Berman, Phys. Rev. **112**, 267 (1958).

[13] R. Plano, Phys. Rev. **119**, 1400 (1960).

[14] L. Rosenson, Phys. Rev. **109**, 958 (1958).

[15] Dudziak, Sagane, and Vedder, Phys. Rev. **114**, 336 (1959).

[16] H. Cramer, Mathematical Methods of Statistics, Princeton, 1946.

[17] Larsen, Lubkin, and Tausner, Phys. Rev. **107**, 856 (1957).

[18] A. O. Vaĭsenberg, Usp. Fiz. Nauk **70**, 429 (1960), Soviet Phys. Uspekhi **3**, 195 (1960).

Translated by E. Marquit
174

SOVIET PHYSICS JETP VOLUME 13, NUMBER 4 OCTOBER, 1961

ON THE KINETIC THEORY OF SHOCK WAVES

G. Ya. LYUBARSKII

Physico-Technical Institute, Academy of Sciences, Ukrainian S.S.R.

Submitted to JETP editor February 13, 1960

J. Exptl. Theoret. Phys. (U.S.S.R.) 40, 1050-1057 (April, 1961)

The structure of a low-intensity shock wave in a monatomic gas is obtained at large distances from the wave front. The calculation is based on a kinetic equation with a simplified collision integral containing a constant collision time. It is shown that in this case various physical quantities approach their limiting values at infinity with a slower rate than in the hydrodynamic theory. Therefore, if the kinetic equation is replaced by a finite system of ordinary differential equations it is impossible in principle to obtain the correct asymptotic solutions of the kinetic equation.

1. INTRODUCTION

THE problem of the structure of the shock waves in a liquid and in a gas has been the subject of a large number of papers. However, as far as the author knows, not one of these papers is devoted to the investigation of the structure of the shock wave at large distances from the wave front (disregarding those calculations of the asymptotic values in which the structure of the shock wave is not taken into account). The reason for this is to be found in the circumstance that in these papers the kinetic equation is replaced by a finite system of ordinary differential equations. In the paper by Becker,[1] this system is the Navier-Stokes equation with account of the heat conductivity. Zoller,[2] using the method of Burnett,[3] wrote down a system of seven differential equations and investigated its properties. Grad,[4] by modifying the method of Burnett, derived a different system of differential equations and used it for the study of the shock waves.

Many other papers differ from the work of Becker, Zoller, and Grad either in that certain simplifying assumptions are introduced or in that they concentrate on the quantitative aspects of the problem or on the numerical solution of the basic system of differential equations.

The above-mentioned authors do not in any way attempt to simplify the collision integral in the kinetic equation. To the contrary, they try to write down the most accurate form possible. However, when the transition from the kinetic equation to the system of differential equations is made, only the coefficients of the equation depend on the form of the collision integral, so that the over-all picture changes only quantitatively when the form of the collision integral is altered.

The paper of Mott-Smith,[5] which stands by itself, also contains no answer to the problem of the asymptotic form of the shock wave, since it is not clear what is the character of the approximations underlying this work.

The aim of the present paper is the determination of the correct form of the asymptotic shock wave on the basis of the simplest kinetic equation, in which the collision integral is written in the radically simplified form (2.1). It will be shown that the hydrodynamic quantities approach their limiting values at great distances from the front of the shock wave as $C_1 \exp\{-C_2|x|^{2/3}\}$ (C_1 and C_2 are certain constant coefficients). On the other hand, the solutions of the ordinary differential equations obtained in references 1, 2, and 4 approach their limiting values exponentially. This fact demonstrates that the replacement of the kinetic equation by a system of differential equations always leads to incorrect asymptotic values.

It is easy to see what the reason for this situation is. At large distances from the wave front, where all hydrodynamic quantities are close to their limiting values, one can linearize the differential equations. In this case the way in which the solution approaches its limiting value is determined by the smallest characteristic denominator. In going from one approximation to the next, the system of differential equations is changed, and in general the smallest characteristic denominator is changed, too. If the characteristic denominators obtained in this way go to zero, no approximation gives the correct asymptotic values. The asymptotic form derived in the present paper shows that this is indeed the case.

2. FORMULATION OF THE PROBLEM

In the present paper we consider the structure of a low intensity shock wave on the basis of the kinetic equation with collision integral. The latter is written in the form

$$J = (f_0 - f)/\tau, \tag{2.1}$$

where $f = f(x, \mathbf{v})$ is the distribution function (the x axis is directed along the direction of motion of the liquid perpendicular to the wave front), τ is the relaxation time, which is assumed constant, and $f_0(x, \mathbf{v})$ is the Maxwell distribution function,

$$f_0(x, \mathbf{v}) = \left[\frac{m}{2\pi kT(x)}\right]^{3/2} n(x) \exp\left[-m\frac{(v_x - u_x)^2 + v_y^2 + v_z^2}{2kT(x)}\right], \tag{2.2}$$

corresponding at every point to the average density $n(x)$, velocity $u(x)$, and energy $\frac{3}{2}n(x)kT(x)$:

$$n(x) = \int f(x, \mathbf{v})\, d\mathbf{v}, \qquad n(x)u(x) = \int v_x f(x, \mathbf{v})\, d\mathbf{v},$$
$$\frac{3}{2} n(x)\, kT(x) = \int \frac{m}{2}\left[(v_x - u(x))^2 + v_y^2 + v_z^2\right] f(x, \mathbf{v})\, d\mathbf{v}. \tag{2.3}$$

This form of the collision integral automatically ensures the fulfillment of the conservation laws for the number of particles, momentum, and energy in the use of the kinetic equation. On the other hand, if the deviation of the distribution function $f(x, \mathbf{v})$ from the Maxwellian form is small, the error caused by the replacement of the exact collision integral by the expression (2.1) is insignificant.

The relations (2.3) together with the kinetic equation

$$v_x \partial f/\partial x = \frac{1}{\tau}(f_0 - f) \tag{2.4}$$

form a system of four equations with the four unknown functions f, n, u, and T. To this we must add the boundary conditions. For a shock wave, these conditions are that as $x \to \pm\infty$ the functions $n(x)$, $u(x)$, and $T(x)$ approach certain limits which we denote by $n_\pm$, $u_\pm$, and $T_\pm$. The distribution function f approaches the Maxwell function.

The system (2.3), (2.4) can be solved by making use of the smallness of the relative discontinuities

$$\varepsilon_1 = (n_+ - n_-)/n_-, \qquad \varepsilon_2 = (u_+ - u_-)/u_-,$$
$$\varepsilon_3 = (T_+ - T_-)/T_-. \tag{2.5}$$

Here it turns out that the results obtained for small distances from the wave front [$x \sim u_-\tau\epsilon^{-1}$; see formula (6.4)] are in agreement with the results of hydrodynamic theory with account of the coefficients of viscosity and heat conductivity. At distances much larger than $u_-\tau\epsilon^{-1}$, the kinetic approach [see formula (7.4)] leads to the conclusion that the hydrodynamic quantities approach their limiting values at a slower rate than in the hydrodynamic theory. This fact is explained physically by the presence of fast particles which penetrate to large distances from the wave front with almost no collisions. It is clear, therefore, that the structure of the shock wave far away from its front is determined by the dependence of the relaxation time τ on the velocity at large velocities. It appears that the hydrodynamic theory predicts correctly only the structure of the steepest part of a low intensity shock wave.

3. DERIVATION OF THE BASIC SYSTEM OF INTEGRAL EQUATIONS

The formal solution of the kinetic equation (2.4) has the form

$$f(x, \mathbf{v}) = \frac{1}{\tau v_x}\int_{-S_{v_x}}^{x} f_0(\xi, \mathbf{v}) \exp\left[\frac{\xi - x}{\tau v_x}\right] d\xi, \tag{3.1}$$

where $S_{v_x} \equiv \infty \operatorname{sgn} v_x$: $S_{v_x} = +\infty$ if $v_x > 0$, and $S_{v_x} = -\infty$ if $v_x < 0$.

Using (3.1), we can eliminate f from the equations (2.3). Introducing the dimensionless variables

$$n' = n/n_-, \qquad T' = T/T_-,$$
$$u' = u/u_-, \qquad x' = x/\tau u_-, \tag{3.2}$$

we obtain the basic system of nonlinear integral equations

$$n'(x') = \sqrt{\frac{\alpha}{\pi}}\int_{-\infty}^{\infty} dv \int_{-S_v}^{x'} \frac{n'(\xi)}{\sqrt{T'(\xi)}}\frac{1}{v}\exp\left[\frac{\xi - x'}{v} - \alpha\frac{(v - u'(\xi))^2}{T'(\xi)}\right] d\xi,$$

$$n'(x')\,u'(x') = \sqrt{\frac{\alpha}{\pi}}\int_{-\infty}^{\infty} dv \int_{-S_v}^{x'} \frac{n'(\xi)}{\sqrt{T'(\xi)}}\exp\left[\frac{\xi - x'}{v} - \alpha\frac{(v - u'(\xi))^2}{T'(\xi)}\right] d\xi,$$

$$\frac{3}{2\alpha} n'(x')\,T'(x') + n'(x')\,u'^2(x')$$
$$= \sqrt{\frac{\alpha}{\pi}}\int_{-\infty}^{\infty} dv \int_{-S_v}^{x'} \frac{n'(\xi)}{\sqrt{T'(\xi)}}\, v \exp\left[\frac{\xi - x'}{v} - \alpha\frac{(v - u'(\xi))^2}{T'(\xi)}\right] d\xi$$
$$+ \frac{1}{\sqrt{\alpha\pi}}\int_{-\infty}^{\infty} dv \int_{-S_v}^{x'} n'(\xi)\sqrt{T'(\xi)}\,\frac{1}{v}\exp\left[\frac{\xi - x'}{v} - \alpha\frac{(v - u'(\xi))^2}{T'(\xi)}\right] d\xi, \quad \alpha = \frac{mu_-^2}{2kT_-}. \tag{3.3}$$

The system (3.3) must be supplemented by the boundary conditions

$$n'(-\infty) = 1, \quad u'(-\infty) = 1, \quad T'(-\infty) = 1;$$
$$n'(+\infty) = 1 + \varepsilon_1, \quad u'(+\infty) = 1 + \varepsilon_2,$$
$$T'(+\infty) = 1 + \varepsilon_3. \tag{3.4}$$

The relaxation time τ does not enter in the relations (3.3) and (3.4). Therefore, it determines only the scale.

It is easily shown that the discontinuities ϵ_1, ϵ_2, and ϵ_3 must satisfy the well-known relations of shock wave theory in order that the system (3.3) with the conditions (3.4) be soluble. We shall therefore regard all discontinuities as known in the following.

4. THE CASE OF LOW-INTENSITY SHOCK WAVES ($\epsilon_j \ll 1$)

The basic system (3.3) is conveniently rewritten in the form

$$\varphi_i\,[y(x), \alpha] = \int_{-\infty}^{\infty} K_i(x-\xi,\ y(\xi),\ \alpha)\,d\xi, \qquad i = 1, 2, 3, \tag{4.1}$$

where

$$y = \{y_1,\ y_2,\ y_3\}, \qquad y_1 = n', \qquad y_2 = u', \qquad y_3 = T';$$
$$\varphi_1 = y_1, \qquad \varphi_2 = y_1y_2, \qquad \varphi_3 = (3/2\alpha)\,y_1y_3 + y_1y_2^2;$$
$$K_1(x, y, \alpha) = \sqrt{\frac{\alpha}{\pi}}\,y_1y_3^{-1/2}\int_0^{S_x}\exp\left[-\frac{x}{v}-\alpha\frac{(v-y_2)^2}{y_3}\right]\frac{dv}{v},$$
$$K_2(x, y, \alpha) = \sqrt{\frac{\alpha}{\pi}}\,y_1y_3^{-1/2}\int_0^{S_x}\exp\left[-\frac{x}{v}-\alpha\frac{(v-y_2)^2}{y_3}\right]dv,$$
$$K_3(x, y, \alpha) = \frac{1}{\sqrt{\pi}}\int_0^{S_x} y_1\left(\sqrt{\frac{\alpha}{y_3}}\,v + \sqrt{\frac{y_3}{\alpha}}\,\frac{1}{v}\right)\exp\left[-\frac{x}{v}-\alpha\frac{(v-y_2)^2}{y_3}\right]dv.$$

Our aim is the solution of this system of integral equations with the assumption that the discontinuities $\epsilon_j \ll 1$. For this purpose we carry out the following transformations. We set

$$y_j(x) = 1 + \varepsilon_j\,\theta(x) + \varepsilon_j\mu_j(x); \quad \theta(x) = 1,$$
$$x > 0; \quad \theta(x) = 0, \ x < 0$$

It is easily seen that the functions $\mu_j(x)$ do not exceed unity in order of magnitude and go to zero as $x \to \pm\infty$.

Let us expand both sides of (4.1) in powers of ϵ_j and discard all terms containing ϵ_j in third or higher order. The resulting relations are then Fourier-transformed. We shall use the notation

$$\bar{\mu}_j(k) = \int_{-\infty}^{\infty}\mu_j(x)\,e^{ikx}\,dx, \qquad \overline{\mu_j^+}(k) = \int_0^{\infty}\mu_j(x)\,e^{ikx}\,dx,$$

$$\overline{\mu_j^-}(k) = \bar{\mu}_j(k) - \bar{\mu}_j^+(k),$$

$$\bar{\mu}_{jl}(k) = \int_{-\infty}^{\infty}\mu_j(x)\,\mu_l(x)\,e^{ikx}\,dx, \quad \overline{\mu_{jl}^+}(k) = \int_0^{\infty}\mu_j(x)\,\mu_l(x)e^{ikx}\,dx.$$

We solve the resultant system of equations with respect to $\bar{\mu}_j(k)$ by expressing the latter in terms of the $\bar{\mu}_{jl}(k)$. We find

$$\varepsilon_\gamma\bar{\mu}_\gamma(k) \doteq \frac{1}{ik}\left\{\varepsilon_\gamma + \frac{1}{2D(k,\alpha)}\sum \varepsilon_j\,\varepsilon_l\,B_{jl\gamma}(k)\right\}$$
$$-\frac{1}{D(k,a)}\sum_{j,l}\varepsilon_j\,\varepsilon_l\,\overline{\mu_j^+}(k)\,B_{jl\gamma}(k)$$
$$-\frac{1}{2D(k,\alpha)}\sum_{j,l}\bar{\mu}_{jl}(k)\,B_{jl\gamma}(k), \tag{4.2}$$

where the functions $B_{jl\gamma}(k)$ and $D(k, \alpha)$ are constructed in the following way. Let us introduce the notation

$$K_{ij}(x, y, \alpha) = \frac{\partial}{\partial y_j}K_i(x, y, \alpha),$$
$$K_{ijl}(x, y, \alpha) = \frac{\partial^2}{\partial y_l\,\partial y_l}K_i(x, y, \alpha),$$
$$G_{ij}(k, \alpha) = \int_{-\infty}^{\infty}K_{ij}(x, 1, \alpha)\,e^{ikx}\,dx,$$
$$G_{ijl}(k, \alpha) = \int_{-\infty}^{\infty}K_{ijl}(x, 1, \alpha)\,e^{ikx}\,dx,$$
$$D(k, \alpha) = \det\left|\frac{G_{ij}(k, \alpha) - G_{ij}(0, \alpha)}{ik}\right|. \tag{4.3}$$

We denote the minors of this determinant by $A_{ij}(k, \alpha)$. Furthermore,

$$B_{jl\gamma}(k) = \sum_m A_{m\gamma}(k, \alpha_0)\,\frac{G_{mjl}(k, \alpha_0) - G_{mjl}(0, \alpha_0)}{ik}. \tag{4.4}$$

Here α_0 is the critical value of the parameter α corresponding to a "shock wave" of zero intensity. For such a wave, the velocity of the liquid u is equal to the velocity of sound c, and therefore $\alpha_0 = mc_-^2/2kT_- = 5/6$. The same value of α_0 is obtained below from the condition of solubility of the problem under consideration. In view of the fact that we are considering small discontinuities, the difference $\alpha - \alpha_0$ is small, and we have therefore replaced α by α_0 in the quadratic terms in (4.4).

The elements of the determinant (4.3) have a comparatively simple form. For example, the element $D_{11}(k, \alpha)$ is equal to

$$D_{11}(k, \alpha) = \sqrt{\frac{\alpha}{\pi}}\int_{-\infty}^{\infty}\frac{ve^{-\alpha(v-1)^2}}{1-ikv}\,dv. \tag{4.5}$$

In the derivation of the relations (4.2) we have made use of the identity

$$\varphi_i(y, \alpha) \equiv \int_{-\infty}^{\infty}K_i(x-\xi;\ y, \alpha)\,d\xi,$$

which has a simple physical meaning: a current with constant density n, velocity u, and temperature T is possible for arbitrary values of n, u, and T.

Let us consider Eq. (4.2) in more detail. In order that the functions $\bar{\mu}_\gamma(k)$ remain finite for $k = 0$, we must require

$$\varepsilon_\gamma + \frac{1}{2D(0,\alpha)} \sum_{j,l} \varepsilon_j \varepsilon_l B_{jl\gamma}(0) = 0. \tag{4.6}$$

It is easily seen that these conditions coincide up to terms of third order with the usual conditions for the discontinuities of the hydrodynamic quantities in a shock wave.

It follows from (4.6) that $D(0, \alpha) \sim \epsilon$. This implies that all terms in (4.2) have the same order of magnitude for small k. This is the explanation for the necessity of including the quadratic terms even in the case of a shock wave of low intensity. As was to be expected, the problem of the shock wave is nonlinear already in the first nonvanishing approximation.

We note finally that the relation $D(0, \alpha) \sim \epsilon$ implies $D(0, \alpha_0) = 0$. This equation leads to the value of α_0 mentioned above.

5. METHOD OF SUCCESSIVE APPROXIMATIONS

The quadratic terms in Eq. (4.2) are not equally important as the linear terms for all values of k, but only for small k, when $D(k, \alpha)$ is not very different from $D(0, \alpha)$, which has the same order of magnitude as the discontinuities ϵ. It is therefore reasonable to represent all coefficients in (4.2) in the form of a sum of their approximate asymptotic expressions for small k and certain corrections of higher order of smallness. Thus we rewrite Eq. (4.2) in the form

$$\begin{aligned} -\frac{1}{ik}\Big[1 + \frac{1}{2[D(\alpha)+ikD_1(\alpha)]} \sum_{j,l} \frac{\varepsilon_j\varepsilon_l}{\varepsilon_\gamma} B_{jl\gamma}(0)\Big] + \bar{\mu}_\gamma(k) \\ + \frac{1}{D(\alpha)+ikD_1(\alpha)} \sum_{j,l} \frac{\varepsilon_j\varepsilon_l}{\varepsilon_\gamma} B_{jl\gamma}(0)\overline{\mu_j^{+}}(k) \\ + \frac{1}{2[D(\alpha)+ikD_1(\alpha)]} \sum_{j,l} \frac{\varepsilon_j\varepsilon_l}{\varepsilon_\gamma} B_{jl\gamma}(0)\,\bar{\mu}_{jl}(k) = F_\gamma(k), \end{aligned} \tag{5.1}$$

where

$$\begin{aligned} F_\gamma(k) = \frac{1}{\varepsilon_\gamma} \sum_{j,l} \varepsilon_j\varepsilon_l \Big[\frac{B_{jl\gamma}(k)}{D(k,\alpha)} - \frac{B_{jl\gamma}(0)}{D(\alpha)+ikD_1(\alpha)}\Big] \\ \times\Big[\frac{1}{2ik} - \overline{\mu_j^{+}}(k) - \frac{1}{2}\bar{\mu}_{jl}(k)\Big]; \end{aligned}$$

$$D(k, \alpha) \approx D(\alpha) + ikD_1(\alpha), \qquad |k| \ll 1. \tag{5.2}$$

It can be shown that the function $F_\gamma(k)$ must be neglected, since it is of higher order of smallness than the terms on the left-hand side of (5.1). We recall that terms of this order have already been neglected earlier.

In reality, however, we cannot discard the function $F_\gamma(k)$, because it is not analytic in the point $k = 0$ on the real axis, in contrast to the coefficients on the left-hand side of (5.1). The presence of a nonanalytic function in the equation leads to a nonanalytic solution. On the other hand, it is well known that the Fourier transform of a nonanalytic function goes to zero as $x \to \pm\infty$ at a considerably slower rate than the Fourier transform of a function which is analytic on the whole real axis.

Neglecting the small term on the right-hand side would thus lead to a serious distortion of the form of the shock wave at large distances from the wave front. The terms neglected earlier have an analytic part which is of the same order of smallness as the function $F_\gamma(k)$, while the remaining nonanalytic part is of even higher order. By keeping the right-hand side of (5.1) we therefore are kept from unwittingly going beyond the accuracy of the approximation.

To solve Eq. (5.1) we first neglect the right-hand side and find the first approximation. We then substitute on the right-hand side of (5.1) the functions μ_j found in first approximation and obtain an equation for the second approximation. There is no sense in trying to improve the accuracy any further in the framework of the Eq. (5.1), since this equation is itself not sufficiently exact for this purpose. We therefore confine ourselves to the above-mentioned two approximations.

6. FIRST APPROXIMATION (AT SMALL DISTANCES FROM THE WAVE FRONT)

As already mentioned, we must neglect the right-hand side of (5.1) for the calculation of the functions μ_j in the first approximation. As a first consequence, we find that then all functions μ_j are identical. Indeed, the coefficients $A_{m\gamma}(0, \alpha_0)$ entering in the expression (4.4) for $B_{jl\gamma}(0)$ are the cofactors of the elements of the determinat $D(0, \alpha_0)$, which is equal to zero. They can therefore be written in the form of a product,

$$A_{m\gamma}(0, \alpha_0) = \rho_m \sigma_\gamma, \tag{6.1}$$

where

$$\rho_m = A_{m1}(0, \alpha_0) / A_{11}(0, \alpha_0), \; \sigma_\gamma = A_{1\gamma}(0, \alpha_0) / A_{11}(0, \alpha_0).$$

It follows from (6.1), (4.4), and (4.6) that the ratios

$$A_{m\gamma}(0, \alpha_0) / \sigma_\gamma, \qquad B_{jl\gamma}(0) / \sigma_\gamma, \qquad \varepsilon_\gamma / \sigma_\gamma, \qquad B_{jl\gamma}(0) / \varepsilon_\gamma$$

are independent of the index γ. The coefficients of Eq. (5.1), therefore, do not depend on the index

γ. Hence all the functions $\bar{\mu}_\gamma$ are identical in this approximation.

With this in mind, we rewrite Eq. (5.1) with the help of (4.6) and obtain

$$-1+\overline{\mu_\gamma^+}(ik-\delta)-\overline{\mu_\gamma^{+2}}\delta=-\overline{\mu_\gamma^-}(ik+\delta)+\overline{\mu_\gamma^{-2}}\delta,$$
$$\delta=D(\alpha)/D_1(\alpha)\approx\alpha-\alpha_0=\alpha-\tfrac{5}{6}. \qquad (6.2)$$

The left-hand side of (6.2) is analytic and bounded in the upper half-plane, and the right-hand side is analytic and bounded in the lower half-plane. According to the Liouville theorem, each side of (6.2) is therefore equal to a constant:

$$-1+\overline{\mu_\gamma^+}(ik-\delta)-\overline{\mu_\gamma^{+2}}\delta=C,$$
$$-\overline{\mu_\gamma^-}(ik+\delta)+\overline{\mu_\gamma^{-2}}\delta=C. \qquad (6.3)$$

The first of these relations can be rewritten in the form

$$-1-\mu_\gamma(+0)-\int_0^\infty e^{ikx'}[\delta\mu_\gamma(x')$$
$$+\mu_\gamma'(x')+\delta\mu_\gamma^2(x')]\,dx'=C.$$

The integral in this relation goes to zero as k → ± ∞. We therefore obtain

$$-1-\mu_\gamma(+0)=C, \qquad \mu_\gamma'+\delta\mu_\gamma+\delta\mu_\gamma^2=0, \qquad x>0.$$

In the same way we obtain from the second equation in (6.3)

$$-\mu_\gamma(-0)=C, \qquad \mu_\gamma'+\delta\mu_\gamma-\delta\mu_\gamma^2=0, \qquad x<0.$$

It follows from these relations that the function $\nu_\gamma(x)=\theta(x)+\mu_\gamma(x)$ is continuous at $x=0$. With the appropriate choice of the separation constant C we have then

$$\nu_\gamma(x)=\frac{1}{1+e^{-\delta x}}.$$

In terms of the dimensional variables this formula has the following form

$$\frac{n(x)-n_-}{n_-}=\frac{u(x)-u_-}{u_-}=\frac{T(x)-T_-}{T_-}$$
$$=\left[1+\exp\left(-x\,\frac{m(u_-^2-c_-^2)}{2kT_-\tau u_-}\right)\right]^{-1} \qquad (6.4)$$

This solution satisfies the conditions at infinity only if $\delta > 0$ or, which is the same thing, $u_- > c_-$. Thus the relative velocity of the gas in front of the shock wave is larger than the velocity of sound.

The relation (6.4) coincides with the well known formula[6] describing the structure of the shock wave in the "approximation of the kinetic coefficients," i.e., under the assumption that the average velocity, density, and temperature change slowly in the diffuse front of the shock wave.

7. STRUCTURE OF THE WAVE AT LARGE DISTANCES

Let us now take account of the function $F_\gamma(k)$ standing on the right-hand side of Eq. (5.1). For this purpose we set

$$\mu_j(k)=\bar{\mu}_{j0}(k)+\bar{\rho}_j(k),$$

where $\bar{\mu}_{j_0}(k)$ are the approximate solutions of (5.1) obtained in Sec. 5, and $\bar{\rho}_j(k)$ are corrections due to the inclusion of right-hand side of (5.1). As has already been shown, the functions $\bar{\rho}_j(k)$ are considerably smaller than the $\bar{\mu}_{j_0}(k)$ for all real values of k. Therefore, the inclusion of the correction terms represents a surpassing of the accuracy at small distances. At large distances, on the other hand, the functions $\rho_j(x')$ play the major role, since the functions $\mu_{j_0}(x')$ go to zero very rapidly.

With this in mind, we calculate the function $\rho_j(x')$ only for large values of x′. To be definite, we consider the region in front of the shock wave $(x' < 0)$. Then

$$\mu_j(x')\approx\rho_j(x')=\frac{1}{2\pi}\int_{-\infty}^{\infty}\bar{\rho}_j(k)\,e^{-ikx'}\,dk, \qquad |x'|\gg\delta^{-2}. \qquad (7.1)$$

The value of this integral for large x′ is determined by the behavior of the function $\bar{\rho}_j(k)$ near its lowest singular point in the upper half-plane. This point is the branch point $k = 0$. Indeed, the integral (4.5) representing the function $D_{11}(k, \alpha)$ coincides in the left half-plane with one analytic function and in the right half-plane with another. All other functions entering in the expression for $F_\gamma(k)$ have the same character. Thus the function $F_\gamma(k)$ coincides in the right half-plane with one analytic function, $F_\gamma^+(k)$, and in the left half-plane with another, $F_\gamma^-(k)$.

The function $\bar{\rho}_\gamma^-(k)$ is analytic in the lower half-plane. With the help of (5.1), it can be continued through the positive half-axis into the right half-plane and through the negative half-axis into the left half-plane. Since the first continuation involves the function $F_\gamma^+(k)$ and the second continuation the function $F_\gamma^-(k)$, the values of $\bar{\rho}_\gamma^-(k)$ are different on the left and right sides of the imaginary axis. The difference between these values is equal to

$$\delta\bar{\rho}_\gamma^-(k)=F_\gamma^+(k)-F_\gamma^-(k).$$

Thus, if we deform the contour of integration in (7.1) in such a way as to make it run along the imaginary axis, we obtain

$$\mu_j(x') = \frac{1}{2\pi}\int_0^{i\infty} \delta\overline{\rho_j^-}(k)\, e^{-ikx'}\, dk, \qquad x' < 0, \qquad |x'| \gg \delta^{-2}. \tag{7.2}$$

Computing this integral by the method of steepest descent, we find

$$\mu_j(x') = \frac{25}{54\sqrt{3}}\frac{|x'|^{5/3}}{\alpha - \alpha_0}\exp\left[-\frac{3}{2}(2\alpha x'^2)^{1/3} - 2(\alpha^2 x')^{1/3} - \frac{4\alpha}{9}\right]. \tag{7.3}$$

In the dimensional variables this relation takes the form

$$\begin{aligned}\frac{n(x) - n_-}{n_-} &= \frac{u(x) - u_-}{u_-} = \frac{T(x) - T_-}{T_-}\\ &= \frac{25}{54\sqrt{3}}\left(\frac{x}{\tau u_-}\right)^{5/3}\frac{2kT_-}{m(u_-^2 - c_-^2)}\exp\Big[-\frac{3}{2}\left(\frac{m}{kT_-}\frac{x^2}{\tau^2}\right)^{1/3}\\ &\quad - 2\left(\frac{m^2u_-^3}{4k^2T_-^2}\frac{x}{\tau}\right)^{1/3} - \frac{2}{9}\frac{mu_-^2}{kT_-}\Big],\\ x < 0, &\qquad |x/\tau c_-| \gg [2kT_-/m(u_-^2 - c_-^2)]^3.\end{aligned} \tag{7.4}$$

Roughly speaking, the difference between the values of n, u, and T and their limiting values goes to zero with increasing $|x|$ as $\exp(-\text{const}\,|x|^{2/3})$, while the hydrodynamic theory leads to a decrease of the type $\exp(-\text{const}\,|x|)$.

The author takes this opportunity to thank A. I. Akhiezer, M. I. Kaganov, I. M. Lifshitz, R. V. Polovin, and Ya. B. Feĭnberg for valuable discussions and interest in this work.

---

[1] R. Becker, Z. Physik **8**, 321 (1922).

[2] D. Burnett, Proc. Lond. Math. Soc. II, **40**, 382 (1935).

[3] K. Zoller, Z. Physik **130**, 1 (1951).

[4] H. Grad, Commun. on Pure and Appl. Math. **2**, 331 (1949).

[5] H. M. Mott-Smith, Phys. Rev. **82**, 885 (1951).

[6] L. D. Landau and E. M. Lifshitz, Механика сплошных сред (Mechanics of Continuous Media) Gostekhizdat (1954).

Translated by R. Lipperheide
175

SOVIET PHYSICS JETP VOLUME 13, NUMBER 4 OCTOBER, 1961

STRUCTURE OF THE TRANSITION LAYER BETWEEN A PLASMA AND A MAGNETIC FIELD

V. P. SHABANSKII

Institute for Nuclear Physics, Moscow State University

Submitted to JETP editor May 12, 1960

J. Exptl. Theoret. Phys. (U.S.S.R.) 40, 1058-1064 (April, 1961)

The structure of the region in which a plasma beam is reflected by a magnetic field has been investigated using the self-consistent microscopic equations of motion for the particles; the structure of the transition layer between a fixed plasma and a magnetic field has also been investigated. In the first case corrections are introduced to take account of the polarization which is produced at high velocities of the incident beam.

1. In a number of problems concerned with the motion of plasma in magnetic fields, it is found that the plasma region and the region occupied by the magnetic field remain separated by boundary regions which exist for finite lengths of time. It is of practical interest to determine the thickness of these transition layers and the variation of particle density and magnetic field inside the layers. It is well-known that the diamagnetism of a plasma with infinite conductivity, which shields it from an external field, is due to true surface currents. If the layer is thin and if the velocity of the beam incident on the magnetic wall is high, the electrons that comprise the shielding current can be relativistic.

The analysis of retardation of a plasma bunch of finite dimensions in a magnetic field has much in common with a problem treated by Veksler.[1] The fact that the kinetic energy of the bunch is converted at the turning point primarily into transverse motion of the electrons[1]

$$w_{\perp}^{-} = m^{-} (v_{\perp}^{-})^2/2 = m^{+} (v_0^{+})^2/2 \tag{1}$$

(m^- and m^+ are the mass of the electron and ion respectively, $v_{\perp}^{-}$ is the electron velocity perpendicular to the motion of the bunch, v_0 is the bunch velocity before retardation) has been noted by Chapman and Ferraro (cf., for example, reference 2).

An extension of Eq. (1) into the relativistic region by simply taking account of the increase in electron mass m^-, as in reference 1, is inexact. Actually, at high velocities of the incident beam (v_0) it is necessary to take account of the polarization of the plasma in the direction of incidence; this process consumes part of the kinetic energy which, in turn, does not enter into the transverse energy of the electrons. Polarization also leads to another effect: the distribution of the longitudinal kinetic energy which is converted into transverse energy of ions and electrons is affected and this effect also acts to reduce the value of $w_{\perp}^{-}$ as compared with that given in Eq. (1). For this reason, at relativistic velocities the transverse energy of the electrons will be smaller than the value which follows from Veksler's analysis, which assumes a relativistic electron mass.[1]

2. We first consider the motion of two particles of different mass in the xy plane in a uniform magnetic field H_0 along the z axis; we assume rigid coupling in the x direction and no coupling in the y direction. The self-field is neglected. This model actually corresponds to the motion of particles in a plasma which is incident from $x = -\infty$ and which is reflected from a magnetic wall in the region $x \geq 0$. The plasma is assumed to be dense enough so that the electric polarization forces in the x direction are large, but rarefied enough so that the field H_0 is not distorted. The equations of motion for each of the particles

$$m\frac{dv_x}{dt} = e\left(E_x + \frac{1}{c}v_y H_0\right), \qquad m\frac{dv_y}{dx} = -\frac{e}{c}v_x H_0 \tag{2}$$

(the conventional notation is used), with rigid coupling in the x direction $v_x^+ = v_x^-$ and the initial condition $v_x^- = v_x^+ = v_0$ at $t = 0$, show that the particle-velocity vectors rotate along appropriate ellipses at the same frequency:

$$\begin{aligned} v_x &= v_x^- = v_x^+ = v_0 \cos\omega t, \\ v_y^- &= v_{y0}^- - \sqrt{m^+/m^-}\, v_0 \cos(\omega t + \pi/2), \\ v_y^+ &= v_{y0}^+ + \sqrt{m^-/m^+}\, v_0 \cos(\omega t + \pi/2), \\ \omega &= eH_0/c\sqrt{m^+m^-} = \sqrt{\omega^-\omega^+}. \end{aligned} \tag{3}$$

Here, ω^+ and ω^- are the Larmor frequencies for the ions and electrons respectively in the field H_0 while $v_0^\pm$ is the initial velocity. Integration of Eq. (3) over a quarter cycle $[t_0 = \pi/2\omega]$ for $v_{y0}^+ = v_{y0}^- = 0$ yields the appropriate semi-axes of the ellipses described by the particles

$$r_0 = x(t_0) = \int_0^{t_0} v_x dt = \sqrt{r^- r^+} = \sqrt{m^- m^+}\, c v_0 / eH_0, \quad y^+(t_0) = -r^-, \quad y^-(t_0) = r^+. \tag{4}$$

Thus, the depth of penetration of the particles into the region of magnetic field is equal to the mean geometric value of the Larmor radii r^+ and r^- while the path traversed by the electron along the boundary $y^-(t_0)$ is m^+/m^- times greater than the path traversed by the ion (cf. Fig. 1). It is apparent from Eq. (3) that at $t_0 = \pi/2\omega$ the proton and the electron exchange kinetic energies:

$$w_\perp^+(t_0) = m^- v_0^2/2, \qquad w_\perp^-(t_0) = m^+ v_0^2/2.$$

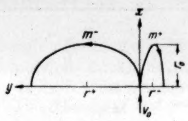

FIG. 1. Trajectories of particles m^+ and m^- in a magnetic field; the field is directed toward the reader and occupies the region $x \geq 0$.

This problem is equivalent to the problem of reflection of plasma from a magnetic wall H_0 when the conditions noted above are satisfied (rarefied plasma and absence of polarization); these conditions are stipulated by

$$m^+ N_0 v_0^2 \ll H_0^2/8\pi, \qquad \delta = \sqrt{m^+ v_0^2 / 4\pi N_0 e^2} \ll r_0,$$

where δ is the Debye polarization length for a particle of energy $m^+ v_0^2$ while r_0 is determined by Eq. (4). These requirements imply

$$m^+ N_0 v_0^2 \ll H_0^2/8\pi \ll m^- c^2 N_0. \tag{5}$$

If the left-hand equality is not satisfied it is necessary to take account of the self magnetic field of the current in the y direction; if the right-hand relation is not satisfied polarization must be taken into account. In particular, it can be seen that if the inverse inequality holds, i.e., $H_0^2/8\pi \gg m^- c^2 N_0$, the coupling between the particles in the x direction is so small that each particle moves in a circle with the appropriate Larmor radius and, in general, there is no transfer of energy.

We show below that if the field is free (that is to say, if in the absence of the plasma it extends over all space) the condition for stationary reflection for a plasma of infinite extent leads to the condition $m^+ v_0^2 N_0 = H_0^2/8\pi$, while the inequality in (5), which allows us to neglect polarization, reduces to the requirements $m^+ v_0^2 / m^- c^2 \ll 1$ or $w_\perp^-(t_0)/m^- c^2 \ll 1$ i.e., the electron velocities $v_\perp$ must be nonrelativistic.

3. A sufficiently small portion of the surface which divides the regions occupied by the magnetic field and the plasma may be regarded as a plane surface; this is taken to be the plane $x = \text{const}$. The problem is formulated as follows. A plasma beam is incident from the region $x = \infty$ in the $-x$ direction, with a given velocity. At $x = -\infty$ there is a field H_0 which is along z; the magnitude of this field is to be determined from the existence condition for the stationary solution.

It is clear from the symmetry of the problem that all quantities can only vary in the x direction and that there are only two particle-velocity components, $v_x^\pm = v^\pm$ and $v_y^\pm$. It will be assumed that the velocities of the ion beam (+) and the electron beam (–) can be different at infinity. This means that in addition to considering reflected plasma beams we can, in rough approximation treat also a fixed plasma. In the first case, the velocities of the electrons and ions are equal at infinity and can be identified with a macroscopic beam velocity which is large enough so that the thermal velocities can be neglected. (A similar formulation of the problem has been considered by Chapman and Ferraro.[2]) In the second case (fixed plasma) the velocities of the particles can be identified with the mean thermal velocities, whose dispersion in direction and absolute magnitude is negligible (i.e., the fixed plasma is approximated by two interpenetrating beams.

The complete system of equations of motion for the particles in the self-consistent fields is

$$m^+ v^+ \frac{dv^+}{dx} = e\left(E + \frac{1}{c} v_y^+ H\right),$$

$$m^- v^- \frac{dv^-}{dx} = -e\left(E + \frac{1}{c} v_y^- H\right),$$

$$m^+ dv_y^+/dx = -eH/c, \qquad m^- dv_y^-/dx = eH/c;$$

$$j_y = eN^+ v_y^+ - eN^- v_y^- = -\frac{c}{4\pi}\frac{dH}{dx}, \qquad \frac{dE}{dx} = 4\pi e(N^+ - N^-),$$

$$N^+ v^+ = N_0 v_0^+, \qquad N^- v^- = N_0 v_0^-. \tag{6}$$

Here, N_0 is the plasma density at infinity (for both beams, incident and reflected, so that the density in one beam is $N_1 = N_0/2$); v_0^+ and v_0^- are the velocities for the positive and negative particles at x

$= +\infty$. The positive direction for the velocity is taken to be from the plasma toward the boundary i.e., in the negative x direction; the remaining notation is conventional.

The temperature and pressure in the x and y directions in the second problem (fixed plasma) are given by the formulas

$$p^{\pm}_{x,\,y} = kT^{\pm}_{x,\,y}N^{\pm} = N^{\pm}m^{\pm}(v^{\pm}_{x,\,y})^2. \qquad (7)$$

We now convert to dimensionless variables in which v, N, H and x are measured in units of

$$v_0^+, \quad N_0, \quad H_1 = (4\pi N_0 m^+)^{1/2} v_0^+,$$
$$x_1 = (m^- c^2 / 4\pi e^2 N_0)^{1/2}. \qquad (8)$$

Then, eliminating E, N^+, N^-, v_y^+ and v_y^- in (6), we obtain the system*

$$\sqrt{\frac{\alpha}{\beta}}\, v^- \frac{dH}{dx} = \left(1 + \alpha \sqrt{\frac{\alpha}{\beta}\frac{v^-}{v^+}}\right) \int_\infty^x H dx,$$

$$v^+ \frac{dv^+}{dx} + \alpha v^- \frac{dv^-}{dx} = -(1+\alpha) H \int_\infty^x H dx,$$

$$\gamma_\alpha v^- \frac{dv^-}{dx} + \gamma H \int_\infty^x H dx = -\int_\infty \left(\frac{1}{v^+} - \frac{1}{\sqrt{\alpha/\beta}\, v^-}\right) dx, \qquad (9)$$

where

$$\alpha = m^-/m^+, \quad \beta = m^-(v_0^-)^2 / m^+(v_0^+)^2 = T_-/T_+,$$
$$\gamma = m^+(v_0^+)^2 / m^- c^2. \qquad (10)$$

The particle velocities in the y direction are:

$$v_y^- = \frac{1}{\sqrt{\alpha}} \int_\infty^x H dx, \qquad v_y^+ = -\sqrt{\alpha} \int_\infty^x H dx. \qquad (11)$$

In the incident-beam problem, we must put $\beta = \alpha$ in (9); in the case of a fixed plasma with equal electron and ion temperatures at infinity, we put $\beta = 1$. It is clear from Eq. (11) that the velocity ratio $v_y^-/v_y^+ = -m^+/m^-$ is the independent of γ and corresponds to the condition that the total y momentum must vanish provided $N^-(x) = N^+(x)$. However, in the presence of polarization the total momentum does not vanish and there is motion of matter in the y direction.

4. In the absence of polarization ($\gamma \ll 1$) the equations can be solved easily. From the third equation in (11) we find that $v^+ = \sqrt{\alpha/\beta}\, v^-$, $N = N^+ = N^- = 1/v^+$ and the system reduces to two equations for v^+ and H:

$$v^+ \frac{dH}{dx} = \int_\infty^x H dx, \qquad v^+ \frac{dv^+}{dx} = -H \int_\infty^x H dx, \qquad (12)$$

where H is measured in units of $H_1\sqrt{1+\beta}$ while x is measured in units of $x_1/\sqrt{1+\alpha}$.

The first integral of these equations gives a relation between v^+ and H:

$$v^+ = 1 - H^2/2 \qquad (13)$$

or, in terms of the usual dimension variables:

$$v^+ = v_0^+ - H^2 / 8\pi m^+ v_0^+ N_0 (1+\beta). \qquad (13')$$

For the incident-beam problem[2] we have $\beta = \alpha \ll 1$, $v_0^- = v_0^+ = v^0$ and Eq. (13′) yields the expression

$$v = v_0 - H^2 / 8\pi m^+ v_0 N_0.$$

The thickness of the transition layer is approximately $x_1/\sqrt{1+\alpha}$. For a fixed plasma Eq. (13′) together with the relation $v^- = \sqrt{\beta/\alpha}\, v^+$ determines the relations between the electron-ion pressure and the field. Using (7) for the pressure and the equation of continuity, we have from Eq. (13′)

$$p_x = p_x^0 - H^2/8\pi, \qquad p_x = p_x^- + p_x^+, \quad p_x^-/p_x^+ = T_x^-/T_x^+ = \beta; \qquad (13'')$$

the first two of these equations coincide with the results of the hydrodynamic analysis.

The value of the magnetic field at the turning point (v = 0) at x = 0 is given by

$$H_0^2/8\pi = m^+(v_0^+)^2 N_0 (1+\beta). \qquad (14)$$

If Eq. (14) is used to eliminate N_0 in Eq. (8) for x_1, which characterizes the thickness of the transition layer, we have

$$x_1 = [2r_0^+ r_0^- \sqrt{\alpha/\beta}\,(1+\beta)]^{1/2},$$

where r_0^- and r_0^+ are the Larmor radii of rotation for electrons and ions with velocities v_0^- and v_0^+ in the field H_0. In the case of an incident beam ($\beta = \alpha \ll 1$) this expression coincides with (4) for r_0 to within a factor $\sqrt{2}$. The difference is explained by the fact that in the present case the particles move in an inhomogeneous self-consistent field.

Substituting Eq. (12) in Eq. (13), we obtain an equation for the magnetic field in the layer:*

---

*If we use the vector and scalar field potentials and eliminate V^+ and V^- rather than E, the system is somewhat more compact; however, the form used in the text is more convenient for the introduction of relativistic corrections.

*We arrive at the same equation in the case of a plasma of equal masses ($m^- = m^+$). We put in Eq. (9) $\alpha = \beta = 1$. Furthermore, in order for this plasma density to coincide with the density of a real electron-ion plasma, we must write in the equation of continuity $N_0/2$ in place of N_0. Then it is apparent that $v^- = v^+$ for any value of γ and the equations in (9) reduce to two identical systems, each of which reduces to Eq. (15). The difference lies only in the fact that we introduce in Eq. (8) for x_1 m^+ in place of m^-, that is to say, the magnitude of the field for which stationary reflection is possible remains the same [Eq. (14)] but the width of the transition layer is increased by a factor of $\sqrt{m^+/m^-}$. This is explained by the absence of the constraining effect of the electrons.

$$\frac{d}{dx}\left\{\left(1-\frac{H^2}{2}\right)\frac{dH}{dx}\right\}=H, \qquad (15)$$

with the boundary conditions H = 0 at x = ∞ and H = $\sqrt{2}$ at x = 0.* Introducing the variable Z = dx/dH we can write Eq. (15) in the form

$$\frac{d}{dH}\left\{\left(1-\frac{H^2}{2}\right)\frac{1}{Z}\right\}=ZH, \qquad Z=\frac{dx}{dH}, \qquad (16)$$

with the boundary condition Z = − ∞ at H = 0. Integrating Eq. (16) and choosing from among the two solutions the one which satisfies the boundary condition, we have

$$Z=-(1-H^2/2)/H\sqrt{1-H^2/4}, \qquad (17)$$

$$x=\frac{1}{2}\ln\frac{(\sqrt{2}-1)(1+\sqrt{1-H^2/4})}{(\sqrt{2}+1)(1-\sqrt{1-H^2/4})}-2\sqrt{1-\frac{H^2}{4}}+\sqrt{2}. \qquad (18)$$

The velocities $v^- = \sqrt{\beta/\alpha}\, v^+$, $v^+ = 1 - H^2/2$ in the x direction are determined from the equations

$$x=\frac{1}{2}\ln\frac{(\sqrt{2}-1)(\sqrt{2}+\sqrt{1+v^+})}{(\sqrt{2}+1)(\sqrt{2}-\sqrt{1+v^+})}-\sqrt{2(1+v^+)}+\sqrt{2}. \qquad (19)$$

In Fig. 2 we show the approximate behavior of H, v and vH = H (1 − $H^2/2$) for the case of a reflected beam ($\beta = \alpha \ll 1$) as a function of the layer depth x. The velocities and energies in the y direction can be found from Eq. (11).

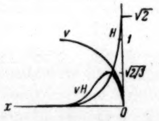

FIG. 2. Behavior of the quantities v, H and vH in the transition layer.

In particular, at the turning point x = 0, H = $\sqrt{2}$, $\int_\infty^x H\,dx = 1$, the velocities and energies in the ordinary variables (when $\alpha \ll 1$) are given respectively by

$$v_y^+=\sqrt{(1+\beta)m^-/m^+}\,v_0^+, \qquad v_y^-=-\sqrt{(1+\beta)m^+/m^-}\,v_0^+,$$
$$w_y^+=m^-(v_0^+)^2(1+\beta), \qquad w_y^-=m^+(v_0^+)^2(1+\beta). \qquad (20)$$

When $\beta = \alpha \ll 1$ (incident beam) the expressions in (20) show that the electrons and ions exchange kinetic energies at the turning point.

At the turning point the velocities v^+ and v^- vanish so that the particle density N and the current density along the y axis become infinite. This effect arises because we have neglected the directional dispersion in the velocity. The mean values of those quantities remain finite in the layer. In order to compute the mean values we must know the number of particles in the layer. This quantity can be determined as follows:*

$$n=\int_0^\infty N v_y^+\,dx\Bigg/\int_0^\infty v_y^+\,dx=\int_{\sqrt{2}}^0\frac{v_y^+}{v^+}Z\,dH\Bigg/\int_{\sqrt{2}}^0 v_y^+ Z\,dH$$
$$=\frac{3}{2\sqrt{2}-1}\approx 1.66. \qquad (21)$$

It is then easy to show that the mean velocities will be $n/\sqrt{2} \sim 1.2$ times smaller than the maximum values given by Eq. (20).

The total current in the y direction can be determined either from the equation for j in (6) or from the expression $I \approx \Gamma = -enN_0\overline{v_y}x$. We find†

$$I=cv_0^+\sqrt{(1+\beta)N_0 m^+/2\pi}. \qquad (22)$$

5. We now consider the case in which polarization must be taken into account. In this case, only the incident-beam problem has any meaning, since the temperature of a fixed plasma at $\gamma = 1$ would be $T^+ \sim 10^9$ deg. On the other hand, beams with velocities $v_0 = \sqrt{m^-c^2/m^+} \sim 7 \times 10^8$ cm/sec, corresponding to $\gamma = 1$, are completely feasible. Hence we can write in Eq. (11) $\alpha = \beta \ll 1$, thereby obtaining the system of equations

$$v^-\frac{dH}{dx}=\int_\infty^x H\,dx, \quad v^-\frac{dv^+}{dx}=-H\int_\infty^x H\,dx, \quad \frac{1}{v^-}$$
$$-\frac{1}{v^+}=\gamma\frac{d}{dx}\left\{H\int_\infty^x H\,dx\right\}. \qquad (23)$$

We shall only find the correction to the velocities obtained in the preceding section, assuming that $\gamma < 1$. In the first approximation ($\gamma = 0$) we have the case already treated, where $v = v^+ = v^-$, $N = N^+ = N^-$, and the magnetic field is given by Eq. (18). In the second approximation, the field remains the same but the mean values of the velocities $\overline{v^-}$ and $\overline{v^+}$ are determined from the third equation in (23).

Using the relations obtained in Sec. 4 we find:

$$\overline{v^-}=\overline{v^+}(1-k_1\gamma), \qquad (24)$$

k_1 is a numerical factor of order unity.

---

*If we neglect the term $H^2/2$ compared with unity in Eq. (15) then this equation coincides with the equation that describes the penetration of a magnetic field into a superconductor. This equation is simpler for the superconductor because the density of the superconducting electrons is assumed to be constant over the entire depth of the layer.

*If n is determined by the expression,

$$n=\int_0^\infty N H\,dx\Bigg/\int_0^\infty H\,dx,$$

then we find n = $\pi/2 \sim 1.6$, which coincides with Eq. (21) in order of magnitude.

†The mean current density $\overline{j} = I/x_1 = cH/4\pi\sqrt{2}\,x_1$ coincides with the expression for the density of surface current in a superconductor in a magnetic field H.

Multiplying the third equation in (23) by v_y^- and integrating over the entire layer, we obtain expressions for the mean velocity and energy of electrons, taking account of polarization in the x direction:

$$\overline{(v_y^-)}_\gamma = \overline{v_y^-}(1 - k_2\gamma),$$

$$\overline{(w_y^-)}_\gamma = \overline{w_y^-}(1 - k_3\gamma) = \frac{3}{4n}\frac{m^+ v_0^2}{2}(1 - k_3\gamma), \qquad (25)$$

where k_2 and k_3 are numerical factors approximately equal to unity.

Thus, the relation $w_y^- = m^+(v_0^+)^2/2$, which applies for low beam velocities, is not satisfied here. The kinetic energy of the electrons along the y axis is smaller than this value for $\gamma \neq 0$. In the second approximation the total energy of the electrons and ions along the y axis is equal to the sum of the energies of the electrons and ions in the beam. This is apparent from the relation $\sqrt{\alpha}\, v_y^- - v_y^+/\sqrt{\alpha}$, which is satisfied for any γ, and from the fact that the field H does not change in the second approximation, so that

$$\sqrt{\alpha}\, v_y^- = \int_\infty^0 H dx = -1.$$

Hence, the effect of polarization is not primarily to change the total kinetic energy of the particles, but rather to affect the redistribution of energy between electrons and ions in the layer in such a way that the transverse energy of the electrons is reduced while that of the ions is increased as compared with the values in the absence of polarization. The effect of polarization on the total energy along the y axis first appears in the next approximation in γ. In this case the thickness of the layer increases and the magnetic field is changed so that in absolute magnitude

$$\sqrt{\alpha}\, v_y^- = v_y^+ / \sqrt{\alpha} = \left| \int_\infty^0 H dx \right| < 1.$$

The remainder of the kinetic energy of the particle goes into polarization energy.

Both effects appear before the relativistic increase in mass; hence in the analysis of retardation of a plasma bunch in an axially symmetric magnetic field[1] with $\gamma \gtrsim 1$ these effects should be considered on equal terms with the latter. The account of these effects should lead to a reduction in the acceleration of electrons in the collision of a fast plasma beam with a magnetic field.

In conclusion I wish to thank S. I. Syrovat-skii for valuable remarks.

---

[1] V. I. Veksler, Doklady Akad. Nauk SSSR **118**, 263 (1958), Soviet Phys. Doklady **3**, 84 (1958).

[2] V. C. A. Ferraro, J. Geophys. Research **57**, 15 (1952).

Translated by H. Lashinsky
176

SOVIET PHYSICS JETP VOLUME 13, NUMBER 4 OCTOBER, 1961

QUANTUM THEORY OF THE SPECTRUM OF EXCITATIONS OF AN ELECTRON GAS IN A MAGNETIC FIELD

P. S. ZYRYANOV

Ural Polytechnic Institute

Submitted to JETP editor July 8, 1960

J. Exptl. Theoret. Phys. (U.S.S.R.) 40, 1065-1071 (April, 1961)

The quantum dispersion equation is found for the longitudinal oscillations of an electron gas in a magnetic field, for the case of an arbitrary energy distribution of the particles. A criterion (with respect to the magnetic field) for the applicability of the hydrodynamical approximation is established. It is shown that as we go from very high magnetic field strengths to low fields the frequency of the longitudinal oscillations changes discontinuously. The longitudinal permittivity of a plasma is calculated.

THE classical kinetic theory of the oscillations of an electron plasma in a homogeneous magnetic field has been studied by many physicists.[1] In all of the papers devoted to this problem it has been assumed that there is a Maxwell distribution of the electron velocities, and no account has been taken of the quantization of the orbital motion of the electrons in the magnetic field. The quantum theory, also with a Maxwell distribution function, has been considered by Bonch-Bruevich and Mironov.[2] They found small quantum corrections to the well known classical results. Effects of a fundamentally quantum nature were not considered. Yakovlev and Kalyush[3] have used the quantum kinetic equation as the basis for a treatment of the oscillations of an electron-ion plasma in a magnetic field with arbitrary distribution functions, but the quantization of the orbital motion in the ground state was not taken into account, and therefore their dispersion equation is not valid for the study of the effect of the quantization of the orbital motion of the electrons on the spectrum of the oscillations. The study of these effects is the main purpose of the present paper.

The classical description of a plasma in a magnetic field is admissible only under the weak-field condition, which corresponds to large values of the quantum number n that quantizes the motion of an electron in the magnetic field; more exactly, the classical description is valid as long as the quantum energy satisfies $\hbar\omega_c \ll E_0$ (E_0 is the energy of the random motion of the particles). In the case $\hbar\omega_c \geq E_0$ small values of the quantum number n play an important part, and therefore one must use a quantum description of the motion of the particles, but one can still treat the electromagnetic field in the plasma by classical theory.

In the first section of the paper we give the method for finding the quantum dispersion equation for electrons in a magnetic field. In the second section we give an essentially quantum-theoretical analysis of this equation. At the end of the paper (the third section) we calculate the longitudinal dielectric constant with an arbitrary energy distribution of the particles.

1. As is well known, the longitudinal and transverse oscillations of a plasma in a magnetic field cannot be separated, but neglect of the retardation in the propagation of the electromagnetic field allows us to make the separation. Small longitudinal oscillations of an electron plasma in a magnetic field can be described by means of linearized equations with a self-consistent field, which have been extended in a paper by the writer[4] to the case of nonstationary states. If in Eq. (3) of that paper we neglect force correlations at small distances and nonlinear terms, the equation is equivalent to the usual equation of motion for the density operator

$$i\hbar\dot{\hat{\rho}} = [\hat{\mathscr{H}}_0, \hat{\rho}] + [\hat{V}, \hat{\rho}_0], \qquad (1)$$

where $\hat{\rho}$ is a small correction to the unperturbed value $\hat{\rho}_0$, and $\hat{V}$ is the self-consistent potential, which is a functional of $\hat{\rho}$.

In the case of a homogeneous magnetic field directed along the z axis, the Hamiltonian operator of an electron is

$$\hat{\mathscr{H}}_0 = \frac{1}{2m}\left(\hat{\mathbf{p}} - \frac{e}{c}\mathbf{A}\right)^2, \qquad \mathbf{A} = \{-Hy, 0, 0\}. \qquad (2)$$

Next, following the work of Ehrenreich and Cohen,[5] we use Eq. (1) to find the equation of motion of the matrix elements of the operator $\hat{\rho}$, which describes the transitions between the stationary states of the system with $\hat{V} = 0$. The wave function $|k_x, k_z, n\rangle$ in the Landau representation is an eigenfunction of the operator $\hat{\mathcal{H}}_0$:

$$\hat{\mathcal{H}}_0 | k_x, k_z, n\rangle = E_{k_z, n} | k_x, k_z, n\rangle, \tag{3}$$

where

$$E_{k_z, n} = \hbar\omega_c\left(n + \frac{1}{2}\right) + \frac{\hbar^2 k_z^2}{2m}, \quad \omega_c = \frac{eH}{mc}, \quad n = 0, 1, 2, \ldots,$$

$$|k_x, k_z, n\rangle = (2\pi\sqrt{\alpha})^{-1} \exp(ik_x x + ik_z z)\, \Phi_n[(y + \alpha^2 k_x)/\alpha]. \tag{4}$$

$\Phi_n(y)$ is a normalized oscillator wave function, and $\alpha^2 = \hbar/m\omega_c$.

By means of Eq. (2) we get the equation of motion for the matrix elements of the operator $\hat{\rho}_0$:

$$\begin{aligned}&(i\hbar\partial/\partial t + E_{k_z+q_z, n} - E_{k_z, n})\\ &\quad\times\langle k_x, k_z, n|\hat{\rho}|k_x + q_x, k_z + q_z, n'\rangle = \{f_0(E_{k_z+q_z, n'})\\ &\quad - f_0(E_{k_z, n})\}\langle k_x, k_z\, n|\hat{V}|k_x + q_x, k_z + q_z, n'\rangle. \end{aligned}\tag{5}$$

In obtaining Eq. (4) we have taken into account the well known property of the unperturbed operator $\hat{\rho}_0$:

$$\hat{\rho}_0 | k_x, k_z, n\rangle = f_0(E_{k_z, n}) | k_x, k_z, n\rangle, \tag{6}$$

where $f_0(E)$ is the energy distribution function of the particles.

Let us expand $\hat{V}(\mathbf{r})$ in Fourier series and transform the matrix element of $\hat{V}(\mathbf{r})$ that appears in Eq. (5) to the form

$$\begin{aligned}&\langle k_x, k_z, n|\sum_{\gamma}\hat{V}(\gamma)\, e^{-i\gamma\mathbf{r}}|k_x + q_x, k_z + q_z, n'\rangle\\ &\quad = \sum_{\gamma_y}\hat{V}(q_x, q_z, \gamma_y)\langle k_x, n|e^{-i\gamma_y y}|k_x + q_x, n'\rangle,\end{aligned}\tag{7}$$

where

$$\begin{aligned}&\langle k_x, n|e^{-i\gamma_y y}|k_x + q_x, n'\rangle = \frac{1}{\alpha}\\ &\quad\times\int dy\, \Phi_n[(y + \alpha^2 k_x)/\alpha]\, e^{-i\gamma_y y}\, \Phi_{n'}[(y + \alpha^2(k_x + q_x))/\alpha\ .\end{aligned}$$

To obtain the dispersion equation it is necessary to make in Eq. (7) an approximation which is equivalent to the approximation of "random phases," namely,

$$\begin{aligned}&\sum_{\gamma_{y_c}}\hat{V}(q_x, q_z, \alpha_y)\langle k_x, n|e^{-i\gamma_y y}|k_x + q_x, n'\rangle\\ &\quad\approx V(q_x, 0, q_z)\ \langle k_x, n|k_x + q_x, n'\rangle.\end{aligned}\tag{8}$$

This approximation admits of the following interpretation. In $\langle k_x, n|e^{-i\gamma_y y}|k_x + q_x, n'\rangle$ one takes the average value of the overlap integral of the wave functions $\Phi_n(y)$ and $\Phi_{n'}(y + \alpha^2 q_x)$ out from under the integral sign, and integration of the rest of the integrand gives the δ function of γ_y.

An analogous approximation is made in finding the dispersion equation for the oscillations of a plasma in a periodic field of ions (cf. e.g., the papers by Kanazawa[6] and by Ehrenreich and Cohen[5]).

Let us express $\hat{V}(\mathbf{q})$ in terms of the matrix element of the operator $\hat{\rho}$, using Poisson's equation:

$$\Delta\hat{V} = -4\pi e^2 N(\mathbf{r}), \qquad N(\mathbf{r}) = \mathrm{Sp}\{\delta(\mathbf{r} - \mathbf{r}')\,\hat{\rho}(\mathbf{r}')\}. \tag{9}$$

Calculating the trace by means of the eigenfunctions (4) and using Eq. (8), we find

$$\begin{aligned}\hat{V}(q_x, 0, q_z) &= G(q_x, 0, q_z)\sum_{\varkappa_x, \varkappa_z n'', n'''}\langle\varkappa_x + q_x, n'''|\varkappa_x, n''\rangle\\ &\quad\times\langle\varkappa_x, \varkappa_z, n''|\hat{\rho}|\varkappa_x + q_x, \varkappa_z + q_z, n'''\rangle,\\ G(q_x, 0, q_z) &= 4\pi e^2(q_x^2 + q_z^2)^{-1}.\end{aligned}\tag{10}$$

Using Eqs. (10) and (8), we rewrite Eq. (5) in the form

$$\begin{aligned}&\left(i\hbar\frac{\partial}{\partial t} + E_{k_z+q_z, n'} - E_{k_z, n}\right)\\ &\quad\times\langle k_x, k_z, n|\hat{\rho}|k_x + q_x, k_z + q_z, n'\rangle\\ &\quad = \{f_0(E_{k_z+q_z, n'}) - f_0(E_{k_z, n})\}\langle k_x, n|k_x + q_x, n'\rangle\\ &\quad\times G(q_x, 0, q_z)\sum_{\varkappa_x, \varkappa_z, n'', n'''}\langle\varkappa_x, \varkappa_z, n''|\hat{\rho}|\varkappa_x\\ &\quad + q_x, \varkappa_z + q_z, n'''\rangle.\end{aligned}\tag{11}$$

From Eq. (10) there follows as the dispersion equation for the longitudinal oscillations of an electron plasma

$$\begin{aligned}1 = &\lim_{\gamma\to 0}\sum_{n, n', k_x, k_z} G(q_x, 0, q_z)|\langle k_x, n|k_x + q_x, n'\rangle|^2\\ &\times[f_0(E_{k_z+q_z, n'})\\ &- f_0(E_{k_z, n})][E_{k_z+q_z, n'} - E_{k_z, n} - \hbar\omega + i\hbar\gamma]^{-1}.\end{aligned}\tag{12}$$

According to reference 7, for $n' \geq n$ the two-center integral that appears in Eq. (12) is given by

$$\begin{aligned}F_{nn'}(\alpha q_x) &= \langle k_x, n|k_x + q_x, n'\rangle\\ &= (n!/n'!)^{1/2}\exp\{-(\alpha q_x/2)^2\}\\ &\quad\times(-\alpha q_x/\sqrt{2})^{n'-n} L_n^{n'-n}(\alpha^2 q_x^2/2),\end{aligned}\tag{13}$$

where L_n^{α} is the associated Laguerre polynomial

$$L_n^{\alpha}(x) = (n!)^{-1} e^x x^{-\alpha}\frac{d^n}{dx^n}(e^{-x}x^{n+\alpha}).$$

Since $F_{nn'}(x)$ does not depend on k_x, the summation over k_x in Eq. (12) gives the total number of allowed values of k_x, which is $(eH/c\hbar) L_x L_y$ (where L_x and L_y are the dimensions of the system along the x and y axes). Replacing the summation over k_z in Eq. (12) by an integration, we rewrite this equation in the form

$$1 = \lim_{\gamma\to 0} \sum_{n,\,n'} G(q_x, 0, q_z) \frac{1}{2\pi^2\alpha^2} [F_{nn'}(\alpha q_x)]^2 \int dk_z [f_0(E_{k_z+q_z,\,n'}) - f_0(E_{k_z,\,n})] [E_{k_z+q_z,\,n'} - E_{k_z,\,n} - \hbar\omega + i\hbar\gamma]^{-1} \tag{14}$$

(the volume $V = L_xL_yL_z$ of the system is taken to be unity).

2. Before going on to the study of the dispersion equation (14), let us rewrite it in terms of dimensionless quantities, taking as the unit of length $\alpha = (c\hbar/eH)^{1/2}$ and as that of energy the quantum $\hbar\omega_c$. Then instead of Eq. (14) we get

$$1 = \lim_{\Gamma\to 0} G(q_x, 0, q_z) \frac{m}{2\pi^2\hbar^2\alpha} \sum_{n,\,n'} [F_{nn'}(q_x)]^2 \int d\zeta [f_0(E_{\zeta+q_z,\,n'}) - f_0(E_{\zeta,\,n})] [n' - n + \tfrac{1}{2}(q_z^2 + 2q_z\zeta) - \Omega + i\Gamma]^{-1}. \tag{15}$$

Let us make some remarks about this equation. Since in obtaining Eq. (15) we imposed no restrictions on the form of $f_0(E)$, the equation holds for arbitrary $f_0(E)$. Furthermore, Eq. (15) gives two branches of the spectrum of excitations. The poles from the denominator in Eq. (15) give the branch of one-particle excitations, and the root of the integral equation (15) with $G(q) \neq 0$ gives the branch of collective oscillations.

We shall consider below the case of a completely degenerate Fermi distribution. The chemical potential μ is determined from the equation $N = -(\partial\chi/\partial\mu)_T$, where N is the number of particles in the system and χ is the thermodynamical potential. For a completely degenerate Fermi gas this last relation takes the form

$$N_0 = \frac{N}{V} = \frac{\sqrt{2}}{\pi^2\alpha^3} \sum_{n=0}^{n_0} (n_0 - n)^{1/2}, \tag{16}$$

where μ is connected with n_0 by the relation $n_0 = \mu/\hbar\omega_c - 1/2$. The limits of the integration over ζ in Eq. (15) are determined as usual from the condition

$$\mu = \hbar^2k_z^2/2m + \hbar\omega_c(n + 1/2).$$

The result of the integration over ζ is the equation (with damping neglected)

$$1 = G(q_x, 0, q_z) \frac{m}{2\pi^2\hbar^2\alpha} \sum_{n,\,n'}^{n_0} [F_{nn'}(q_x)]^2 \frac{1}{q_z} \times \left\{ \ln \frac{\Omega - (n'-n) - \sqrt{2}(n_0 - n')^{1/2} + q_z/2}{\Omega - (n'-n) + \sqrt{2}(n_0 - n')^{1/2} + q_z/2} + \ln \frac{\Omega - (n'-n) - \sqrt{2}(n_0 - n)^{1/2} - q_z^2/2}{\Omega - (n'-n) + \sqrt{2}(n_0 - n)^{1/2} - q_z^2/2} \right\}. \tag{17}$$

First of all, Eq. (17) must give the well known classical results, in particular the results of the hydrodynamical approximation, namely the equation

$$1 = \frac{\omega_0^2}{\omega^2}\cos^2\vartheta + \frac{\omega_0^2}{\omega^2 - \omega_c^2}\sin^2\vartheta \tag{18}$$

ϑ is the angle between the vectors **q** and **H**, and $\omega_0^2 = 4\pi e^2 N_0/m$ is the square of the Langmuir frequency.

Since Eq. (18) does not involve any characteristics of the energy distribution of the particles in the ground state, and also does not involve the magnitude of the vector **q**, to derive Eq. (18) from Eq. (17) we must take the limit as $q \to 0$. To do this we separate out from the double sum over n and n′ the terms with $n = n'$. For $q_z \ll \Omega$ the sum of these terms gives the expression

$$\Omega_0^2\Omega^{-2} \exp\{-{}^1/_2 q^2 \sin^2\vartheta\} \cos^2\vartheta \qquad (\Omega_0^2 = \omega_0^2/\omega_L^2). \tag{19}$$

For $q_z \ll \Omega$ we can transform the sum with $n' \neq n$ to the form

$$2G(q_x, 0, q_z) \frac{\sqrt{2}m}{\pi^2\hbar^2\alpha} \times \sum_{n;\,n'>n}^{n_0} F_{nn'}^2(q_x) \frac{(n_0 - n)^{1/2}(n_0 - n')^{1/2}}{\Omega^2 - (n' - n)^2}(n' - n). \tag{20}$$

Using Eqs. (19) and (20), we can write Eq. (17) in the form

$$1 = \frac{\Omega_0^2}{\Omega^2} \exp\left\{-\frac{1}{2}q^2\sin^2\vartheta\right\}\cos^2\vartheta + \sum_{n=0}^{n_0-1}\sum_{l=1}^{n_0-n} \frac{C_{l,\,n}(q_x, q_z)}{\Omega^2 - l^2};$$

$$C_{l,\,n}(q_x, q_z) = G(q_x, 0, q_z) \frac{2\sqrt{2}m}{\pi^2\hbar^2\alpha} F_{n,n+l}^2(q_x) \times [(n_0 - n)^{1/2} - (n_0 - n - l)^{1/2}]\, l. \tag{21}$$

For $q_x \to 0$ and $q_z \to 0$ we get from Eq. (21) the equation (18).

In order to get the second term in the right member of Eq. (18) we must have $n_0 \geq 1$. For $n_0 < 1$ this term is zero, i.e., the frequency of the wave with $\mathbf{q} \perp \mathbf{H}$ is zero. Since Eq. (18) is valid only for $n_0 < 1$ and $q_x \to 0$, the criterion for the applicability of the hydrodynamic approximation reduces to the inequalities

$$H \leqslant \frac{c\hbar}{e}\left(\frac{\pi^2 N_0}{\sqrt{2}}\right)^{2/3}, \qquad \frac{c\hbar}{2eH} q_x^2 \ll 1. \tag{22}$$

In the case of very strong magnetic field $n_0 \ll 1$, i.e., in the case in which quantum theory is essential, Eq. (17) has for any value of q the solution

$$\omega^2 = \omega_0^2 \exp\left\{-\frac{\hbar c}{2eH} q^2 \sin^2\vartheta\right\}\cos^2\vartheta + \frac{\hbar^2 q^4}{4m^2}\cos^4\vartheta. \tag{23}$$

Let us make a closer analysis of the dispersion equation (17) in the case of ϑ close to $\pi/2$, or small values of q_z. It follows from Eq. (21) that as the magnetic field strength decreases (i.e., as n_0 increases) new terms are added to the sums over n and l, and this leads to discontinuous changes of the frequency ω. For example, for $n_0 < 1$ the frequency ω is determined from the equation

$$\omega^2 = \omega_0^2 \exp\{-(c\hbar/2eH)\, q^2 \sin^2\vartheta\} \cos^2\vartheta, \tag{24}$$

and for $n_0 = 1$ it is determined from the equation

$$1 = \left(\frac{\omega_0^2}{\omega^2}\cos^2\vartheta + \frac{\omega_0^2}{\omega^2-\omega_c^2}\sin^2\vartheta\right)\exp\left\{-\frac{c\hbar}{2eH}\, q^2\sin^2\vartheta\right\}. \tag{25}$$

The appearance of the second term in the brackets is due to transitions between n = 0 and n = 1. There is an analogy between the behavior of an electron plasma in a magnetic field and that of a plasma in the periodic field of a lattice, in which latter case the role of the quantum number n is played by the band number. Transitions between states with different values of n in the magnetic-field case correspond to interband transitions in the case of the periodic field. In this analogy the difference is that in the case of filled bands the neglect of interband transitions leads to the absence of plasma waves, whereas the neglect of transitions between levels with different values of n leads only to the absence of plasma waves with $\vartheta = \pi/2$. This can be seen from Eq. (21). The first term in the right member of Eq. (21) does not include transitions between states of different n, since it is obtained on the condition $n' = n$; the transitions between states n' and n with $n' \neq n$ are taken into account in the second term.

3. Let us consider the expression for the longitudinal dielectric constant. We introduce $\mathbf{P}(\mathbf{q}, t)$, the Fourier component of the polarization operator, which is connected with the corresponding component of the electric field, $\mathbf{E}(\mathbf{q}, t)$, and the dielectric constant by the well known relation

$$\mathbf{P}(\mathbf{q}, t) = \frac{1}{4\pi}[\varepsilon(\omega, \mathbf{q}) - 1]\,\mathbf{E}(\mathbf{q}, t). \tag{26}$$

Then on taking into account the connection of $\mathbf{E}(\mathbf{q}, t)$ with the potential, that of the polarization with the charge density, and also the relation (26), we get for $\epsilon(\mathbf{q}, \omega)$ the expression in terms of dimensionless quantities:

$$\varepsilon(\omega, \mathbf{q}) = 1 - \lim_{\Gamma\to 0} G(q_x, 0, q_z)\frac{m}{2\pi\hbar^2\alpha}\sum_{nn'} F_{nn'}^2(q_x) \times \int d\zeta\, [f_0(E_{\zeta+q,\,n'}) - f_0(E_{\zeta,\,n})]\,[n' - n + \tfrac{1}{2}(q_z^2 + 2q_z\zeta) - \Omega + i\Gamma]^{-1}. \tag{27}$$

Without taking a concrete form for the function f_0, for small q_z we can write expressions for the real and imaginary parts ϵ' and ϵ'' of the complex quantity ϵ. We get for ϵ' and ϵ'' the expressions

$$\varepsilon'(\omega, \mathbf{q}) = 1 - \frac{2e^2m\alpha}{\pi\hbar^2\Omega^2}\cos^2\vartheta\exp\left\{-\frac{1}{2}q_x^2\right\}\sum_n\int f_0(E_{\zeta,n})\,d\zeta - \frac{2e^2m\alpha}{\pi\hbar^2}\sum_{n;\,n'>n}\frac{C_{nn'}(q, q_x)}{\Omega^2-(n'-n)^2},$$

$$C_{nn'} = F_{nn'}^2(q_x)\,(n'-n)\,q^{-2}\int d\zeta\,[f_0(E_{\zeta,n'}) - f_0(E_{\zeta,n})]; \tag{28}$$

$$\varepsilon''(\omega, \mathbf{q}) = \frac{2e^2m\alpha}{\hbar^2q^2}\exp\left\{-\frac{1}{2}q_x^2\right\}\sum_n\int d\zeta f_0(E_{\zeta,n}) \times \left[\delta\left(\frac{1}{2}q^2\cos^2\vartheta + q\zeta\cos\vartheta - \Omega\right) - \delta\left(\frac{1}{2}q^2\cos^2\vartheta - q\zeta\cos\vartheta + \Omega\right)\right] + \frac{2e^2m\alpha}{\hbar^2q^2}\sum_{n',\,n;\,n'\neq n}\int d\zeta\,[f_0(E_{\zeta,n'}) - f_0(E_{\zeta,n})]\,F_{nn'}^2(q_x)\,\delta[n' - n - \Omega]. \tag{29}$$

The first term in ϵ' is due to transitions without change of the quantum number n, and the second to transitions between states with different values of n. In the language of the band model, the first term describes "intraband" transitions and the second, "interband" transitions. In ϵ'' the first term contains the "intraband" transitions and describes the well known mechanism of damping of the oscillations that was established by Landau.[8] The second term is due to the "interband" transitions and for q = 0 describes "interband" optical absorption. This is natural, since for q = 0 the transverse dielectric constant, which describes the interaction of light with matter, coincides with the longitudinal dielectric constant, which is due to collective oscillations of the electrons. This result was first established by Wolff,[9] and has also been found by Fröhlich and Pelzer.[10]

---

[1] A. I. Akhiezer and L. E. Pargamanik, Уч. зап. ХГУ (Science Notes, Khar'kov. State Univ.) **27**, 75 (1948). E. P. Gross, Phys. Rev. **82**, 232 (1951). G. V. Gordeev, JETP **23**, 660 (1952). M. E. Gertsenshteĭn, JETP **27**, 180 (1954). Al'pert, Ginzburg, and Feĭnberg, Распространение радиоволн (The Propagation of Radio Waves), Gostekhizdat, 1953. A. G. Sitenko and K. N. Stepanov, JETP **31**, 642 (1956), Soviet Phys. JETP **4**, 512 (1957).

[2] V. L. Bonch-Bruevich, Физика твердого тела **2**, 489 (1960), Soviet Phys.-Solid State.

[3] V. A. Yakovlev and A. V. Kalyush, JETP **39**, 308 (1960), Soviet Phys. JETP **12**, 219 (1961).

[4] P. S. Zyryanov, JETP **35**, 448 (1958), Soviet Phys. JETP **8**, 309 (1959).

[5] H. Ehrenreich and M. H. Cohen, Phys. Rev. **115**, 786 (1959).

[6] H. Kanazawa, Prog. Theoret. Phys. **13**, 227 (1955).

[7] Erdelyi, Magnus, Oberhettinger, and Tricomi, Higher Transcendental Functions, New York, 1953, Vol. 2.

[8] L. D. Landau, JETP **16**, 574 (1946).

[9] P. A. Wolff, Phys. Rev. **92**, 18 (1953).

[10] H. Fröhlich and H. Pelzer, Proc. Phys. Soc. **A68**, 525 (1955).

Translated by W. H. Furry
177

SOVIET PHYSICS JETP VOLUME 13, NUMBER 4 OCTOBER, 1961

COMMUTATION FUNCTION OF A NONLINEAR MESON FIELD

D. IVANENKO and D. F. KURDGELAIDZE

Moscow State University

Submitted to JETP editor July 16, 1960

J. Exptl. Theoret. Phys. (U.S.S.R.) 40, 1072-1075 (April, 1961)

A new definition of the commutation function is proposed. Nonlinear meson fields are considered and, in particular, an expression for the commutation function is presented.

THE usual definition of the commutation function of the boson field

$$D(s) = [\overline{\Psi}(x),\ \Psi(x')]_-, \qquad s^2 = -x_\mu^2, \tag{1}$$

[where $\Psi(s)$ is the sum of solutions over the wave vector k] cannot be used in the nonlinear theory, in view of the violation of the superposition principle. The right half of (1) now depends on the wave vector. We therefore propose to start at the very outset from the more general definition

$$D(s) = \sum_{k,\omega}\sum_{k'\omega'}\sum{}' [\overline{\Psi}_{k,\omega}(0),\ \Psi_{k'\omega'}(x - x')]_-\ \rho(k, \omega)\ \rho(k', \omega'), \tag{2}$$

where $\rho(k, \omega)$ is a certain weighting function.

The summation Σ' is over the physically admissible independent wave solutions of the field equation. In the particular case of the linear theory, where $\rho(k, \omega) = 2|\omega|\delta(k_\mu^2)$, we obtain the well-known result (1). In the case

$$\Psi_k(x) = a_k\varphi_k(x), \qquad [\bar{a}_k, a_{k'}]_- = f(k)\delta_{kk'} \tag{3}$$

we obtain from (2)

$$D(s) = \sum_{k,\omega}\sum{}' \eta(k, \omega)\,\varphi_k(x - x'),$$

$$\eta(k, \omega) = f(k)\,\varphi_k(0)\,\rho(k, \omega), \tag{4}$$

where $\varphi_k(x)$ is the wave solution.

In the linear theory the function D(s) is, for any value of $\rho(k, \omega)$, a four-dimensional radially-symmetrical solution of the field equation, made up of the wave solutions. In the case of nonlinear theory this is possible only for a very special choice of $\rho(k, \omega)$. In particular, the simplest choice of the function $2|\omega|\delta(k_\mu^2)$ for $\rho(k, \omega)$, as will be shown later, is found to be unsatisfactory.

If we consider a neutral meson field, obeying the equation

$$(\partial^2/\partial x_\mu^2 + \lambda\varphi^2)\varphi = 0, \tag{5}$$

for which it is natural to take the commutator between the functions $\varphi_k(x)$ and $\varphi_{-k}(x)$ [in nonquantum theory $\varphi_k(x) = \varphi_{-k}(x)$], then its energy can be represented in the form

$$H_k = \frac{1}{4V}\int\left\{\left[\frac{\partial\varphi_k}{\partial x_n}, \frac{\partial\varphi_{-k}}{\partial x_n}\right]_+ - \left[\frac{\partial\varphi_k}{\partial x_4}, \frac{\partial\varphi_k}{\partial x_4}\right]_+ \right.$$
$$\left. + k_0^2[\varphi_k, \varphi_{-k}]_+ + \frac{\lambda}{2}[\varphi_k^3, \varphi_{-k}]_+\right\} d^3x. \tag{6}$$

Calculating further the time average of the energy (with $k_0 = 0$) we obtain[1] ($C = 2/3$):

$$H_k = \frac{C}{2}\omega_k\left(1 - \frac{\lambda}{8\omega_k}[a_k, a_{-k}]_+\right)\frac{1}{2}[a_k, a_{-k}]_+,$$
$$\omega_k = \frac{k}{|k|}\left[k^2 + \frac{\lambda}{2}[a_k, a_{-k}]_+\right]^{1/2}. \tag{7}$$

We introduce the canonical coordinates

$$q_k = a_k \exp(-i\Omega_k t), \qquad \dot{p}_k = -\partial H_k/\partial q_k,$$
$$\Omega_{-k} = -\Omega_k, \qquad q_{-k} = q_k^*. \tag{8}$$

Under the assumption

$$[q_k, q_{-k}]_- = f(k) \tag{*}$$

we obtain

$$p_k(t) = \frac{C}{2}\Omega_k q_k^*, \qquad \Omega_k = \frac{k}{|k|}\left[k^2 + \frac{3\lambda}{4}[a_k, a_{-k}]_+\right]^{1/2}. \tag{9}$$

From this we get

$$[\Omega_k q_k, q_k]_- = [\Omega_k q_k^*, q_k^*]_- = 0,$$
$$[\Omega_k q_k^*, q_k]_- = -[\Omega_k q_k, q_k^*]_- = -2/C. \tag{10}$$

Under condition (*), which is equivalent to the approximation $[a_k, a_{-k}]_+ \approx 2a_k^2$, i.e., to neglect of the quantum character of this expression in the formulas for ω_k and Ω_k, we obtain

$$f(k) = 2/C\Omega_k \quad a_k = \xi_k\sqrt{2/C|\Omega_k|}, \quad a_{-k} = \xi_{-k}\sqrt{2/C|\Omega_{-k}|},$$
$$[\xi_k, \xi_{-k}]_- = 1. \tag{11}$$

Let us attempt now to calculate the sought commutation function D(s) by means of formula (2), using (3) and (11), and assuming $\rho(\mathrm{k}, \omega)$ to have a form analogous to that of the linear case

$$\rho(k, \Omega_k) = \delta\left(\Omega_k + \sqrt{k^2 + \tfrac{3}{2}\beta_k^2}\right) + \delta\left(\Omega_k - \sqrt{k^2 + \tfrac{3}{2}\beta_k^2}\right),$$

$$\beta_k^2 \equiv \lambda a_k^2. \tag{12}$$

We then obtain

$$D_{nl}(s) = \sum_{n=0}^{\infty} A_n D_l(\alpha_n s), \qquad \alpha_n = (2n+1)\lambda a_k \,\mathrm{const},$$

$$A_n = A(n), \tag{13}$$

where $D_l(s)$ is the commutation function of the linear theory.

The result obtained, in view of the known divergence of the linear function $D_l(s)$, is unsatisfactory (from the point of view of constructing a complete field theory). This does not apply, however, to the expressions (2) or (11). Within the limits of assumption (*) Eq. (11) is valid, and we shall make use of it, as well as of (2). What is unsatisfactory is the choice of the form (12) for $\rho(\mathrm{k}, \omega)$.

Inasmuch as we expect no divergences in the linear theory, we must review the definition of the nonlinear commutation function. In this connection we assume that the commutation function is a four-dimensional radially-symmetrical solution of the field equation not only in the linear but also in the nonlinear theory. If we start from such an assumption we obtain for the weighting function $\rho(\mathrm{k}, \omega)$, subject to assumption (3), as the main result of the present investigation, a Fredholm integral equation of the first kind.

$$D(s) = (2\pi)^{-4} \int \sum{}' [\overline{\Psi}_k(0), \Psi_k(x-x')]_- \rho(k, \omega) d^3k d\omega. \tag{14}$$

Here $D(s)$ is a radially-symmetrical solution of the nonlinear equation of the field.

The summation Σ', as already indicated, is carried out over the physically admissible independent wave solutions $\Psi_{\mathrm{k}}(x)$. Thus, Eq. (14) establishes with the aid of the function $\rho(\mathrm{k}, \omega)$ the connection between the wave solutions and radially-symmetrical solutions of the nonlinear field equation.

The condition imposed on (14) is

$$D(0) = 0, \qquad \int \rho(k, \omega) d^3k d\omega = 1. \tag{15}$$

In this connection, let us analyze in greater detail the radially-symmetrical solution of the initial nonlinear generalized Klein-Gordon equation (5).

Equation (5) has in the real domain two independent wave solutions

$$\varphi = \varphi_0 \,\mathrm{cn}\,(k_\mu^{(1)} x_\mu + c_1; k_1), \qquad \omega_{(1)}^2 = k_{(1)}^2 + \lambda\varphi_0^2, \qquad k_1^2 = 1/2,$$

$$\varphi = \varphi_0 \,\mathrm{sn}\,(k_\mu^{(2)} x_\mu + c_2;\ i\,|k_2|)$$

$$= \frac{\varphi_0}{\sqrt{2}} \frac{\mathrm{sn}\,(k_\mu^{(1)} x_\mu + \sqrt{2}c_2;\ k_1)}{\mathrm{dn}\,(k_\mu^{(1)} x_\mu + \sqrt{2}c_2;\ k_1)}, \ |k_2| = 1,$$

where $\mathrm{k}_\mu^{(1)} = \sqrt{2}\mathrm{k}_\mu^{(2)}$.

As wave solutions, both solutions are physically admissible. However, Eq. (5) has two independent radially-symmetrical solutions, corresponding to the two independent wave solutions mentioned, namely cn(u) and sn(u). The radially symmetric solution corresponding to sn(u) is in this case complex (when $\lambda > 0$ and $s^2 > 0$). In this connection we neglect both the radially-symmetrical solution corresponding to the wave solution sn(u) and the wave solution sn(u) itself. The real radially-symmetrical solution of Eq. (5) is given by the following formulas (see reference 1)

$$\underset{(\lambda s^2>0)}{\varphi(s, k_1)} = \begin{cases} \left(\dfrac{2}{\lambda s_0^2(2-k_2^2)}\right)^{1/2} \left(\dfrac{s_0}{s}\right) \mathrm{dn}\left[\dfrac{\ln(s_0/s)}{\sqrt{2-k_2^2}}\right], & 0 < k_2^2 = k_1^{-2} \leqslant 1, \quad \text{(16a)} \\ \left(\dfrac{2k_1^2}{\lambda s_0^2(2k_1^2-1)}\right)^{1/2} \left(\dfrac{s_0}{s}\right) \mathrm{cn}\left[\dfrac{\ln(s_0/s)}{\sqrt{2k_1^2-1}}\right], & \tfrac{1}{2} < k_1^2 \leqslant 1, \quad \text{(16b)} \\ 0 & 0 \leqslant k_1^2 \leqslant \tfrac{1}{2}, \quad \text{(16c)} \end{cases}$$

where k_1 and k_2 are the moduli of the corresponding elliptic functions.

When $\mathrm{k}_2 = 0$ and $\mathrm{k}_2^2 = 1$ we have

$$\varphi(s, k_2 = 0) = \sqrt{\frac{1}{\lambda s_0^2}} \left(\frac{s_0}{s}\right),$$

$$\varphi(s, k_2^2 = 1) = \sqrt{\frac{2}{\lambda s_0^2}} \frac{1}{1 + (s/s_0)^2}. \tag{17}$$

This last particular solution was used by Borgart as a commutation function.[2]

In the region $0 < \mathrm{k}_2^2 = \mathrm{k}_1^{-2} \le 1$ we have $\mathrm{k}_2' = \sqrt{1 - \mathrm{k}_2^2} \le \mathrm{dn}(u) \le 1$, and therefore the function tends to zero only as $s \to \infty$. On the other hand, in the region $1/2 < \mathrm{k}_1^2 < 1$ the function cn(u) executes infinite oscillations as $s \to 0$, and we can put

$$\varphi(0, k_1) = 0, \qquad \tfrac{1}{2} < k_1^2 \leqslant 1. \tag{18}$$

This behavior of the proposed commutation function, which falls off like $1/s$ as $s \to \infty$ and which vanishes on the average as $s \to 0$, corresponds very closely to the conditions imposed by Heisenberg[3] on the commutation function of the nonlinear spinor field. Therefore our commutation function can be employed in analogous problems.

Thus, for D(s) we can take a radially-symmetrical solution of the form (16b). With this the integral equation (14) can be simplified by approximately replacing the elliptic functions with trigonometric ones. We then obtain for the weighting function the expression

$$\rho(k,\ \omega) \approx \frac{\mathrm{const}}{[a_k,\ a_{-k}]_-} \int \cos\left(\frac{\ln(s_0/s)}{\sqrt{2k_1^2 - 1}}\right) \cos(k_\mu x_\mu) \frac{d^4x}{s}, \quad (19)$$

where $[a_k, a_{-k}]_-$ can be determined from (3) and (11).

The results obtained can subsequently be used for specific calculations, by obvious generalization to the case of other boson and spinor nonlinear fields and by establishing a connection with the Greenians and other singular functions.

Note added in proof (March 12, 1961). A similar suggestion is made by H. Mitter in the case of a spinor nonlinear field. We are grateful to him and to H. P. Dürr for supplying us with a preprint.

---

[1] D. F. Kurgelaidze, JETP **38**, 842 (1959), Soviet Phys. JETP **9**, 594 (1959).

[2] A. Borgart, Trudy, First All-Union Inter-University Theoretical Conference, Uzhgorod, 1958.

[3] Heisenberg, Dürr, Mitter, Schlieder, and Yamazaki, Z. Naturforsch. **14a**, 441 (1959).

Translated by J. G. Adashko
178

SOVIET PHYSICS JETP VOLUME 13, NUMBER 4 OCTOBER, 1961

ON THE USE OF AN ARBITRARY GAUGE OF THE ELECTROMAGNETIC POTENTIALS IN THE DISPERSION METHOD

V. D. MUR and V. D. SKARZHINSKII

P. N. Lebedev Physics Institute, Academy of Sciences, U.S.S.R.

J. Exptl. Theoret. Phys. (U.S.S.R.) **40**, 1076-1079 (April, 1961)

Submitted to JETP editor July 22, 1960

The problem of the use of an arbitrary gauge of the electromagnetic potential of quantum electrodynamics within the framework of the dispersion method is considered. Several formulae are obtained which are generalizations of known expressions.

IT is well known that owing to gauge invariance of quantum electrodynamics all physically meaningful quantities are independent of the gauge of the electromagnetic potentials. However there exist quantities in the theory which are not independent of the gauge, like, for example, the propagator, the vertex function, and diverse matrix elements. It is therefore desirable to discuss them in a general gauge. In particular, this facilitates the evaluation of these quantities.

In the dispersion method such an approach is difficult since there exists no unique method which would allow to determine the dependence on the gauge for a number of quantities. In particular, when writing matrix elements in covariant notation the summation over intermediate states, e.g. in reduction formulae, are usually carried out in the diagonal gauge ($d_l = 1$).

In the present paper[*] we shall study the systematic treatment of an arbitrary gauge in the dispersion method.

1. It is well known that the quantized vector potential of the free electromagnetic field[†] whose Lagrangian is given by

$$L(x) = -\frac{1}{2}\frac{\partial A_\mu(x)}{\partial x^\nu}\frac{\partial A_\mu(x)}{\partial x^\nu} \tag{1.1}$$

can be written in the form

$$A_\mu(x) = (2\pi)^{-3/2}\int d^4k\sqrt{2k_0}\,\theta(k_0)\,\delta(k^2)\,e_\mu^\lambda\,\{e^{ikx}c_\lambda^+(\mathbf{k}) + e^{-ikx}c_\lambda^-(\mathbf{k})\}, \tag{1.2}$$

while the commutation relations for the operators $c_\lambda^\pm(\mathbf{k})$ follow from the form of the Lagrangian (the structure of the operator is that of the energy-momentum 4-vector P_μ), from the requirement of a positive energy and from translational invariance:

$$\partial A_\mu(x)/\partial x^\nu = i\,[P_\nu, A_\mu(x)]. \tag{1.3}$$

The operator $A_\mu(x)$ is determined up to a gauge transformation

$$A_\mu(x) \to A'_\mu(x) = A_\mu(x) + \partial f(x)/\partial x^\mu, \tag{1.4}$$

where $f(x)$ is, generally speaking, an arbitrary operator function. Expressing $A_\mu(x)$ in terms of $A'_\mu(x)$ by means of the implicit equation (1.4) and inserting in (1.1) we obtain

$$L(A_\mu(x)) = L'(A'_\mu(x)), \tag{1.5}$$

where L' indicates the change in the form of the Lagrangian induced by the gauge transformation (1.4). As a result of the change of $L(x)$ the equation for $A_\mu(x)$ changes into

$$\Box A'_\mu(x) = -\partial\Box f(x)/\partial x^\mu. \tag{1.6}$$

We note that in a gauge transformation both the change of $A_\mu(x)$ to $A'_\mu(x)$ and the change indicated by (1.5) has to be considered in order to maintain the original quantization scheme, i.e., the meaning and the commutation relations of the operators $c_\lambda^\pm(\mathbf{k})$. In particular, then also the form of the energy-momentum vector P_μ remains unchanged.

We now are going to find a class of functions $f(x)$ which obey the following conditions: (i) the operators $A'_\mu(x)$ are Hermitian; (ii) the operators $A'_\mu(x)$ are translationally invariant:

$$\partial A'_\mu(x)/\partial x^\nu = i\,[P_\nu, A'_\mu(x)]; \tag{1.7}$$

(iii) the gauge transformation (1.4) has to lead to the known expression for the photon propagator

---

[*] The basic results of this work have already been utilized in a previous paper[1] by the present authors.

[†] Due to the gauge invariance of the S-matrix (see reference 2, p. 247) the results obtained below are valid also for interacting fields.

$$D_{\mu\nu}(k) = -\frac{1}{k^2+i\varepsilon}\left\{\left(\delta_{\mu\nu}-\frac{k_\mu k_\nu}{k^2}\right)+d_l\,\frac{k_\mu k_\nu}{k^2}\right\}, \qquad (1.8)$$

where the range of the quantities d_l has to include at least the values $d_l = 0$ and $d_l = 1$. These correspond to the important cases of the transversal and diagonal gauge respectively.

These requirements substantially restrict the form of $f(x)$. As can be easily seen, (1.7) leads to a linear dependence of $f(x)$ on the field operators. Condition (i) restricts $f(x)$ to the class of functions of the form

$$\partial f(x)/\partial x^\mu = (2\pi)^{-3/2}\int d^4k\,\sqrt{2k_0}\,\theta(k_0)\,\delta(k^2) \times k_\mu(e^\lambda k)\,f_\pm(k^2)\,[e^{ikx}c^+_\lambda(\mathbf{k}) \pm e^{-ikx}c^-_\lambda(\mathbf{k})], \qquad (1.9)$$

where $f_+(k^2)$ and $if_-(k^2)$ are arbitrary real functions. Condition (iii) allows to connect $f_\pm(k^2)$ with the longitudinal part of $D_{\mu\nu}(k)$. We obtain immediately (see reference 2, p. 259)

$$f_+(k^2) = (\sqrt{d_l}-1)/k^2, \qquad if_-(k^2) = \sqrt{d_l-1}/k^2, \qquad (1.10)$$

and the requirement $d_l \geq 0$ eliminates the second possibility.

From (1.9) and (1.10) one sees that $\partial\Box f(x)/\partial x^\mu \neq 0$, and thus (1.6) differs considerably from the equation for $A_\mu(x)$. We do not consider here the specialized gauge transformation with $\Box f(x) = 0$.

The relations (1.2), (1.4), (1.9), and (1.10) allow to write $A'_\mu(x)$ in the form

$$A'_\mu(x) = (2\pi)^{-3/2}\int d^4k\,\sqrt{2k_0}\,\theta(k_0)\,\delta(k^2)\,\tilde{e}^\lambda_\mu(k)\,\{e^{ikx}\,c^+_\lambda(\mathbf{k}) + e^{-ikx}c^-_\lambda(\mathbf{k})\}, \qquad (1.11)$$

where

$$\tilde{e}^\lambda_\mu(k) = e^\lambda_\mu + k_\mu\,k^{-2}\,(e^\lambda k)\,(\sqrt{d_l}-1). \qquad (1.11')$$

The pole $k^2 = 0$ in the integrals of the form

$$\int d^4k\,\varphi(k)\,\delta(k^2)/k^2$$

is understood to be taken as a principal value. In actual calculations it is convenient to utilize

$$\mathrm{P}x^{-1}\delta(x) = -\delta'(x).$$

We note that due to

$$\partial A'^{\pm}_\mu(x)/\partial x^\mu = \sqrt{d_l}\,\partial A^\pm_\mu(x)/\partial x^\mu \qquad (1.12)$$

the admissible states remain unchanged, and the relation

$$\langle\Phi_{\mathrm{adm}},\, A'_\mu(x)\,\Phi_{\mathrm{adm}}\rangle = \langle\Phi_{\mathrm{adm}},\, A_\mu(x)\,\Phi_{\mathrm{adm}}\rangle \qquad (1.13)$$

insures the correspondence with Maxwell's equations. Indeed, one sees from (1.13) that the appearance of d_l in the propagator $D_{\mu\nu}(k)$ is associated with a change in the unphysical part of $A_\mu(x)$.

We can thus say that a gauge transformation which obeys the above specified conditions turns out to change the polarization vectors e^λ_μ into $\tilde{e}^\lambda_\mu$ in the expansion (1.2) of the operators $A_\mu(x)$ in terms of the operators $c^\pm_\lambda(\mathbf{k})$. In the following we shall omit the prime in $A'_\mu(x)$.

It is easy to see that the dependence of matrix elements on d_l when separating them out from the dependence on photons is exactly the same. For example, the matrix element $\langle\alpha\,|\,F\,|\,\beta;\ \mathbf{k}\lambda\rangle$ of an arbitrary operator F (the indices **k** and λ denote a photon of momentum **k** and polarization λ) in the diagonal gauge due to considerations of covariance can be written in the form $\langle\alpha\,|\,F\,|\,\beta;\ \mathbf{k}\lambda\rangle = e^\lambda_\mu F_\mu$. After a gauge transformation this changes to $\langle\alpha\,|\,F\,|\,\beta;\ \mathbf{k}\lambda\rangle = \tilde{e}^\lambda_\mu(\mathrm{k})\,F_\mu(d_l)$. In case of gauge invariance of F_μ the whole dependence of the matrix element $\langle\alpha\,|\,F\,|\,\beta;\ \mathbf{k}\lambda\rangle$ on d_l is contained in $\tilde{e}^\lambda_\mu(\mathrm{k})$.

2. When investigating matrix elements it is frequently necessary to bring them into a covariant form. The use of an arbitrary gauge introduces certain changes into the expressions which give the operators $c^\pm_\lambda(\mathbf{k})$ in terms of $A_\mu(x)$. One can easily show that

$$\tilde{e}^\lambda_\mu(\mathbf{k})\,c^\pm_\lambda(\mathbf{k}) = \frac{\mp i}{(2\pi)^{3/2}}\frac{1}{\sqrt{2k_0}}\int d\mathrm{x}\,e^{\mp ikx}\,\frac{\overleftrightarrow{\partial}}{\partial x^0}A_\mu(x). \qquad (2.1)$$

In order to split off $c^\pm_\lambda(\mathbf{k})$ we introduce the vectors $\bar{e}^\lambda_\mu(\mathrm{k})$ which are taken to be orthogonal to $\tilde{e}^\lambda_\mu(\mathrm{k})$:

$$\bar{e}^\lambda_\mu(k) = e^\lambda_\mu + k_\mu\,(e^\lambda k)\,k^{-2}\,(1/\sqrt{d_l}-1). \qquad (2.2)$$

Indeed,

$$\bar{e}^\lambda_\mu(k)\,\tilde{e}^\lambda_\nu(k) = \delta_{\mu\nu}; \qquad \bar{e}^\lambda_\mu(k)\,\tilde{e}^\nu_\mu(k) = \delta_{\lambda\nu}. \qquad (2.3)$$

From (2.1) and (2.3) we obtain

$$c^\pm_\lambda(\mathbf{k}) = \frac{\mp i}{(2\pi)^{3/2}}\frac{1}{\sqrt{2k_0}}\,\bar{e}^\lambda_\mu(k)\int d\mathrm{x}\,e^{\mp ikx}\,\frac{\overleftrightarrow{\partial}}{\partial x^0}A_\mu(x). \qquad (2.4)$$

This way one has to exchange the polarization vectors e^λ_μ for $\bar{e}^\lambda_\mu(\mathrm{k})$ in the usual reduction formulae when one goes to arbitrary gauge.

However, it is more convenient to use (2.4) in a somewhat changed form, namely, in terms of $\tilde{e}^\lambda_\mu$ instead of $\bar{e}^\lambda_\mu$ (see the concluding remarks of section 1.). Using the relation

$$\bar{e}^\lambda_\mu(k) = \tilde{e}^\lambda_\mu(k) + k_\mu\,(e^\lambda k)\,k^{-2}(1/\sqrt{d_l}-\sqrt{d_l}), \qquad (2.5)$$

we obtain from (2.4)

$$c^\pm_\lambda(\mathbf{k}) = \mp\frac{i}{(2\pi)^{3/2}}\frac{1}{\sqrt{2k_0}}\,\tilde{e}^\lambda_\mu(k)\int d\mathrm{x}\,e^{\mp ikx}\,\frac{\overleftrightarrow{\partial}}{\partial x^0}A_\mu(x) \mp\frac{i}{(2\pi)^{3/2}}\frac{k_\mu}{\sqrt{2k_0}}\frac{(e^\lambda k)}{k^2}\left(\frac{1}{\sqrt{d_l}}-\sqrt{d_l}\right)\int d\mathrm{x}\,e^{\mp ikx}\,\frac{\overleftrightarrow{\partial}}{\partial x^0}A_\mu(x). \qquad (2.6)$$

When utilizing (2.4) and (2.6) to bring matrix elements into covariant form there appear different Green's functions which can be expressed in terms of G, $D_{\mu\nu}$ and Γ_μ. These, and also the second term of (2.6) can be brought to a simpler form by means of the relations[3]

$$k_\mu D_{\mu\nu}(k) = -k_\nu d_l/(k^2 + i\varepsilon)\ ,$$
$$k_\mu \Gamma_\mu(p, p-k) = G^{-1}(p) - G^{-1}(p-k). \qquad (2.7)$$

3. In the dispersion method, frequent use is made of expansions into intermediate states, in which the eigenfunctions of the free field energy-momentum operator are taken as the complete set of states. In quantum electrodynamics such a set of intermediate states is taken which besides the transverse photons contains also the longitudinal and scalar photons. Therefore in the sum over intermediate states

$$\langle\alpha|AB|\beta\rangle = \Sigma\langle\alpha|A|n\rangle\langle n|B|\beta\rangle$$

the summation over the polarization λ goes from 0 to 3. Writing the matrix elements of A and B which contain the polarization index in arbitrary gauge in the form

$$\tilde{e}^\lambda_\mu(k)A_\mu, \qquad \tilde{e}^\lambda_\mu(k)B_\mu,$$

we find that instead of $e^\lambda_\mu e^\lambda_\nu = \delta_{\mu\nu}$ there appears, according to (1.11′),

$$\tilde{e}^\lambda_\mu(k)\,\tilde{e}^\lambda_\nu(k) = (\delta_{\mu\nu} - k_\mu k_\nu/k^2) + d_l k_\mu k_\nu/k^2.$$

In conclusion the authors express their deep gratitude to V. Ya. Faĭnberg and E. S. Fradkin for stimulating discussions and continuing interest in the work.

---

[1] V. D. Mur and V. D. Skrazhinskii, JETP **38**, 1817 (1960), Soviet Phys. JETP **11**, 1308 (1960).

[2] N. N. Bogolyubov and D. V. Shirokov, Введение в теорию квантованных полей (Introduction into the Theory of Quantized Fields), Interscience, 1959.

[3] E. S. Fradkin, JETP **29**, 258 (1955), Soviet Phys. JETP **2**, 361 (1956).

Translated by M. Danos
179

SOVIET PHYSICS JETP VOLUME 13, NUMBER 4 OCTOBER, 1961

RESONANCE CHARGE EXCHANGE IN HYDROGEN AND SODIUM

Yu. E. MURAKHVER

Leningrad Physico-Technical Institute, Academy of Sciences, U.S.S.R.

Submitted to JETP editor July 21, 1960; resubmitted December 6, 1960

J. Exptl. Theoret. Phys. (U.S.S.R.) 40, 1080-1084 (April, 1961)

Two problems are considered within the framework of the parametric method: 1) Resonance charge exchange of protons in atomic hydrogen. Its probability at all velocities can be expressed through a single integral involving Hankel functions. A numerical calculation is carried out for a single value of the velocity v of the relative motion of the nuclei. 2) Single resonance charge exchange of Na^+ ions in sodium. Up to the present, charge exchange involving complex atoms has been considered in the hydrogen-like approximation. In this article, the calculation is based on analytical wave functions and the analytical expression for the field of the atomic core. These expressions approximate the corresponding quantities computed by the Hartree-Fock method. Results are obtained for all values of v (within the limits of applicability of the parametric method).

1. INTRODUCTION

COLLISIONS between atomic systems for which the energy of the relative motion is of the order 1 ev and higher are most conveniently studied by means of the parametric method.[1-5]

We shall consider the charge exchange

$$(A+e)+B\to A+(B+e), \tag{1}$$

where A and B are certain atomic systems. Its probability is given with sufficient accuracy by the formula*

$$w_{n_An_B}=|A_{n_An_B}|^2=\Big|\int_{-\infty}^{\infty}\exp\Big\{-i\frac{v^2}{2}t+iE_{n_B}t-iE_{n_A}t+i\int\langle\psi_{n_B}|V_A|\psi_{n_B}\rangle\,dt-i\int\langle\psi_{n_A}|V_B|\psi_{n_A}\rangle\,dt\Big\}\,dt\int\psi^*_{n_B}(\mathbf{r}-\mathbf{s})\,[V_B(|\mathbf{r}-\mathbf{s}|)-\langle\psi_{n_A}|V_B|\psi_{n_A}\rangle]\,e^{i\mathbf{v}\mathbf{r}}\,\psi_{n_A}(\mathbf{r})\,d\mathbf{r}\Big|^2, \tag{2}$$

in which ψ_{n_A} (or ψ_{n_B}) and E_{n_A} (or E_{n_B}) are the eigenfunction and energy, respectively, of an electron bound to nucleus A (or B) in the state n_A (or n_B); V_A and V_B are the interaction energies between the electron and nuclei A and B; s is the trajectory of the relative motion of the "nuclei." Formula (2) is valid for $w_{n_An_B}\ll 1$. Its derivation can be found, for example, in the paper of Bates.[5]

For (symmetric) resonance, when $E_{n_A}=E_{n_B}$,

$$\langle\psi_{n_A}|V_B|\psi_{n_A}\rangle=\langle\psi_{n_B}|V_A|\psi_{n_B}\rangle$$

(and v^2/Z_A and $v^2/Z_B\ll 1$, where Z_A and Z_B are the effective charges of nuclei A and B), formula (2) gives a value of $w_{n_An_B}$ much greater than unity. In this case, we should use, instead of (2),

$$w_{n_An_B}=\sin^2|A_{n_An_B}|. \tag{3}$$

In fact, (3) coincides with the formula for the probability of resonance charge exchange obtained by Firsov[3] and Demkov[4] if in the latter the molecular terms are calculated in the first-order approximation of perturbation theory. For $|A_{n_An_B}|^2\ll 1$, formula (3) goes over into (2).

2. RESONANCE CHARGE EXCHANGE OF PROTONS IN ATOMIC HYDROGEN

By (2) and (3), the probability of the process is given by the formula

$$w=\sin^2|J_1-J_2|, \tag{4}$$

where

$$J_1=\frac{1}{\pi}\int_{-\infty}^{\infty}\exp\Big(-i\frac{v^2}{2}t\Big)\,dt\int\frac{1}{|\mathbf{r}-\mathbf{s}|}\exp(-r-|\mathbf{r}-\mathbf{s}|+i\mathbf{v}\mathbf{r})\,d\mathbf{r},$$

$$J_2=\frac{1}{\pi}\int_{-\infty}^{\infty}\exp\Big(-i\frac{v^2}{2}t\Big)[s^{-1}+(s^{-1}+1)\,e^{-2s}]\,dt\int\exp(-r-|\mathbf{r}-\mathbf{s}|+i\mathbf{v}\mathbf{r})\,d\mathbf{r}.$$

As usual, we neglect the curvature of the trajectory of the relative motion of the nuclei, i.e., we set

$$\mathbf{s}=\boldsymbol{\rho}+\mathbf{v}t,\qquad \boldsymbol{\rho}\mathbf{v}=0 \tag{5}$$

---

*Atomic units are used throughout.

(ρ is the collision parameter). In the case of resonance, this introduces no error.

The integral J_1 has been calculated by Brinkman and Kramers.[1]

$$J_1 = \frac{2\rho^2}{v(1+v^2/4)} K_2(\rho\sqrt{1+v^2/4}).$$

We shall now consider the determination of J_2 (see Appendix). The occurrence of this term results from the physical condition that the chosen perturbation be a minimum (in a certain sense), or more precisely, from the fact that the mean value of the perturbation in the state described by the electronic wave function is equal to zero. We find that

$$J_2 = \frac{32}{\pi v} \int_{-\infty}^{\infty} \Big[K_0(\rho|\xi|) - K_0(\rho\sqrt{4+\xi^2}) - \frac{2\rho}{\sqrt{4+\xi^2}} K_1(\rho\sqrt{4+\xi^2}) \Big] \Big\{ \frac{2}{(2v\xi)^3} [K_0(\rho R_+) - K_0(\rho R_-)] + \frac{\rho}{2(2v\xi)^2} \Big[\frac{K_1(\rho R_+)}{R_+} + \frac{K_1(\rho R_-)}{R_-} \Big] \Big\} d\xi,$$

$$R_\pm = \sqrt{1+(\xi \pm v/2)^2}. \tag{7}$$

Bassel and Gerjuoy[6] derived an expression for the probability of the process [where the term (7) was written as a single integral of more complex form]. Along with this, they obtained, by Born's method, an analytical expression for the probability of the process as a function of the scattering angle. Hence the calculations by Born's method in explicit form can be advanced somewhat further. This method, however, is applicable only at large velocities, while the parametric method permits the construction of an approximation that is suitable for small v.

The numerical calculations were performed for an energy 100 kev ($v = 2$). Here $|J_1 - J_2|^2 \ll 1$ for all ρ, and the total cross section was calculated from the formula

$$\sigma = \int_0^\infty |J_1 - J_2|^2 \, 2\pi\rho \, d\rho. \tag{8}$$

Our curve for the probability $|J_1 - J_2|^2$ and the curve given by Bassel and Gerjuoy[6] turned out to be identical.

For the total cross section, we found the value $\sigma = 0.34$. The following values were found by Bassel and Gerjuoy,[6] Jackson and Schiff[7] (in whose paper the term $\langle \psi_{nA} | V_B | \psi_{nA} \rangle$ was replaced by s^{-1}), and Brinkman and Kramers[1] (the perturbation contains only the term V_B): $\sigma_{BG} = 0.32$, $\sigma_{JS} = 0.26$, and $\sigma_{BK} = 1.26$. Hence, for medium v ($v^2 \sim 1$), the results of Jackson and Schiff[7] are more accurate than those of Brinkman and Kramers,[1] while for large v ($v^2 \gg 1$), the value σ_{BK}, and not σ_{JS}, coincides with the accurate value.[6]

3. RESONANCE CHARGE EXCHANGE OF SINGLY CHARGED POSITIVE SODIUM IONS IN SODIUM

We shall calculate this process in order to see how accurately the universal formulas obtained in a number of papers* on the basis of the approximation involving hydrogen-like functions describes a single charge exchange.

We assume that the charge exchange involves only the outer 3s electron and we employ the analytical wave functions[9] and the analytical expression for the field of the atomic core obtained by I. V. Abarenkov (private communication);

$$\psi_{30}(r) = 0.1704(1 - 5.268r + 4.013r^2)e^{-r}r \tag{9}$$

(this function was normalized to 4π);

$$V_B(r) = r^{-1}\{1 + 15.85e^{-3.6r} - 5.85e^{-16.1r} - 75.2\,r\,e^{-0.9r}\}. \tag{10}$$

Proceeding along the lines indicated in the Appendix, we obtain an expression for the probability amplitude of the process A in terms of a large number of integrals of the form†

$$J_{mn}(\alpha,\beta) = \int_{-\infty}^{\infty} \exp\Big(-i\frac{v^2}{2}t\Big)dt \int \exp(-\alpha r - \beta|\mathbf{r}-\mathbf{s}| + i\mathbf{v}\mathbf{r}) r^{m-1} |\mathbf{r}-\mathbf{s}|^{n-1} d\mathbf{r} = (-1)^{m+n}(\partial^{m+n}/\partial\alpha^m \partial\beta^n) J_{00}(\alpha,\beta); \tag{11}$$

$$J_{00}(\alpha,\beta) = \frac{8\pi}{v(\alpha^2-\beta^2)} \Big[K_0\Big(\rho\sqrt{\beta^2+\frac{v^2}{4}}\Big) - K_0\Big(\rho\sqrt{\alpha^2+\frac{v^2}{4}}\Big) \Big]. \tag{12}$$

The extremely cumbersome calculations were carried out by the method suggested by Demkov,[4] i.e., the cross section was determined from the formula

$$\sigma = \tfrac{1}{2}\pi\rho_0^2 + \int_{\rho_0}^{\infty} |A|^2 \, 2\pi\rho \, d\rho, \tag{13}$$

where ρ_0 is the largest root of the equation

$$|A|^2 = 1/2 \tag{14}$$

(in the case of those v for which $|A|^2 < 1/2$, we take $\rho_0 = 0$). The results are shown in the table, in which σ_1 are the results of the present work, σ_2 are those obtained previously,[8] and σ_e are the

---

*In the papers of Firsov[3] and Demkov,[4] the corresponding calculations were limited to small v; the present author obtained results[8] which were valid for both small and large v.

†We do not include the term $\langle \psi_{n_A} | V_B | \psi_{n_A} \rangle$ here.

Cross section	v^2			
	0.00026	0.0037	6	$v \to \infty$
σ_1	385	270	0,00167	$3.8 \cdot 10^4 \, v^{-12}$
σ_2	388	272	0,00915	$1.3 \cdot 10^3 \, v^{-12}$
σ_e	329	164	—	—

experimental data.[10] The table also gives expressions for $\sigma(v)$ as $v \to \infty$.

For the lowest value of the velocity ($v^2 = 0.00026$), the cross section was also calculated by Firsov's method.[3] The value obtained here is somewhat greater (by less than 10%) than that shown in the table.

It is seen from the table that for small v (in the case of resonance charge exchange), the hydrogen-like approximation is accurate. In view of the fact that, for small v, the cross section has the form[4]

$$\sigma(v) = (a - b \ln v^2)^2, \tag{15}$$

its value at two points completely determines the shape of the curve.

For large v, the calculations with hydrogen-like functions lead to results that are correct only as regards the order of magnitude. This is explained by the fact that there is such a sizable decrease in the effective distance of charge exchange that the detailed behavior of the wave function and the perturbation energy close to the origin prove to be important. The size of the cross section is then determined by two competitive factors: 1) At small distances between the electron and the incident nucleus, the effective charge is much larger than in the hydrogen-like approximation. 2) The probability of the electron being close to the nucleus is much less than in the hydrogen-like approximation.

It should be noted that, at very large v, inelastic transitions of 2p and 2s, and then 1s electrons begin to play the main role as the energy increases.* If we estimate the charge-exchange cross section for $v^2 \gg 400$ (energy much greater than 200 Mev), when captures of 1s electrons are most important, then it turns out that it is of the same order of magnitude as in the case of the capture of an electron bound to a "bare" sodium nucleus by another such nucleus (i.e., the result obtained by Brinkman and Kramers[1] is 2×10^7 times that shown in the fourth column of the table ($v \to \infty$).

Thus, for v^2 in the range

$$6 < v^2 < 400 \tag{16}$$

the charge-exchange cross section drops much more slowly than v^{-12}, and only for v^2 of the order 1000 does it begin to fall off like v^{-12}. If it is necessary to make a rough estimate of the cross section in the range (16), its value for $v^2 = 6$ (third column of the table) should be matched to the value for v^2 of the order 1000.

In conclusion, the author tanks G. F. Drukarev for valuable advice and A. Ya. Chernyak for performing the tedious calculations.

APPENDIX

Using the Fourier transformation

$$r^{-1} e^{-\gamma r} = \frac{1}{2\pi^2} \int \frac{\exp(i\mathbf{kr})\, d\mathbf{k}}{\gamma^2 + k^2},$$

we rewrite the expression for J_2 in the form

$$J_2 = \frac{8}{\pi^2 v} \int_{-\infty}^{\infty} \left[\frac{1}{\sqrt{x^2+\rho^2}} - \left(1 + \frac{1}{\sqrt{x^2+\rho^2}}\right) \exp(-2\sqrt{x^2+\rho^2}) \right]$$

$$\times\, dx \iiint_{-\infty}^{\infty} \frac{\exp(ix\xi + i\rho\eta)\, d\xi\, d\eta\, d\zeta}{[1 + (\xi + v/2)^2 + \eta^2 + \zeta^2]^2 [1 + (\xi - v/2)^2 + \eta^2 + \zeta^2]^2}.$$

Integrating over x, we obtain (see ref. 11, p. 281)

$$J_2 = \frac{16}{\pi^2 v} \int_{-\infty}^{\infty} g(\xi)\, d\xi \iint_{-\infty}^{\infty} \exp(i\rho\eta)\, d\eta\, d\zeta\, [1 + (\xi + \tfrac{1}{2} v)^2$$

$$+ \eta^2 + \zeta^2]^{-2}\, [1 + (\xi - \tfrac{1}{2} v)^2 + \eta^2 + \zeta^2]^{-2},$$

where

$$g(\xi) = K_0(\rho\,|\xi|) - K_0(\rho\sqrt{4+\xi^2})$$

$$- \frac{2\rho}{\sqrt{4+\xi^2}} K_1(\rho\sqrt{4+\xi^2}).$$

We break up the integrand into simpler fractions and carry out a change of variables. We then obtain

$$J_2 = \frac{32}{\pi v} \int_{-\infty}^{\infty} g(\xi)\, d\xi \int_{0}^{\infty} J_0(\rho r) \left\{ \frac{1}{(2v\xi)^2} [[1 \right.$$

$$+ (\xi + \tfrac{1}{2} v)^2 + r^2]^{-2} + [1 + (\xi - \tfrac{1}{2} v)^2 + r^2]^{-2}]$$

$$+ \frac{2}{(2v\xi)^3} \left[\left[1 + \left(\xi + \frac{v}{2}\right)^2 + r^2 \right]^{-1} - \left[1 + \left(\xi - \frac{v}{2}\right)^2 \right. \right.$$

$$\left. \left. \left. + r^2 \right]^{-1} \right] \right\} r\, dr,$$

from which (see reference 11, p. 260) we arrive at the final formula (7).

---

*Since the second factor indicated above is not involved in these transitions.

[1] H. C. Brinkman and H. A. Kramers, Proc. Acad. Sci. Amsterdam **33**, 973 (1930).

[2] J. W. Frame, Proc. Cambridge Phil. Soc. **27**, 511 (1931).

[3] O. B. Firsov, JETP **21**, 1001 (1951).

[4] Yu. N. Demkov, Ученые записки ЛГУ (Scientific Papers, Leningrad State Univ.) **8**, 74 (1952).

[5] D. R. Bates, Proc. Roy. Soc (London) A247 294 (1958).

[6] R. H. Bassel and E. Gerjuoy, Phys. Rev. 117, 749 (1960).

[7] J. D. Jackson and H. Schiff, Phys. Rev. 89, 359 (1953).

[8] Yu. E. Murakhver, Вестник ЛГУ Leningrad State Univ. Reports, No. 4 (1961).

[9] V. Ya. Vel'dre, Izv. Akad. Nauk LatvSSR, No. 5, 105 (1956).

[10] A. M. Bukhteev and Yu. F. Bydin, Izv. Akad. Nauk SSSR, Ser. Fiz. 24, 964 (1960), Columbia Tech. Transl., in press.

[11] I. M. Ryzhik and I. S. Gradshteĭn, Таблицы интегралов, сумм, рядов и произведений (Tables of Integrals, Sums, Series, and Products), Gostekhizdat, Moscow, 1951.

Translated by E. Marquit
180

SOVIET PHYSICS JETP VOLUME 13, NUMBER 4 OCTOBER, 1961

DOUBLE DISPERSION RELATIONS AND PHOTOPRODUCTION OF PIONS

N. F. NELIPA

P. N. Lebedev Physics Institute, Academy of Sciences, U.S.S.R.

Submitted to JETP editor August 3, 1960; resubmitted January 4, 1961

J. Exptl. Theoret. Phys. (U.S.S.R.) **40**, 1085-1092 (April, 1961)

A set of integral equations is obtained for the partial photoproduction amplitudes. It differs from that previously found in that besides the partial amplitudes for scattering of pions on nucleons it also contains the partial amplitudes for nucleon pair annihilation into two pions and the photoproduction of pions on pions. These amplitudes are related to the partial amplitudes for scattering of pions by pions.

1. Dispersion relations in energy and momentum transfer simultaneously (double dispersion relations) were proposed by Mandelstam[1] for transition amplitudes. Thereafter Chew and Mandelstam[2] developed a method, applicable at low energies, for reducing the double dispersion relations to single dispersion relations for partial amplitudes. Further development of the Mandelstam representation was accomplished by Cini and Fubini[3] and Ter-Martirosyan.[4]

Because certain complications arose (see Appendix 1) when the Chew-Mandelstam method was applied to an analysis of meson* photoproduction on nucleons, it became of interest to discuss this process in the framework of the Cini–Fubini–Ter-Martirosyan method, after generalizing it to take into account the spin of the interacting particles.

In Sec. 2 we discuss the kinematics of a process involving two nucleons, a meson and a photon. In Sec. 3 we write in invariant form the amplitude for meson photoproduction. In Sec. 4 we derive one-dimensional dispersion relations for the meson photoproduction amplitude from the two-dimensional relations. The resultant one-dimensional dispersion relations differ from those obtained previously[5] by an extra term. Because of this term certain expressions must be added to previously obtained dispersion relations for the amplitudes, as well as for the partial amplitudes:† these expressions are found in Sec. 5.

From the dispersion relations for the partial amplitudes one obtains easily integral equations for partial photoproduction amplitudes. The latter differ from those found previously[5] in that they contain in addition to the meson-nucleon partial scattering amplitude also the partial amplitude for nucleon pair annihilation into two mesons and the photoproduction of mesons on mesons.

The partial amplitude for nucleon pair annihilation into two mesons may be determined by making use of the integral equations formulated by Frazer and Fulco;[6] the partial amplitudes for meson photoproduction on mesons can be obtained from the integral equations derived by Gourdin and Martin.[7] Thus, in principle, a complete solution of the problem in question is possible.

The resultant expressions are rather complicated. In order to better explain their structure we give in Sec. 6 the main expressions for the simplest case when the charge of the particles and the spin of the nucleon are assumed to be zero.

2. Let k, q, p_1 and p_2 be the momentum four-vectors of the photon, meson and nucleons respectively. We consider the processes

$$\gamma + N_1 \rightarrow N_2 + \pi, \qquad \text{I}$$

$$\pi + N_1 \rightarrow N_2 + \gamma, \qquad \text{II}$$

$$N_1 + N_2 \rightarrow \pi + \gamma. \qquad \text{III}$$

Let us introduce the invariants

$$s\,(p_1 + k)^2, \qquad s_c = (p_1 + q)^2, \qquad t = (p_1 + p_2)^2. \tag{2.1}$$

In the barycentric frame of process I, these expressions can be rewritten as:*

$$s = (p_{10} + k_0)^2 = W^2 = (E_k + |\mathbf{k}|^2)^2 = (E_\mu + E_M)^2,$$

$$s_c = M^2 + \mu^2 - 2E_k E_\mu - 2\,|\mathbf{p}_1|\,|\mathbf{q}|\,x,$$

$$t = 2M^2 - 2E_k E_M + 2\,|\mathbf{p}_1|\,|\mathbf{p}_2|\,x, \tag{2.2}$$

---

*In what follows we understand by the term meson the pion.

†The expansion in angular variables of the amplitude for nucleon pair annihilation into a meson and photon needed here is given in Appendix 2.

*We assume in what follows that $ab = a_0 b_0 - \mathbf{a}\cdot\mathbf{b}$, $p^2 = M^2$, $q^2 = \mu^2$.

where $x = \cos\theta$, θ being the angle between the photon and meson momenta, $E_k = \sqrt{\mathbf{k}^2 + M^2}$, $E_\mu = \sqrt{\mathbf{q}^2 + \mu^2}$, $E_M = \sqrt{\mathbf{q}^2 + M^2}$, where M and μ are the mass of the nucleon and the meson, and **k** and **q** are the momentum of the photon and the final meson.

In the barycentric frame of process III we find

$$\begin{aligned} t &= 4(\mathbf{p}^2 + M^2) = (\sqrt{\mathbf{q}'^2 + \mu^2} + |\mathbf{q}'|)^2, \\ s_c &= M^2 + \mu^2 - 2E_pE_{q'} + 2|\mathbf{p}||\mathbf{q}'|y, \\ s &= M^2 + \mu^2 - 2E_pE_{q'} - 2|\mathbf{p}||\mathbf{q}'|y, \end{aligned} \tag{2.3}$$

where $y = \cos\varphi$, φ being the angle between the directions of motion of the initial and final particles, $E_p = \sqrt{\mathbf{p}^2 + M^2}$, $E_{q'} = \sqrt{\mathbf{q}'^2 + \mu^2}$, where **p** and **q′** are the momentum of the nucleon-antinucleon pair and the final meson.

3. The transition matrix element for the photoproduction of mesons on nucleons can be written in the case of pseudoscalar coupling as follows:[5]

$$\begin{aligned} \langle\pi|R|\gamma\rangle &= \tfrac{1}{2} i (2\pi)^4 (k_0 q_0 p_{10} p_{20})^{-1/2} \delta(p_2 + q - p_1 - k) \\ &\times \sum_i \hat{T}_i^{1\rho} \bar{u}(p_2)\, P_i^{\alpha\beta}(k, p_1, p_2, \gamma)\, u(p_1)\, e_\alpha^\nu k_\beta; \end{aligned} \tag{3.1}$$

$$P_i^{\alpha\beta} = \begin{cases} \gamma_5(p_1^\alpha p_2^\beta - p_1^\beta p_2^\alpha), \quad i = 1; & -\tfrac{1}{2}\gamma_5[\gamma^\alpha(p_1^\beta + p_2^\beta) - \gamma^\beta(p_1^\alpha + p_2^\alpha)], \quad i = 2; \\ -\tfrac{1}{2}\gamma_5[\gamma^\alpha(p_1^\beta - p_2^\beta) - \gamma^\beta(p_1^\alpha - p_2^\alpha)], \quad i = 3; & -\gamma_5(\gamma^\alpha\gamma^\beta - \gamma^\beta\gamma^\alpha), \quad i = 4; \end{cases} \tag{3.2}$$

Here ρ is a variable describing the charge of the produced meson ($\rho = 1, 2, 3$).

The coefficients $\hat{T}_i^\rho$ are functions of the energy s, the momentum transfer t, and the isotopic spins of the meson and nucleon.* The latter dependence may be made explicit by writing

$$\hat{T}_i^\rho(s, t) = \delta_{3\rho} T_i^{(1)} + \tau_\rho T_i^{(2)} + \tfrac{1}{2}[\tau_\rho \tau_3] T_i^{(3)}. \tag{3.3}$$

The coefficients T_i^j possess the following symmetry properties under the exchange $s \to s_c$, $t \to t$:

$$T_i^j(s, s_c) = \eta_i^j T_i^{*j}(s_c, s), \tag{3.4}$$

$$\eta_i^j = \begin{vmatrix} 1 & 1 & -1 & 1 \\ 1 & 1 & -1 & 1 \\ -1 & -1 & 1 & -1 \end{vmatrix}. \tag{3.5}$$

4. The double dispersion relations for the amplitude $T_i^j(s, s_c, t)$ are of the form:

$$\begin{aligned} T_i^j(s, s_c, t) &= O_i^j + \frac{1}{\pi^2} \int_{(M+\mu)^2}^{\infty} ds' \int_{4\mu^2}^{\infty} dt' \frac{A_{i13}^j(s', t')}{(s' - s)(t' - t)} \\ &+ \frac{1}{\pi^2} \int_{(M+\mu)^2}^{\infty} ds_c' \int_{4\mu^2}^{\infty} dt' \frac{A_{i23}^j(s_c', t')}{(s_c' - s_c)(t' - t)} \\ &+ \frac{1}{\pi^2} \int_{(M+\mu)^2}^{\infty} ds' \int_{(M+\mu)^2}^{\infty} ds_c' \frac{A_{i12}^j(s', s_c')}{(s' - s)(s_c' - s_c)}. \end{aligned} \tag{4.1}$$

Here

$$O_i^j = r_i^j/(\mu^2 - t) + R_i^j/(M^2 - s) + \eta_i^j R_i^j/(M^2 - s_c),$$

R_i^j, r_i^j are quantities characterizing the one-nucleon and one-meson contributions.

We restrict ourselves to the low energy region where it is legitimate to ignore inelastic processes. Then the double dispersion relations may be reduced[3,4] to approximate single dispersion relations (at fixed t):

$$\begin{aligned} T_i^j(s, t) &= O_i'^j + \frac{1}{\pi} \int_{(M+\mu)^2}^{\infty} ds' \operatorname{Im} T_i^j(s', t) \left[\frac{1}{s' - s} + \eta_i^j \frac{1}{s_c' - s_c}\right] \\ &+ \frac{1}{\pi} \int_{4\mu^2}^{\infty} \operatorname{Im} H_i^j(t', s, s_c) \frac{dt'}{t' - t}, \end{aligned} \tag{4.2}$$

where $O_i'^j = O_i^j + C_i^j(1 + \eta_i^j)$, with the C_i^j being slowly varying functions of s, s_c, t, which may in first approximation be taken as constant, and the H_i^j are amplitudes for the process III.* The relation (4.2) is applicable as long as $s - M^2 < 4M\mu$, $s_c - M^2 < 4M\mu$, $t \leq 9\mu^2$.

5. The above dispersion relations for the amplitude for the photoproduction of mesons on nucleons, Eq. (4.2), differ from those obtained previously[5] by the presence of two additional terms (an integral term and a one-meson term). When these terms are taken into account the dispersion relations for the amplitude in the barycentric frame may be written as

$$\operatorname{Re} U_i = (\,.\,.\,.\,.\,.\,) + \overline{U}_i. \tag{5.1}$$

Into the brackets one should substitute the expressions given by Eqs. (6.8) – (6.9) of Logunov, Tavkhelidze and Solov'ev or Eqs. (9.1) – (9.4) of Chew, Goldberger, Low and Nambu,[5] whereas

$$\begin{aligned} \overline{U}_1 &= C_i^j(1 + \eta_i^j) + \frac{1}{\pi} \mathrm{P} \int_{4\mu^2}^{\infty} \frac{dt'}{t' - t} (\alpha_{12} \operatorname{Im} B_2 \\ &+ \alpha_{13} \operatorname{Im} B_3 + \alpha_{14} \operatorname{Im} B_4), \end{aligned} \tag{5.2}$$

$$\begin{aligned} \overline{U}_3 &= C_i^j(1 + \eta_i^j) + \frac{1}{\pi} \mathrm{P} \int_{4\mu^2}^{\infty} \frac{dt'}{t' - t} (\alpha_{31} \operatorname{Im} B_1 \\ &+ \alpha_{32} \operatorname{Im} B_2 + \alpha_{33} \operatorname{Im} B_3 + \alpha_{34} \operatorname{Im} B_4), \end{aligned} \tag{5.3}$$

where the B_i are amplitudes of process III in the barycentric frame (see Appendix 2), and

---

*Expressions for the transition amplitude in the barycentric frame are given in reference 5.

*To avoid misunderstanding we note that the H_i^j are the same amplitudes as the T_i^j but taken in the physical region of process III.

$$\alpha_{11} = 0, \quad \alpha_{12} = -\frac{M\nu_1}{(W-M)\,k_0}\,\frac{1}{|\mathbf{p}|},$$

$$\alpha_{13} = \frac{1}{|\mathbf{k}|}\left[\frac{W^2 - M^2 - 2M\nu_1}{2(W-M)(E+M)} - 1\right],$$

$$\alpha_{14} = -\left[\frac{W^2 - M^2 - 2M\nu_1}{2(W-M)}E + \frac{M\nu_1(\mathbf{k}'\mathbf{k})}{(W-M)\,k_0}\right]\frac{1}{\mathbf{p}^2|\mathbf{k}|},$$

$$\alpha_{31} = -i\,\frac{W-M}{4Ek_0|\mathbf{p}|}, \quad \alpha_{32} = -\frac{1}{2k_0|\mathbf{p}|},$$

$$\alpha_{33} = -\frac{1}{2|\mathbf{k}|(E+M)}\left[1 - \frac{(W-M)\,M}{2E}\right],$$

$$\alpha_{34} = \left\{\frac{(W-M)\,M}{4E} + \frac{1}{2}\left[E - \frac{(\mathbf{k}'\mathbf{k})}{k_0}\right]\right\}\frac{1}{\mathbf{p}^2|\mathbf{k}|}.$$

The expression for $\overline{U}_2$ may be obtained from that for $\overline{U}_1$ by replacing everywhere $W \pm M$ by $W \mp M$ and -1 by $+1$, and the expression for $\overline{U}_4$ may be obtained from that for $\overline{U}_3$ by replacing everywhere $-(W-M)$ by $(W+M)$.

The dispersion relations for the partial amplitudes are similarly modified:*

$$\mathrm{Re}\, M^{(\lambda)}_{l,i} = (\,.\,.\,.\,) + M'^{(\lambda)}_{l,i}. \tag{5.4}$$

Into the brackets one must substitute expressions determined by Eq. (28) of Solov'ev,[5] whereas

$$M'^{(\lambda)}_{l,i} = \overline{M}^{(\lambda)0}_{l,i} + \frac{1}{\pi}\,\mathrm{P}\int\limits_{4\mu^2}^{\infty} dt' \left\{\mathrm{P}_{li}\left[\frac{1}{t'-t}\sum_{b=1}^{4}\sum_{m=1}^{4}\sum_{l'=0}^{\infty}\alpha_{jb}\tau_{bml'}\right]\right.$$

$$\left.\times\,\mathrm{Im}\, b^{(\lambda)}_{ml'}\right\} = \overline{M}^{(\lambda)0}_{li} + \frac{1}{\pi}P\int\limits_{4\mu^2}^{\infty} dt' \sum_{ml'}{}' \varepsilon^{(\lambda)}_{li,l'm}\,\mathrm{Im}\, b_{ml'}; \tag{5.5}$$

$$\varepsilon^{(\lambda)}_{li,l'_1} = \int\limits_{-1}^{+1}\frac{dx}{t'-t}P_{li}\left[\alpha'_{j1}\frac{2j+1}{\sqrt{j(j+1)}}P'_j(y)\right],$$

$$\varepsilon^{(\lambda)}_{li,l'_2} = \int\limits_{-1}^{+1}\frac{dx}{t'-t}P_{li}\left[-\alpha'_{j2}\frac{\sqrt{(j+1)(2j+1)}}{j}P'_{j-1}(y)\right.$$

$$\left. - \alpha'_{j3}\sqrt{\frac{2j+1}{j+1}}P'_j(y) + \alpha'_{j4}\frac{1}{j}\sqrt{\frac{2j+1}{j+1}}P''_{j-1}(y)\right], \tag{5.6}$$

$$\varepsilon^{(\lambda)}_{li,l'_3} = \int\limits_{-1}^{+1}\frac{dx}{t'-t}P_{li}\left[-\alpha'_{j2}\frac{2j+1}{j(j+1)}P'_j(y) + \alpha'_{j4}\frac{2j+1}{j(j+1)}P''_j(y)\right],$$

$$\varepsilon^{(\lambda)}_{li,l'_4} = \int\limits_{-1}^{+1}\frac{dx}{t'-t}P_{li}\left[\alpha'_{j2}\frac{\sqrt{j(2j+1)}}{j+1}P'_{j+1}(y)\right.$$

$$\left. + \alpha'_{j3}\sqrt{\frac{2j+1}{j}}P'_j(y) + \alpha'_{j4}\frac{\sqrt{2j+1}}{(j+1)\sqrt{j}}P''_{j+1}(y)\right].$$

Here $b_{ml'}$ are the partial amplitudes for process III, $\alpha' = \alpha/K_j$, K_j being coefficients connecting the amplitudes A_i with the U_i, and τ_{bm} are the coefficients that accompany $b_{l',j}$ in the expansions (A.10).

By making use of the unitarity condition $\mathrm{Im}\, b_{ml'}$ may be expressed in terms of the partial amplitudes for the processes of nucleon pair annihilation into two mesons and photoproduction of mesons on mesons.* The indicated amplitudes may be determined by making use of the integral equations derived by Frazer and Fulco[6] and Gourdin and Martin.[7] In other words, the expression for the additional integral (5.5) in the dispersion relations for the partial photoproduction amplitudes may be considered as known. Consequently one obtains for the amplitude for photoproduction of mesons on nucleons integral equations that differ from the ones obtained previously[5] in the structure of the inhomogeneous term, which contains, in particular, a contribution from $\pi\pi$ scattering.

6. As can be seen, the resultant expressions are rather complicated. To better understand their structure we show below the main expressions in the form that they take when it is assumed that all particles are neutral and that the nucleon has spin zero (the spin of the photon is taken, as before, to be unity, and the meson to be pseudoscalar). In that case in the expression (3.1) for the amplitude of the process only one function (T_1) will be different from zero.

In place of the dispersion relations (5.1) we obtain

$$\mathrm{Re}\, U(W, \nu_1) = Q + \frac{1}{\pi}\mathrm{P}\int\limits_{M+\mu}^{\infty} dW'$$

$$\times\left[\frac{1}{W'^2 - W^2} + \frac{1}{W'^2 + W^2 - 4M\nu_1 - 2M^2}\right]\mathrm{Im}\, U(W', \nu_1), \tag{6.1}$$

where

$$Q = r\left(\frac{1}{W^2 - M^2} + \frac{1}{W^2 - M^2 - 4M\nu_1}\right) + \Delta\overline{U},$$

$$\nu_1 = \frac{|\mathbf{k}|(\omega - |\mathbf{q}|x)}{2M},$$

$$\Delta\overline{U} = C^l_i(1 + \eta^l_i) + \frac{1}{\pi}\mathrm{P}\int\limits_{4\mu^2}^{\infty}\frac{dt'}{t'-t}\alpha_{31}\,\mathrm{Im}\, B$$

— a quantity characterizing the contribution of process III.

In the static limit ($M \to \infty$) one gets with the help of Eqs. (5.4) in this model the following dispersion relation for, for example, the partial amplitude E_1:

$$\mathrm{Re}\, E_1(\varepsilon) = N + \frac{\varepsilon^2 q}{\pi}\mathrm{P}\int\limits_{\mu}^{\infty}\left(\frac{1}{\varepsilon' - \varepsilon} + \frac{1}{\varepsilon' + \varepsilon}\right)\frac{1}{\varepsilon'^2 q'}\,\mathrm{Im}\, E_1(\varepsilon')\, d\varepsilon', \tag{6.2}$$

where E_1 is the amplitude for meson production in the P state by an electric quadrupole photon, $N = M^0 + M'_1$, $\epsilon = W - M$, $\epsilon' = W' - M$. The corresponding integral equation is written as:†

---

*At that the coefficients $b_{ml'}$ are related to the coefficients $b_{l',j}$ that appear in Eq. (A.12), as follows:

$$i2^{-1/2}b_{l',j(0)} = b_{1l'}, \quad i2^{-1/2}b_{l'+1,j} = b_{2l'},$$

$$i2^{-1/2}b_{l',j} = b_{3l'}, \quad i2^{-1/2}b_{l'-1,j} = b_{4l'}.$$

*See Appendix 3.

†Here one should keep in mind that $\mathrm{Im}\, E_1 = E_1 h^*$ where h is the meson-nucleon scattering amplitude.

$$X_1(\varepsilon) = N' + \frac{1}{\pi}\int_{\mu}^{\infty} d\varepsilon' \left[\frac{1}{\varepsilon' - \varepsilon - i\delta} + \frac{1}{\varepsilon' + \varepsilon - i\delta}\right] X_1(\varepsilon')\, h^*(\varepsilon'), \tag{6.3}$$

where

$$X_1 = E_1 / \varepsilon^2 q, \qquad N' = N / \varepsilon^2 q.$$

The solution of this equation has been given by Omnes[8] [Eqs. (5.3) – (5.9)]. The situation is analogous in the approximation under discussion for the other multipole as well.

APPENDIX 1

We consider first the case when the mesons are produced only in s and p states (i.e., we limit ourselves to photons with energies close to threshold). Then the nonvanishing coefficients M_{li} in the expansion of the amplitude $T_i(s, x)$ in the angular variables x can be written as

$$M_{03}(s) = \frac{2}{3}\int_{-1}^{+1} T_2'(s, x)\, dx, \tag{A.1}$$

if the mesons are produced in s states, and as

$$M_{11}(s) = -\frac{1}{2}\int_{-1}^{+1} T_2' x\, dx + \frac{1}{2}\int_{-1}^{+1} T_1'\, dx + \int_{-1}^{+1} T_4'\, dx,$$

$$M_{12}(s) = \int_{-1}^{+1} T_4'\, dx, \qquad M_{13}(s) = \frac{1}{6}\int_{-1}^{+1} T_1'\, dx + \frac{1}{6}\int_{-1}^{+1} T_2' x\, dx, \tag{A.2}$$

if the mesons are produced in p states.

Here

$$M_{l1} = M_{l_-} - M_{l_+}, \qquad M_{l2} = (l+1)\, M_{l_+} + l M_{l_-},$$

$$M_{l3} = E_{i_+} \quad M_{l4} = E_{l_-}, \qquad T_1' = -WT_1 / K_2,$$

$$T_2' = 3WT_2 / 2iK_1, \qquad T_4' = -4WT_4 / (W - M)\, K_2.$$

The coefficients $M_{l\pm}(s)$ and $E_{l\pm}(s)$ depend on the energy only and constitute the amplitudes for meson photoproduction with relative orbital angular momentum l, by magnetic and electric multipoles respectively, when the total angular momentum of the system is $l \pm 1/2$.

We make use of the double dispersion relations (4.1) to deduce the analytic properties of the amplitude M_{li} in the complex s plane. After substitution of Eq. (4.1) into Eqs. (A.1) and (A.2) there will appear in the latter equations denominators of the form $s_C' - s_C$, $s' - s$ and $t' - t$.

The vanishing of the denominator $s' - s$ gives rise to a series of branch points on the positive real axis of s; the first one of these branch points is at $s = (M + \mu)^2$ (see the figure). The vanishing of the denominators $s_C' - s_C$ and $t' - t$ with $x = 1$ results, after Eq. (2.2) is taken into account, in the equations:

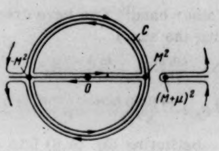

$$s^2 s_c' + s\,(s_c'^2 + M^2\mu^2 - M^4 - s_c'\mu^2 - 2s_c' M^2) + M^2(-s_c' M^2 + 2M^4 + s_c'\mu^2 - M^2\mu^2) = 0,$$

$$s^2 + s\,(t' - 2M^2 - \mu^2) + \mu^4 M^2 / t' + M^4 - \mu^2 M^2 = 0. \tag{A.3}$$

For x = 0 these equations become instead:

$$s^2 + 2\,(s_c' - M^2 - \mu^2/2)\, s - M^4 + M^2\mu^2 = 0,$$

$$s^2 + 2\,(t' - M^2 - \mu^2/2)\, s + M^4 - M^2\mu^2 = 0. \tag{A.4}$$

The singularities due to the pole terms appearing in Eq. (4.1) are obtained by setting in the above equations $s_C' = M^2$ and $t' = \mu^2$.

An analysis making use of Eqs. (A.3) and (A.4) shows that the partial amplitudes are analytic functions in the entire s plane except for a cut along the real axis from $(M + \mu)^2$ to ∞ and from M^2 to $-\infty$ and also along the circumference of the circle C (see the figure). The existence of singularities lying in the complex plane considerably complicates the situation.* The analytic properties of the partial amplitudes M_{li} for other values of l will be the same provided that the expressions for them contain no coefficients with $W = \sqrt{s}$, which introduce additional branch points.

APPENDIX 2

We give here the angular expansion of the amplitude for the process $\gamma + \pi \rightarrow N + \overline{N}$, which was used in deriving Eq. (5.5). The matrix element for this process is given by

$$\langle \pi\gamma \,|\, R \,|\, N\overline{N} \rangle = \frac{1}{2}\, i\,(2\pi)^4 \delta\,(p_1 + p_2 - k - q)(p_{10} q_0 k_0 p_{20})^{-1/2} \times \sum_i \hat{H}_i^{\rho} \bar{u}\,(p_2)\, \overline{P}_i^{\alpha\beta}(k, p_1, p_2, \gamma)\, v\,(p_1) e_\alpha^{\nu} k_\beta. \tag{A.5}$$

In order to obtain $\overline{P}_i^{\alpha\beta}$ it is necessary to replace p_1 by $-p_1$ in the appropriate expressions (3.2) for $P_i^{\alpha\beta}$.

Since in the barycentric frame we have on the one hand†

$$\bar{u}\Phi_1 v = -2ik_0 E\,(\mathbf{k}'\,\mathbf{e}),$$

$$\bar{u}\Phi_2 v = E^{-1}(p_1 k)\,(\sigma\,[\mathbf{e}\mathbf{k}']) + E^{-1}(\mathbf{k}'\mathbf{e})\,(\sigma\,[\mathbf{k}\mathbf{k}']) + iE^{-1}Mk_0\,(\mathbf{k}'\mathbf{e}),$$

$$\bar{u}\Phi_3 v = -E^{-1}(p_2 k)\,(\sigma[\mathbf{e}\mathbf{k}']) + E^{-1}(\mathbf{k}'\mathbf{e})\,(\sigma\,[\mathbf{k}\mathbf{k}']) + iE^{-1}Mk_0\,(\mathbf{k}'\mathbf{e}),$$

$$\bar{u}\Phi_4 v = \frac{2ik_0}{E}(\mathbf{k}'\mathbf{e}) + 2(\sigma\,[\mathbf{e}\mathbf{k}]) - \frac{2}{E\,(E+M)}(\mathbf{k}'\,\mathbf{e})\,(\sigma\,[\mathbf{k}'\mathbf{k}]) + \frac{2\,(\mathbf{k}'\mathbf{k})}{E\,(E+M)}\,(\sigma[\mathbf{k}'\mathbf{e}]), \tag{A.6}$$‡

---

*An analogous situation occurs for meson-nucleon scattering.[9]

†At that $\overline{P}_{1,4} = \Phi_{1,4}$, $\Phi_2 = \overline{P}_2 + \overline{P}_3$, $\Phi_3 = \overline{P}_2 - \overline{P}_3$.

‡$[\mathbf{k}\mathbf{k}'] = \mathbf{k} \times \mathbf{k}'$.

and on the other hand[10] (we have dropped the factor preceding the sum)

$$\langle \pi\gamma | R | N\bar{N} \rangle = \frac{i\,(\mathbf{k}'\mathbf{e})}{|\mathbf{k}|} B_1 + \frac{(\sigma\,[\mathbf{k}'\mathbf{e}])}{|\mathbf{k}'|} B_2 + \frac{(\sigma\,[\mathbf{k}\mathbf{e}])}{|\mathbf{k}|} B_3 + \frac{(\sigma\,[\mathbf{k}'\mathbf{k}])\,(\mathbf{k}'\mathbf{e})}{\mathbf{k}'^2\,|\mathbf{k}|}\; B_4, \tag{A.7}$$

we find by substituting Eq. (A.6) into Eq. (A.5) and comparing the result with Eq. (A.7) that

$$-B_1/|\mathbf{p}|k_0 = 2EH_1^\rho - MH_2^\rho/E - 2H_4^\rho/E,$$

$$B_2 = -H_2^\rho\,(\mathbf{k}'\,\mathbf{k})/E + 2\,(\mathbf{k}'\,\mathbf{k})\,H_4^\rho/E\,(E+M) + k_0 H_3^\rho\,|\mathbf{p}|,$$

$$B_3 = -2H_4^\rho|\mathbf{k}|, \qquad B_4/\mathbf{p}^2|\mathbf{k}| = -H_2^\rho/E - 2H_4^\rho/E\,(E+M). \tag{A.8}$$

Determining from here H_1^ρ we get

$$H_1(t,y) = \frac{B_1(t,y)}{2Ek_0\,|\mathbf{p}|} - \frac{B_3(t,y)}{2E\,(E+M)\,|\mathbf{k}|} - \frac{MB_4(t,y)}{2E\,\mathbf{p}^2\,|\mathbf{k}|},$$

$$H_2(t,y) = \frac{B_3(t,y)}{|\mathbf{k}|\,(E+M)} - \frac{EB_4(t,y)}{\mathbf{p}^2\,|\mathbf{k}|},$$

$$H_3(t,y) = \frac{B_2(t,y)}{|\mathbf{p}|\,k_0} - \frac{(\mathbf{k}'\mathbf{k})\,B_4(t,y)}{\mathbf{p}^2 k_0^2}, \qquad H_4(t,y) = -\frac{B_3(t,y)}{2\,|\mathbf{k}|}, \tag{A.9}$$

where (see reference 10)

$$i\sqrt{2}\,B_1(t,y) = b_{l',j(0)}\frac{2j+1}{\sqrt{j\,(j+1)}}P_j'(y),$$

$$-i\sqrt{2}\,B_2(t,y) = b_{l'+1,j}\,\frac{\sqrt{(j+1)\,(2j+1)}}{j}P_{j-1}'(y) - b_{l',j}\frac{2j+1}{j\,(j+1)}P_j'(y) - b_{l'-1,j}\frac{\sqrt{j\,(2j+1)}}{j+1}P_{j+1}'(y),$$

$$-i\sqrt{2}\,B_3(t,y) = -b_{l'+1,j}\sqrt{\frac{2j+1}{j+1}}P_j'(y) + b_{l'-1,j}\sqrt{\frac{2j+1}{j}}P_j'(y),$$

$$-i\sqrt{2}\,B_4(t,y) = b_{l'+1,j}\frac{1}{j}\sqrt{\frac{2j+1}{j+1}}P_{j-1}''(y) - b_{l',j}\frac{2j+1}{j\,(j+1)}P_j''(y) + b_{l'-1,j}\frac{1}{j+1}\sqrt{\frac{2j+1}{j}}P_{j+1}''(y). \tag{A.10}$$

Here j and l' are the total and orbital angular momenta of the final nucleon-antinucleon system.

APPENDIX 3

Expanding both sides of the equation

$$\operatorname{Im} B(t,y) = \int dy'\, d\varphi_{y'} T^+_{\pi\gamma\to\pi\pi} T_{\pi\pi\to N\bar{N}} \tag{A.11}$$

in polynomial-matrices[10]

$$\operatorname{Im}\sum b_{ik}(t)\,L_{ik}(y) = \sum\int dy'\,d\varphi_{y'}F^+_{\alpha\beta}(t)\,L^+_{\alpha\beta}(y')\,G_{mn}(t)\,L_{mn}(z) \tag{A.12}$$

and making use of the normalization condition of the polynomial-matrices, we obtain

$$\operatorname{Im}\sum b_{ik}(t)\,L_{ik}(y) = 4\pi\sum F^+_{\alpha m}(t)\,G_{mn}(t)\,L_{\alpha n}(y), \tag{A.13}$$

where $F_{\alpha m}$ and G_{mn} are the partial amplitudes for the processes of meson photoproduction on mesons and nucleon pair annihilation into two mesons. A comparison of the coefficients of identical L_{ik} and $L_{\alpha n}$ gives as a result an expression for the $\operatorname{Im} b_{ik}$ in terms of the partial amplitudes $F_{\alpha m}$ and G_{mn}.

---

[1] S. Mandelstam, Phys. Rev. **112**, 1344 (1958).

[2] G. F. Chew and S. Mandelstam, Phys. Rev. **119**, 467 (1960).

[3] M. Cini and S. Fubini, Ann. of Phys. **10**, 352 (1960).

[4] K. A. Ter-Martirosyan, JETP **39**, 827 (1960), Soviet Phys. JETP **12**, 575 (1960).

[5] Chew, Goldberger, Low, and Nambu, Phys. Rev. **106**, 1345 (1956). Logunov, Tavkhelidze, and Solov'ev, Nucl. Phys. **4**, 427 (1957). L. D. Solov'ev, Nucl. Phys. **5**, 256 (1958).

[6] W. Frazer and J. Fulco, Phys. Rev. **117**, 1603 (1960).

[7] M. Gourdin and A. Martin, Nuovo cimento **15**, 78 (1960).

[8] R. Omnes, Nuovo cimento **8**, 316 (1958).

[9] S. W. MacDowell, Phys. Rev. **116**, 774 (1959).

[10] V. I. Ritus, Thesis, Physics Institute, Academy of Sciences (1958); JETP **40**, 352 (1961), Soviet Phys. JETP **13**, 240 (1961). L. I. Lapidus, JETP **34**, 922 (1958), Soviet Phys. JETP **7**, 638 (1958).

Translated by A. M. Bincer
181

SOVIET PHYSICS JETP VOLUME 13, NUMBER 4 OCTOBER, 1961

NUCLEON-NUCLEON INTERACTION AT AN ENERGY OF 9 Bev

I. M. GRAMENITSKII, I. M. DREMIN, V. M. MAKSIMENKO, and D. S. CHERNAVSKII

P. N. Lebedev Physics Institute, Academy of Sciences, U.S.S.R.

Submitted to JETP editor September 21, 1960

J. Exptl. Theoret. Phys. (U.S.S.R.) 40, 1093-1100 (April, 1961)

The pole approximation[3,4] is employed to describe peripheral collisions of nucleons at 9 Bev. The results of the calculations are compared with the experimental data,[1,2] and the agreement is found to be satisfactory. The region of applicability of the pole approximation is estimated and the possibility of obtaining information on the properties of the π-meson propagation function and πN interaction cross section as a function of the square of the π-meson 4-momentum (k^2) is discussed.

INTRODUCTION

An abundance of experimental data on the nucleon-nucleon (hereafter, NN) interaction at an energy of 9 Bev is now available.[1,2] On the other hand, the recently suggested pole method of calculating strong interactions has been further developed.[3-5] It is therefore of interest to compare the theoretical data on the NN interaction at 9 Bev with the experimental data.

It should be noted that certain experimental data[1,2] (for example, the strongly anisotropic c.m.s. angular distribution of the nucleons, the c.m.s. asymmetry of charged particles, etc.) directly indicate the important role of peripheral interactions in this process. One can state in advance that these data cannot be explained with the aid of the statistical theory[6-8] of central nucleon-nucleon collisions.

METHOD

We shall not consider here all the aspects of the pole method, which has been described in detail in references 3 — 5; we shall discuss only the assumptions on which it is based.

1. The propagation function of the intermediate meson in the general case should have the form

$$D(k^2) = \frac{1}{k^2+\mu^2} + \int_{(3\mu)^2}^{\infty} \frac{\rho(\varkappa)}{k^2+\varkappa}\, d\varkappa, \qquad (1)$$

where $\rho(\kappa)$ is an essentially positive function which is not yet known; k is the 4-momentum of the intermediate meson, $k^2 = k^2 - k_0^2$, $\hbar = c = 1$; μ is the π-meson mass. In the one-meson pole approximation, only the first (pole) term in expression (1) is taken into account; it is seen from (1) that the influence of the second term is important only for $k^2 \geq (3\mu)^2$.

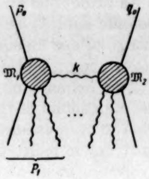

FIG. 1.

2. The cross section for the interaction between a π-meson and a nucleon depends on the energy ω (in the c.m.s. of the nucleon and π meson) and also (if the π meson is virtual) on the quantity k^2. In the general case, we can write

$$\sigma(\omega, k^2) = \sigma(\omega, k^2 = -\mu^2) - \Sigma(\omega, k^2). \qquad (2)$$

The first term represents here the cross section for the interaction between a real π meson ($k^2 = -\mu^2$) of energy ω and a nucleon. The role of the second term has not yet been investigated in detail.* It, too, is neglected in the pole method.

3. Only the one-meson diagram is considered in the pole method (Fig. 1). Diagrams in which the nucleons exchange two, three, etc. mesons are not considered. The basic question that arises in the estimate of the permissibility of this simplification is not the extent of contribution to the cross section, but whether there is significant interference between the one-meson diagram and the multimeson diagrams. In fact, if the interference is not significant, then the contributions of the various diagrams to the cross section are additive; the

---

*Generally speaking, the sign of the second term cannot be determined beforehand. It is very likely to be negative [i.e. $\sigma(k^2)$ decreases with an increase in k^2].

calculation of the one-meson diagram is of value in itself, and can be used to describe part of the experimental data. The question of interference is complicated and merits special investigation. We present here only a number of arguments indicating that this effect plays an unimportant role.

In the case of the one-meson exchange, two groups of particles are produced from nodes 1 and 2. These groups of particles have anisotropic distributions (in the c.m.s.) and are emitted in different directions. The greatest interference between the one-meson matrix element and the two-meson (in general, multi-meson) matrix element occurs when the angular distributions are similar.

In this case, however, interference will occur only if all the quantum numbers characterizing each group of particles [the intrinsic angular momentum (spin) J, its projection on any axis m_y, the parity I, the isotopic spin T, etc.] coincide. In the case of exchange of one meson, T = $\frac{1}{2}$, $\frac{3}{2}$; $m_y = \frac{1}{2}$. (Here m_y is the projection of the spin on the momentum of the primary nucleon in the system in which the momentum of the entire group of particles is zero.) If it is assumed that the quantities T, T_z, and m_y in multi-meson exchange are distributed at random, then one can estimate the probability that they all coincide with the corresponding quantities for one-meson exchange. For the two-meson exchange, the requirement that only the quantities T, T_z, and m_y coincide leads to the probability $W \sim 0.1$. The requirement that all other quantities coincide (total angular momentum J and parity I) can only reduce this estimate.

Using the three assumptions enumerated above, we can write an expression for the inelastic NN-interaction cross section:

$$\sigma_{NN}(E_0) = \frac{2}{(2\pi)^3 p_0^2 E_0^2} \int dz\, dy \sqrt{z^2 - m^2\mu^2} \sqrt{y^2 - m^2\mu^2}$$
$$+ \left\{\frac{1}{\mu^2 + \varkappa^2} - \frac{1}{\mu^2 + \varkappa^2 + 4p_0 P_1}\right\}$$
$$\times \begin{cases} \frac{10}{9}\sigma_{3/2}(z)\,\sigma_{3/2}(y) + \frac{16}{9}\sigma_{3/2}(z)\,\sigma_{1/2}(y) + \frac{1}{9}\sigma_{1/2}(z)\,\sigma_{1/2}(y)\,\text{for}\,pp \\ \frac{14}{9}\sigma_{3/2}(z)\,\sigma_{3/2}(y) + \frac{8}{9}\sigma_{3/2}(z)\,\sigma_{1/2}(y) + \frac{5}{9}\sigma_{1/2}(z)\,\sigma_{1/2}(y)\,\text{for}\,pn \end{cases}$$

Here

$$z = \tfrac{1}{2}(\mathfrak{M}_1^2 - m^2 - \mu^2), \qquad y = \tfrac{1}{2}(\mathfrak{M}_2^2 - m^2 - \mu^2), \qquad (3)$$

$\sigma_{3/2}(z)$ is the cross section for the interaction between a π meson and nucleon at an energy $\omega_L = z/m$ in the isospin state $\frac{3}{2}$ etc.; $\kappa^2 = 2(E_0E_1 - p_0P_1) - \mathfrak{M}_1^2 - m^2$ (the quantity κ^2 reflects the virtualness of the π meson and is of the order of magnitude $k^2/2$); E_0, p_0, and m are the c.m.s. energy, momentum, and mass of the primary nucleon; E_1 and p_1 are the energy and momentum of the entire group of particles emitted from node 1; $\mathfrak{M}_1 = \sqrt{E_1^2 - P_1^2}$ is the energy of this group of particles in its rest system; E_2, P_2 and $\mathfrak{M}_2$ are the corresponding quantities for node 2.

Hereafter, for convenience, we shall call these groups of particles isobars and carry out the calculations in two steps: a) the calculation of the production of the two isobars (with masses $\mathfrak{M}_1$ and $\mathfrak{M}_2$) and b) their decay into secondary particles. This procedure is used primarily to facilitate the calculations, but it is also justified physically, since the time for the production of the isobars, as a rule, is much smaller than the time for their decay. In fact, the production of an excited state is a one-quantum process, and its time in the rest system of the isobar is estimated from the uncertainty relation $\tau_1 \Delta E \sim \hbar$ (ΔE is the excitation energy). The decay of the excited state is a multi-quantum classical process and the time for it is $\tau_2 \Delta E \gg \hbar$. More precisely, $\tau_2 \Delta E \sim n\hbar$, where n is the value of the action in the decay and has the order of magnitude of the number of secondary particles. The case n = 1 (decay into one π meson) occurs primarily at $\omega_L \approx 200$ Mev (the so-called Tamm isobar[13]). However, here, too $\tau_2 \gg \tau_1$, but for other reasons due to the resonance character of the πN interaction in this energy region.

According to the sense of this method, one should insert in (3) the experimental cross section for the πN interaction instead of $\sigma(\omega)$. Hence, to calculate NN interactions of different types at 9 Bev, it is necessary to have the following data on the πN interaction in the energy region $\omega_L \leq 2.5$ Bev:

a) The elastic and inelastic cross sections for the πN interaction and also the c.m.s. angular and momentum distributions of the secondary nucleons. These data were taken from experimental investigations.[9-12]*

b) The multiplicity and prong distribution in inelastic πN interactions for the individual isospin states of the πN system. These data cannot be taken directly from the experiments. Since the experimental data are, as a rule, averaged over the isospin, we calculated these characteristics on the basis of the statistical theory.[6-8] It should be kept in mind here that in this energy region the statistical theory formulas for suitably chosen parameters are empirical formulas describing the experiment. Actually, all the calculations with formula (3) have to be performed numerically.

---

*We note that the elastic πN interaction in the energy region 1 Bev < ω_L < 2.5 Bev is basically of a diffraction character.

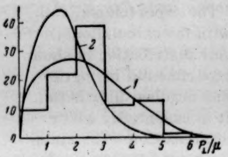

FIG. 2. Transverse momentum distribution of the nucleons (curves 1 and 2 are the theoretical curves for variants I and II, respectively; the histogram represents the experimental data[1,2]).

First, we calculated by formula (3) the total cross section σ_{NN}, which proved to be 18 mb. Here we imposed no additional restrictions on the value of the "virtualness" k^2. The basic contribution to the cross section came from cases with a virtualness not exceeding $(7\mu)^2$.

According to the experimental data, the cross section for the processes observed in references 1 and 2 was 21 mb. It thus follows that the pole approximation (if it is valid in the region $k^2 \lesssim (7\mu)^2$, can be used to describe a basic part of the experimental data. We therefore compared the results of the calculations with all the experimental material without an additional selection.

However, it was not clear beforehand whether the above assumptions were valid for large values of the quantity $k^2 \sim (7\mu)^2$. It was clear, however, that the smaller the value of k^2, the more justified were the assumptions. We therefore carried out the calculations with an additional restriction on the magnitude of the virtualness: $k^2 \le (3\mu)^2$.* [In this case, the term $(\mu^2 + \kappa^2 + 4p_0P_1)^{-1}$ in formula (3) is replaced by an expression of the form $(\delta^2 + \mu^2)^{-1}$, where $\delta^2 = k^2_{\max} = (3\mu)^2$.] In this variant, the cross section σ_{NN} turned out to be 4 mb. It thus follows that this variant can describe only a small part of the experimental data ($\sim 20\%$); the results of the calculations in this case are valid only with a special selection of the experimental cases in which the value of the transferred momentum is small (these selection criteria are discussed below).

By carrying out the calculations for both variants and comparing them with the experiments, we hoped to obtain information on the applicability of the pole method in the region of k^2 between $(3\mu)^2$ and $(7\mu)^2$.

RESULTS OF THE CALCULATIONS AND COMPARISON WITH EXPERIMENTAL DATA

1. The transverse momentum distribution of the nucleons ($p\perp$) is shown in Fig. 2 for the two methods of calculation: variant I with no restriction on k^2 (curve 1) and variant II with $k^2 \le (3\mu)^2$ (curve 2). The experimental histogram is also shown in the figure. The curves and the histogram are normalized here (and below) to the same area. It is seen from the curves that in variant II practically all the nucleons have $p\perp \le 2.5\,\mu$; the experimental distribution is significantly broader. Hence, to compare the experimental data with other characteristics obtained from the calculations by variant II, we selected from the former only those cases which satisfied the condition $p^r_\perp \le 2.5$ (where $p^r_\perp$ is the transverse momentum of the recoil proton).

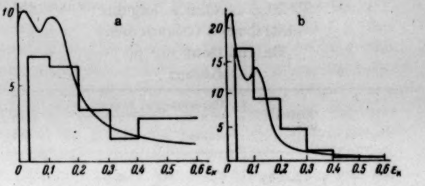

FIG. 3. Energy distribution of the recoil nucleons in the laboratory system: a – variant I, b – variant II; curves – theoretical results, histograms – experimental data (the kinetic energy of the recoil nucleons is laid off along the abscissa axis in fractions of the nucleon mass).

Comparison of the experimental histogram with the curves obtained from variant I indicates satisfactory agreement. A difference (double the experimental error) occurs only in the interval $p\perp = 0 - 1\,\mu$.

It should be noted that, in the theoretical calculation, the basic contribution in this region comes from cases in which two "ordinary" isobars with $\mathfrak{M} = 1.3$ m and isospin $^3/_2$ are produced, i.e., the isobars involved in the resonance scattering of 200-Mev π mesons.[13] On the other hand, there are grounds for assuming (see below) that a large number of these cases were missed in the experiments. This discrepancy can thus be attributed to "technical" rather than physical factors.

2. The energy distribution of the recoil nucleons is shown in Fig. 3a. Two facts are striking. First, the recoil nucleon spectrum drops sharply beginning with $\epsilon_{\text{kin}} \sim 150$ Mev. This is characteristic for the picture of peripheral collisions and does not occur for "central" collisions. Second, the spectrum is not monotonic; a second weak maximum appears at $\epsilon_{\text{kin}} = 120$. This maximum is due to the contribution of cases in which one of the isobars has a mass $\mathfrak{M} = 1.3$ m. Unfortunately, the experimental accuracy at the present time is insufficient for the separation of this maximum. It

---

*This variant already has been partially considered by Dremin and Chernavskii.[4]

TABLE I. C.m.s. angular distribution of nucleons. Calculations for pp collisions.

Cosine interval	Percentage of cases	
	variant I	variant II
1 —0.95	70	89.0
0.95—0.9	9	3.3
0.9 —0,85	4.2	3.2
0.85—0.8	3.9	2.5
0.8 —0.75	2.3	
0.75—0.7	1.4	
0,7 —0,6	2.3	
0,6 —0.5	2.2	2.0
0,5 —0.0	4.7	

is possible that it can be observed more easily at a higher nucleon energy.

Comparison of this curve with the experimental data indicates good agreement, except for the interval $\epsilon_{\mathrm{kin}} \leq 30$ Mev. However, in the experiment, cases in which the recoil nucleons had energies $\epsilon_{\mathrm{kin}} \leq 30$ Mev were simply discarded. On the other hand, according to the theoretical curve, about 10% of the cases are of this energy. It should be noted that the contribution to this region comes mainly from cases in which two isobars are produced with equal masses $\mathfrak{M}_1 = \mathfrak{M}_2 = 1.3$ m.

An estimate (based on the statistical accuracy of the experiment) indicates that the "missing" of such cases is quite real. In this connection, it should be noted that the contribution of these cases to the transverse momentum curve may also have been "missed," as was already pointed out above.

The energy distribution of the recoil nucleons calculated by variant II is shown in Fig. 3b. Also shown there are the experimental data selected in accordance with the criterion $p_\perp^r \leq 2.5\,\mu$. The agreement is good.

3. The c.m.s. angular distribution of the nucleons is shown in Table I. It is quite anisotropic both in variants I and II. The experimental data are not in contradiction with the calculations.

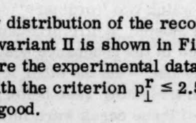

FIG. 4. π-meson c.m.s. angular distribution for variant I (pp interaction); the curves represent the theoretical results and the histogram represents the experimental data. [1,2]

4. The π-meson angular distribution is shown in Fig. 4 along with the experimental histogram. It is seen that the π-meson angular distribution is anisotropic, although it is essentially wider than the nucleon angular distribution. The small difference in the low-angle region is apparently due to the same "technical" factors mentioned above. The difference in the large-angle region (the theoretical curve goes above the experimental points) may have a physical basis. On the whole, we consider the agreement to be satisfactory.

TABLE II. Multiplicity and prong distribution

Character of the star	Percentage of stars				
	Variant I			Variant II*	
	calc.	statistical theory	expt.	calc.	expt.
	pp interactions				
Two-prong	35	32.8	46±5.4	35	35±14
Four-prong	58.9	58.5	44.7±5.3	63.4	35±18
Six-prong	6,0	8.6	8.1±2.2	1.6	6±3
Eight-prong	0.1	0.1	0.62±0.62	—	—
Mean multiplicity	3.46	3,53	3.2	3.4	3.42
	pn interactions (variant I)				
One-prong	18.4	14,5	35.1±6.1		
Three-prong	65.2	59.4	53.2±7.5		
Five-prong	15.7	25.0	9.6±3.2		
Seven-prong	0.7	1.1	2.1±1.5		
Mean multiplicity	2.96	3.25	2.6		
Charged particle asymmetry	0.47	0	0.4±0.2		

*The experimental data refer to cases in which the transverse momentum of the recoil proton is $\leq 2.5\,\mu$. The theoretical calculations, in variant II took this into account.

5. We calculated the number of charged particles produced in πN interactions at energies ω_L from 0.7 to 2 Bev by means of the statistical theory.*

The probability for the production of the corresponding isobars was calculated on the basis of expression (3).

In variant I, we calculated the multiplicity and the prong distribution for pp and pn collisions. The results are shown in Table II, which lists also the experimental data and (for comparison) the results of the statistical theory calculations for central NN collisions under the assumption of the production of a single system of mass $\mathfrak{M} = 5$ Bev.

---

*Here we took into account the contribution of the diffraction part of the interaction which constitutes ~ 30% at an energy $\omega_L > 1$ Bev. The determination of the number of "prongs" is in the latter case trivial. In the energy region $\omega_L < 200$ Mev, where the interaction is elastic, the number of prongs was found from considerations of charge symmetry.

Attention is drawn to the fact, first, that the calculated multiplicity in peripheral collisions was found to be of the same order as in central collisions. The reason for this is that the multiplicity is a weak function of the energy, and the production of two "isobars" of smaller mass can give the same multiplicity as the production of one "compound" system of large mass. Second, the other enumerated characteristics (for example, the c.m.s. asymmetry of the charge distribution) listed in Table II are essentially different from the results of the statistical theory calculations for "central" collisions (in general, no asymmetry can occur there).

The experimental data do not contradict the obtained values (within the limits of two times the error), but it cannot be stated that there is full agreement. The calculated multiplicity is somewhat greater than the observed one, but the calculated charge asymmetry is in agreement with that observed.

In variant II, the calculations were performed only for pp interactions under an additional condition: we selected only cases in which a proton was emitted "backward" in the c.m.s. The results of these calculations are shown in Table II along with the experimental data selected in accordance with the criterion $p_{\perp}^{r} \leq 2.5\,\mu$. The agreement is good.

CONCLUSIONS

The comparison of the theoretical results with experiment indicates that the peripheral one-meson interaction calculated by the pole method satisfactorily describes the basic part of the experimental data, and, consequently, the pole approximation is applicable in the region $k^2 \lesssim (7\,\mu)^2$ important to the calculations.* This can serve as an indication that, first, the nonpole term in the propagation function (1) is small in the region $k^2 \lesssim (7\mu)^2$ in comparison with the pole term, and, second, the cross section is a smooth, slowly-varying function of k^2 up to $k^2 \sim (7\mu)^2$ [This, of course, does not exclude the possibility that the nonpole terms in (1) and (2) are both large, but in the region $k^2 \leq (7\mu)^2$ they offset one another.]

The marked difference between the calculations and experiment as regards the multiplicity indicates that the role of the second term in (2) is more important than the second term in (1). Indeed, if we allow for the drop in the cross section with an increase in k^2, we could reduce the role of the cases of high multiplicity in the calculation and bring about agreement with experiment; the inclusion of the second term in the propagation function can only increase the multiplicity.

Hence it seems that such experiments and the improvement of their accuracy can provide information (although indirectly) on very important quantities in contemporary theoretical physics, the functions $\rho(\kappa)$ and $\sigma(k^2)$. This is of interest, since thus far there are no other experimental sources of such information. The fact that the results of the calculations by the second variant $[k^2 \leq (3\mu)^2]$ are in good agreement with part of the experimental stars (selected in accordance with the criterion $p_\perp \leq 2.5\,\mu$) is important in this situation only as an additional confirmation; they do not give any new information.

Comparison of the absolute values of the cross sections indicates that the contribution of interactions of another type (for example, multi-meson, K-meson, central, etc.) can constitute 20 — 30% of the total cross section. However, it is not possible to separate them by their total mass in a given experiment, since it is difficult, at present, to indicate criteria for such a separation.*

In conclusion, the authors take this opportunity to express their gratitude to E. L. Feĭnberg and V. I. Veksler for their constant interest in this work and valuable comments.

---

[1] Bogachev, Bunyatov, Gramenitskii, Lyubimov, Merekov, Podgoretskii, Sidorov, and Tuvdendorzh, JETP **37**, 1225 (1959), Soviet Phys. JETP **10**, 872 (1960).

[2] Wang Shu-Fen, Visky, Gramenitskii, Grishin, Lebedev, Dalkhazhav, Nomofilov, Podgoretskii, and Strel'tsov, JETP **39**, 957 (1960), Soviet Phys. JETP **12**, 663 (1961).

[3] G. F. Chew and F. E. Low, Phys. Rev. **113**, 1640 (1959).

[4] I. M. Dremin and D. S. Chernavskii, JETP **38**, 229 (1960), Soviet Phys. JETP **11**, 167 (1960).

[5] V. B. Berestetskii and I. Ya. Pomeranchuk, JETP **39**, 1078 (1960), Soviet Phys. JETP **12**, 752 (1961).

[6] E. Fermi, Progr. Theoret. Phys. (Kyoto) **5**, 570 (1950); Phys. Rev. **81**, 683 (1951).

---

*A similar calulation and comparison with the experimental data at 200 Bev[14,15] gives additional information on the character of the pole approximation at larger k^2. This question has been considered separately.[16]

*A large multiplicity in a star (as was explained above) cannot serve as such a criterion.

[7] S. Z. Belen'kii and L. D. Landau, Usp. Fiz. Nauk 56, 309 (1955).

[8] Belen'kii, Maksimenko, Nikishov, and Rozental', Usp. Fiz. Nauk 62, No. 2, 1 (1957).

[9] H. Bethe and F. de Hoffman, Mesons and Fields, Row, Peterson and Co., New York, 1955, vol. 2.

[10] Burrowes, Caldwell, Frisch, Hill, Ritson, Schluter, and Wahlig, Phys. Rev. Lett. 2, 119 (1959).

[11] Chretien, Leitner, Samios, Schwartz, and Steinberger, Phys. Rev. 108, 383 (1957).

[12] R. C. Whitten and M. M. Block, Phys. Rev. 111, 1675 (1958).

[13] Tamm, Gol'fand, and Faĭnberg, JETP 26, 649 (1954).

[14] S. A. Slavatinskii, Moscow Cosmic Ray Conf. 1959.

[15] N. A. Dobrotin, 1960 Annual Intern. Conf. on High Energy Physics at Rochester.

[16] I. M. Dremin and D. S. Chernavskii, JETP (in press).

Translated by E. Marquit
182

SOVIET PHYSICS JETP VOLUME 13, NUMBER 4 OCTOBER, 1961

EFFECT OF UNRESOLVED STRUCTURES ON THE LINE WIDTH IN ELECTRONIC PARAMAGNETIC RESONANCE

R. Kh. TIMEROV

Physico-Technical Institute, Kazan' Branch, Academy of Sciences, U.S.S.R.

Submitted to JETP editor September 21, 1960

J. Exptl. Theoret. Phys. (U.S.S.R.) 40, 1101-1105 (April, 1961)

The electronic paramagnetic resonance line width in solid paramagnetic salts is computed by taking into account the unresolved fine and hyperfine structures.

1. A single resonance line is usually observed in magnetically concentrated paramagnetic salts of elements of the first transition group. Fine and hyperfine splittings, which appear in dilute samples in the form of corresponding structures, are not resolved in the case of concentrated specimens because of the strong exchange interaction. Similarly, in magnetic dipole-dipole interactions they make their contribution to the width of the natural observed line and are also subject to the narrowing action of exchange. This fact, which is used to explain the divergence between experiment and theories which take into account only the dipole splitting of the magnetic resonance line,[1,2] has been little studied quantitatively.

The equation for the absorption curve is derived below by the method suggested by Kubo and Tomita,[3] taking into account the contribution of the unresolved fine and hyperfine structures in solid magnetically concentrated salts of elements of the first transition group.

2. Kubo and Tomita[3] have shown that the spectral density $I(\omega)$ of the absorption line in magnetic resonance is determined by the Fourier transform of the autocorrelation functions $G(t)$ of the component of the magnetic moment along the applied alternating magnetic field

$$I(\omega) = \frac{1}{2\pi}\int_{-\infty}^{\infty} G(t)e^{-i\omega t}dt, \tag{1}$$

where

$$G(t) = \langle\{\hat{M}_x(t)\,\hat{M}_x\}\rangle. \tag{2}$$

Here the symmetrized product $\{\hat{M}_X(t)\hat{M}_X\}$ is averaged with the density matrix, which can be replaced by a constant for not very low temperatures ($kT \gg \hbar\omega$). $\hat{M}_X(t)$ is the magnetization operator in the Heisenberg representation

$$\hat{M}_x(t) = \exp(it\hat{\mathcal{H}}/\hbar)\,\hat{M}_x\exp(-it\hat{\mathcal{H}}/\hbar), \tag{3}$$

where $\hat{\mathcal{H}}$ is the Hamiltonian of the system in the absence of the alternating field.

On consideration of the effects of motion and exchange, the Hamiltonian $\hat{\mathcal{H}}$ splits into two parts:

$$\hat{\mathcal{H}} = \hat{\mathcal{H}}_1 + \hat{\mathcal{H}}_2 + \hat{\mathcal{H}}', \tag{4}$$

such that $\hat{\mathcal{H}}_1 + \hat{\mathcal{H}}_2 = \hat{\mathcal{H}}_0$ is the unperturbed Hamiltonian defining the basis functions and $\hat{\mathcal{H}}'$ is the perturbation, whence

$$[\hat{\mathcal{H}}_1,\ \hat{\mathcal{H}}_2] = [\hat{\mathcal{H}}_2,\ \hat{M}_x] = 0. \tag{5}$$

Solving the equation of motion $i\hbar\hat{M}_X(t) = [\hat{M}_X(t), \hat{\mathcal{H}}_0 + \hat{\mathcal{H}}']$ by the method of successive approximations, we obtain an expansion of $G(t)$ in a series:

$$G(t) = \sum_{n=0}^{\infty} G_n(t), \tag{6}$$

the first three terms of which describe the basic characteristics of the effect of motion and exchange on magnetic resonance, according to which we can establish $G(t)$ in the form

$$G(t) = \sum_{\alpha}\langle|\hat{M}_{x\alpha}|^2\rangle \times\exp\left\{i\omega_\alpha t - \sum_{\gamma}\sigma^2_{\alpha\gamma}\int_0^t (t-\tau)\,d\tau\exp(i\omega_\gamma\tau)\,f_{\alpha\gamma}(\tau)\right\}, \tag{7}$$

with accuracy which is sufficient for our purposes; here $\sigma^2_{\alpha\gamma}$ is the second moment of the broadening perturbation

$$\sigma^2_{\alpha\gamma} = \langle|[\hat{M}_{x\alpha},\ \hat{\mathcal{H}}'_\gamma]|^2\rangle/\langle|\hat{M}_{x\alpha}|^2\rangle, \tag{8}$$

$f_{\alpha\gamma}(\tau)$ is the correlation function:

$$f_{\alpha\gamma}(\tau) = \langle\{[\hat{M}_{x\alpha},\ \hat{\mathcal{H}}'_\gamma(\tau)][\hat{\mathcal{H}}'_{-\gamma}(0),\ \hat{M}_{x,-\alpha}]\}\rangle/\langle|[\hat{M}_{x\alpha}, \hat{\mathcal{H}}'_\gamma(0)]|^2\rangle. \tag{9}$$

The quantities $\hat{M}_{X\alpha}$, $\hat{\mathcal{H}}'_\gamma(t)$, ω_α, and ω_γ are defined by the relations

$$\exp\,[it\hat{\mathcal{H}}_1+\hat{\mathcal{H}}_2)/\hbar]\,\hat{M}_x\exp\,[-\,it(\hat{\mathcal{H}}_1+\hat{\mathcal{H}}_2)/\hbar]$$

$$=\exp\,(it\hat{\mathcal{H}}_1/\hbar)\,\hat{M}_x\exp\,(-\,it\hat{\mathcal{H}}_1/\hbar)=\sum_\alpha\hat{M}_{x\alpha}\exp\,(i\omega_\alpha t), \tag{10}$$

$$\exp\,[it\,(\hat{\mathcal{H}}_1+\hat{\mathcal{H}}_2)/\hbar]\,\hat{\mathcal{H}}'\exp\,[-\,it\,(\hat{\mathcal{H}}_1+\hat{\mathcal{H}}_2)/\hbar]$$

$$=\exp\,(it\,\hat{\mathcal{H}}_2/\hbar)\Big[\sum_\gamma\hat{\mathcal{H}}'_\gamma\exp\,(i\omega_\gamma t)\Big]\exp\,(-\,it\,\hat{\mathcal{H}}_2/\hbar)$$

$$=\sum_\gamma\hat{\mathcal{H}}'_\gamma(t)\exp\,(i\omega_\gamma t). \tag{11}$$

3. For the description of the behavior of the lowest spin levels of a system of N identical magnetic ions of a solid paramagnetic salt, the Hamiltonian $\hat{\mathcal{H}}$ is introduced:

$$\hat{\mathcal{H}}=\hat{\mathcal{H}}_z+\hat{\mathcal{H}}_{\mathrm{fs}}+\hat{\mathcal{H}}_{\mathrm{hfs}}+\hat{\mathcal{H}}_{ss}+\hat{\mathcal{H}}_e, \tag{12}$$

where we have the operators $\hat{\mathcal{H}}_Z$ = Zeeman energy, $\hat{\mathcal{H}}_{\mathrm{fs}}$ = fine structure, $\hat{\mathcal{H}}_{\mathrm{hfs}}$ = hyperfine structure, $\hat{\mathcal{H}}_{\mathrm{ss}}$ = magnetic dipole-dipole interaction, and $\hat{\mathcal{H}}_{\mathrm{e}}$ = exchange interaction.

The local electric field at the position of location of the magnetic ion is frequently a combination of a strong field of cubic symmetry and a weak field of lower, usually axial, symmetry.[4] Then

$$\hat{\mathcal{H}}_z=-\,g_{\parallel}\beta\sum_k\hat{S}_{z'k}\hat{H}_{z'k}-g_{\perp}\beta\sum_k(\hat{S}_{x'k}H_{x'k}+\hat{S}_{y'k}H_{y'k}), \tag{13}$$

$$\hat{\mathcal{H}}_{\mathrm{fs}}=\hbar D\sum_k[\hat{S}^2_{z'k}-\tfrac{1}{3}S\,(S+1)]. \tag{14}$$

For simplicity, we shall take the operators $\hat{\mathcal{H}}_{\mathrm{hfs}}$ and $\hat{\mathcal{H}}_{\mathrm{e}}$ to be isotropic:

$$\hat{\mathcal{H}}_{\mathrm{hfs}}=\hbar A\sum_k\hat{\mathbf{S}}_k\hat{\mathbf{I}}_k,\qquad\hat{\mathcal{H}}_e=\hbar\sum_{i>j}\sum J_{ij}\hat{\mathbf{S}}_i\hat{\mathbf{S}}_j,$$

$$\hat{\mathcal{H}}_{ss}=g^2\beta^2\sum_{i>j}\sum r_{ij}^{-3}[\hat{\mathbf{S}}_i\hat{\mathbf{S}}_j-r_{ij}^{-2}(\hat{\mathbf{S}}_i\mathbf{r}_{ij})(\hat{\mathbf{S}}_j\mathbf{r}_{ij})]. \tag{15}$$

Here D and A are constants of the fine and hyperfine structures, $J_{ij}=J_{ji}$ = exchange integral, and r_{ij} = distance between the i-th and j-th magnetic ions.

Introducing the angles ϑ_k and φ_k, which are formed by the axis z'_k of the local field at the kth magnetic ion with the laboratory system of axes xyz (z ∥ H), we can represent $\hat{\mathcal{H}}_Z$ and $\hat{\mathcal{H}}_{\mathrm{fs}}$ in the form

$$\hat{\mathcal{H}}'_z=\hat{\mathcal{H}}_{0z}+\hat{\mathcal{H}}'_z,\qquad\hat{\mathcal{H}}_{0z}=-\,g\beta H\sum_k\hat{S}_{zk}=-\,\hbar\omega_z\sum_k\hat{S}_{zk}, \tag{16}$$

$$\hat{\mathcal{H}}'_z=-\,\Delta g\beta H\sum_k[\hat{S}_{zk}(\cos^2\vartheta_k-\tfrac{1}{3})+\tfrac{1}{3}(\hat{S}_{+k}\exp(-\,i\varphi_k)+\hat{S}_{-k}\exp(i\varphi_k))\sin\vartheta_k\cos\vartheta_k],$$

$$\hat{\mathcal{H}}_{\mathrm{fs}}=\hbar D\sum_k\{[\hat{S}^2_{zk}-\tfrac{1}{3}S\,(S+1)]-[\hat{S}^2_{zk}-\tfrac{1}{4}(S_+S_-+S_-S_+)_k]\sin^2\vartheta_k+\tfrac{1}{4}[(\hat{S}_z\hat{S}_++\hat{S}_+\hat{S}_z)_k\exp(-\,i\varphi_k)$$

$$+(\hat{S}_z\hat{S}_-+\hat{S}_-\hat{S}_z)_k\exp(i\varphi_k)]\sin\vartheta_k\cos\vartheta_k+\tfrac{1}{4}[\hat{S}^2_{+k}\exp(-\,2i\varphi_k)+\hat{S}^2_{-k}\exp(2i\varphi_k)]\sin^2\vartheta_k\},$$

$$g=\tfrac{1}{3}(g_{\parallel}+2g_{\perp}),\qquad\Delta g=g_{\parallel}-g_{\perp},\qquad\hat{S}_{\pm k}=\hat{S}_x\pm i\hat{S}_y. \tag{17}$$

The exchange forces are relatively short range and are effective only in salts with rather high concentrations of magnetic ions. Therefore, in a sufficiently magnetically concentrated salt, $\hat{\mathcal{H}}'_Z+\hat{\mathcal{H}}_{\mathrm{fs}}+\hat{\mathcal{H}}_{\mathrm{hfs}}+\hat{\mathcal{H}}_{\mathrm{ss}}$ can be regarded as a perturbation relative to $\hat{\mathcal{H}}_{0Z}+\hat{\mathcal{H}}_{\mathrm{e}}$, i.e.,

$$\hat{\mathcal{H}}_1=\hat{\mathcal{H}}_{0z},\quad\hat{\mathcal{H}}_2=\hat{\mathcal{H}}_e,\quad\hat{\mathcal{H}}'=\hat{\mathcal{H}}'_z+\hat{\mathcal{H}}_{\mathrm{fs}}+\hat{\mathcal{H}}_{\mathrm{hfs}}+\hat{\mathcal{H}}_{ss}. \tag{18}$$

Experimentally, this corresponds to the case of observation of a single line of electron paramagnetic resonance without resolution of any structure.

It can be shown that the contributions to the spectral density $I(\omega)$ (1) from the different parts of the perturbation $\hat{\mathcal{H}}'$ (18) can be computed separately. The effect of exchange $\hat{\mathcal{H}}_{\mathrm{e}}$ does not appear on this part of the width of the absorption peak, which is associated with the anisotropic part of the Zeeman energy (since $[\hat{\mathcal{H}}'_Z,\mathcal{H}_{\mathrm{e}}]=0$), and the term $\hat{\mathcal{H}}_Z$ will be omitted in the consideration of exchange narrowing in solid salts.

We can represent the correlation function $f_{\alpha\gamma}(\tau)$ of the exchange motion in the form[3]

$$f_e(\tau)=\exp\,(-\,\tfrac{1}{2}\omega_e^2\tau^2), \tag{19}$$

where ω_e = exchange frequency.

In the case of strong exchange $\langle|\hat{\mathcal{H}}'|^2\rangle\ll\langle|\hat{\mathcal{H}}_{\mathrm{e}}|^2\rangle$, if we follow the scheme of Sec. 2 (for details see references 3 and 5), we obtain a Lorentz distribution for $I(\omega)$ with a half-width $\Delta\omega$:

$$\Delta\omega=\Delta\omega_{\mathrm{fs}}+\Delta\omega_{\mathrm{hfs}}+\Delta\omega_{ss}. \tag{20}$$

The dipole half-width $\Delta\omega_{\mathrm{ss}}$ is known in general form.[3] Therefore, we write down the explicit expressions only for $\Delta\omega_{\mathrm{fs}}$ and $\Delta\omega_{\mathrm{hfs}}$:

$$\Delta\omega_{\mathrm{fs}}=(\pi/2)^{1/2}P\omega_e^{-1}[\xi_0^2+(\xi_1^2+\xi_{-1}^2)\exp\,(-\,\omega_z^2/2\omega_e)$$

$$+\,\xi_1\exp\,(-\,2\omega_z^2/\omega_e^2)], \tag{21}$$

where

$$\xi_0^2 = \tfrac{4}{5} N^{-1} \sum_k \left(1 - \tfrac{3}{2} \sin^2 \vartheta_k\right)^2,$$

$$\xi_1^2 = \tfrac{3}{2} \xi_{-1}^2 = \tfrac{4}{5} N^{-1} \sum_k \sin^2 \vartheta_k \cos^2 \vartheta_k,$$

$$\xi_2^2 = \tfrac{1}{5} N^{-1} \sum_k \sin^4 \vartheta_k, \qquad P = D^2 \left[S(S+1) - \tfrac{3}{4}\right],$$

$$\omega_e^2 = 2J^2 S(S+1), \qquad J^2 = N^{-1} \sum_{i \neq j}\sum J_{ij}^2.$$

Here ϑ_k is the angle between the axis of the local electric field at the kth ion and the constant magnetic field H; J^2 is the mean square of the exchange integral existing at a single ion. If the exchange takes place only with z nearest neighbors, then $J^2 = z\mathcal{J}^2$, where $\mathcal{J}^2$ is the mean square of the exchange integral for a pair of nearest neighbors.

For powders and supercooled liquids, the distribution of the axes of the local fields can be taken as isotropic in the mean; then

$$\Delta\omega_{fs} = \frac{2}{15} (\pi)^{1/2} \left\{\frac{D^2 [S(S+1) - {}^3/_4]}{\sqrt{J^2 S(S+1)}}\right\} \times \left[\frac{3}{5} + \exp\left(-\frac{\omega_z^2}{4J^2 S(S+1)}\right) + \frac{2}{5} \exp\left(-\frac{\omega_z^2}{J^2 S(S+1)}\right)\right], \tag{23}$$

The contribution $\Delta\omega_{hfs}$ of the isotropic hyperfine structure (15), in accord with reference 5, is equal to

$$\Delta\omega_{hfs} = \tfrac{1}{2} (\pi/3)^{1/2} \left[\frac{A^2 I(I+1)}{\sqrt{J^2 S(S+1)}}\right] \left\{1 + \exp\left[\frac{-3\omega_z^2}{4J^2 S(S+1)}\right]\right\}, \tag{24}$$

where I is the nuclear spin.

At frequencies $\omega_z^2 \leq J^2 S(S+1)$, the exponents in (21), (23), and (24) should be kept, while at frequencies $\omega_z^2 \gg J^2 S(S+1)$, they can be neglected.

This peculiarity of the frequency dependence of $\Delta\omega_{fs}$ and $\Delta\omega_{hfs}$ is completely analogous to the well-known "$^{10}/_3$ effect" in the theory of dipole broadening.[1,5]

With the help of Eqs. (21) and (24) for monocrystals, and (23) and (24) for powders and supercooled liquids, we can estimate the part of the absorption line broadening due to unresolved structures.

We note that the contribution of the fine structure $\Delta\omega_{fs}$ (21) depends significantly on the angle ϑ and can be the reason for the occasional observance of anisotropy of line width in monocrystals. Since, in the single crystals of $CrCl_3$, at a frequency of 37,000 Mc, the line width at $\vartheta = 0$ and $\vartheta = 90°$ is given respectively by $\Delta H_{\parallel} = (140 \pm 5)$ oe and $\Delta H_{\perp} = (98 \pm 3)$ oe.[6] We estimate the exchange integral from the well-known relation of the theory of the molecular field $3k\Theta = 2JzS(S+1)$. The Curie temperature Θ for $CrCl_3$ is 27° K[7] z = 6.[8] It suffices to set $D = 0.1\ \text{cm}^{-1}$, in order to obtain $2(\Delta\omega_{\parallel} - \Delta\omega_{\perp}) = 38.3$ oe from Eqs. (21), (22).

Thus, from systematic measurements of the electron paramagnetic resonance line width, we can estimate the value of the fine and hyperfine splittings, even if the corresponding structures are not resolved.

The author thanks S. A. Al'tshuler for direction and constant attention to the work, and B. M. Kozyrev for discussion of the results.

---

[1] J. H. Van Vleck, Phys. Rev. **74**, 1168 (1948).

[2] P. W. Anderson and P. R. Weiss, Revs. Modern Phys. **25**, 269 (1953).

[3] R. Kubo and K. Tomita, J. Phys. Soc. Japan **9**, 888 (1954).

[4] S. A. Al'tshuler and B. M. Kozyrev, Usp. Fiz. Nauk **63**, 533 (1957).

[5] D. Kivelson, J. Chem. Phys. **27**, 1087 (1957).

[6] G. A. Egorov and Yu. V. Yablokov, JETP **39**, 265 (1960), Soviet Phys. JETP **12**, 190 (1961).

[7] J. W. Leech and A. J. Manuel, Proc. Phys. Soc. (London) **B69**, 210 (1956).

[8] B. F. Ormont, Структуры неорганических веществ (Structures of Inorganic Materials) (Gostekhizdat, 1950).

Translated by R. T Beyer.
183

SOVIET PHYSICS JETP VOLUME 13, NUMBER 4 OCTOBER, 1961

PHASE SHIFT ANALYSIS OF pp SCATTERING AT 95 Mev

V. A. BOROVIKOV, I. M. GEL'FAND, A. F. GRASHIN, and I. Ya. POMERANCHUK

Submitted to JETP editor October 6, 1960

J. Exptl. Theoret. Phys. (U.S.S.R.) 40, 1106-1111 (April, 1961)

A five-parameter analysis of the experimental data on pp-scattering at 95 Mev (cross section, polarization, depolarization) is performed by a new numerical method (the "ravine" method). We obtain a broad complex range of solutions, which cannot be described by specifying the local minima and error matrices as in the well known "local" technique. The region obtained can be divided into two comparatively small regions by including some data on rotation of polarization R, obtained by extrapolating from energies of 150, 210, and 310 Mev.

1. PHASE-SHIFT ANALYSIS PROCEDURE

AT the present time the universally adopted procedure for processing of experimental data, particularly the phase-shift procedure, is as follows. We minimize the square of the deviation

$$\chi^2(\delta) = \sum\left[\frac{y(\delta) - y_e}{\Delta_e}\right]^2, \qquad (1)$$

where $y(\delta)$ are the theoretical data (cross sections, etc.) as functions of certain parameters (phase shifts) $\delta = \delta_1, \delta_2 \ldots, \delta_n$, subject to determination from corresponding experimental data y_e (Δ_e — experimental errors); the sum extends over different points on the specified curves. The problem thus reduces formally to a determination of local minima of the function (1) in many-dimensional space of the parameters δ (the phase space), for which we usually employ the method of gradient descent from a series of randomly drawn points. The local minima obtained are called solutions, and their accuracy is specified in terms of an error matrix, which outlines certain many-dimensional ellipsoids in phase space (see, for example, references 1 — 4).

In the simplest cases the solution obtained in this manner can give a correct idea of the phase-space regions that satisfy the experimental data. However, if the number of dimensions and surfaces (1) is large and the surfaces have various undulations and troughs, the method is laborious and does not provide a sufficient assurance that all the regions with small values of χ^2 has been determined. This is not surprising, for two reasons:

1) It is difficult to trace a function that has essentially different values in a tremendous number of points. Thus, for example, in nine-parameter analysis with a range of variation $-\pi/2 \ll \delta \ll \pi/2$, with a spacing of 0.1 — 0.2, the number of points to be investigated for each phase is $10^{10} - 10^{14}$.

2) In any case of considerable complexity, the method of gradient descent is unjustifiably cumbersome, since it forces us to trace the most minute details of the relief, details which usually have no physical meaning, and we cannot extricate ourselves from individual 'cavities' in which we "get stuck." In addition, the method is essentially suitable for finding those individual cavities (local minima) which have usually the sense of a sort of 'fine structure' in broader regions containing low values.

Thus, instead of finding local minima it is desirable to carry out a direct "probing" of the phase space in order to find the entire region with low values of χ^2 and to obtain a more complete and accurate idea of the possible values of the phase shift. However, a direct "probing" of an entire phase space with a large number of dimensions is impossible in practice, and we must therefore use a method which works predominantly in regions with low values of χ^2. In this problem we use for this purpose a new numerical method (the method of "ravines") proposed by Gel'fand (more details about this method will be published separately). A characteristic feature of this method are "jumps" of finite length along the "ravines" of low values of χ^2. If the network of "ravines" is not too badly tangled up, this method yields relatively rapidly all regions with low values of χ^2. This situation obtains in "well organized" functions, such as the many-dimensional functions usually encountered in practical problems.

To complete the analysis we must choose some criterion for solving the problem. We use the simplest method of drawing the obtained points, assuming the solution to include all the regions of the phase space with values $\chi^2(\delta) \le \chi^2_{\max}$. In this problem we assume $\chi^2_{\max} = 2\overline{\chi^2}$ where $\overline{\chi^2}$ is the mean mathematical expectation. By plotting the theoretical curves corresponding to the phase shifts obtained in this manner we can ascertain that they agree sufficiently well with the experimental points.

We do not give a more detailed analysis of the region of solutions for the following reasons. Regions with low values of χ^2 are large and complex, and therefore any attempt to describe them by specifying the local minima and the error matrix, as is customary in the old procedure, may lead to a loss of large regions in which the true solution may be located. Upon sufficient improvement of the experimental data (improvement of the set of data through supplementary polarization experiments or by reducing the errors), the form of the surface (1) apparently becomes simpler and is converted into a certain small number of sufficiently narrow, clearly separated "troughs" of paraboloidal type. In this case it would be easy to investigate in detail the regions for solution and to find reliable limits. Further, the existing experimental data contain many systematical errors. Thus, new data on the cross section for 98 Mev (Harwell) differ greatly in a certain range of angles from those used in this investigation (Harvard). An analogous situation takes place for depolarization at 150 Mev. This leads to a certain distortion and to a shift in the level lines in phase space.

In making up the squared deviation (1), all the phases corresponding to large orbital momenta were considered in the one-meson approximation (with meson-nucleon constant $g^2 = 14.5$), as proposed in reference 5. The choice of values of momenta, starting with which the phase becomes "fixed" in the one-meson approximation, is based on estimates of the two-meson corrections obtained by Galanin et al.[6]

2. ANALYSIS OF DATA FOR 95 — 98 Mev

We processed the data on the cross section $\sigma(\theta)$ and polarization $P(\theta)$ for fourteen scattering angles[7] jointly with data on depolarization $D(\theta)$ for five scattering angles.[8] The independently varied parameters were five proper phase shifts with allowance for the Coulomb interaction (called BB shifts by Stapp et al.[2]), viz: $\delta_0(^1S_0)$, $\delta_2(^1D_2)$, $\delta_1^0(^3P_0)$, $\delta_1^1(^3P_1)$, and $\delta_1^2(^3P_2)$.

In the determination of the phase shifts $\epsilon_2(^3P_2 - {}^3F_2)$ and $\delta_3^2(^3F_2)$, connected with δ_1^2, it is necessary to take into account the fact that the one-meson approximation gives only the real parts of the scattering matrix. For this reason we specified in the one-meson approximation the following matrix elements[5]

$$\xi_2 = \operatorname{Re}[S^2_{1,3}/2i], \qquad \eta_3^2 = \operatorname{Re}[(S_3^2 - e^{2i\Phi_3})/2i],$$

(Φ_3 — Coulomb phase), which leads to the relations*

$$\operatorname{tg} \varepsilon_2 = 2\xi_2/[\sin 2\delta_1^2 - 2\eta_3^2 - \sin 2\Phi_3],$$

$$\sin 2\delta_3^2 = 2\eta_3^2 + \sin 2\Phi_3 - 2\xi_2 \operatorname{tg} \varepsilon_2.$$

Starting with the state $^3F_4$, all the contributions were taken into account in the form of a closed sum (one-meson amplitudes), and the imaginary parts of the scattering matrix were thus neglected.

As a result of the analysis we obtained a large complex region of solutions, which cannot be described by specifying the local minima and error matrices. We obtained several hundreds of points with $\chi^2 \le 2\overline{\chi^2}$ ($\overline{\chi^2} = 28$), which lie within the limits

$$-25° \leqslant \delta_0 \leqslant 25°, \qquad -4° \leqslant \delta_2 \leqslant 9°, \qquad -20° \leqslant \delta_1^0 \leqslant 35°,$$
$$-13° \leqslant \delta_1^1 \leqslant 9°, \qquad 9° \leqslant \delta_1^2 \leqslant 18°.$$

In an examination of the topography of the resultant region, we see that it has a tendency to split, in accordance with the phase shifts $^1S_0$ and $^3P_0$, into two regions (which we designate I and II), each of which is subdivided in turn into two others, corresponding to $^3P_1$ and $^1D_2$. In places where the proposed separations lie, there are low 'mountain ranges' with $\chi^2 \approx 3\overline{\chi^2}$. Figure 1 and the table show some of these points: 1 — 4 from region I and 5 and 6 from region II. These points were chosen from among all those obtained so as to include as fully as possible the entire resultant region of solutions.

Figures 2, 3, and 4 show the curves corresponding to the chosen points for the depolarization

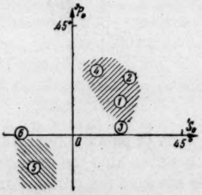

FIG. 1

---

*tg = tan.

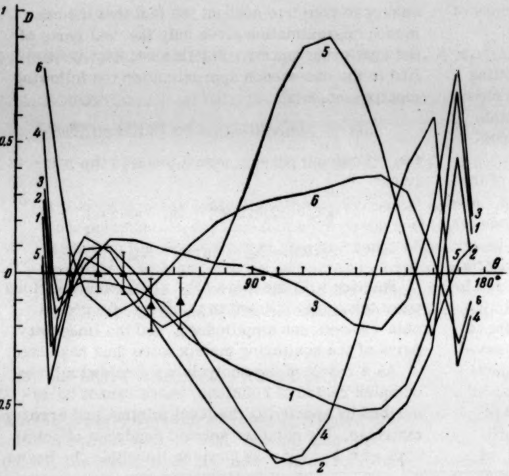

FIG. 2

Certain solutions (points) from the resultant region of phase space (in degrees)

Point	χ^2	$^1S_0$	$^1D_2$	$^3P_0$	$^3P_1$	$^3P_2$
1	25	20.3	6.0	14.4	—11.5	13.2
2	44	23.5	4.0	24.1	—8.7	12.5
3	59	20.2	6.8	3.7	—14.9	11.8
4	24	9.8	—3.5	26.0	—2.6	15.3
5	24	—16.9	7.2	—13.5	7.0	15.8
6	37	—20.5	—1.7	0.5	—10.6	13.8

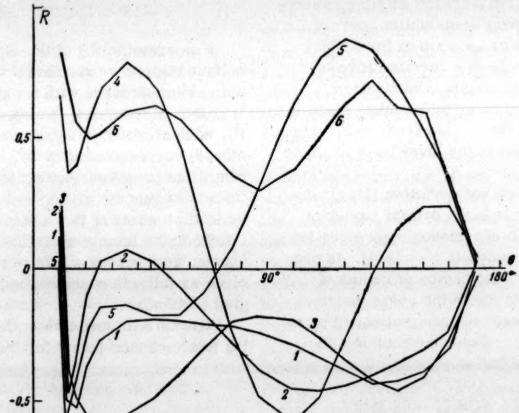

FIG. 3

D(θ) and rotations of polarization R(θ) and A(θ). Figure 2 shows also the experimental curves.[8] We do not give the curves for the cross section and polarization, for in practice the various solutions merge, within the limits of experimental errors, and differ somewhat in the interference region θ ≈ 10°.

Figures 2 – 4 show that a measurement of D(θ) for θ ≈ 120° and R(θ) for θ ≈ 30 and 120° would bring us much closer to a single-valued solution with relatively low tolerances in all the phases. Extrapolating the available data for R(θ) at energies 150, 210, and 310 Mev, we can assume that for 95 Mev the rotation of the

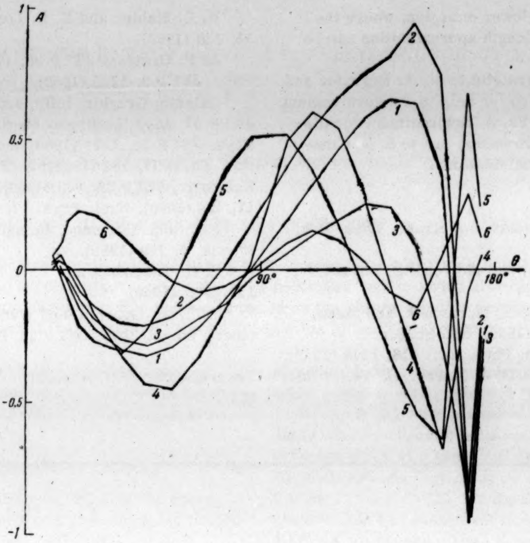

FIG. 4

polarization $R \approx -0.2$ at $\theta \approx 30°$. The addition of such data would shrink and sharply demarcate the foregoing regions and would yield two relatively small regions (two solutions):

I. $\delta_0 \approx 20°$, $\delta_2 \approx 6°$, $\delta_1^0 \approx 15°$, $\delta_1^1 \approx -12°$, $\delta_1^2 \approx 13°$;

II. $\delta_0 \approx -17°$, $\delta_2 \approx 7°$, $\delta_1^0 \approx -13°$, $\delta_1^1 \approx 7°$, $\delta_1^2 \approx 16°$.

In particular, only points with a positive ^1D phase shift, $\delta_2 \approx 4 - 8°$, would remain. We note that both solutions differ little in cross section and in polarization in the interference region.

For the foregoing solutions we obtained continuations in the region of high energies — solutions I and II for 150 Mev[9] and solutions I and II for 310 Mev,[3] respectively.

In carrying out the phase-shift analysis, we also undertook to ascertain whether it is possible to obtain from the available experimental data the "peripheral" phases, for which the main contribution should be made by the one-meson approximation, and to verify thereby the correctness of the estimate of the accuracy of the one-meson approximation, obtained by calculating the two-meson phases (see reference 6). For 95 Mev we can already regard as peripheral the F phase shifts and the mixing parameter ξ_2, which for this reason were 'fixed' in the one-meson approximation. However, the analysis was repeated with varying these phase shifts (four additional parameters). With this, the dimensions of the solution region increased and very low values $\chi^2 \approx 10$ were obtained at the minima (with $\overline{\chi^2} = 24$). To illustrate the permissable tolerances in the ^3F phase shifts we give one point with $\chi^2 = 26$:

$$\delta_0 = 21.1°, \quad \delta_2 = 6.1°, \quad \delta_1^0 = 3.2°, \quad \delta_1^1 = 10.1°,$$
$$\delta_1^2 = 8.9°, \quad \xi_2 = 4.3° (-3.4°), \quad \eta_3^2 = -11.8° (0.8°),$$
$$\delta_3^3 = 6.3° (0°), \quad \eta_3^4 = 2.3° (0.3°).$$

(the parentheses contain also the theoretical values of ξ_2 and ^3F phase shifts assumed in the five-parameter analysis).

The results obtained allow to conclude that it is impossible to obtain with any degree of reliability the values of ξ_2 and ^3F shifts from the available data, and it can only be stated that the one-meson values for these phase shifts do not contradict the experiment.

We note in conclusion that of the two regions of solutions indicated above, region I is preferred since it is characterized by positive values of the ^1S phase shift, and this agrees better with the positive ^1S phase at lower energies, where the effective scattering length approximation can be employed.

The authors are grateful to M. A. Evgrafov and I. I. Piatetskii-Shapiro for help in the development of the procedure, to Ya. A. Smorodinskii for discussions and useful remarks, and to S. L. Ginzburg for help in the calculations.

---

[1] Anderson, Gilcksman, and Kruse, Phys. Rev. **100**, 279 (1955).

[2] Stapp, Ypsilantis, and Metropolis, Phys. Rev. **105**, 302 (1957).

[3] Gziffra, MacGregor, Moravcsik, and Stapp, Phys. Rev. **114**, 880 (1959), MacGregor, Moravcsik, and Stapp, Phys. Rev. **116**, 1248 (1959), M. H. MacGregor and M. J. Moravcsik, Phys. Rev. Lett. **4**, 524 (1960).

[4] R. C. Stabler and E. L. Lomon, Nuovo cimento **15**, 150 (1960).

[5] A. F. Grashin, JETP **36**, 1717 (1959), Soviet Phys. JETP **9**, 1223 (1959).

[6] Galanin, Grashin, Ioffe, and Pomeranchuk, JETP **37**, 1663 (1959) and **38**, 375 (1960), Soviet Phys. JETP **10**, 1179 (1960) and **11**, 347 (1960); Nuc. Phys. **17**, 181 (1960); A. F. Grashin and I. Yu. Kobzarev, JETP **38**, 863 (1960), Soviet Phys. JETP **11**, 624 (1960); Nucl. Phys. **17**, 218 (1960).

[7] Palmieri, Cormack, Ramsey, and Wilson, Ann. Physik, **5**, 299 (1958).

[8] E. H. Thorndike and T. R. Ophel, Phys. Rev. **119**, 362, (1960).

[9] Gel'fand, Grashin, and Ivanova, JETP **40**, 1338 (1961), Soviet Phys. JETP **13**, in press.

Translated by J. G. Adashko
184

SOVIET PHYSICS JETP VOLUME 13, NUMBER 4 OCTOBER, 1961

RECONSTRUCTION OF THE ENERGY GAP IN A SUPERCONDUCTOR BY MEASUREMENT OF SOUND ATTENUATION

V. L. POKROVSKII and V. A. TOPONOGOV

Institute of Radiophysics and Electronics, Siberian Section, Academy of Sciences, U.S.S.R.

Submitted to JETP editor October 10, 1960

J. Exptl. Theoret. Phys. (U.S.S.R.) **40**, 1112-1114 (April, 1961)

A method is indicated for the reconstruction of the energy gap $\Delta(\mathbf{n})$ as a function of direction in an anisotropic superconductor on the basis of measurements of sound absorption $\alpha(\mathbf{n})$ in the low-temperature region. The method is based on the simple relation between the level lines of $\Delta(\mathbf{n})$ and $\alpha(\mathbf{n})$ on a stereographic projection of the Fermi surface.

IT was shown earlier[1] that ultrasonic damping $\alpha_s(\mathbf{q})$ in an anisotropic superconductor in the direction $\mathbf{n} = \mathbf{q}/q$ is determined by the asymptotic formula

$$\ln\left[(\alpha_s(\mathbf{q})/\omega_s(\mathbf{q})\right] = -\Delta_{min}^{(\mathbf{n})}/T, \tag{1}$$

where $\Delta_{\min}^{(\mathbf{n})}$ is the minimum value of the energy gap $\Delta(\mathbf{n})$ in the vicinity of a stereographic projection of the Fermi surface perpendicular to $\mathbf{n}$. Equation (1) is applicable in the temperature region determined by the inequality

$$1 < T_k/T < (2/\alpha)\ln(v_F/c), \tag{2}$$

where v_F is the Fermi velocity, c = sound velocity, α = coefficient of anisotropy, equal to the ratio of $\Delta(\mathbf{n})$ on the Fermi surface to the minimum value of Δ_0.

The purpose of the present work is a detailed analysis of the problem of the possibility of reconstruction of the function $\Delta(\mathbf{n})$ according to the given measurements of $\alpha_s(\mathbf{q})$, and the demonstration of a simple experimental procedure for reconstructing the gap. We shall assume that the type of Fermi surface is known from other experiments. In what follows, the Fermi surface is assumed to be singly connected. We shall also assume that the lattice possesses radial symmetry. For simplicity, we introduce the notation $\Delta_{\min}^{(\mathbf{n})} = f(\mathbf{n})$.

We consider a great circle on the sphere $C(\mathbf{n})$, perpendicular to the direction $\mathbf{n}$. Let $P(\mathbf{n})$ be the point on $C(\mathbf{n})$ at which $\Delta(\mathbf{n})$ takes its minimum value $f(\mathbf{n})$. Then the level line $\Gamma_{f(\mathbf{n})}$ of the function $\Delta(\mathbf{n})$ passing through $P(\mathbf{n})$ is tangent to the circle $C(\mathbf{n})$. From this it is evident that Γ_a is the envelope of a family of circles $C(\mathbf{n})$ for which $f(\mathbf{n}) = a$. In this way a method is given for constructing the function $\Delta(\mathbf{n})$ in terms of $f(\mathbf{n})$. However, in this case certain peculiarities can arise which we shall consider in examples.

1. Let $\Delta(\mathbf{n})$ have a total of two minima in diametrically opposite points which we shall take to be the poles of a spherical system of coordinates. We shall assume that $\Delta(\vartheta, \varphi)$ is a monotonic function of $\vartheta\ (0 < \vartheta < \pi/2)$ for fixed φ. We shall also assume that a certain level line Γ_a of the function $\Delta(\mathbf{n})$ is not convex. Then there exists a circle $C(\mathbf{n}_a)$ which is tangent to Γ_a at two points P_1, P_2 (Fig. 1). On an arbitrary circle which is tangent to Γ_a on the non-convex cut P_1P_2, the minimum of $\Delta(\mathbf{n})$ is less than a. It is then evident that one cannot define the function $\Delta(\mathbf{n})$ on the segment P_1P_2 of the curve Γ_a. The set of such segments for all Γ_a forms a region in which $\Delta(\mathbf{n})$ cannot be defined ("white spot").

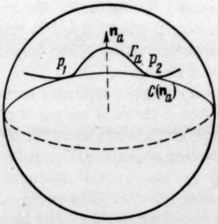

FIG. 1

We consider two families of circles tangent to Γ_a "on the left" (P_1) and "on the right" (P_2). It is obvious that these families are tangent to the circle $C(\mathbf{n}_a)$. For the function $f(\mathbf{n})$ this corresponds to the fact that its level line Γ_a has an angle point at $\mathbf{n}_a$.

2. Let there exist four absolute minima (in

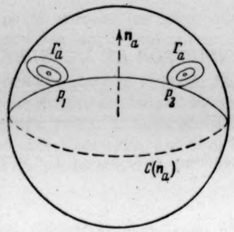

FIG. 2

two pairs of diametrically opposite points). Then, for certain values of a, the level lines Γ_a are split into four unconnected closed curves (Fig. 2). There exists a circle $C(\mathbf{n}_a)$ tangent to both these curves. In this case, just as in the previous, there are two families of circles tangent to Γ_a which are joined by $C(\mathbf{n}_a)$. Just as in case 2, this leads to a "white spot" for the function $\Delta(\mathbf{n})$, and to angle points for level lines of the function $f(\mathbf{n})$.

Thus, there are angle points of the level lines for the function $f(\mathbf{n})$. If $f(\mathbf{n})$ does not have these singularities, then $\Delta(\mathbf{n})$ is defined everywhere. Now let the function $f(\mathbf{n})$ be known. We shall take the level line γ_a of the function $f(\mathbf{n})$. For each point of $\mathbf{n}$ of the line γ_a we construct a circle $C(\mathbf{n})$ and find the envelope of the resultant family of circles. According to what has been pointed out above, this is also the level line Γ_a of the function $\Delta(\mathbf{n})$.

In experiment, the level line γ_a will be a certain broken curve consisting of segments of large circles. For each segment of the circle it is necessary to construct its center on the sphere. Joining all the points constructed in this fashion, we obtain an approximation of the level line Γ_a of the function $\Delta(\mathbf{n})$.

It is necessary to give separate consideration to the case in which there is an angle point on γ_a. In this case, for sufficiently detailed measurement, the two neighboring segments of circles on the line approximating γ_a intersect at an angle which is strongly different from π. The two points on the line Γ_a corresponding to them will be sufficiently far removed from one another. According to what has been observed in connection with the examples considered above, it is not necessary to join such points, since they form the boundary of a "white spot."

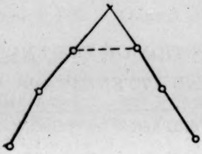

FIG. 3

What has been said above needs to be made more precise. For experiments close to the angle point, the line γ_a will be the characteristic situation schematically drawn in Fig. 3. In this case, it is necessary to draw the line through the experimental points so that only a single angle is obtained that differs strongly from π. Evidently, after the initial measurements, it will be necessary to carry out more detailed measurements close to the points which can be shown to be angle points.

As has been shown,[1] for superconductors with a Fermi surface of the corrugated plane type, Eq. (1) is found to be invalid even at temperatures satisfying condition (2) in that region of directions of sound propagation which are not parallel to any normal to the Fermi surface. In this case, the following formula holds:

$$\ln(\alpha_s/\omega_s) \approx -\Delta_0/T. \tag{3}$$

This means that $f(\mathbf{n})$ is constant in some region on the sphere. Reconstruction of $\Delta(\mathbf{n})$ in terms of $f(\mathbf{n})$ is carried out in this case also by the method described above.

The situation becomes complicated if the Fermi surface is not singly connected. In this case, to reconstruct $\Delta(\mathbf{n})$ by means of $f(\mathbf{n})$, it is necessary to apply the procedure that has been described, but it is not possible to show to just which of the unconnected parts of the Fermi surface the level lines that have been found belong.

---

[1] V. L. Pokrovskii, JETP **40**, 898 (1961), Soviet Phys. JETP **13**, 628 (1961).

Translated by R. T. Beyer
185

SOVIET PHYSICS JETP VOLUME 13, NUMBER 4 OCTOBER, 1961

STABILITY OF A PLASMA PINCH WITH ANISOTROPIC PARTICLE VELOCITY DISTRIBUTION AND ARBITRARY CURRENT DISTRIBUTION

V. F. ALEKSIN and V. I. YASHIN

Physico-Technical Institute, Academy of Sciences, Ukrainian S. S. R.

Submitted to JETP editor October 13, 1960

J. Exptl. Theoret. Phys. (U.S.S.R.) **40**, 1115-1118 (April, 1961)

The necessary conditions for stability of a plasma with an anisotropic distribution of particle velocities located in a helical magnetic field are derived on the basis of kinetic theory without taking close collisions into account.

In Suydam's work[1], a necessary condition for stability of a plasma pinch with arbitrary electric current distribution is obtained in the magnetohydrodynamic approximation. The magnetohydrodynamic approximation is only valid for perturbations with frequency and growth rate significantly lower than the frequency of close collisions. To investigate perturbations of frequency significantly greater than the frequency of the close collisions, a kinetic analysis is necessary. For perturbations in the region in which the "drift" approximation is applicable, a stability criterion can be obtained from the generalized energy principle.[2]

In this paper, the stability of a cylindrical plasma pinch with an anisotropic particle velocity distribution is investigated with the aid of the generalized energy principle and with account the charge neutrality of the plasma.[3] As in Suydam's work,[1] the magnetic lines of force are assumed to be helical, with pitch depending on the distance from the symmetry axis. We note that the "drift" approximation is not valid for particles in the tail of the equilibrium distribution. The number of these particles is small and therefore, as shown by Sagdeev and Shafranov,[4] the oscillation build-up effects that lead to instability, produced by them, are also small. No such instabilities exist in the case of a "cut-off" equilibrium distribution.

In this paper we obtain the necessary conditions for stability of a plasma pinch with anisotropic particle-velocity distribution. One of these criteria, which places a limit on the magnetic field gradient and on the particle distribution function, is the analog of Suydam's condition. Two other criteria with a local character are related to the possible appearance of "kinetic" instabilities caused by the anisotropy in the distribution function. These conditions have the same form as in the case of an unbounded homogeneous plasma.

A necessary condition for the stability of a plasma is that the energy change, δW, resulting from a small possible perturbation be greater than or equal to zero. Choosing the displacement vector of the plasma, $\boldsymbol{\xi}(\mathbf{r})$, in the form

$$\xi(\mathbf{r}) = [\xi_r(r),\ \xi_\varphi(r),\ \xi_z(r)] \exp(ikz + im\varphi) \qquad (1)$$

and minimizing the previously obtained[3] expression for δW with respect to the displacement components $\xi_\varphi(r)$ and $\xi_z(r)$, we find

$$\delta W = \pi \int_0^R r\,dr \left(A\frac{\xi^2}{r^2} + 2B\frac{\xi\xi'}{r} + C\xi'^2 \right). \qquad (2)$$

Here $\xi = \xi_r$; the prime signifies differentiation with respect to r;

$$A = \gamma n_z^4 + \eta(g^2r^2 - n_\varphi^4) - r\frac{d}{dr}(\eta n_\varphi^2) - \frac{[\gamma n_z^2(mr^{-1}n_z - kn_\varphi) + \eta n_\varphi(gn_z + k)]^2}{\gamma(mr^{-1}n_z - kn_\varphi)^2 + \eta g^2}, \qquad (3)$$

$$B = -\eta n_\varphi^2 + k^2\gamma\eta/[\gamma(mr^{-1}n_z - kn_\varphi)^2 + \eta g^2], \qquad (4)$$

$$C = g^2\gamma\eta/[\gamma(mr^{-1}n_z - kn_\varphi)^2 + \eta g^2], \qquad (5)$$

where

$$\mathbf{n} = \mathbf{H}/H, \quad g = kn_z + mr^{-1}n_\varphi, \quad \eta = H^2/4\pi + p_\perp - p_\parallel,$$
$$\gamma = H^2/4\pi + 2p_\perp + 2q,$$

$p_\parallel$ and $p_\perp$ are the longitudinal and transverse components of the pressure tensor, and R is the radius of the pinch. The quantity q is related to the anisotropy of the particle distribution function $f_0^{(i)}(r, v_\parallel, v_\perp)$:

$$q = \frac{1}{2}\sum_i m_i \iint \frac{H^3}{v_\parallel}\mu^2\frac{\partial f_0^{(i)}}{\partial\varepsilon}d\mu\,d\varepsilon - \Big(\sum_i e_i \iint \frac{H^2}{v_\parallel}\mu\frac{\partial f_0^{(i)}}{\partial\varepsilon}d\mu\,d\varepsilon\Big)^2 \Big/ 2\sum_i \frac{e_i^2}{m_i}\iint \frac{H}{v_\parallel}\frac{\partial f_0^{(i)}}{\partial\varepsilon}d\mu\,d\varepsilon. \qquad (6)$$

The variables of integration, μ and ε, are given in terms of the longitudinal and transverse velocity components by $\mu = v_\perp^2/2H$ and $\varepsilon = {}^1\!/_2(v_\parallel^2 + v_\perp^2)$. The summation in Eq. (6) is over the particle types (m_i and e_i are the mass and charge of particles of the i-th type).

In the derivation of (2) it was assumed that the displacement ξ_r is zero on the boundary of the plasma and on the axis of the cylinder. In order that the quadratic form (2) be non-negative, it is necessary that the coefficient of ξ'^2 be positive. We find another necessary condition by minimizing δW with respect to ξ. This minimization leads to the Euler equation

$$\xi'' + \left(\frac{d}{dr}\ln Cr\right)\xi' - \frac{1}{Cr^2}\left(A - r\frac{dB}{dr}\right)\xi = 0. \qquad (7)$$

If ξ satisfies Eq. (7), then the expression under the integral sign in (2) is a perfect differential, so that

$$\int r\,dr\left(A\frac{1}{r^2}\xi^2 + 2B\frac{1}{r}\xi\xi' + C\xi'^2\right) = B\xi^2 + Cr\xi\xi'. \qquad (8)$$

Equation (7) is an equation with a regular singularity at $r = a$, where $g(a) = 0$. The general solution of Eq. (7) has a branch point or pole at $r = a$ and can be represented in the form

$$\xi = (r-a)^{s_1}u_1(r) + (r-a)^{s_2}u_2(r), \qquad (9)$$

where $u_1(r)$ and $u_2(r)$ are functions analytic at $r = a$ and $s_{1,2} = -{}^1\!/_2 \pm {}^1\!/_2(1 - 4M^2)^{1/2}$ are the roots of the indicial equation

$$s^2 + s + M^2 = 0, \qquad M^2 = \left[\left(\frac{\nu}{\nu'}\right)^2\nu^2\left(1 + \frac{\eta}{\gamma} + r\frac{\eta'}{\eta n_\varphi^2}\right)\right]_{r=a},$$

$$\nu = \frac{n_\varphi}{rn_z} = \frac{H_\varphi}{rH_z}. \qquad (10)$$

For all values of M^2, the displacement ξ is infinite at $r = a$. Therefore we substitute in Eq. (2) for δW values of ξ which satisfy Eq. (7) for all r except in the interval $a - \varepsilon < r < a + \varepsilon$, in which we choose ξ constant:

$$\xi = \varepsilon^{s_1}u_1(a) + \varepsilon^{s_2}u_2(a). \qquad (11)$$

The width, 2ε, of the interval is chosen to be such that when $u_1(r)$ and $u_2(r)$ are expanded in powers of $r - a \approx \varepsilon$, only the first term need be kept. In the following determination of the sign of δW, the values of $u_1(a)$ and $u_2(a)$ at $r = a$ are not essential and are chosen to be equal to unity.

If the roots of the indicial equation (10) are real ($4M^2 \leq 1$), we find

$$\delta W = 2\pi\varepsilon^{2s_2+1}\left[r\eta n_\varphi^2 n_z^2(\nu'/\nu)^2\right]_{r=a}(|s_2| - M^2) \geqslant 0. \qquad (12)$$

If the roots s_1 and s_2 are complex ($1 - 4M^2 = -\rho < 0$), then the energy change δW has the form

$$\delta W = \tfrac{1}{2}\pi\left[r\eta n_\varphi^2 n_z^2(\nu'/\nu)^2\right]_{r=a}\left[(1 - 2M^2)(1 + \cos 2\psi) + \rho\sin 2\psi\right], \qquad (13)$$

where $\psi = {}^1\!/_2\rho\ln\varepsilon + \Phi$ with Φ a constant phase.

It is easy to see that the right hand side of (13) can be made negative by a suitable choice of the interval width, 2ε. Thus, for the stability of the plasma it is necessary that the inequalities

$$H^2/4\pi + p_\perp - p_\parallel \geqslant 0, \qquad H^2/4\pi + 2p_\perp + 2q \geqslant 0, \qquad (14)$$

$$4\left(\frac{H_\varphi}{rH_z}\right)^2\left[1 + \frac{H^2/4\pi + p_\perp - p_\parallel}{H^2/4\pi + 2p_\perp + 2q} + r\frac{H^2}{H_\varphi^2}\frac{d}{dr}\ln(H^2/4\pi + p_\perp - p_\parallel)\right]$$
$$\leqslant\left(\frac{d}{dr}\ln\frac{H_\varphi}{rH_z}\right)^2 \qquad (15)$$

hold at all points, with $m \neq 0$.

In the isotropic case, $f_0^{(i)} = f_0^{(i)}(r, v_\parallel^2 + v_\perp^2)$, the inequalities (14) are automatically fulfilled and (15) becomes the stability criterion obtained by Suydam[1] in the magnetohydrodynamic approximation. This shows that collisions do not affect the stability condition (15) in an isotropic plasma. We note that the inequalities (14) are identical with the stability criteria for an unbounded homogeneous plasma.[5]

In the case $m = 0$, the stability conditions can be obtained directly from (2); they are

$$\eta = H^2/4\pi + p_\perp - p_\parallel \geqslant 0, \qquad \gamma = H^2/4\pi + 2p_\perp + 2q \geqslant 0,$$

$$\eta(\gamma - \eta)\left[\gamma(rn_\varphi^2)' + \eta n_z^2\right] - r\gamma'\eta^2 n_z^2 - r\eta'\gamma^2 n_\varphi^2$$
$$+ \eta(\gamma n_\varphi^2 + \eta n_z^2)^2\left[(k^2r^2 + 1)n_z^2 - 2n_\varphi^2\right] \geqslant 0. \qquad (16)$$

We note that the criteria (16) are not valid if the magnetic lines of force are circular ($n_z = 0$). This is due to the fact that when $n_z = 0$, integrals along the lines of force which are zero for $n_z \neq 0$ contribute to the expression for the energy change δW. We have obtained the stability criteria for $n_z = 0$ in a previous paper.[3]

In conclusion, the authors thank A. I. Akhiezer and K. N. Stepanov for useful advice and criticism.

---

[1] B. R. Suydam, Физика горячей плазмы и термоядерные реакции (Physics of Hot Plasma and Thermonuclear Reactions) Glavatom, **1**, 89 (1959).

[2] M. D. Kruskal and S. R. Oberman, ibid. **1**, 42 (1959).

[3] V. F. Aleksin and V. I. Yashin, JETP **39**, 822 (1960), Soviet Phys. JETP **12**, 572 (1961).

[4] R. Z. Sagdeev and V. D. Shafranov, JETP **39**, 181 (1960), Soviet Phys. JETP **12**, 130 (1961).

[5] A. B. Kitsenko and K. N. Stepanov, JETP **38**, 1841 (1960), Soviet Phys. JETP **11**, 1323 (1960).

Translated by M. Bolstęrli
186

SOVIET PHYSICS JETP VOLUME 13, NUMBER 4 OCTOBER, 1961

LOSSES OF ELECTRONS IN SYNCHROTRONS DUE TO THE QUANTUM CHARACTER OF THE RADIATION

P. S. LANDA

Moscow State University

Submitted to JETP editor October 18, 1960

J. Exptl. Theoret. Phys. (U.S.S.R.) 40, 1119-1123 (April, 1961)

By means of an approximate solution of the nonstationary Fokker-Planck equation, an explicit expression which includes effects of the nonlinearity of the phase oscillations, is obtained for the probability of electron loss. It is shown that inclusion of the nonlinearity leads to an increase of the probability of electron loss, but this increase is quite insignificant and is of the order of unity. A simple approximate formula for calculating electron-loss probabilities is proposed.

THE effect of the quantum nature of the radiation of electromagnetic waves by a beam of electrons being accelerated in a synchrotron on the phase of the alternating electric field at the instant an electron passes through an accelerating section is equivalent to the effect of white noise. As the result of the action of this noise, the phase can pass through an unstable value and the electron will then be lost. A knowledge of the probability of electron loss is necessary for the correct choice of the parameters of a synchrotron. Quite a number of papers have been devoted to this problem, for example references 1 — 5. In some of them (cf. reference 1) the damping of the phase oscillations is not taken into account; in others a linearized problem is solved and only the mean-square deviation of the phase from its equilibrium value is calculated (for example, reference 2); in still others there is an incomplete inclusion of effects of the nonlinearity of the phase oscillations (references 3 — 5). For example, in Matveev's papers[3-5] the value of the unstable phase is calculated with the nonlinear equation, but the statistical problem of the probability of reaching this unstable phase is solved by linearization of the original equation. Naturally such an approach can lead to errors, since the equation that describes the phase fluctuations is essentially nonlinear.

In the present paper full account is taken of both the nonlinear character of the equation and the damping of the phase oscillations. As a particular example the data so obtained are compared with the results of Matveev.[3-5]

As is well known,[1-5] the equation for the synchrotron phase oscillations is analogous to the equation of the physical pendulum with displaced equilibrium position:

$$\ddot{\psi} + \gamma\dot{\psi} + f^2 [\cos\varphi_s - \cos(\varphi_s + \psi)] = \frac{k\omega\alpha}{\lambda E_s}\Big[W_s - \sum_i \varepsilon_i \delta(t - t_i)\Big]. \tag{1}$$

Here $\psi = \varphi - \varphi_s$, where φ_s is the equilibrium value of the phase;

$$\gamma = (4 - \alpha)\frac{2\omega r_0}{3R}\left(\frac{E_s}{m_0c^2}\right)^3, \quad \alpha = \frac{\delta R / R}{\delta E / E}, \quad f^2 = \frac{k\omega^2\alpha}{2\pi\lambda}\frac{eV_0}{E_s},$$

α is the spacing coefficient, R the radius of the electron orbit, E_s the equilibrium value of the electron energy, $r_0 = e^2/m_0c^2$, $\omega = c/R\lambda$, $\lambda = 1 + L/2\pi k$, L is the total length of the straight sections in the circumference of the synchrotron, k is the harmonic number of the high-frequency field at which the acceleration is produced, and V_0 is the amplitude of the high-frequency field.

The right member of Eq. (1) characterizes the emission of radiation by the electron and is assumed to be small. The concrete conditions assumed for this smallness will be indicated later. The first term in the right member of Eq. (1) is proportional to the equilibrium power radiated by the electron,

$$W_s = 2ce^2 / 3\lambda R^2 (E_s / m_0c^2)^4;$$

the second represents a random succession of short pulses, equivalent to white noise with the spectral density

$$N = (k^2\omega^2\alpha^2 / \lambda^2E_s^2)\langle\varepsilon^2\rangle\bar{n},$$

where $\langle\epsilon^2\rangle$ is the mean square value of the energy of the emitted photons, and n is the mean number of photons per unit time. The values of $<\epsilon^2>$ and n have been calculated by Matveev[5]:

$$\langle\varepsilon^2\rangle=\left(\frac{55}{24\sqrt{3}}\right)\left(\frac{hc^2e^2}{\lambda R^3}\right)\left(\frac{E_s}{m_0c^2}\right)^7, \qquad \bar{n}=\frac{5}{2\sqrt{3}R}\frac{e^2}{h}\frac{E_s}{m_0c^2}.$$

Let us introduce a function $U(\psi)$, which characterizes the potential energy of the phase oscillations:*

$$U(\psi)=\Omega^2\left[1-\cos\psi+\operatorname{ctg}\varphi_s(\psi-\sin\psi)\right], \qquad \Omega^2=f^2\sin\varphi_s.$$

The function $U(\psi)$ has extrema at the points $\psi = 2\pi n$ and $\psi = -2\varphi_S + 2\pi n$, $n = 0, \pm 1, \pm 2, \ldots$. We shall be interested in the positions of the maxima of $U(\psi)$ that are closest to the equilibrium value $\psi = 0$: $\psi_1 = -2\varphi_S$ and $\psi_2 = 2(\pi - \varphi_S)$. To these values of ψ there correspond maximum values of $U(\psi)$ given by

$$U(\psi_1)=2\Omega^2\left[-\varphi_s\operatorname{ctg}\varphi_s+1\right],$$

$$U(\psi_2)=2\Omega^2\left[(\pi-\varphi_s)\operatorname{ctg}\varphi_s+1\right].$$

If $\varphi_S \neq \pi/2$, then $U(\psi_1) \neq U(\psi_2)$, and the loss of a particle occurs whenever the phase ψ reaches that one of the extremal values at which the maximum of $U(\psi)$ is the smaller.

Let us rewrite Eq. (1) in the form

$$\ddot{\psi}+\gamma\dot{\psi}+dU/d\psi=\xi(t), \tag{2}$$

where

$$\xi(t)=\frac{k\omega\alpha}{\lambda E_s}\left[W_s-\sum_i\varepsilon_i\delta(t-t_i)\right]$$

is white noise with zero mean value.

We now introduce a new variable Q to characterize the total energy of the phase oscillations:

$$Q=\dot{\psi}^2/2+U(\psi).$$

Multiplying both sides of Eq. (2) by $\dot{\psi}$, we get an exact equation for Q:

$$\dot{Q}=-\gamma\dot{\psi}^2+\dot{\psi}\xi(t). \tag{3}$$

If the damping coefficient γ of the phase oscillations is small in comparison with the average frequency of the oscillations and if the emission of radiation is so small that

$$\left\langle\left[\int_t^{t+\tau}\dot{\psi}\xi(t)\,dt\right]^2\right\rangle^{1/2}\ll U_{max}$$

(here the brackets $< >$ denote the statistical average, and τ is an interval of time of the order of the mean period of the oscillations), then we can average the right member of Eq. (3) over the period.

Generally speaking, the quantities φ_S, γ, f^2, and N are functions of the time, since as a particle is accelerated its energy E_S changes, and consequently there is also a change of its equilibrium phase φ_S. The radiation effect, however, is important only in the final stage of the acceleration process, in which the change of energy occurs very slowly, so that we can regard the quantities E_S and φ_S as constant over the period of the phase oscillations. Moreover, in many cases one is interested in motion of a particle along an orbit with constant energy, with the radiation loss on the average compensating the energy of the high-frequency field.

Let us introduce the quantity $\overline{\dot{\psi}^2}$ averaged over the period (cf. reference 1):

$$\overline{\dot{\psi}^2}\equiv f_1(Q)=I_1(Q)/I_2(Q), \tag{4}$$

where

$$I_1(Q)=\int_{\Phi_{min}}^{\psi_{max}}\sqrt{2\left[Q-U(\psi)\right]}\,d\psi,$$

$$I_2(Q)=\int_{\psi_{min}}^{\psi_{max}}d\psi/\sqrt{2\left[Q-U(\psi)\right]}.$$

Here ψ_{min} and ψ_{max} are the extreme values of the phase in the oscillations, i.e., the two solutions of the equation $U(\psi) = Q$ that are closest to $\psi = 0$.

Substituting the expression (4) in Eq. (4), we get an approximate equation for the energy of the phase oscillations:

$$\dot{Q}=-\gamma f_1(Q)+\dot{\psi}\xi(t). \tag{5}$$

This equation describes a Markov process, and consequently for the calculation of the statistical characteristics of Q we can use the Fokker-Planck equation:

$$\frac{\partial w}{\partial t}=-\frac{\partial}{\partial Q}\left\{\left[-\gamma f_1(Q)+a(Q)\right]w\right\}+\frac{1}{2}\frac{\partial^2}{\partial Q^2}\left[b(Q)w\right]. \tag{6}$$

Here $w(Q, t)$ is the probability density distribution for the quantity Q; $a(Q) = <\dot{\psi}\xi(t)>$ is the mean value of the random process $\xi(t)\dot{\psi}$, which is different from zero because of the correlation between $\dot{\psi}$ and $\xi(t)$; and $b(Q)$ is the spectral density of the process $\dot{\psi}\xi(t)$. The quantities $a(Q)$ and $b(Q)$ can be calculated by a method analogous to that given in the appendix to a paper by Stratonovich.[6] We get as the result:

$$a(Q)=N/2, \qquad b(Q)=Nf_1(Q). \tag{7}$$

A knowledge of the nonstationary solution of the Fokker-Planck equation enables us to calculate the probability for loss of the electron. As has been stated, the electron will be lost if ψ reaches the value ψ_1 or ψ_2, i.e., the energy Q exceeds the value U_{max} that corresponds to the smaller of the values $U(\psi_1)$ and $U(\psi_2)$. Thus mathematically our problem reduces to that of the reaching of a boundary, and for the case of a constant boundary the approximate solution of this problem has been given in many papers.

---

*ctg = cot.

In the present paper we use the results of preceding papers,[7,8] and from these it follows that in the case of sufficiently small fluctuations of the radiation the number of electrons in the synchrotron should decrease with time according to the law $n(t) = n_0 e^{-\beta t}$, where β is the probability per unit time of loss of an electron. The quantity β can be expressed approximately in terms of the stationary solution of Eq. (6) that satisfies the condition that the probability flux vanishes:

$$\beta = \tfrac{1}{2}\gamma f_1(U_{max}) w(U_{max}). \tag{8}$$

As is well known, the stationary solution $w(Q)$ is of the form

$$w(Q) = \frac{C_0}{f_1(Q)} \exp\left\{-2\frac{\gamma}{N}Q + \int \frac{dQ}{f_1(Q)}\right\} = C_0 I_2(Q) e^{-2\gamma Q/N}. \tag{9}$$

Since for small fluctuations of the radiation $w(Q)$ has a sharply marked maximum near $Q = 0$, for the calculation of C_0 we can set $f(Q) \approx Q$. This will be justified if $N/\gamma\Omega^2 \ll 1$. Besides this we assume that $N/\gamma\Omega^2 \ll U_{max}$. Then, apart from a term $\sim \exp(-2\gamma U_{max}/N)$, we get

$$C_0 \approx \gamma\Omega/\pi N. \tag{10}$$

Substituting Eqs. (9) and (10) in Eq. (8), we have

$$\beta = (\gamma^2\Omega/\pi N) I_1(U_{max}) \exp(-2\gamma U_{max}/N). \tag{11}$$

For comparison we shall calculate β in the case of linearization of the equation of the phase oscillations. Furthermore, as Matveev has done,[4] we shall take the depth of the potential well from the nonlinear theory, and shall determine the permissible limits on the deviations in the framework of the linear theory from the requirement that the depths of the potential well be the same in the linear and nonlinear theories. Then for the calculation of β we need only set $I_1(U_{max}) = \pi U_{max}/\Omega$. We then have

$$\beta_{lin} = (\gamma^2 U_{max}/N) \exp(-2\gamma U_{max}/N). \tag{12}$$

As we see, the expressions (11) and (12) differ by a factor $\mu = \Omega I_1(U_{max})/\pi U_{max}$. A calculation shows that $\mu > 1$, i.e., when the nonlinearity is taken into account we get a larger value for the probability of loss of an electron.

In the general case the value of the quantity μ must be determined graphically, since one cannot get an analytic expression for $I_1(U_{max})$. There is, however, one practically important case — that in which the mean radiation loss per revolution is small in comparison with eV_0 and the beam of electrons revolves in a constant orbit with constant energy (the mean radiation loss being compensated by the energy of the high-frequency electric field) — for which the value of μ can be calculated analytically. In fact, in this case $U_{max} = 2f^2$, $\Omega = f$, $I_1(U_{max}) = 8f$, and consequently $\mu = 4/\pi$. Calculation shows that also for other values of φ_s the quantity μ is close to unity. For example, for $\varphi_s = 3\pi/4$ we have $\mu = 1.15$. Therefore it is probably suitable for practical purposes to use the simplified formula (12) and, if the correction is important, to introduce a correction factor $\mu = 1.2$.

The expressions (11) and (12) are valid in the case of motion of the electron along an orbit with constant energy. If the energy of the electron is changing, but so slowly that during the time in which a stationary distribution is established (a time of the order $1/\gamma$) it does not change much, the expressions (11) and (12) remain valid, except that we must regard β as a function of the time. In this case the number of particles in the synchrotron falls off with time according to the law

$$n(t) = n_0 \exp\left(-\int_0^t \beta dt\right).$$

In the case in which the change of energy of the electron is not slow, one can use the method of majorants.[4,5]

---

[1] N. M. Blachman, On the Effect of Noise in Nonlinear Automatic Control Systems. First IFAC (Intl. Feder. for Automatic Control) Congress, Moscow, 1960.

[2] M. Sands, Phys. Rev. **97**, 470 (1955).

[3] A. N. Matveev, JETP **33**, 913 (1957), Soviet Phys. JETP **6**, 702 (1958).

[4] A. N. Matveev, JETP **33**, 1254 (1957), Soviet Phys. JETP **6**, 965 (1958).

[5] A. N. Matveev, Dissertation, Moscow State University, 1958.

[6] R. L. Stratonovich, Радиотехника и электроника (Radio Engineering and Electronics) **3**, 497 (1958).

[7] R. L. Stratonovich and P. S. Landa, Изв. высших уч. зав., Радиофизика (News of Higher Educational Institutions, Radiophysics) **2**, 37 (1959).

[8] P. S. Landa, Автоматика и телемеханика (Automation and Telemechanics) **21**, 36 (1960).

Translated by W. H. Furry
187

SOVIET PHYSICS JETP VOLUME 13, NUMBER 4 OCTOBER, 1961

SUPERFLUIDITY IN A FERMI SYSTEM IN THE PRESENCE OF PAIRS WITH NONZERO ANGULAR MOMENTUM

L. P. GOR'KOV and V. M. GALITSKII

Institute for Physics Problems, Academy of Sciences, U.S.S.R.

Submitted to JETP editor October 25, 1960

J. Exptl. Theoret. Phys. (U.S.S.R.) **40**, 1124-1127 (April, 1961)

A picture is proposed for the superfluid state in a Fermi system when the Cooper pairs have a nonzero angular momentum. It is shown that if the system does not have a total angular momentum, the ground state will be isotropic. The Fermi excitation spectrum has its usual form with an isotropic gap.

In all the papers on the theory of superconductivity (cf., for example, references 1, 2, etc.) it is assumed that the Cooper pairs[3] are formed in an S state. But it is obvious that one can generalize the Cooper phenomenon in a system of Fermi particles to the case where the attraction between a pair of particles occurs in a state with nonzero relative angular momentum. In particular, Pitaevskii[4] has shown that for a pair of excitations in He^3 there is an attraction in the higher harmonics. It is of interest to study the characteristics of the superfluid state that develops in a Fermi system at sufficiently low temperatures because of this type of interaction. Such an attempt was made in a recent paper by Anderson and Morel,[5] but their results seem to us to be incorrect. In the following we shall investigate this question, using a generalization of the method[6] proposed by one of us in the theory of superconductivity.

Let the interaction between two particles have the following form

$$V(\mathbf{p}-\mathbf{p}') = \sum_l V_l P_l(\theta) \tag{1}$$

in the momentum representation, i.e., in the neighborhood of the Fermi surface, the interaction depends on the angle between the vectors $\mathbf{p}$ and $\mathbf{p}'$ and is independent of their magnitudes. For simplicity, we assume[1,2] that the interaction is equal to zero* when $|v(p-p_0)|$, $|v(p'-p_0)| > \tilde{\omega}$ and restrict ourselves to the weak binding approximation.

Let us assume that the relation between the quantities V_l is such that the Cooper pairs which are formed have orbital angular momentum l and spin s.* As was done in reference 6, we then consider the value at absolute zero of the average of a product of four fermion operators $\langle N|\psi_1\psi_2\psi_3^+\psi_4^+|N\rangle$ over the exact ground state for a fixed number of particles. We shall assume that the total angular momentum is zero in the ground state. The operators $\psi_1\psi_2$ which annihilate, and $\psi_3^+\psi_4^+$ which create two particles, contain terms corresponding to the creation and annihilation of bound pairs. At absolute zero the pairs, which obey Bose statistics, are in a state of Bose "condensation," i.e. the number of pairs in states with their momentum equal to zero is comparable to the total number of particles in the system. Therefore the matrix element $\langle N+2|\psi^+\psi^+|N\rangle$ can be replaced by a c-number. In doing this we must remember that, because of the nonzero orbital angular momentum of the pair, the operator $\psi^+\psi^+$ can create a pair with any one of $(2l+1)$ values of the angular momentum projection, and consequently contains $2l+1$ components, corresponding to transitions

$$\langle N+2, l, m|\psi^+\psi^+|N, 0\rangle$$

from the ground state of the N particle system to the ground state of the $(N+2)$-particle system with angular momentum projection m along some direction. In the light of these remarks it is clear that the generalization of the method of reference 6 to the present case consists in introducing $2l+1$ functions $F^+_{m\alpha\beta}(x-x')$ and $F_{m\alpha\beta}(x-x')$:

$$F^+_{m\alpha\beta}(x-x') = \langle N+2, l, m|T(\psi^+_\alpha(x), \psi^+_\beta(x'))|N, 0\rangle,$$

$$F_{m\alpha\beta}(x-x') = \langle N, 0|T(\psi_\alpha(x), \psi_\beta(x')|N+2, l, m\rangle$$

---

*In our case, $\tilde{\omega}$ is of the order of the Fermi energy.

*In accordance with the Pauli principle, even l is possible for $s=0$, odd l for $s=1$. We shall omit the spin in the following discussion, since it can be included in a trivial fashion in the final formula (12).

in place of the functions F and F^+ of reference 6. We shall therefore, in particular, assume that in the expansion of the average of a product of four ψ-operators, the term containing the product of the functions F and F^+ has the form

$$\langle T(\psi_\alpha(1)\psi_\beta(2)\psi_\gamma^+(3)\psi_\delta^+(4))\rangle$$

$$\rightarrow \sum_m F_{m\alpha\beta}(x_1 - x_2)\, F^+_{m\gamma\delta}(x_3 - x_4)$$

As we shall see later, we thus obtain a consistent picture of the superfluid state of the system.

Repeating the derivation[6] of the equations for the Green's function $G_{\alpha\beta}(x - x') = -i < T(\psi_\alpha(x)\psi^+_\beta(x')) >$ and for each of the $2l + 1$ quantities F^+_m, we get the following system of equations for the Fourier components of these functions:

$$(\omega - \xi)\hat{G}(p) - i\sum_m \hat{\Delta}_m(p)\hat{F}^+_m(p) = 1,$$

$$(\omega + \xi)\hat{F}^+_m(p) + i\hat{\Delta}^+_m(p)\hat{G}(p) = 0. \tag{3}$$

Here $\xi = v(p - p_0)$, the symbols $\hat{G}$, etc, denote the matrix form of the spinor indices of the corresponding quantities, and the products $\hat{\Delta}\hat{F}^+$ and $\hat{\Delta}^+\hat{G}$ are the ordinary matrix product. The quantities $\hat{\Delta}_m$ and $\hat{\Delta}^+_m$ have the following meaning:

$$\hat{\Delta}_m(p) = (2\pi)^{-4}\int V(\mathbf{p} - \mathbf{p}')\,\hat{F}_m(p')\,d^3p'\,d\omega,$$

$$\hat{\Delta}^+_m(p) = (2\pi)^{-4}\int V(\mathbf{p} - \mathbf{p}')\,\hat{F}^+_m(p')\,d^3p'\,d\omega. \tag{4}$$

Since the total angular momentum of the system is zero, $\hat{G}_{\alpha\beta}(p)$ is isotropic, and has the form

$$\hat{G}_{\alpha\beta}(p) = \delta_{\alpha\beta}G(p),$$

where $G(p)$ is independent of the direction of p. As for the matrices $\hat{F}_m$ and $\hat{F}^+_m$, from the commutation relations for Fermi operators we find for $t = t'$:

$$F_{m\alpha\beta}(\mathbf{r} - \mathbf{r}', 0) = -F_{m\beta\alpha}(\mathbf{r}' - \mathbf{r}, 0); \tag{5}$$

$$F^+_{m\alpha\beta}(\mathbf{r} - \mathbf{r}', 0) = -F^+_{m\beta\alpha}(\mathbf{r}' - \mathbf{r}, 0),$$

$$\{F^+_{m\alpha\beta}(\mathbf{r} - \mathbf{r}', 0)\}^* = -F_{m\alpha\beta}(\mathbf{r} - \mathbf{r}', 0). \tag{6}$$

According to (2), the functions $\hat{F}^+_m$ and $\hat{F}_m$ correspond to creation and annihilation of pairs of particles in a state with angular momentum l and projection m. It is therefore obvious that $\hat{F}_m(p)$ and $\hat{F}^+_m(p)$ have the structure of the corresponding spherical harmonic, i.e., they are proportional to

$$Y_{lm}(\theta, \varphi) = \left[\frac{2l + 1}{4\pi}\,\frac{(l - |m|)!}{(l + |m|)!}\right]^{1/2} P_l^m(\theta)\,e^{im\varphi},$$

where $P_l^m(\theta)$ are the associated Legendre polynomials. This assumption is justified later; on this basis we can write

$$\hat{F}^+_{m\alpha\beta}(p) = F^*_m(p)\,\hat{I}^s_{\alpha\beta}Y^*_{lm}(\theta, \varphi),$$

$$\hat{F}_{m\alpha\beta}(p) = -F_m(p)\,\hat{I}^s_{\alpha\beta}Y_{lm}(\theta, \varphi), \tag{7}$$

where the sign is chosen in agreement with Eq. (6). The matrix $\hat{I}$ reflects the dependence of the wave function of the pair on the spin variables. It is obvious that when the angular momentum l in which the pairing occurs is even, it follows from (6) that $I_{\alpha\beta} = -I_{\beta\alpha}$, i.e., the particles are in a singlet state. In the opposite case, the spin of the pair is unity and $I^S_{\alpha\beta} = I^S_{\beta\alpha}$. In both cases we shall assume that $I^2_{\alpha\beta} = \delta_{\beta\alpha}$

Using the addition theorem for the Legendre polynomials

$$P_l(\gamma) = \sum_m \frac{(l - |m|)!}{(l + |m|)!}\,P_l^m(\theta)\,P_l^m(\theta')\,e^{im(\varphi - \varphi')}, \tag{8}$$

we find from (1), (4), and (7),

$$\hat{\Delta}^+_{m\alpha\beta}(p) = \Delta^*_m\hat{I}^s_{\alpha\beta}Y_{lm}(\theta, \varphi), \quad \hat{\Delta}_{m\alpha\beta}(p) = -\Delta_m\hat{I}^s_{\alpha\beta}Y_{lm}(\theta, \varphi); \tag{9}$$

$$\Delta^*_m = \left(\frac{V_l}{2l + 1}\,\frac{mp_0}{2\pi^2}\right)\int\frac{d\omega}{2\pi}\int_{-\tilde{\omega}}^{\tilde{\omega}} d\xi\,F^*_m(p, \omega) \tag{10}$$

and similarly for Δ_m.

Substituting (7) and (9) in (3), we find

$$F^*_m(p) = -i\Delta^*_m G(p)/(\omega + \xi), \quad G(p) = \frac{\omega + \xi}{\omega^2 - \varepsilon_p^2},$$

$$F^*_m(p) = -i\,\frac{\Delta^*_m}{\omega^2 - \varepsilon_p^2}, \tag{11}$$

where the spectrum $\epsilon_p = \sqrt{\xi^2 + |\Delta|^2}$ has a gap $|\Delta|$ equal to

$$|\Delta|^2 = \sum_m |\Delta_m|^2\,\frac{2l + 1}{2}\,\frac{(l - |m|)!}{(l + |m|)!}\,(P_l^m(\theta))^2.$$

Since $G(p)$ is isotropic, all the $|\Delta_m|^2$ are equal, and according to Eq. (8),

$$|\Delta|^2 = \tfrac{1}{2}|\Delta_m|^2(2l + 1)(2s + 1)P_l(\theta = 0).$$

Substitution of (11) in (10) gives for the value of the gap:

$$|\Delta| = 2\tilde{\omega}\exp\{-2\pi^2(2l + 1)/mp_0|V_l|\}. \tag{12}$$

Thus if the pairs are formed in a state with angular momentum l, the gap size is determined only by the interaction component V_l. If an attraction of a pair of particles through the interaction (1) occurs for several harmonics, then as we see from (12), it follows from energy considerations that pairing of the particles will occur with the angular momentum for which the value of $|V_l|/(2l+1)$ is largest.

The Fermi energy spectrum is isotropic and has the usual form.[1,2] In addition, in a system of uncharged fermions in the superfluid state, there is an acoustic vibration branch. Therefore the specific heat of such a system at low temperatures is

$$C_s = \frac{2\sqrt{3}}{5}\frac{T^3}{v^3} + \frac{mp_0}{\pi^2}\sqrt{\frac{2\pi\Delta^3}{T^3}}\,\Delta e^{-\Delta/T},$$

The term in T^3, which comes from the acoustic branch, is important only at the very lowest temperatures, because the range of temperatures within which the superfluid state exists is exponentially small.

In reference 5, the spectrum

$$\varepsilon_p = [\xi^2 + |\Delta_m|^2 (P_l^m(\theta))^2]^{1/2}$$

was found. This is physically absurd since it gives an anisotropic spectrum in an isotropic system, to say nothing of the fact that it gives a zero gap at the points where $P_l^m(\theta) = 0$.

In conclusion we note that, within the framework of the isotropic model, when the interaction has the form (1), it is difficult to think of an experiment for determining the angular momentum value for which the pairing of particles in the superfluid phase occurs.

The authors express their gratitude to L. D. Landau and L. P. Pitaevskii for value comments.

---

[1] Bardeen, Cooper and Schrieffer, Phys. Rev. **108**, 1175 (1957).

[2] N. N. Bogolyubov, JETP **34**, 58 (1958), Soviet Phys. JETP **7**, 41 (1958).

[3] L. Cooper, Phys. Rev. **104**, 1189 (1956).

[4] L. P. Pitaevskii, JETP **37**, 1794 (1959), Soviet Phys. JETP **10**, 1267 (1960).

[5] P. Anderson and P. Morel, Phys. Rev. Letters **5**, 136 (1960).

[6] L. P. Gor'kov, JETP **34**, 735 (1958), Soviet Phys. JETP **7**, 505 (1958).

Translated by M. Hamermesh
188

SOVIET PHYSICS JETP VOLUME 13, NUMBER 4 OCTOBER, 1961

DISPERSION RELATIONS FOR VERTEX PARTS

Yu. M. MALYUTA

Physics Institute, Academy of Sciences, Ukrainian S.S.R.

Submitted to JETP editor October 26, 1960

J. Exptl. Theoret. Phys. (U.S.S.R.) 40, 1128-1133 (April, 1960)

The primitive diagrams are found and the location of the nearest singularities for the $\Lambda\Lambda\pi$, $\Lambda\Sigma\pi$ and $\Sigma\Sigma\pi$ vertex parts are determined by making use of the Nambu-Symanzik majorization method. Our investigation differs from Nambu's study of the hyperon form factor[1] in that we do not restrict ourselves to the consideration of a simplified model but study the situation that arises when all strongly interacting particles are allowed to interact.

1. INTRODUCTION

RECENTLY in the theory of dispersion relations the method of majorization[1,2] for the determination of the location of the nearest singularities of scattering amplitudes was developed. The idea of the method consists of the following.

Consider a connected diagram of arbitrary order[*]

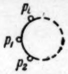

(1)

where p_i is the sum of the momenta acting on the i-th external vertex. The matrix element corresponding to diagram (1) is a function of the invariants constructed from the vectors p_i. We are interested in the analytic properties of the matrix element as a function of one of the invariants with the remaining ones held constant.

Let us formulate the basic theorem of the majorization method.[†][1,2]

Let A′ and A be two connected diagrams with equal numbers of external vertices:

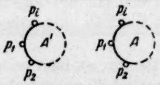

(2)

Let diagram A′ reduce to diagram A according to the rules of majorization given in Fig. 1,[‡] and

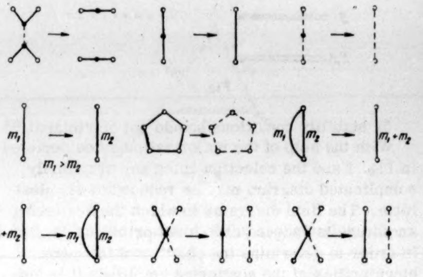

Fig. 1

in accordance with selection rules (see below). Then the nearest singular point of diagram A will lie no further than the nearest singular point of diagram A′, provided that the set of vectors p_i is Euclidean.[*]

Let us list the selection rules.

1) In the majorization process the baryon number and strangeness must be conserved;[†]

2) a strongly connected diagram should be majorized by a strongly connected diagram;[‡]

3) internal pion lines attached to external vertices should not be removed if as a result the structure of the diagram is broken;

4) it is desirable to keep cubic type vertices (this simplifies the investigation);

---

[*] Without loss of generality we discuss the scalar version of the theory. Divergent diagrams are regularized by the auxiliary masses method.[3]

[†] The formulation is given in graphical language, in a form convenient for subsequent applications.

[‡] In Fig. 1 are shown the majorization rules for a pion-nucleon theory. These rules may be expanded by replacing the nucleon line by a kaon or hyperon line, or by a line denoting an arbitrary nucleus or hyperfragment (for the notation for the lines see Sec. 2)

[*] The set of vectors p_i is Euclidean if the Gram determinants composed of these vectors are nonnegative.

[†] To simplify the discussion we do not take into account other conservation laws, connected with inversions and gauge invariance.

[‡] The majorization of a strongly connected diagram by a weakly connected diagram is forbidden because this would result in a loss of information about the analyticity properties of the scattering amplitude.

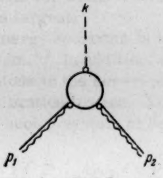

Fig. 2

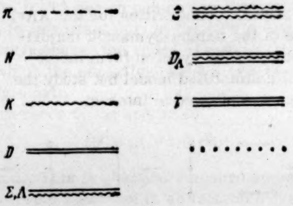

Fig. 3

5) stability conditions should not be violated.[4,5]

With the help of the majorization rules depicted in Fig. 1 and the selection rules any arbitrarily complicated diagram may be reduced to simplest form. The final diagrams to which the scattering amplitude is reduced are called primitive diagrams. In order to determine the position of the nearest singularities of the scattering amplitude it is sufficient to determine the position of the nearest singularities of the primitive diagrams.

In this work concrete applications of the majorization of the vertex part shown in Fig. 2 are presented.

2. MAJORIZATION OF THE VERTEX PART

We introduce graphic notation for the strongly interacting particles (see Fig. 3). Other nuclei and hypernuclei may be analogously denoted by an appropriate number of straight and wavy lines, representing the baryon number and strangeness.

Strong interactions of the cubic type are shown in Fig. 4.[6]*

We consider the vertex part shown in Fig. 2 and find its primitive diagrams. The vertex part depends on the following invariants:†

$$p_1^2 = \lambda^2, \qquad p_2^2 = \sigma^2, \qquad k^2 = (p_1 + p_2)^2,$$

where λ and σ are hyperon masses ($\lambda \leq \sigma$). We are interested in the analytic properties as a function of k^2. It is easy to verify that the set of

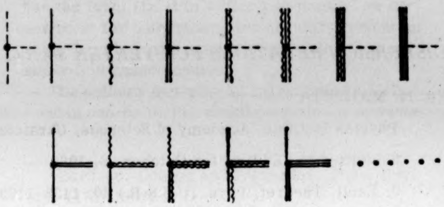

Fig. 4

vectors p_1, p_2 and k is Euclidean provided that k^2 lies in the interval

$$(\lambda - \sigma)^2 \leqslant k^2 \leqslant (\lambda + \sigma)^2. \tag{3}$$

Therefore if the singular points of the primitive diagrams fall within the interval (3), then the nearest of these will be the nearest singular point of the vertex part.

Let us enumerate the elements of which the vertex part is composed:

a) the baryon line, joining the external hyperon lines;

b) the strangeness line, joining the external hyperon lines;

c) baryon closed loops and strangeness closed loops;

d) lines a), b), and c) may coincide with each other forming various virtual particles;

e) pion lines act as connecting links between all lines, including pion lines;

f) an external pion line may be attached to any line.

We first replace the closed loops c) by pion closed loops in accordance with Fig. 1 and the selection rules,* and lower the masses of the virtual Σ hyperons to the masses of the Λ hyperons (in accordance with Fig. 1). Following this operation the vertex part will contain only the elements a), b), e), f) and coincidences only between a) and b).

We extract from the vertex part under discussion the weakly connected diagrams shown in Fig. 5.

The diagram of Fig. 5a need not be considered since it contains a self-energy part on the free hyperon line and, consequently, the corresponding matrix element vanishes. The diagram of Fig. 5b reduces to a strongly connected diagram since the self-energy part on the virtual pion line may be included in the external source.

---

*To simplify the discussion we assume the pion to be scalar.

†Our metric is 1, −1, −1, −1.

*It is possible in this way to obtain higher degree vertices involving pion lines. However they can be reduced to the cubic type by the removal of the relevant pion lines.

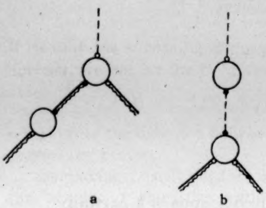

Fig. 5

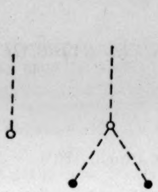

Fig. 6

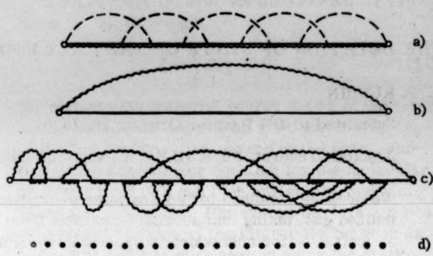

Fig. 7

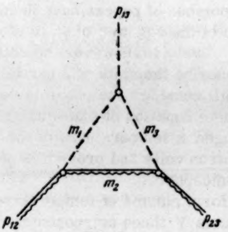

Fig. 8

The strongly connected diagrams may be majorized (in accordance with Fig. 1 and the selection rules) by diagrams obtained by attaching in all possible ways the elements depicted in Fig. 6 to the chains shown in Fig. 7 (the dots in Fig. 7 stand for all possible strongly connected combinations and variations of the chains indicated above). The diagrams resulting from the chains of Fig. 7b, c, d may in turn be majorized (in accordance with Fig. 1 and the selection rules) by the diagrams resulting from Fig. 7a.* We finally obtain the single primitive diagram shown in Fig. 8 by majorizing the diagrams resulting from the chain in Fig. 7a (in accordance with Fig. 1 and the selection rules), and making use of the method of induction.

3. DETERMINATION OF THE POSITION OF THE SINGULARITIES

Taking into account the results obtained by Karplus, Sommerfield and Wichmann,[4] and by Tarski,[5] we determine the position of the nearest lying singularities for the vertex parts $\Lambda\Lambda\pi$, $\Lambda\Sigma\pi$, and $\Sigma\Sigma\pi$.

The matrix element corresponding to the primitive diagram of Fig. 8 has the form

$$G = \text{const}\cdot\int_0^1 d\alpha_1\int_0^1 d\alpha_2\int_0^1 d\alpha_3\,\frac{\delta(1-\alpha_1-\alpha_2-\alpha_3)}{(\alpha_1 m_2 m_3+\alpha_2 m_1 m_3+\alpha_3 m_1 m_2)\,V(p\alpha)},$$

where

$$V(p\alpha)=\alpha_1^2+\alpha_2^2+\alpha_3^2+2\alpha_1\alpha_2 y_{12}+2\alpha_1\alpha_3 y_{13}+2\alpha_2\alpha_3 y_{23},$$

$$p_{ij}^2=m_i^2+m_j^2-2m_i m_j y_{ij},\qquad y_{ij}=\cos\theta_{ij},\qquad 0\leqslant\theta_{ij}\leqslant\pi.$$

It follows from the work of the above mentioned authors[4,5] that the position of the nearest singularity for $G(k^2)$ is determined as

$$\bar{k}^2=\begin{cases}(m_1+m_3)^2, & \text{if}\quad \theta_{12}+\theta_{23}\leqslant\pi\\ m_1^2+m_3^2-2m_1m_3\cos(\theta_{12}+\theta_{23}), & \text{if}\quad \theta_{12}+\theta_{23}>\pi.\end{cases}$$

Let us find the position of the nearest singularity for the vertex part $\Lambda\Lambda\pi$:

$$\theta_{12}=\theta_{23}=86.5^\circ,\qquad \theta_{12}+\theta_{23}<\pi,\qquad \bar{k}^2=4\mu^2;$$

for the vertex part $\Lambda\Sigma\pi$:

$$\theta_{12}=86.5^\circ,\qquad \theta_{23}=120^\circ,\ \theta_{12}+\theta_{23}>\pi,\qquad \bar{k}^2=3.78\,\mu^2;$$

and for the vertex part $\Sigma\Sigma\pi$:

$$\theta_{12}=\theta_{23}=120^\circ,\qquad \theta_{12}+\theta_{23}>\pi,\qquad \bar{k}^2=3\mu^2.$$

The author is grateful to N. N. Bogolyubov and A. A. Logunov for valuable advice and remarks.

---

*The majorization of these diagrams is based on the circumstance that $m+\kappa>\lambda+2\mu$, where m, κ λ, μ are the nucleon, kaon, hyperon and pion masses respectively.

[1] Y. Nambu, Nuovo cimento 9, 610 (1958).

[2] K. Symanzik, Progr. Theoret. Phys. 20, 690 (1958).

[3] N. N. Bogolyubov and D. V. Shirkov, Introduction to Quantum Field Theory, Interscience, 1959.

[4] Karplus, Sommerfield, and Wichmann, Phys. Rev. 114, 376 (1959).

[5] J. Tarski, J. Math. Phys. 1, 149 (1960).

[6] P. Matthews, Relativistic Quantum Theory of the Interactions of Elementary Particles (Russ. Transl.), IIL, 1959.

Translated by A. M. Bincer
189

SOVIET PHYSICS JETP VOLUME 13, NUMBER 4 OCTOBER, 1961

THE EQUATION OF STATE OF PARTIALLY IONIZED HYDROGEN

L. P. KUDRIN

Submitted to JETP editor October 29, 1960

J. Exptl. Theoret. Phys. (U.S.S.R.) **40**, 1134-1139 (April, 1961)

We propose a method for approximate evaluation of the thermodynamic functions of a partially ionized gas, taking into account deviations from ideality. We obtain an equation of state and an ionization formula which is appreciably different from the Saha formula.

1. A large number of papers have been devoted to a discussion of the equation of state of a totally ionized gas. There is, however, no satisfactory theory to describe the state of a partially ionized gas. We shall consider one possible derivation of an approximate equation of state, using as an example hydrogen at temperatures of the order of several electron volts and pressures of the order of tens of atmospheres.

Let a uniform plasma of temperature T contain within a volume V three components: neutral hydrogen atoms, electrons, and ions. Since the plasma is electrically neutral,

$$n_{i0} = n_{e0}, \qquad (1)$$

where n_{e0} and n_{i0} are the average electron and ion densities, respectively.

The effects of the interaction between particles in the plasma lead to a change in the atomic energy levels and also to the so-called "cut-off" of the atomic partition function, manifest spectroscopically by the vanishing of Fraunhofer lines corresponding to relatively high values of the principal quantum number. The discrete states near the continuum vanish for two reasons. First, because the broadening of the levels caused by the interaction between the atom and the charged component of the plasma or the other atoms may turn out to be comparable with the spacing of the levels, so that levels with relatively high values of the principal quantum number overlap. Second, the action of the quasi-static microfield of the plasma on the atom causes ionization of the upper atomic levels.

Generally, one must take both these effects into account when evaluating the partition function. If, however, the electron density exceeds about 10^{17} cm^{-3}, the second effect is dominant (strong electrical microfield) and one can neglect the first one. Margenau and Lewis[1] have, for instance, studied this problem in detail in their survey article.

We shall consider the influence of the screened electrical charges on the atom. One can describe this influence in the adiabatic approximation by the perturbation of the atom by an electrical field **F**:

$$\mathbf{F} = \sum_i \mathbf{E}_i(\mathbf{r}_i) = e \sum_i \mathbf{r}_i r_i^{-3} (1 + \varkappa r_i) \exp(-\varkappa r_i), \qquad (2)$$

where $\kappa = (r_0^3 kT/3)^{-1/2}$ is the inverse Debye radius (in atomic units) and r_0 the average distance between the ions.

Hoffman and Theimer[2] obtained the statistical distribution of the field. If the ion and electron densities are not too small, one can use for the evaluation of the field distribution the so-called "nearest neighbor" approximation which takes only the influence of the nearest ion on the atom into account. The probability of finding a perturbing ion at a distance r from the atom is then given by an expression of the form

$$dP(r) = 4\pi n \exp\left\{-\frac{U(r)}{kT} - 4\pi n \int_0^r r'^2 \exp\left[-\frac{U(r')}{kT}\right] dr'\right\} r^2 dr, \qquad (3)$$

where U(r) is the potential energy for the interaction between the ion and a hydrogen atom and n the ion density in the plasma.

When the Stark effect in a strong electrical field is evaluated one determines the value of the critical field $F_0^{m_0}$ for which the spectral line corresponding to an initial state of the atomic electron with principal quantum number m_0 vanishes.[3] A classical calculation of the threshold for ionization gives the following value for the critical field $F_0^{m_0}$:

$$F_0^{m_0} = e/16 m_0^4 a_0^2, \qquad (4)$$

where a_0 is the Bohr radius.

A comparison with the quantum-mechanical calculation and with experiment (see reference 3) shows that $F_0^{m_0}$ can be approximated with fair accuracy by an expression of the form

$$F_0^{m_0} = e/8m_0^4a_0^2. \qquad (5)$$

If we take the screening of the perturbing ion into account, we get for the field acting upon the atom

$$F(r) = er^{-2}(1 + \varkappa r)\,e^{-\varkappa r}, \qquad (6)$$

where r is the distance between the atom and the perturbing proton.

Comparing Eqs. (5) and (6) we get for the quantum number at which the partition function must be cut off:

$$m_0 = 2^{-3/4}(r/a_0)^{1/2}(1 + \varkappa r)^{-1/4}e^{\varkappa r/4}. \qquad (7)$$

It is necessary to note that the electrical field inside the plasma can be different from the field used in the proposed model. It is thus necessary to compare the theory with an experiment on the vanishing of spectral lines in a plasma, and we shall do this below.

The partition function of the atom as a function of the distance r between the atom and the perturbing ion,

$$Z(r) = 2\sum_{n=1}^{m_0} g_n \exp[-E_n(r)/kT], \qquad (8)$$

contains E_n, the energy of the atomic levels in an external electrical field, and g_n, the statistical weight of the corresponding levels. One can show that for electron densities less than 10^{20} cm^{-3} we do not introduce a serious error if we write Z(r) in the form

$$Z(r) = 2\sum_{n=1}^{m_0} n^2 \exp[-I_n(r)/kT], \qquad (9)$$

$$I(r) = I_0(1 - 1/m_0^2(r)), \qquad (10)$$

where $I_0 = e^2/2a_0 = 13.53$ ev (ionization potential of hydrogen), $I_n = I(r)/n^2$. We have assumed here that the energy levels of the hydrogen atom are unperturbed and that the cut-off occurs at $n = m_0$.

We take the energy of the m_0 level as the zero point of the energy, i.e., we assume that E_{m_0} is the boundary of the discrete and the continuous spectra of the relative motion of the electron and the proton. This corresponds clearly to an effective lowering of the ionization potential [see Eq. (10)]. We assume then that upon going over into the continuous spectrum the electron moves in a potential caused by all the free charged particles in the plasma, i.e., in the Debye potential. We note that this assumption is not an obvious one and needs further justification. A rough estimate shows that this assumption introduces an error of the second order. We shall return in a later paper to a detailed study of this problem.

If we average (9) over the distribution dP(r) given by Eq. (3) we get

$$Z = \int_0^\infty Z(r)\,dP(r). \qquad (11)$$

To evaluate the potential energy U(r) of the interaction between an ion and an atom for $r \sim a_0$ (a_0 is the Bohr radius) we use the well-known solution of the Schrödinger equation for the molecular hydrogen ion.[4] We can then neglect the screening of the perturbing ion. However, when $1/\kappa > r \gg a_0$ the potential energy of the interaction between an ion and an atom is evaluated by using the Stark-effect perturbation theory. When $r > 1/\kappa$ the potential U(r) = 0.

2. We write for the free energy of the neutral component in an external field

$$F_a = -N_akT\ln[(MkT/2\pi\hbar^2)^{3/2}eVZ/N_a], \qquad (12)$$

where Z is given by Eq. (11), M is the proton mass, N_a is the number of atoms, and V is the volume of the system.

In the Debye approximation we have for the free energy of the charged component

$$F_{\mathrm{ch}} = F_{\mathrm{id}} - \tfrac{2}{3}e^3\sqrt{\pi/kTV}\,(N_e + N_i)^{3/2}, \qquad (13)$$

where F_{id} is the free energy of a perfect gas of electrons and ions and N_e and N_i are, respectively, the numbers of electrons and ions. We have not taken into account in Eq. (13) terms quadratic in the charged component density since the logarithmic term tends to zero for hydrogen (see reference 5), and the other terms give a small contribution.

The condition of chemical equilibrium

$$\mu_a = \mu_i + \mu_e \qquad (14)$$

(where μ_a, μ_i, and μ_e are respectively the chemical potentials of the atoms, the ions, and the electrons) leads, if we use (12) and (13), to the following ionization equation:

$$n_{e0}^2/n_a = Z^{-1}g_e^2(mkT/2\pi\hbar^2)^{3/2}\exp\{4e^3(2\pi n_{e0})^{1/2}/(kT)^{3/2}\}, \qquad (15)$$

where $g_e^2 = 4$. Equation (15) is the analogue of Saha's ionization formula (see, for instance, reference 6). In the derivation of the Saha formula one does not take into account that the free particles form an imperfect gas and the ionization potential is essentially put equal to the perturbing potential, i.e., one assumes that only the ground state of the atom gives a contribution to the partition function of the neutral component. The ionization potential obtained in the present paper takes into account the deviation of the electron and the proton gas from perfect gases. It is necessary to change the ratio between the neutral and the charged components as compared to the one given by the Saha formula also because of the effective lowering of the ionization potential and because excited states of the hydrogen atom must be taken into account.

The partition function Z is a function of the ion density, i.e., it depends not only on the temperature, but also on the density in the plasma. Conversely, the ion density depends on Z, i.e., it is a self-consistent problem. We obtain the equation of state by differentiating $F = F_a + F_{ch}$ with respect to the volume, keeping T, N_e, and N_a fixed:

$$P = (n_a + 2n_{e0})\,kT - \tfrac{2}{3}e^3\sqrt{2\pi/kT}\,n_{e0}^{3/2} + kTn_a\lambda;$$
$$\lambda = -\partial\ln Z/\partial\ln n_{e0}, \qquad 0 < \lambda < 1. \tag{16}$$

Using (15) and (16) we get an ionization formula from which we can calculate the electron density (and the degree of ionization) for a given temperature T and pressure P:

$$n_{e0}^2(1+\lambda) = Z^{-1}g_e^2(mkT/2\pi\hbar^2)^{3/2}\,[P/kT - 2n_{e0}$$
$$+ \tfrac{2}{3}(2\pi)^{1/2}e^3(n_{e0}/kT)^{3/2}]\exp\{4e^3(2\pi n_{e0})^{1/2}(kT)^{3/2}\}. \tag{17}$$

For comparison we give here the usual Saha formula for hydrogen:

$$n_{e0}^2 = \tfrac{1}{2}g_e^2(mkT/2\pi\hbar^2)^{3/2}\,[P/kT - 2n_{e0}]e^{-I_0/kT}. \tag{18}$$

3. We consider now some effects which may lead to an additional change in the atomic levels and thus to a change in the partition function. If because of the perturbation the electron makes a transition into a state with a sufficiently large principal quantum number (in our conditions ~ 6 to 10), the radius of its Bohr orbit will become appreciable. The electron then moves slowly between the atoms and the position is nearly the same as if a slow free electron moved through the gas. The presence of other atoms will change the energy of the excited state which we are considering on two grounds: firstly, the average potential energy of the field in which the electron moves is changed, and secondly, the bound proton will cause a polarization of the atoms. The result of these two effects is a shift in the level[7]

$$\Delta = a\hbar n_a/2\pi m - 10e^2\alpha n_a^4, \tag{19}$$

where a is the magnitude of the effective radius of the elastic scattering of slow electrons by a hydrogen atom and α the polarizability of the atom.

One shows easily that in the range of temperatures and pressures considered both these effects are small, i.e.,

$$|\Delta E/E| \ll 1. \tag{20}$$

Account of the dipole-dipole interactions between the atoms also leads to an insignificantly small correction. To estimate the contribution from this interaction we can use perturbation theory. It turns out that this effect is comparable with the Stark effect only when

$$5\cdot10^{-18}\,n_a/n_{e0}^{2/3} \sim 1, \tag{21}$$

but this condition is known not to be satisfied under the conditions we consider here.

4. To estimate Z we use a rough model. Let

$$U(r) = \begin{cases} +\infty, & r \leqslant r_1 \\ -U_0, & r_1 < r \leqslant r_2. \\ 0, & r > r_2 \end{cases} \tag{22}$$

From Eq. (3) we then get

$$dP(r) = \begin{cases} 0, & r \leqslant r_1 \\ dP_1(r), & r_1 < r \leqslant r_2, \\ dP_2(r), & r > r_2 \end{cases}$$

$$P_2 = \left(\frac{r}{r_0}\right)^3\exp\left\{\left[1-\exp\left(\frac{U_0}{kT}\right)\right]\left(\frac{r_2}{r_0}\right)^3 + \left(\frac{r_1}{r_0}\right)^3\right\}\exp\left[-\left(\frac{r}{r_0}\right)^3\right],$$
$$P_1 = \exp\left(\frac{U_0}{kT}\right)P_2; \tag{23}$$

In (23) r_0 is evaluated from the equation

$$4\pi nr_0^3/3 = 1. \tag{24}$$

However, r_0 is not the quantity that corresponds to the most probable value of the field F. The lower T, the greater the difference between that value and r_0. We estimate

$$Z = \int_0^\infty Z(r)\,dP(r)$$

for $n_i = 10^{17}$ cm^{-3} ($r_0 = 253.7$) and kT = 1.1 ev. Using simple functions for Z (r) we get approximately $Z = 2.25 \times 10^6$.

On the other hand, if we substitute in (9) the value $r_0 = 253.7$ we get $Z = 2.15 \times 10^6$.

From the estimate which we have just given it is clear that we can evaluate Z approximately from the equation

$$Z = Z(r_0) = 2\exp\left\{\frac{I_0}{kT}\left(1-\frac{1}{m_0^2}\right)\right\}$$
$$= \left[1 + \int_2^{m_0}\exp\left\{-\frac{I_0}{kT}\left(1-\frac{1}{m_0^2}\right)\left(1-\frac{1}{x^2}\right)\right\}x^2dx\right], \tag{25}$$

where m_0 is given by Eq. (7).

For actual calculations using Eqs. (16) and (18) one can use the following expressions to work with

$$\tilde{n}_e^2(1+\lambda) = (A_1T^{3/2}/Z)[A_2P/T - 2\tilde{n}_e$$
$$+ A_3(\tilde{n}_e/T)^{3/2}]\exp\{A_4^2\tilde{n}_e^{1/2}/T^{3/2}\}, \tag{26}$$

$$A_2P/T = \tilde{n}_a(1+\lambda) + 2\tilde{n}_e - A_3(\tilde{n}_e/T)^{3/2}, \tag{27}$$

$$\tilde{n}_a = [A_2P/T - 2\tilde{n}_e + A_3(\tilde{n}_e/T)^{3/2}](1+\lambda)^{-1}, \tag{28}$$

where

P, atm	T, ev	$10^{-18} n_{e0}$ (Saha)	$10^{-18} n_{e0}$
1	1	$6.21 \cdot 10^{-2}$	$6.88 \cdot 10^{-2}$
	2	0,153	0.154
	3	0,102	0.103
	5	$6.12 \cdot 10^{-2}$	$6.13 \cdot 10^{-2}$
	10	$3.06 \cdot 10^{-2}$	$3.06 \cdot 10^{-2}$
5	1	0.148	0.176
	2	0.749	0.752
	3	0.510	0.513
	5	0.306	0,306
	10	0.153	0,153
10	1	0.212	0.259
	2	1,446	1.595
	3	1.020	1.029
	5	0,612	0.613
	10	0.306	0,307
15	1	0.262	0.322
	2	2,14	2.29
	3	1.53	1,59
	5	0.918	0.919
	10	0.459	0.468
20	1	0.303	0.378
	2	2,78	3.18
	3	2.04	2.09
	5	1,22	1,23
	10	0,612	0.613
50	1	0.484	0,662
	2	5.54	6,19
	3	5.06	5.00
	5	3,06	3.05
	10	1.53	1,53
100	1	0.688	1.021
	2	11.74	14.83
	3	10.06	11.69
	5	6.12	7.26
	10	3.06	2.99
200	1	0.976	1,57
	2	20.15	23.02
	3	19.83	21.99
	5	12.23	14.06
	10	6.12	7.04
500	1	1.55	2.89
	2	38.43	48.30
	3	47.69	53.46
	5	30.52	31.21
	10	15.31	15.49

$$A_1 = 1.1869 \cdot 10^4, \qquad A_2 = 0{,}6125,$$

$$A_3 = 9{,}1281 \cdot 10^{-2}, \qquad A_4 = 0.2738;$$

$$n_e \equiv n_{e0} \cdot 10^{-18}, \qquad \tilde{n}_a \equiv n_a \cdot 10^{-18},$$

where we now must express P in atmospheres and T in electron volts.

In the Table we have given values for n_{e0} calculated from Eqs. (26) to (28) for different pressures and temperatures. The calculation was performed on an electronic computer. We also give for comparison the corresponding values for the electron densities in a perfect plasma, calculated with the Saha formula.

We must note that the Debye approximation used here limits the validity of the theory to values of the electron density and the temperature which satisfy the well-known Kirkwood-Onsager inequality

$$e^2 n_{e0}^{1/3} / kT \ll 1. \tag{29}$$

5. Yamamoto[8] has investigated experimentally the vanishing of spectral lines in a plasma which is caused by interactions in the plasma. The analysis of the experiment given by the author is incorrect and we proceeded therefore as follows to compare the results of the present paper with that experiment. We calculated from Eq. (26) the electron density n_{e0} for the values of P and T corresponding to the experiment and then for that value of the density we used Eq. (7) to find the value of m_0. This calculation gave $m_0 \sim 8$ (P = 1 atm, T ~ 1.5 ev). The experimental value was $m_0 = 7$. We can clearly say that although such a comparison with experiment is an insufficient one, there is no discrepancy between the theory and this particular experiment.

In conclusion I express my gratitude to D. F. Zaretskii for a discussion of the results of this paper.

---

[1] H. Margenau and M. Lewis, Revs. Modern Phys. **31**, 569 (1959).

[2] H. Hoffman and O. Theimer, Astrophys. J. **127**, 477 (1958).

[3] H. Bethe, Handb. Phys. **241**, 273 (1933).

[4] E. Teller, Z. Physik **61**, 458 (1930).

[5] A. A. Vedenov and A. I. Larkin, JETP **36**, 1133 (1959), Soviet Phys. JETP **9**, 806 (1959).

[6] A. Unsöld, Physik der Sternatmosphären, Springer, 1938.

[7] E. Fermi, Nuovo cimento **11**, 157 (1934).

[8] M. Yamamoto, J. Phys. Soc. Japan **14**, 1739 (1959).

Translated by D. ter Haar
190

SOME ISOTOPIC RELATIONS FOR REACTIONS OF THE TYPE $\pi N \to \pi\pi N$

V. N. STREL'TSOV

Joint Institute for Nuclear Research

Submitted to JETP editor October 29, 1960

J. Exptl. Theoret. Phys. (U.S.S.R.) 40, 1140-1142 (April, 1961)

Isotopic relations are utilized in an analysis of experimental data for reactions of the type $\pi N \to \pi\pi N$ from the point of view of resonant $\pi\pi$ interactions.

THE model of resonant $\pi\pi$ interactions in states with definite isotopic spin ($T_{\pi\pi}$) values for the $\pi\pi$ system[1-7] has recently attracted attention as a means of explaining various experimental results. In particular, these considerations have been used to explain the mechanism of reactions of the type $\pi N \to \pi\pi N$.[4-7] The presence in such reactions of resonant $\pi\pi$ interactions with definite $T_{\pi\pi}$ can be examined with the aid of the isotopic relations which apply in this case (see, for example, references 1 and 2).

We shall analyze the experimental data using the somewhat more general relations, which are satisfied when the $\pi\pi$ interaction in the state with some value of the isotopic spin ($T'_{\pi\pi}$) is much smaller than the interaction in another state (the two other states), i.e.,

$$|a(T'_{\pi\pi})| \ll a|(T''_{\pi\pi})| \qquad (|a(T'_{\pi\pi})| \ll |a(T''_{\pi\pi})|,\ |a(T'''_{\pi\pi})|).$$

Then we have the following relations among the total and differential cross sections:*

I. $|a(0)| \ll a|(2)|$

$$\sigma(\pi^- n \to \pi^-\pi^- p) = 9\sigma(\pi^- p \to \pi^0\pi^0 n);$$

II. $|a(1)| \ll a|(2)|$

$$\sigma(\pi^- n \to \pi^-\pi^0 n) = \tfrac{1}{4}\sigma(\pi^- n \to \pi^-\pi^- p) = \sigma(\pi^- p \to \pi^-\pi^0 p),$$
$$d\sigma(\pi^- p \to \pi^-\pi^0 p) = d\sigma(\pi^- p \to \pi^0\pi^- p),$$
$$d\sigma(\pi^- n \to \pi^-\pi^0 n) = d\sigma(\pi^- n \to \pi^0\pi^- n);$$

IIa. $|a(1)| \ll |a(0)|,\ |(a(2)| \qquad (|a(1)| \gg |a(0)|,\ |a(2)|)$

$$d\sigma(\pi^- p \to \pi^-\pi^+ n) = d\sigma(\pi^- p \to \pi^+\pi^- n);$$

III. $|a(2)| \ll |a(1)|$

$$\sigma(\pi^- n \to \pi^-\pi^- p) = 0,\ d\sigma(\pi^- p \to \pi^-\pi^0 p) = d\sigma(\pi^- p \to \pi^0\pi^- p)$$
$$d\sigma(\pi^- n \to \pi^-\pi^0 n) = d\sigma(\pi^- n \to \pi^0\pi^- n).$$

At present, a more or less definite examination of relations I — III for the total cross section is possible only at an energy of about 1.5 Bev. The cross section ratios

$$\beta = \frac{\sigma(\pi^- n \to \pi^-\pi^- p)}{\sigma(\pi^- p \to \pi^0\pi^0 n)}, \qquad \gamma = \frac{\sigma(\pi^- n \to \pi^-\pi^- p)}{\sigma(\pi^- p \to \pi^-\pi^0 p)},$$
$$\delta = \frac{\sigma(\pi^- n \to \pi^-\pi^0 n)}{\sigma(\pi^- p \to \pi^-\pi^0 p)}$$

computed from the experimental data[8-10] for cases I and II are given in the table. From the table it is clear that $\beta \ll 9$, i.e., the condition $|a(0)| \ll |a(2)|$ is not fulfilled at 1.5 Bev. The values obtained for γ and δ also differ from those possible in case II.

Energy E_{lab}, Bev	I	II	
	β	γ	δ
1.37 [8]		0.7±0.6	3.1±1.1
1.5 [9,10]	$0.41\pm0.12 \leqslant \beta^* \leqslant 2.0\pm0.8$	0.36±0.09	2.1±0.3

*The value of β is obtained from only the data of Walker et al.[10] The limits given for β correspond to two different assumptions on the magnitude of the cross section $\sigma_1(\pi^- p \to \pi^0 n)$ [namely, $\sigma_1 = 0$ and $\sigma_1 = \sigma(\pi^- p \to \pi^- p)$], since there are experimental results only for the sum of the cross sections σ_1 and $\sigma(\pi^- p \to \pi^0\pi^0 n)$.

Condition II, moreover, is also in disagreement with the different shapes of the angular distributions of π^0 and π^- mesons in the $\pi^- p \to \pi^-\pi^0 p$ reaction. It follows, therefore, that $|a(1)|$ cannot be small. The condition that the $\pi^- n \to \pi^-\pi^- p$ reaction cross section be small (III) is apparently not fulfilled by any of the data on the $\pi^- n(\pi^+ p)$ interaction at 0.5, 1.37, and 1.5 Bev.[8-11]* Thus, the data under consideration give no indication that any of the quantities $|a(T_{\pi\pi})|$ is small.

By using only the conditions on the differential cross sections, we can analyze the data on the $\pi^- p$ interaction separately in a similar manner. The results obtained by Alles-Borelli et al.[13] at 960 Mev show that the energy distributions of π^+ and

---

*The equality of differential cross sections, for example $d\sigma(\pi^- p \to \pi^-\pi^0 p) = d\sigma(\pi^- p \to \pi^0\pi^- p)$, indicates clearly that the angular and energy distributions of the π^0 and π^- mesons are identical in the $\pi^- p \to \pi^-\pi^0 p$ reaction.

*It should be noted that, at 0.75 Bev,[12] only one case of $\pi^+ p \to \pi^+\pi^+ n$ has been observed, compared with eight $\pi^- p \to \pi^-\pi^+ n$ cases. However, the statistics are clearly not good enough to allow a definite conclusion.

π^- mesons in the $\pi^- p \to \pi^-\pi^+ n$ interaction cannot be resonant in the states with $T_{\pi\pi} = 0$ or 2. To see whether the interaction in the state with $T_{\pi\pi} = 1$ is strong, it would be necessary to measure the cross section for the $\pi^- n \to \pi^-\pi^- p$ reaction, which would be zero if such were the case. However, it turns out that along with this, the equality

$$d\sigma(\pi^- p \to \pi^-\pi^+ n) = d\sigma(\pi^- p \to \pi^+\pi^- n)$$

again must hold, and, since it does not hold, the $\pi\pi$ interaction in the $T_{\pi\pi} = 1$ state can likewise not be resonant. Similar conclusions follow also from other experiments performed at energies around 1 Bev[14] and 1.85 Bev.[15]

Thus, the analysis of experimental data in reactions of the type $\pi N \to \pi\pi N$ at energies 0.96 – 1.85 Bev gives no indication whatsoever of the presence of resonant $\pi\pi$ interaction in a state with definite $T_{\pi\pi}$.* Moreover, $|a(2)|$ is not small even at 500 Mev.†

This approach allows us to obtain some information on the nature of the interaction of the system of two π mesons in $\pi N \to \pi\pi N$ reactions near the meson production threshold. Near threshold the π mesons are in a relative S state and therefore the isotopic spin $T_{\pi\pi}$ cannot be 1. It is interesting to see where P-waves begin to be important, i.e., at what energy $|a(1)|$ is no longer small. The difference in the angular and energy distributions of π^+ and π^- mesons in the $\pi^- p \to \pi^-\pi^+ n$ reaction at 290 Mev[16] apparently indicates the presence of P-waves in the $\pi\pi$ system. If the $\pi\pi$ system at threshold is in a mixture of only $T = 0$ and $T = 2$ states, then an admixture of P states will show itself as a difference in the angular and energy distributions of π^+ and π^- mesons in this reaction.

In conclusion, we give some isotopic relations which may be useful in future analyses of experimental data. They are for the case that the interaction in the πN subsystem in the final state occurs predominantly in a state with definite isotopic spin, for example, in the $T_{\pi N} = 3/2$ ("isobar") state, and in addition the inequality $|a(T'_{\pi\pi})| \ll |a(T''_{\pi\pi})|$ holds for the $\pi\pi$ system. For $|a(2)| = 0$,* we obtain the following equations for the total cross sections:

$$\sigma(\pi^- n \to \pi^-\pi^0 n) = \sigma(\pi^- n \to \pi^-\pi^- p) = 0,$$
$$\sigma(\pi^- p \to \pi^-\pi^0 p) = \sigma(\pi^- p \to \pi^0\pi^0 n) = \tfrac{2}{5}\,\sigma(\pi^- p \to \pi^-\pi^+ n).$$

For $|a(0)| = 0$ these relations are identical with those which hold in the case $T_{\pi N} = T = 3/2$, where T is the isotopic spin of the initial state.

The author thanks L. I. Lapidus, V. I. Ogievetskii, and M. I. Podgoretskii for appraising these results and for valuable comments, and also S. A. Bunyatov and A. V. Efremov for aid in this work.

---

*It should be noted that if the $\pi N \to \pi\pi N$ reaction goes only through the nucleon "isobar" ($J = T = 3/2$), then a resonant $\pi\pi$ interaction in a state with definite $T_{\pi\pi}$ is obviously impossible. Therefore, if the "isobar" model is valid in the energy range 1–1.5 Bev (as is apparently indicated by the results in references 14 and 17) such a resonant $\pi\pi$ interaction is impossible.

†Of course, these conclusions do not exclude the possibility that the $\pi\pi$ interaction is resonant for certain values of the relative momentum of the π mesons.

*The case $|a(1)| = 0$ is impossible; that is, if the πN interaction is strong in a state with definite $T_{\pi N}$, then the $\pi\pi$ interaction in the $T = 1$ state cannot be small.

---

[1] F. J. Dyson, Phys. Rev. **99**, 1037 (1955).

[2] G. Takeda, Phys. Rev. **100**, 440 (1955).

[3] W. R. Fraxer and I. R. Fulco, Phys. Rev. Lett. **2**, 365 (1959); Phys. Rev. **117**, 1609 (1960).

[4] F. Bonsignori and F. Sellery, Nuovo cimento **15**, 465 (1960).

[5] F. Sellery, Nuovo cimento **16**, 1775 (1960).

[6] P. Carruthers and H. A. Bethe, Phys. Rev. Lett. **4**, 536 (1960).

[7] Itabashi, Kato, Nakagawa, and Takeda, preprint.

[8] V. P. Kenney, Phys. Rev. **104**, 784 (1956).

[9] W. D. Walker and J. Crussard, Phys. Rev. **98**, 1416 (1955).

[10] Walker, Crussard, and Koshiba, Phys. Rev. **95**, 852 (1954).

[11] W. J. Willis, Phys. Rev. **116**, 753 (1959); Blevis, Block, and Leitner, Phys. Rev. **112**, 1287 (1958).

[12] M. Blau and A. R. Oliver, Phys. Rev. **102**, 489 (1956).

[13] Alles-Borelli, Bergia, Perez Ferreira, and Waloschek, Nuovo cimento **14**, 211 (1959).

[14] Derado, Lütjens, and Schmitz, Ann. Physik **4**, 103 (1959); I. Derado and N. Schmitz, Phys. Rev. **118**, 309 (1960).

[15] R. C. Whitten and M. M. Block, Phys. Rev. **111**, 1676 (1958).

[16] Batusov, Bogachev, and Sidorov in B. M. Pontecorvo's report to the Ninth High-Energy Physics Conference, Kiev, 1959.

[17] S. I. Lindenbaum and R. M. Sternheimer, Phys. Rev. **106**, 1107 (1957).

Translated by M. Bolsterli

SOVIET PHYSICS JETP VOLUME 13, NUMBER 4 OCTOBER, 1961

EXCITATION SPECTRUM OF A PARTICLE SYSTEM IN AN EXTERNAL FIELD

V. M. ELEONSKII

Ural Polytechnic Institute

Submitted to JETP editor October 29, 1960

J. Exptl. Theoret. Phys. (U.S.S.S.) 40, 1143-1147 (April, 1961)

A set of equations defining the excitation spectrum and decay of the initial individual excitation is derived from the linearized Hartree equations by taking the initial conditions into account. The quantum dispersion relation and its classical analog, which specify the collective excitation spectrum of a system in an external field, are deduced.

A linear approximation of the Hartree self-consistent field method has been used many times to determine the spectrum of collective and single-particle excitations of systems of interacting particles.[1,2] A consistent application of this method should obviously include the formulation and solution of the initial-condition problem (the Cauchy problem). In the present paper we show that for a given approximation Heitler's formalism[3] not only yields the spectrum of the collective and single-particle excitations of the system in an external field, but determines the decay of an initial individual or collective state.

We consider a system of interacting particles in an external field. The operator equation for the density matrix, in a representation determined by the eigenvalues of the particle states in the external field, has the form

$$\{i\hbar\,\partial/\partial t - E_n + E_{n'}\}\,\rho\,(nn') = \sum_{ll'}\Big\{\rho\,(ll')\;\rho\,(mm')\;G^{nl'}_{ml}\,\delta\,(n'm') - \rho\,(mm')\;\rho\,(ll')\;G^{m'l'}_{n'l}\,\delta\,(nm)\Big\} \equiv \sum_{ll'} G^{nl'}_{n'l}\{\rho(ll')\;\rho\,(n'n') - \rho\,(nn)\,\rho\,(ll')\} + \Delta\rho(nn'); \qquad (1)$$

$$G^{nl'}_{n'l} = \int dx\,dy\;G\,(x-y)\,\overset{+}{\psi}_n(x)\,\overset{+}{\psi}_{l'}(y)\,\psi_{n'}(x)\,\psi_l(y). \qquad (1')$$

Here $G(x-y)$ is the kernel of the interaction between particles, and $\psi_l(x)$ satisfies the equation

$$\{T\,(p) + U\,(x)\}\,\psi_l(x) = E_l\psi_l\,(x).$$

Averaging the operator equation for the density matrix over the state of the system (in the occupation-number space) and using further the Hartree approximation in which the diagonal elements of the averaged density matrix are replaced by the distribution functions of the non-interacting particles in the external field:

$$\langle\rho\,(ll')\;\rho\,(nn)\rangle \to \langle\rho\,(ll')\rangle\,\langle\rho\,(nn)\rangle \to f\,(E_n)\,\langle\rho\,(ll')\rangle,$$

we obtain in the linear approximation $\langle\Delta\delta\,(nn')\rangle \to 0$, i.e., a system of Hartree equations, which is a natural generalization of the system considered by Ehrenreich and Cohen[2]

$$\{i\hbar\,\partial/\partial t - E_n + E_{n'}\}\,\langle\rho\,(nn')\rangle = \Delta f\,(nn')\sum_{ll'} G^{nl'}_{n'l}\,\langle\rho\,(ll')\rangle,$$
$$\Delta f\,(nn') = f(E_{n'}) - f(E_n). \qquad (2)$$

We assume that in the system of linearlized Hartree equations the self action of the particles has been eliminated, so that

$$\sum_{ll'} G^{nl'}_{n'l}\,\langle\rho\,(ll')\rangle \to \sum_{ll' \neq nn'} G^{nl'}_{n'l}\,\langle\rho\,(ll')\rangle.$$

We proceed to analyze the Hartree system with allowance for an initial condition in the form

$$\langle\rho\,(n_0n_0')\rangle_{t\to 0^+} = 1,\quad \langle\rho\,(nn')\rangle_{t\leqslant 0} = 0, \qquad nn' \neq n_0n_0'.$$

Using the expansion

$$\langle\rho\,(nn')\rangle = \frac{1}{2\pi i}\int dE\,\rho_{nn'\,|\,n_0n_0'}(E)\exp\,[-iEt/\hbar],$$

we find that allowance for the initial condition leads to the system

$$D_{nn'}(E)\,\rho_{nn'|n_0n_0'}(E) = \Delta f\,(nn')\sum_{ll'} G^{nl'}_{n'l}\,\rho_{ll'|n_0n_0'}(E) + \delta\,(n_0n_0'\,|\,nn'),$$
$$D_{nn'}(E) = E - E_n + E_{n'}. \qquad (3)$$

Following Heitler's formalism[3] we introduce for $ll' \neq n_0n_0'$ a new matrix, defined by the relation

$$\rho_{ll'|n_0n_0'}(E) = U_{ll'|n_0n_0'}(E)\,D^{-1}_{ll'}(E)\,\rho_{n_0n_0'|n_0n_0'}(E),$$

$$D^{-1}_{nn'}(E) = \mathrm{P}\,[E - E_n + E_{n'}]^{-1} - i\pi\delta\,(E - E_n + E_{n'}).$$

The system of homogeneous equations

$$U_{nn'|n_0n_0'}(E) = \Delta f\,(nn')\sum_{ll'} G^{nl'}_{n'l}D^{-1}_{ll'}(E)\,U_{ll'|n_0n_0'}(E) \qquad (4)$$

determines the introduced matrix for $nn' \neq n_0n_0'$, and the relation

$$\rho_{n_0n_0'|n_0n_0'}(E) = [D_{n_0n_0'}(E) + \frac{i}{2}\Gamma_{n_0n_0'}(E)]^{-1}, \qquad (5)$$

$$\frac{1}{2}\Gamma_{n_0n_0'}(E) = i\Delta f(n_0n_0')\sum_{ll'} G^{n_0l'}_{n_0'l} D^{-1}_{ll'}(E)\, U_{ll'|n_0n_0'}(E) \qquad (6)$$

determines the behavior of the initial condition.

The quantity $\Gamma_{n_0n_0'}(E)$ is, generally speaking, complex and determines the line width of the single-particle transition $n_0' \rightarrow n_0$ and the energy shift of the single-particle transition. We note that $\Gamma_{n_0n_0'}(E)$ vanishes when $n_0' = n_0$, corresponding to the absence of a shift and to the natural width of the single-particle level.

To separate the spectrum of the collective fluctuations, we parametrize the resultant system of equations. Actually, expanding the interaction kernel in the expression for the matrix element of the transition $G^{nl'}_{n'l}$ in a Fourier series

$$G^{nl'}_{n'l} = \sum_q G(q)\,(n|e^{iqx}|n')\,(l'|e^{iqx}|l),$$

and introducing the generalized collective operator

$$U_q(E;\ n_0n_0') = \sum_{ll'} (l'|e^{iqx}|l)\, D^{-1}_{ll'}(E)\, U_{ll'|n_0n_0'}(E), \qquad (7)$$

we find that the width and the shift of the energy of the single-particle transition are expressed in terms of the introduced quantity as follows:

$$\frac{1}{2}\Gamma_{n_0n_0'}(E) = i\Delta f(n_0n_0')\sum_q G(q)\,(n_0|e^{iqx}|n_0')\,U_q(E;\ n_0n_0'). \qquad (8)$$

By simple transformation of the system of homogeneous equations for $U_{nn'|n_0n_0'}$ we find that the collective operator $U_q(E;\ n_0n_0')$ should satisfy the equation

$$\{1 - G(q)\sum_{nn'} \Delta f(nn')\, D^{-1}_{nn'}(E)\, |(n|e^{iqx}|n')|^2\}\, U_q(E;\ n_0n_0')$$
$$= \sum_{q' \neq q} G(q')\, U_{q'}(E;\ n_0n_0')$$
$$\times \sum_{nn'} \Delta f(nn')\, D^{-1}_{nn'}(E)\,(n|e^{iq'x}|n')\,(n'|e^{iqx}|n), \qquad (9)$$

the structure of which is such as to permit the separation

$$U_q(E;\ n_0n_0') = U_q(E)\, U(n_0n_0'),$$

which leads to the possibility of existence of a collective-excitation spectrum $E(q)$ independent of the quantum numbers of the individual initial condition. This last circumstance is again a consequence of the elimination of terms corresponding to the self-action of the particles from the initial Hartree equations.

Neglecting the right half in the complete system (9), we arrive to a quantum dispersion relation in closed form

$$1 = G(q)\sum_{nn'} \mathrm{P}\frac{f(E_{n'}) - f(E_n)}{E - E_n + E_{n'}}\, |(n|e^{iqx}|n')|^2$$
$$- i\pi G(q)\sum_{nn'} \delta(E - E_n + E_{n'})$$
$$\times [f(E_{n'}) - f(E_n)]\, |(n|e^{iqx}|n')|^2, \qquad (10)$$

solution of which determines the spectrum of the collective fluctuations of the system of interacting particles.

Relation (5) together with the expression (8) determines the energy shift and the line width of the initial individual excitation of the system in the presence of collective excitation with a spectrum defined by the dispersion relation (10). To find the classical analog of the dispersion relation (10), we change in this expression from summation over (n, n') to summation over $(n, \Delta n = n' - n)$ and take account of the fact that in the classical approximation the main contribution is due to the eigenvalues $n \gg \Delta n \gg 1$. Since the quasi-classical matrix elements approach zero rapidly with increasing Δn and change little with changing n when the difference Δn is fixed, we use, on going to the classical dispersion relation, the expansion

$$E - E_{n+\Delta n} + E_n \rightarrow E - (\partial E_n/\partial n)\,\Delta n = E - \hbar\omega(n)\,\Delta n,$$
$$f(E_{n+\Delta n}) - f(E_n) \rightarrow (\partial f(E_n)/\partial E_n)\,\hbar\omega(n)\,\Delta n,$$

where, according to reference 4,

$$\omega(n) = \partial E_n/\partial I, \qquad I = \frac{1}{2\pi}\oint p\,dx.$$

In addition, it is necessary to take account of the fact that the matrix element of the transition goes in the classical limiting case into the corresponding Fourier component of a function defined on the classical trajectory of the particle. After simple transformations we obtain a classical analog of the dispersion relation (10)

$$1 = G(q)\sum_{n,\,\Delta n} \mathrm{P}\frac{\hbar\omega(n)\,\Delta n}{E - \hbar\omega(n)\,\Delta n}\,\frac{\partial f(E_n)}{\partial E_n}\left|\int dt\, e^{iqx(t) - i\omega(n)\Delta n t}\right|^2$$
$$- i\pi G(q)\sum_{n,\,\Delta n} \delta(E - \hbar\omega(n)\,\Delta n)$$
$$\times\ \frac{\partial f(E_n)}{\partial E_n}\,\hbar\omega(n)\,\Delta n\left|\int dt\, e^{iqx(t) - i\omega(n)\Delta n t}\right|^2, \qquad (10')$$

where $x(t)$ is a solution of the classical problem of the motion of a particle in an external field.

The dispersion relations (10) and (10′) obtained above lead, in the case of infinitesimally small wave numbers $(q \to 0)$, to generalized Lorentz dispersion sums. For particles that are free in the ground state the complete system of equations for the collective operator coincides identically with the cut-off system and (10) goes into the well known Klimontovich-Silin dispersion equation.[1] We note that the Hartree-Fock approximation leads in this situation to a system that determines a collective operator analogous to the complete system (9).

For a system in a periodic field, in the approximation

$$(n, \mathbf{k} \,|\, e^{i\mathbf{qr}} \,|\, \mathbf{k}', n') \to (u_{\mathbf{k},n} \,|\, u_{\mathbf{k}+\mathbf{q},n'})\, \delta(\mathbf{k}' - \mathbf{k} - \mathbf{q}),$$

where $(n, \mathbf{k} \,|\, \mathbf{r}) \equiv u_{\mathbf{k}}, n(\mathbf{r}) e^{\prime \mathbf{k} \cdot \mathbf{r}}$ defines the state of a particle with quasi-momentum $\mathbf{k}$ in band n, corresponding to conservation of the quasi-momentum in the single-particle transition $\mathbf{k}'$, n' → $\mathbf{k}$, n, the dispersion relation (10) goes into the dispersion equation of the band model.[2] Finally, for a system of particles in a constant homogeneous magnetic field, in the approximation

$$(k_x, n, k_z \,|\, e^{i\mathbf{qr}} \,|\, k_z', n', k_x')$$
$$\to \delta(k_z' - k_z - q_z)\, \delta(k_x' - k_x - q_x)\, (\chi_n \,|\, \chi_{n'})\, \delta(q_y),$$

where $(\chi_n \,|\, \chi_{n'})$ is the overlap integral of the oscillator functions, corresponding to the Landau representation,[4] we arrive at the dispersion equation obtained by Zyryanov.[5]

Let us turn now to an examination of the "collective" initial condition, which is an assembly of initial conditions with definite wave number values

$$R_q(0) = \sum_{n_0 n_0'} (n_0 \,|\, e^{iqx} \,|\, n_0')\, \rho^{(0)}(n_0 n_0'). \tag{11}$$

Parametrizing relation (5), which determines the behavior of each individual initial condition, we find that the quantity

$$R_q(E) = \sum_{n_0 n_0'} (n_0 \,|\, e^{iqx} \,|\, n_0')\, \rho_{n_0 n_0' | n_0 n_0'}(E), \tag{12}$$

which characterizes the behavior of the assembly of initial conditions with definite wave number values, is determined by the relation

$$R_q(E) = \sum_{n_0 n_0'} \frac{(n_0 \,|\, e^{iqx} \,|\, n_0')}{D_{n_0 n_0'}(E) + i\Gamma_{n_0 n_0'}(E)/2}\, \rho^{(0)}(n_0 n_0'). \tag{13}$$

Relation (13) in general does not lend itself to separation in the right-hand part of the 'collective' initial condition. However, in the approximation $\langle D^{-1} \rangle_{\text{av}} = \langle D \rangle_{\text{av}}^{-1} + \ldots$ we find that

$$R_q(E) = [D_q(E) + i\Gamma_q(E)/2]^{-1} R_q(0), \tag{14}$$

where the fluctuation propagation function

$$D_q(E) = \sum_{n_0 n_0'} D_{n_0 n_0'}(E)\, (n_0 \,|\, e^{iqx} \,|\, n_0')\, \rho^{(0)}(n_0 n_0')$$

is the propagation function of the single-particle transition averaged over the initial state, and the decay of the fluctuations is determined by the averaged width

$$\tfrac{1}{2}\Gamma_q(E) = iG(q) F(q, q)\, U_q(E) + i \sum_{q' \neq q} G(q')\, F(q, q')\, U_{q'}(E),$$

$$F(q, q') = \sum_{n_0 n_0'} \Delta f(n_0 n_0')\, (n \,|\, e^{iq'x} \,|\, n_0')\, (n_0' \,|\, e^{iqx} \,|\, n_0)\, \rho^{(0)}(n_0 n_0').$$

In conclusion we note that parametrization of the initial Hartree equations leads in the presence of self-action to a system of inhomogeneous equations for the collective operator $U_q(E; n_0 n_0')$, of the form

$$\begin{aligned} U_q(E; n_0 n_0') = {} & \{1 - G(q) \sum_{nn'} \Delta f(nn')\, D_{nn'}^{-1}(E)\, |(n \,|\, e^{iqx} \,|\, n')|^2\}^{-1} \\ & \times \Big\{ \sum_{nn'} \Delta f(nn')\, D_{nn'}^{-1}(E)\, (n \,|\, e^{iqx} \,|\, n')\, G_{n_0 n}^{n_0' n} \\ & + \sum_{q' \neq q} G(q')\, U_{q'}(E; n_0 n_0') \\ & \times \sum_{nn'} \Delta f(nn')\, D_{nn'}^{-1}(E)\, (n \,|\, e^{iq'x} \,|\, n')\, (n' \,|\, e^{iqx} \,|\, n) \Big\}. \end{aligned} \tag{15}$$

In this case the state of collective fluctuations of the system is determined not only by the excitation spectrum $E = E(q)$, but by the quantum numbers of the initial individual excitation (n_0, n_0'). The system given above for the definition of $U_q(E; n_0 n_0')$, together with the expression for $\rho_{n_0 n_0' | n_0 n'}(E)$, analogous to that given above, determines the decay of the initial individual state and the excitation of collective fluctuations in the system of interacting particles.

For particles that are free in the ground state the equation for the collective operator $U_q(E; k_0, k_0')$ is greatly simplified and turns into the analog of the following equation[1]

$$\begin{aligned} \rho_{\mathbf{k}}(t) = {} & \frac{1}{2\pi i} \oint ds e^{st} \\ & \times \Big\{ 1 - G(k) \int \frac{f(\mathbf{p} + \hbar\mathbf{k}/2) - f(\mathbf{p} - \hbar\mathbf{k}/2)}{m^{-1}kp - is}\, d^3p \Big\}^{-1} \\ & \times \int \frac{\varphi_{\mathbf{k}}(0, \mathbf{p})}{s + im^{-1}\mathbf{kp}}\, d^3p, \end{aligned}$$

which determines the time variation of the Fourier component of the density fluctuation $\rho_{\mathbf{k}}(t)$ in terms of the initial value of the perturbed particle distribution function of the system, $\varphi_{\mathbf{k}}(0, \mathbf{p})$.

---

[1] Yu. L. Klimontovich and V. P. Silin, Usp. Fiz. Nauk 70, 247 (1960), Soviet Phys.-Uspekhi 3, 84 (1960).

[2] H. Ehrenrich and M. H. Cohen, Phys. Rev. 115, 786 (1959).

[3] W. Heitler. The Quantum Theory of Radiation, Oxford 1954.

[4] L. D. Landau and E. M. Lifshitz, Quantum Mechanics, I. Pergamon, 1948.

[5] P. S. Zyryanov, JETP 40, 1065 (1961), this issue p. 751.

Translated by J. G. Adashko
192

SOVIET PHYSICS JETP VOLUME 13, NUMBER 4 OCTOBER, 1961

SCATTERING OF LOW-ENERGY PHOTONS ON A SYSTEM WITH SPIN ½

V. A. PETRUN'KIN

P. N. Lebedev Physics Institute, Academy of Sciences, U.S.S.R.

Submitted to JETP editor November 1, 1960

J. Exptl. Theoret. Phys. (U.S.S.R.) **40**, 1148-1154 (April, 1961)

An expression for the scattering cross section of low-energy photons on a system with spin $1/2$ is obtained within the framework of the local theory, with an accuracy up to terms quadratic in frequency. In addition to the constants e, M, and λ (which represent the charge, mass, and anomalous moment of the system respectively), three other parameters, α, β, and $\langle r_e^2 \rangle$ (representing, respectively, the electric and magnetic polarizabilities and the mean-square radius of the charge distribution of the system) also appear in the cross-section formula.

1. INTRODUCTION

LOW[1] and Gell-Mann and Goldberger[2] have investigated the scattering amplitude of light on a system with spin $1/2$ within the framework of the local theory. It has been shown that, from the requirement of the relativistic and gauge invariance of the theory, one can draw definite conclusions concerning the scattering amplitude, with an accuracy up to terms linear in frequency. For a comparison of the theory with experiment, it would be interesting to obtain not the amplitude but the differential cross section. It is the purpose of the present paper to obtain a formula for the cross section with an accuracy up to terms quadratic in the frequency. To this end, it is necessary to take into account in the expression for the amplitude the quadratic terms which interfere with the Thompson scattering amplitude and thus contribute to the quadratic terms in the expression for the cross section, in addition to the linear terms. No complete derivation of a general formula for the light-scattering cross section on a system with spin $1/2$ has been given in the literature, although the importance of the quadratic terms was indicated, and the calculation of some of them carried out, by Klein[3] and Baldin.[4] (A preliminary report was presented by Baldin at the Elementary Particle Conference in Padua in 1957.)

It is also interesting to obtain the general formula for the cross section in order to find such characteristics of the nucleons as their electrical (α) and magnetic (β) polarizability. In the conclusion, we shall dwell briefly on the possibility of obtaining numerical estimates of α and β from the presently-available experimental data on the Compton effect on protons.[5,6]

2. CALCULATION OF THE SCATTERING AMPLITUDE

Within the assumptions made by Low,[1] we can write the following expression, quadratic in e, for the matrix element for the scattering of a photon with four-momentum k and polarization **e** on a nucleon* with momentum p. The scattered photon then has a momentum k′ and a polarization **e**′:

$$\langle \mathbf{e}'k'p's' \,|\, S \,|\, \mathbf{e}kps \rangle = -\frac{2i}{\sqrt{4kk'}} \Big\langle p's' \Big| \, e^2 \mathbf{e}\mathbf{e}' \int \Phi\,(x) \Phi\,(x)$$

$$\times \exp\,[i\,(k - k')\,x]\,dx \Big| ps \Big\rangle$$

$$-\frac{1}{\sqrt{4kk'}} \Big\langle p's' \Big| \int P\,[j\,(x)\,\mathbf{e}', j\,(y)\,\mathbf{e}]$$

$$\times \exp\,[i\,(ky - k'x)]\,dxdy \Big| ps \Big\rangle \qquad (1)$$

where p′ is the momentum of the final nucleon, s′ and s are the projections of the spin of the initial and final nucleons, (kx) is the scalar product of the four-vectors, and $\Phi(x)$ and $j_\nu(x)$ are time-dependent operators of the meson field and of the current in the electromagnetic representation of the interaction.

We shall change Eq. (1) over to time-independent operators, using the transformation

$$A\,(x) = e^{iH_0 t} A\,(\mathbf{x})\,e^{-iH_0 t},$$

where H_0 is the total Hamiltonian of the meson and nucleon fields.

Writing the P-product explicitly and letting the operator H_0 operate on the indices of the matrix element, we obtain, after an integration with respect to t,

---

*Henceforth, we use the word nucleon as an abreviation for a "system with spin ½."

$$\langle|S|\rangle = -\frac{2\pi}{\sqrt{4kk'}}\,\delta(E(p') + k' - E(p) - k)\,\Big[2i\Big\langle\Big|e^2\mathbf{e}\mathbf{e}'\int\Phi^*(\mathbf{x})\Phi(\mathbf{x})\exp[i(\mathbf{k}-\mathbf{k}')\mathbf{x}]\,d\mathbf{x}\Big|\Big\rangle$$

$$+\Big\langle\Big|\int\mathbf{j}(\mathbf{x})\mathbf{e}'\exp[-i\mathbf{k}'\mathbf{x}]\,d\mathbf{x}\,\frac{1}{i(H_0 - E(p) - k)}\int\mathbf{j}(\mathbf{y})\mathbf{e}\,\exp[i\mathbf{k}\mathbf{y}]\,d\mathbf{y}\Big|\Big\rangle$$

$$+\Big\langle\int\mathbf{j}(\mathbf{y})\mathbf{e}\exp[i\mathbf{k}\mathbf{y}]\,d\mathbf{y}\,\frac{1}{i(H_0 - E(p) + k')}\int\mathbf{j}(\mathbf{x})\mathbf{e}'\exp[-i\mathbf{k}\mathbf{x}]\,d\mathbf{x}\Big|\Big\rangle\Big]. \tag{2}$$

We shall expand the last two terms in Eq. (2) in terms of the total system of physical states of the meson-nucleon field. We then have

$$\langle|S|\rangle = -\frac{2\pi}{\sqrt{4kk'}}\,\delta(E(p') + k' - E(p) - k)\,\Big[2i\Big\langle\Big|e^2\mathbf{e}\mathbf{e}'\int\Phi^*(\mathbf{x})\Phi(\mathbf{x})\exp[i(\mathbf{k}-\mathbf{k}')\mathbf{x}]\,d\mathbf{x}\Big|\Big\rangle$$

$$+\sum_N\frac{\Big\langle\Big|\int\mathbf{j}(\mathbf{x})\mathbf{e}'\exp[-i\mathbf{k}'\mathbf{x}]\,d\mathbf{x}\Big|N\Big\rangle\Big\langle N\Big|\int\mathbf{j}(\mathbf{y})\mathbf{e}\exp[i\mathbf{k}\mathbf{y}]\,d\mathbf{y}\Big|\Big\rangle}{i[E_N - E(p) - k]} + \sum_N\frac{\Big\langle\Big|\int\mathbf{j}(\mathbf{y})\mathbf{e}\exp[i\mathbf{k}\mathbf{y}]\,d\mathbf{y}\Big|N\Big\rangle\Big\langle N\Big|\int\mathbf{j}(\mathbf{x})\mathbf{e}'\exp[-i\mathbf{k}'\mathbf{x}]\,d\mathbf{x}\Big|\Big\rangle}{i[E_N - E(p) + k']}\Big]. \tag{3}$$

In order to obtain the momentum-conservation law explicitly, we shall use the translational invariants of the matrix element. We show the detailed calculations only for the first term in Eq. (3):

$$\Big\langle p's'\Big|e^2\mathbf{e}\mathbf{e}'\int\Phi^*(\mathbf{x})\Phi(\mathbf{x})\exp[i(\mathbf{k}-\mathbf{k}')\mathbf{x}]\,d\mathbf{x}\Big|ps\Big\rangle$$

$$= \exp[-i(\mathbf{p}'-\mathbf{p})\mathbf{a}]\Big\langle p's'\Big|e^2\mathbf{e}\mathbf{e}'\int\Phi^*(\mathbf{x}-\mathbf{a})$$

$$\times\,\Phi(\mathbf{x}-\mathbf{a})\exp[i(\mathbf{k}-\mathbf{k}')\mathbf{x}]\,d\mathbf{x}\Big|ps\Big\rangle$$

$$= \exp[-i(\mathbf{p}'+\mathbf{k}'-\mathbf{p}-\mathbf{k})\mathbf{a}]$$

$$\times\Big\langle p's'\Big|e^2\mathbf{e}\mathbf{e}'\int\Phi^*(\mathbf{x}')\Phi(\mathbf{x}')$$

$$\times\exp[i(\mathbf{k}-\mathbf{k}')\mathbf{x}']\,d\mathbf{x}'\Big|ps\Big\rangle. \tag{4}$$

Integrating the right- and left-hand sides of Eq. (4) with respect to **a**, we finally obtain

$$\Big\langle\Big|e^2\mathbf{e}\mathbf{e}'\int\Phi^*(\mathbf{x})\Phi(\mathbf{x})\exp[i(\mathbf{k}-\mathbf{k}')\mathbf{x}]\,d\mathbf{x}\Big|\Big\rangle$$

$$= \frac{(2\pi)^3\,\delta(\mathbf{p}'+\mathbf{k}'-\mathbf{p}-\mathbf{k})}{\mathbf{V}}\Big\langle\Big|e^2\mathbf{e}\mathbf{e}'$$

$$\times\int\Phi^*(\mathbf{x})\Phi(\mathbf{x})\exp[i(\mathbf{k}-\mathbf{k}')\mathbf{x}]\,d\mathbf{x}\Big|\Big\rangle.$$

It can easily be seen that the coefficient ahead of the matrix element, appearing as a result of the transformation carried out, is equal to 1.* Henceforth, we shall write the matrix elements of operators containing integrals as

$$\Big\langle\Big|e^2\mathbf{e}\mathbf{e}'\int\Phi^*(\mathbf{x})\Phi(\mathbf{x})\exp[i(\mathbf{k}-\mathbf{k}')\mathbf{x}]\,d\mathbf{x}\Big|\Big\rangle$$

$$= (2\pi)^3\,\delta(\mathbf{p}'+\mathbf{k}'-\mathbf{p}-\mathbf{k})$$

$$\times\Big[\frac{1}{V}\Big\langle\Big|e^2\mathbf{e}\mathbf{e}'\int\Phi^*(\mathbf{x})\Phi(\mathbf{x})\exp[i(\mathbf{k}-\mathbf{k}')\mathbf{x}]\,d\mathbf{x}\Big|\Big\rangle\Big].$$

We assume the quantity in the brackets to be finite.

From the translational invariance of the two terms of Eq. (3), we can easily obtain the expressions

$$\langle|S|\rangle = -\frac{(2\pi)^4}{\sqrt{4kk'}}\,\delta(p'+k'-p-k)\,\Big\{\frac{2i}{V}\Big\langle\Big|e^2\mathbf{e}\mathbf{e}'\int\Phi^*(\mathbf{x})\,\Phi(\mathbf{x})\,\exp[i(\mathbf{k}-\mathbf{k}')\,\mathbf{x}]\,d\mathbf{x}\Big|\Big\rangle$$

$$+\sum_{\nu\sigma}\Big[\frac{\langle|\mathbf{j}(0)\mathbf{e}'|\nu\sigma\mathbf{k}\rangle\langle\nu\sigma\mathbf{k}|\mathbf{j}(0)\mathbf{e}|\rangle}{i[E_\nu(k) - M - k]} + \frac{\langle|\mathbf{j}(0)\mathbf{e}|\nu\sigma-\mathbf{k}'\rangle\langle\nu\sigma-\mathbf{k}'|\mathbf{j}(0)\mathbf{e}'|\rangle}{i[E_\nu(k') - M + k']}\Big]$$

$$+\sum_{N'}\Big[\frac{\Big\langle\Big|\int\mathbf{j}(\mathbf{x})\mathbf{e}'\exp[-i\mathbf{k}'\mathbf{x}]\,d\mathbf{x}\Big|N'\mathbf{k}\Big\rangle\Big\langle N'\mathbf{k}\Big|\int\mathbf{j}(\mathbf{y})\,\mathbf{e}\exp[i\mathbf{k}\mathbf{y}]\,d\mathbf{y}\Big|\Big\rangle}{i[E_{N'} - M - k]\,V^2}$$

$$+\frac{\Big\langle\Big|\int\mathbf{j}(\mathbf{y})\mathbf{e}\exp[i\mathbf{k}\mathbf{y}]\,d\mathbf{y}\Big|N-\mathbf{k}'\Big\rangle\Big\langle N-\mathbf{k}'\Big|\int\mathbf{j}(\mathbf{x})\mathbf{e}\exp[-i\mathbf{k}'\mathbf{x}]\,d\mathbf{x}\Big|\Big\rangle}{i[E_{N'} - M + k']\,V^2}\Big]\Big\}. \tag{5}$$

We have separated the single-nucleon term explicitly, and set the momentum of the initial nucleon $\mathbf{p} = 0$ (in the laboratory system). The indices ν and σ indicate the summation over positive and negative energies and over the projections of the nucleon spin in the intermediate state. It would be more consistent to work with positive energies only, adding to the single-nucleon expression those terms of the sum over all excited states which contain a pair in the intermediate state in addition to the nucleon. However, it is simpler for us to carry out the summation over negative energies.†

The amplitude component due to the contribution of single-nucleon terms can be calculated directly if we use the total formula for the matrix element of the current operator connecting single-nucleon states:‡

---

*This is true for the limiting case V → ∞.

†See Heitler^7 pp. 213-214 concerning the equivalence of the results obtained.

‡See reference 1, Eq. (3.1).

$$\langle p_2|j_\mu(0)|p_1\rangle = i\bar{u}(p_2)\left[e\gamma_\mu f(\Delta p^2) - \sigma_{\mu\nu}\Delta p_\nu \lambda' g(\Delta p^2)\right]u(p_1),$$
$$\Delta p = p_2 - p_1, \qquad \lambda' = \lambda e/2M, \qquad \sigma_{\mu\nu} = i(\gamma_\nu\gamma_\mu - \gamma_\mu\gamma_\nu)/2. \tag{6}$$

The calculation of the single-nucleon part of Eq. (5), using Eq. (6), leads to the expression

$$\sum_{\nu\sigma}[\ldots] = iN(p')N(p)$$
$$\times\Big\langle\Big|\frac{e^2f^2}{M}\mathbf{ee}' - i\frac{e^2f}{2M}\frac{k}{M}(f+2\lambda g)\,\boldsymbol{\sigma}\,[\mathbf{e}'\mathbf{e}]$$
$$- i\frac{e^2}{2M}\frac{k}{M}(f+\lambda g)^2\,\boldsymbol{\sigma}\,[[\mathbf{ne}]\,[\mathbf{n}'\mathbf{e}']]$$
$$- i\frac{e^2f}{2M}\frac{k}{M}(f+\lambda g)\left((\mathbf{en}')(\boldsymbol{\sigma}[\mathbf{n}'\mathbf{e}']) - (\mathbf{e}'\mathbf{n})(\boldsymbol{\sigma}[\mathbf{ne}])\right)$$
$$-\frac{1}{2}\frac{e^2}{2M}\left(\frac{k}{M}\right)^2(f+\lambda g)^2\left(\mathbf{ee}'(1-\cos^2\theta) - (\mathbf{en}')(\mathbf{e}'\mathbf{n})\right.$$
$$\left.\times(1-\cos\theta)\right)$$
$$-\frac{1}{2}\frac{e^2}{2M}\left(\frac{k}{M}\right)^2(2\lambda gf + \lambda^2g^2)(\mathbf{en}')(\mathbf{e}'\mathbf{n})\Big|\Big\rangle,$$
$$N(p') = \sqrt{{}^1\!/_2\,(1 + M/E(p'))}, \qquad N(p) = 1, \quad \mathbf{p} = 0. \tag{7}^*$$

In deriving Eq. (7), we have changed over to two-row matrices, and have limited ourselves to terms quadratic in frequency. Terms quadratic in k and containing the operator $\boldsymbol{\sigma}$ have been dropped, since their contribution to the cross section is of the order of k^3 and less. The functions f and g characterizing the spread of the charge and of the magnetic moment of a nucleon in the non-relativistic approximation can be written as

$$f(\Delta p^2) = 1 - \tfrac{1}{6}\langle r_e^2\rangle k^2, \quad g(\Delta p^2) = 1 - \tfrac{1}{10}\langle r_\mu^2\rangle k^2.$$

where $\langle r_e^2\rangle$ and $\langle r_\mu^2\rangle$ are the mean-square radii of the charge and of the magnetic moment. In our approximation, we must, in the expression for the amplitude, set the functions f and g equal to one in all terms except the term $e^2f^2M^{-1}\mathbf{e}\cdot\mathbf{e}'$.

As was shown by Low,[1] the sum of the first and third terms in Eq. (5) does not contribute to the single-nucleon term in the approximation linear in k. For the problem on hand, let us first construct the general form of the terms quadratic in k that are due to this sum and that do not contain the operator $\boldsymbol{\sigma}$. From $\mathbf{e}$, $\mathbf{e}'$, $\mathbf{k}$, and $\mathbf{k}'$ one can write the general expression

$$\gamma_1\mathbf{ee}'k^2 + \gamma_2(\mathbf{ee}')(\mathbf{kk}') + \gamma_3(\mathbf{ek}')(\mathbf{e}'\mathbf{k}). \tag{8}$$

Expressions of the type $\mathbf{e}\times\mathbf{k}$, $\mathbf{e}'\times\mathbf{k}'$, $\mathbf{e}\times\mathbf{k}'$, $\mathbf{e}'\times\mathbf{k}$ can be reduced, as can easily be ascertained, to the form (8). γ_1, γ_2, and γ_3 denote still unknown coefficients, whose meaning must be explained. To this end, we shall use the formula proved in reference 1

$$k_ik_jg_{ij} = k'k\Big\langle\Big|\int P\,[\rho(x)\,\rho(y)]\exp[i(ky - k'x)]\,dx\,dy\Big|\Big\rangle, \tag{9}$$

where g_{ij} is defined in the following way

$$\langle|S|\rangle = -e_i'e_jg_{ij}/\sqrt{4kk'}.$$

Equation (9) is obtained as a result of the gauge invariance of the theory. Carrying out a transformation of the right-hand side of Eq. (9), analogous to those carried out earlier, we easily find that

$$k_i'k_jg_{ij} = i(2\pi)^4\delta(p' + k' - p - k)\Big\{\text{single-nucleon term}$$
$$- kk'k_i'k_j\sum_{N'}\Big[\frac{\big\langle 0\big|\int\rho(\mathbf{x})\,\mathbf{x}_i d\mathbf{x}\big|N'0\big\rangle\big\langle N'0\big|\int\rho(\mathbf{y})\,y_j d\mathbf{y}\big|0\big\rangle}{(E_{N'} - M)V^2}$$
$$+ \frac{\big\langle 0\big|\int\rho(\mathbf{y})\,y_j\,d\mathbf{y}\big|N'0\big\rangle\big\langle N'0\big|\int\rho(\mathbf{x})\,\mathbf{x}_i\,d\mathbf{x}\big|0\big\rangle}{(E_{N'} - M)V^2}\Big]\Big\}.$$

Under the summation sign we have the equivalent of a symmetrical tensor α_{ij}. For a particle with spin ½, this tensor should be of the form $\alpha\delta_{ij}$. Thus, transitions to other states make an additional contribution of the form $\alpha k^2\mathbf{k}\cdot\mathbf{k}'$, in addition to the single-nucleon term. It is natural to name the constant

$$\alpha = \sum_{N'}\Big[\frac{\big\langle 0\big|\int\rho(\mathbf{x})\,x_i d\mathbf{x}\big|0N'\big\rangle\big\langle 0N'\big|\int\rho(\mathbf{y})\,y_i d\mathbf{y}\big|0\big\rangle}{(E_{N'} - M)V^2}$$
$$+ \frac{\big\langle 0\big|\int\rho(\mathbf{y})\,y_i d\mathbf{y}\big|0N'\big\rangle\big\langle 0N'\big|\int\rho(\mathbf{x})\,x_i d\mathbf{x}\big|0\big\rangle}{(E_{N'} - M)V^2}\Big] \tag{10}$$

the electrical polarizability of the nucleon.[4] Comparing the left-hand side of Eq. (9) with the right-hand one we see that, to have an equality, it is necessary that $\gamma_2 + \gamma_3 = 0$ and $\gamma_1 = -\alpha$. The equality of the single-nucleon terms on the left- and right-hand sides follows automatically from the requirement that the single nucleon terms should vanish for an exchange of $\mathbf{e} \to \mathbf{k}$ and $\mathbf{e}' \to \mathbf{k}'$ which, as can easily be checked, is satisfied in our case. As a result, we obtain the following form of the matrix element for the process under consideration

$$\langle|S|\rangle = -\frac{i(2\pi)^4}{\sqrt{4kk'}}\delta(p' + k' - p - k)\,\{\langle|(\ldots)$$
$$-\alpha k^2\mathbf{ee}' - \beta\,[\mathbf{ke}]\,[\mathbf{k}'\mathbf{e}']|\rangle\}. \tag{11}$$

The symbol . . . denotes the single-nucleon term in the amplitude, and $\beta = -\gamma_2 = +\gamma_3$.

In order to explain the physical meaning of the constant β, we shall carry out a Foldy transformation[8] of the expressions that lead to the term $\beta\mathbf{k}\times\mathbf{e}\cdot\mathbf{k}'\times\mathbf{e}'$. This transformation means that $\exp(i\mathbf{q}\cdot\mathbf{r})$ is transformed in the corresponding matrix elements according to the identity

---

*$[\mathbf{n}\,\mathbf{e}] = \mathbf{n}\times\mathbf{e}$.

$$\mathbf{e}e^{i\mathbf{qr}} = \int_0^1 \{\operatorname{grad}(\mathbf{er}e^{is\mathbf{qr}}) - i\,[\mathbf{r}\,[\mathbf{qe}]]\,e^{is\mathbf{qr}}\}\,ds. \tag{12}$$

After substituting, we see that β is given by the following approximation:

$$\beta \sim \sum_{N'} \Big[\frac{\left\langle 0 \middle| \int [\mathbf{j}(\mathbf{x})\,\mathbf{x}]\,d\mathbf{x} \middle| N'0 \right\rangle \left\langle N'0 \middle| \int [\mathbf{j}(\mathbf{y})\,\mathbf{y}]\,d\mathbf{y} \middle| 0 \right\rangle}{(E_{N'} - M)\,V^2} + \frac{\left\langle 0 \middle| \int [\mathbf{j}(\mathbf{y})\,\mathbf{y}]\,d\mathbf{y} \middle| N'0 \right\rangle \left\langle N'0 \middle| \int [\mathbf{j}(\mathbf{x})\,\mathbf{x}]\,d\mathbf{x} \middle| 0 \right\rangle}{(E_{N'} - M)\,V^2} \Big]. \tag{13}$$

The "approximately-equal" sign, rather than the equality sign, is used above, since, in general, other terms not written here may also contribute to β. This problem requires additional investigation.

The first term in Eq. (13) has no simple physical meaning, while the second term, like α, can be called the magnetic polarizability. Henceforth, we shall define the magnetic polarizability as the sum of all contributions to β, i.e., as β itself.

3. DIFFERENTIAL CROSS SECTION

The differential cross section is given by the equation*

$$d\sigma = \frac{1}{4kk'}\,|Q|^2\,\frac{d\mathbf{p}'\,d\mathbf{k}'}{J\,(2\pi)^3}\,\delta(\mathbf{p}' + \mathbf{k}' - \mathbf{p} - \mathbf{k})\,\delta(E(p') + k' - E(p) - k),$$

where Q is the expression inside the braces in Eq. (11), and J is the current density of the colliding particles.

Averaging and summing up over the spin projections of the nucleons and of the photon polarization, we obtain a formula for the differential cross section for the scattering of an unpolarized photon beam on unpolarized nucleons:

$$\begin{aligned}\frac{d\sigma}{d\Omega} = \frac{1}{2} r_0^2 \Big\{ \Big[1 - 2\frac{k}{M}(1 - \cos\theta) &+ 3\left(\frac{k}{M}\right)^2 (1 - \cos)^2 \Big] (1 + \cos^2\theta) \\ &+ \left(\frac{k}{M}\right)^2 [(1 - \cos\theta)^2 + f(\theta)] \\ &- \Big[\frac{2}{3}\langle r_e^2\rangle M^2 + 2\frac{\alpha M^3}{e^2}\Big]\left(\frac{k}{M}\right)^2 (1 + \cos^2\theta) \\ &- 4\frac{\beta M^3}{e^3}\left(\frac{k}{M}\right)^2 \cos\theta \Big\}, \\ r_0 = e^2/M, \qquad f(\theta) &= a_0 + a_1\cos\theta + a_2\cos^2\theta, \\ a_0 = 2\lambda + \tfrac{9}{2}\lambda^2 + 3\lambda^3 + \tfrac{3}{4}\lambda^4, \qquad a_1 &= -4\lambda - 5\lambda^2 - 2\lambda^3, \\ a_2 &= 2\lambda + \tfrac{1}{2}\lambda^2 - \lambda^3 - \tfrac{1}{4}\lambda^4. \end{aligned} \tag{14}$$

In deriving Eq. (14), the terms containing powers of frequency higher than k^2 were neglected. Equation (14) contains the three additional constants α, β, and $\langle r_e^2 \rangle$, as compared with the formula of Powell[10] for the scattering of light on a charged particle with anomalous momentum λ. The value of $\langle r_e^2 \rangle$ can be obtained from experiments on the structure of the nucleon. We can attempt to determine the constants α and β from protons by comparing Eq. (14) with the experimental data. The reader may refer to such a comparison carried out by Gol'danskii et al.[6]

4. CONCLUSION

We shall make a few comments concerning the role of the separate terms in Eq. (14), and the region of its applicability. The role of the separate terms is characterized by the following data:

	10–20 Mev	50–60 Mev	90–100 Mev
Term containing λ:	1%	10%	50%
Term containing $\langle r_e^2 \rangle$:	0.3%	4%	12%

Henceforth, we put $\frac{1}{2}(e^2/M)^2 = 1$. In the estimates, we have put $\lambda = 1.7$ and $\sqrt{\langle r_e^2 \rangle} = 0.8 \times 10^{-13}$ cm. We cannot give a good estimate of the terms containing α and β, since there is no rigorous theory concerning these parameters. The estimate of the quantity

$$\alpha' = \frac{1}{3}\frac{e^2}{\hbar c}\,\langle r_e^2\rangle\,\frac{\hbar}{Mc} + \alpha,$$

carried out by Baldin[4] has yielded the following results:

$$0{,}4\cdot 10^{-42}\,\mathrm{cm}^3 \leqslant \alpha' \leqslant 1{,}5\cdot 10^{-42}\ \mathrm{cm}^3.$$

The lower limit of this estimate has been obtained from the relation between the polarizability and the amplitude of the electrical-dipole photoproduction of π mesons. The upper limit of the estimate has been obtained by an analysis of the experimental data on the Compton effect. Gol'danskii, et al.[6] have obtained the value of $\alpha = (0.9 \pm 0.2) \times 10^{-42}$ cm^3. It is easily concluded from this that the contribution of the term containing α may amount to 5 to 12%. No reliable theoretical estimates of β are at present available. From the fact that the measured cross section is not greatly different from the cross section given by the formula of Powell, we can conclude that the contribution of the term containing β is not greater than the contribution of that containing α.

Thus, each of the terms containing α and β makes a contribution of about 10%, in its order of magnitude. This indicates that we have to be very careful in determining α and β directly from experiments by comparing Eq. (14) with experimental data. This is because we do not have an exact estimate of the terms neglected in Eq. (14). We can expect that the contribution of the consecutive terms of the expansion will amount to $\sim k/\mu$ (where μ is the meson mass) of the contribution of terms containing α and β. If we want to fit the experimental data on the Compton effect on a proton with an accuracy of 5%, then Eq. (14) is satisfactory in the 0 — 70 Mev energy range. If we want to determine the parameters α and β to within 10 to 20% by comparing Eq. (14) with experimental data, then experiments on γ-ray scattering at 10 — 30 Mev energy are necessary, which are at present already on the border-line of experimental feasibility. A more exact evaluation of this limit depends on the estimate of the neglected terms in the amplitude, which has so far not been carried out.

---

*See reference 9, p. 292.

In conclusion, the author wishes to thank A. M. Baldin for proposing the subject, and for his constant interest in the work.

Note added in proof (April 7, 1961): A more exact analysis shows that the summation over negative energies in the single-nucleon term (see footnote 3) does not take into account all the intermediate states involving pairs, but accounts only for those which correspond to usual diagrams of the perturbation theory. The remaining states should be included in the sum over N′.

---

[1] F. E. Low, Phys. Rev. 96, 1428 (1954).

[2] M. Gell-Mann and M. L. Goldberger, Phys. Rev. 96, 1433 (1954).

[3] A. Klein, Phys. Rev. 99, 998 (1955).

[4] A. M. Baldin, Nucl. Phys. 18, 310 (1960).

[5] C. Oxley, Phys. Rev. 110, 733 (1958).

[6] Gol'danskii, Karpukhin, Kutsenko, and Pavlovskaya, JETP 38, 1695 (1960), Soviet Phys. JETP 12, 1223 (1960).

[7] W. Heitler, The Quantum Theory of Radiation, Oxford, 1954.

[8] L. L. Foldy, Phys. Rev. 92, 178 (1953).

[9] A. I. Akhiezer and V. B. Berestetskii, Квантовая электродинамика (Quantum Electrodynamics), 2nd Ed., Fizmatgiz, 1959.

[10] J. L. Powell, Phys. Rev. 75, 32 (1949).

Translated by H. Kasha
193

UNSTABLE PARTICLE IN THE LEE MODEL

Ya. B. ZEL'DOVICH

Submitted to JETP editor November 11, 1960

J. Exptl. Theoret. Phys. (U.S.S.R.) 40, 1155-1159 (April, 1961)

We consider an unstable particle which can decay according to V → N + θ in the Lee model of a nonrelativistic second-quantized theory. Perturbation theory for an eigenstate expansion of any initial state is generalized to the case of an unstable particle. A quantity playing the role of the norm of the state of such a particle is defined. A new method is given for finding the amount of time a stable V′ particle, which can undergo virtual transitions to the N + θ state, spends in each of its two possible states. This method is then applied to an unstable V particle, and a definite value is obtained for the amount of time it spends in each state; however, this value is found to be complex.

WE follow Lee[1] and consider a system consisting of three particles, V, N, and θ, whose interaction leads to the decay V → N + θ. Unlike Lee, however, we assume that $m_V > m_N + m_\theta$, so that the V particle is unstable and decays spontaneously into an N and a θ. Then the set of stationary states with positive real energy E does not include V states. In the spectrum of this system, the unstable V will appear simply as a resonance in the θ and N states at a given energy E_0 (with $E_0 > m_N + m_\theta$, and some resonance width γ). It is clear, furthermore, that in the nonstationary problem the wave function of the system will have a term proportional to $\exp(-iE't) = \exp(-iE_0 t - \gamma t)$, describing V decay.

In the case of a stable V particle, the interaction gives rise to a term in its wave function which describes an admixture of the N + θ state. In configuration space and in the simplest case of an S wave, this mixed state is described by a wave function of the form $f(r) = Ce^{-\kappa r}/r$, where r is the distance between the N and the θ.[2] It is then easy to normalize the physical V state and to calculate how much bare V and how much N + θ it contains.

The wave function of an unstable V particle is a superposition of the bare V wave function and a diverging N + θ function, which in configuration space (in the case of an S wave) is of the form $f(r) = Ce^{ikr}/r$.

At first sight such a state cannot be normalized, and it would then seem that it is impossible to find the amount of bare V in the unstable physical V state. It will be shown below, however, that if one uses the techniques developed for the description of unstable states in the Schrödinger quantum mechanics of a single particle,[3] one can uniquely answer all questions for unstable particles which are solvable in an elementary way for stable ones.

With this in mind, we start with a new definition of the concept of the fractional amount of a given state, using first the case of stable particles (for which everything is clear).

Consider an eigenstate Ψ of a Hamiltonian H including interaction ($H\Psi = E\Psi$), and let this state be written in the form

$$\Psi = \left| a\psi_V + \int f(r)\, d\tau\, \psi_N \psi_\theta \right| 0 \Big\rangle \tag{1}$$

where ψ_V is the creation operator for a bare V particle, ψ_N and ψ_θ are creation operators for N and θ particles, and $|0\rangle$ is the vacuum state.* The normalization condition is

$$|a|^2 + \int |f(r)|^2\, d\tau = 1. \tag{2}$$

The usual procedure is the following. We suppose that the interaction leading to the transformation V → N + θ is instantaneously turned off (the Hamiltonian changes from H to H_0). In the system described by H_0, the number of V particles is conserved, and the number of N + θ particles is conserved separately, and therefore the fraction of such states at the instant before the interaction was turned off is given, respectively, by $|a|^2$ and $\int |f(r)|^2\, d\tau$.

Our new approach is the following. We apply to the system in state Ψ a small perturbation of the form $\delta H = \delta_V \psi_V^* \psi_V$. In the first approximation the energy is perturbed by an amount

---

*The wave function could also be written in Fock space as a column, each row of which corresponds to a different number of particles. Then the row with amplitude a would correspond to V, while that with amplitude f(r) would correspond to N + θ.

$$\delta E = K\delta_V. \qquad (3)$$

The coefficient K in this formula is then the fraction of bare V in the physical V state. The principle behind this new approach can be explained by analogy: the fraction of iron in a mixture of iron and wood filings can be found by placing the mixture in a weak magnetic field (which will not destroy the mixture), and measuring the force on it; the usual approach corresponds to destroying the mixture (by sorting).

In the same way one can find the fraction of $N + \theta$ by turning on, for instance, a perturbation of the form $\delta_2 H = \delta_N \psi_N^* \psi_N$ and calculating the first-order correction to the energy

$$\delta E = q\delta_N. \qquad (4)$$

The fraction of $N + \theta$ is then given by q. The normalization of Ψ leads to the identity $K + q = 1$.

For a stable particle the new approach gives exactly the same result as the usual one.

This new approach, however, can be applied also to the case of an unstable particle. Then for a particle whose wave function is of the form

$$\Psi_V = \left| a\psi_V + \int f(r)\, d\tau\, \psi_N \psi_\theta \right| 0 \Big\rangle, \qquad (5)$$

we obtain[3]

$$K = a\tilde{a}^* \Big/ \left[a\tilde{a}^* + \int f(r) \tilde{f}^*(r)\, d\tau \right], \qquad (6)$$

$$q = \int f(r) \tilde{f}^*(r)\, d\tau \Big/ \left[a\tilde{a}^* + \int f(r) \tilde{f}^*(r)\, d\tau \right], \qquad (7)$$

where $\tilde{a}$ and $\tilde{f}$ correspond to the solution with the complex conjugate boundary conditions. In the simplest case of an S wave and a real coupling constant g, we have $f(r) = Ce^{ikr}/r$, $\tilde{f}^* = f$, and $\tilde{a}^* = a$, and then the integral in Eqs. (6) and (7) becomes

$$4\pi C^2 \int e^{2ikr} dr.$$

For an unstable particle the k here is complex, and e^{2ikr} increases exponentially as $r \to \infty$. Now as has been shown elsewhere,[3] the integral can be given a well defined meaning, and it turns out to be equal to $-4\pi C^2/2ik$. Thus for S waves the fraction of bare V in the physical V state is

$$K = \frac{a^2}{a^2 - 4\pi C^2/2ik}, \qquad (8a)$$

and the fraction of $N + \theta$ is

$$q = -\frac{4\pi C^2/2ik}{a^2 - 4\pi C^2/2ik}. \qquad (8b)$$

These formulas are analytic continuations of the corresponding formulas* for the stable particles, where for S waves one finds

$$f(r) = C\frac{1}{r} e^{-\varkappa r}, \quad K = \frac{|a|^2}{|a|^2 + 4\pi |C|^2/2\varkappa},$$
$$q = \frac{4\pi |C|^2/2\varkappa}{|a|^2 + 4\pi |C|^2/2\varkappa}. \qquad (9)$$

In particular, if we let m_V approach $m_N + m_\theta$, i.e., go to the boundary between stable and unstable V, we find that K approaches zero and q approaches 1, independently of whether we approach this boundary from the region of stable or unstable V. Some artificiality in this concept of the "fraction of the state" for the unstable particle is manifested by the fact that K and q are then complex.

For particles with spin, in which case the decay products have orbital angular momentum, the wave function has a nonintegrable singularity at $r = 0$. This difficulty exists both for the stable and unstable cases, and can be removed only by a cutoff for small r (or a form factor in the interaction). On the other hand, it is a simple matter[3] to eliminate difficulties connected with the fact that f(r) increases exponentially for large r when $l \neq 0$ for the unstable-particle case.

Let us now consider the Cauchy problem. Let the initial wave function be of the form

$$\Psi(t = 0) = \left| b\psi_V + \int h(r)\, d\tau\, \psi_N \psi_\theta \right| 0 \Big\rangle \qquad (10)$$

with arbitrary b and h(r). It can be shown that the leading term in the solution is then of the form

$$\Psi(t) = ne^{-iE't}\Psi_V = ne^{-iE't} \left| a\psi_V + \int f(r) \psi_N \psi_\theta d\tau \right| 0 \Big\rangle, \qquad (11)$$

and that the coefficient n in this expression is given by

$$n = \frac{(\tilde{\Psi}_V^* \Psi(t=0))}{(\tilde{\Psi}_V^* \Psi_V)} = \frac{1}{a^2 - 4\pi C^2/2ik} \left[ab + \int h(r)\, C\frac{e^{ikr}}{r} d\tau \right]. \qquad (12)$$

The specific expression on the right side of our equation is correct for the simplest case of an S wave and a real coupling constant g, for which $f(r) = Ce^{ikr}/r$.

Thus also in the Cauchy problem the denominator of Eq. (8a) represents the norm of the state for the decaying particle. For an S wave and a real coupling constant g in the interaction term $g(\psi_V^* \psi_N \psi_\theta + \psi_N^* \psi_\theta \psi_V)$ we find that the quantities entering into (1) are

$$f(r) = Ce^{-\varkappa r}/r, \ C = 2agm_r/4\pi, \ m_{\text{пр}} = m_N m_\theta/(m_N + m_\theta),$$
$$\varkappa = \sqrt{2m_r (m_N + m_\theta - m_V)};$$

and that the quantities entering into (5) are

$$f(r) = Ce^{ikr}/r, \qquad C = 2agm_r/4\pi,$$
$$k = \sqrt{2m_r (m_V - m_N - m_\theta - i\gamma)} \approx k_0 - i\gamma m_r/k_0,$$
$$k_0 = \operatorname{Re} k = \sqrt{2m_r (m_V - m_N - m_\theta)},$$
$$\gamma = -\operatorname{Im} E_V = (g^2/2\pi)\, m_r k_0.$$

---

*Since $C \sim a$ and C/a is real, Eqs. (9) can be written without the absolute value sign on a and C, which emphasizes their resemblance to (8a) and (8b).

Now introducing the decay probability $w = 2\gamma$, writing $\Delta = m_V - m_N - m_\theta$, and expressing g^2 and k_0 in terms of these quantities, we arrive at the fraction of $N + \theta$ in the unstable V state (for $w \leq k_0$), namely

$$q = iw / 16\pi\Delta. \tag{13}$$

The m_V that enters into all these expressions is the renormalized mass.

We shall not go into the simple operations which lead one to the above results, but shall merely describe the basic assumptions. The Lee model is an example of a theory in which there are particles which can decay into each other. In this particular case it is possible to solve the problem completely because one needs to consider only a finite number of different kinds of states (for instance V and N, θ in one problem, or V, θ and N, 2θ in another problem).

In the Lee model this happens because of selection rules of the same kind as charge conservation. In particular, V + N (the baryon number) is conserved, and $V + \theta$ (the electric charge) is conserved. These selection rules, however, would not lead one to the goal if it were not for the fact that at the same time anti-particles and therefore θ, $\overline{\theta}$ pair creation, etc., were not excluded from consideration.

A consistent relativistic theory cannot exist without antiparticles, and therefore it is logical to make still another simplifying assumption by considering the nonrelativistic problem in which the particle energy is $E = E_0 + p^2/2m$, so that one need not introduce the factor $1/2\omega$ into the θ normalization. At the same time, the concept of wave-function and mass (or energy) renormalization is maintained in the nonrelativistic theory. The description of real and virtual decay in a second-quantized nonrelativistic theory, and in particular the definition of the "fraction of a state" in virtual decay (i.e., for a stable state) has been given elsewhere[2] [in particular, Eqs. (28) and (26) of the cited reference].

As has been mentioned by N. A. Dmitriev, the expression

$$N = \int [\psi^2(r) - (Ce^{ikr}/r)^2]\, d\tau - 4\pi C^2 / 2ik \tag{14}$$

which plays the role of the norm in an unstable-state solution of a Schrödinger problem,[3] (the analog of this expression is

$$N = a^2 - 4\pi C^2 / 2ik \tag{15}$$

of the present paper), has already essentially appeared in some work of Ning Hu,[4] involving dispersion relations.

Indeed, according to Heisenberg, a normalized stable (bound) state whose asymptotic wave function is of the form $\psi = Ce^{-\kappa r}/r$ leads to a residue in the scattering amplitude S(k) at the pole corresponding to the state, that is at $k = i\kappa$, given by

$$\oint_{k=i\kappa} S(k)\, dk = 8\pi^2 |C|^2. \tag{16}$$

Using the fact that the bound-state function is real, we write this result for an unnormalized function in the form

$$\oint_{k=i\kappa} S(k)\, dk = 8\pi^2 C^2 \Big/ \int \psi^2(r)\, d\tau \tag{17}$$

Ning Hu gives a similar expression [Eq. (28) in his cited work] for the residue at $k = k_1$, with $\operatorname{Im} k_1 < 0$, which corresponds to an unstable state. His expression is

$$2ik_1 \left(\frac{dS}{dk}\right)_{k=-k_1} = 2k_1 \int_0^R (r\psi)^2\, dr + i\,[R\psi(R)]^2, \tag{18}$$

where $\psi(r)$ is the unstable-state solution whose asymptotic form is $\psi = e^{ik_1 r}/r$. We choose R so large that ψ is essentially in its asymptotic form, and introduce C by writing $\psi = Ce^{ik_1 r}/r$ for $r \geq R$. Some elementary operations lead to

$$\begin{aligned} \oint_{k=k_1} S(k)\, dk &= -2\pi i \left(\frac{dS}{dk}\right)^{-1}_{k=-k_1} \\ &= 2\pi C^2 \Big/ \int_0^R \psi^2 r^2\, dr + \frac{i}{2k_1}[R\psi(R)]^2 \\ &= 2\pi C^2 \Big/ \int_0^R \psi^2 r^2 dr + \frac{i}{2k_1} C^2 e^{2ik_1 R} \\ &= 8\pi^2 C^2 \Big/ \int_0^\infty \left[\psi^2 - \left(\frac{Ce^{ik_1 r}}{r}\right)^2\right] d\tau - \frac{4\pi C^2}{2ik_1}. \end{aligned} \tag{19}$$

The resemblance of (17) to (19) is obvious.

I take this opportunity to express my gratitude to N. A. Dmitriev for valuable discussion and for aid in the work.

---

[1] T. D. Lee, Phys. Rev. **95**, 1329 (1954).

[2] Ya. B. Zel'dovich, JETP **33**, 1488 (1957), Soviet Phys. JETP **6**, 1148 (1958).

[3] Ya. B. Zel'dovich, JETP **39**, 776 (1960), Soviet Phys. **12**, 542 (1961).

[4] Ning Hu, Phys. Rev. **74**, 131 (1948).

Translated by E. J. Saletan
194

SOVIET PHYSICS JETP VOLUME 13, NUMBER 4 OCTOBER, 1961

ON THE POLARIZATION OF RECOMBINATION RADIATION

B. A. LYSOV, L. P. BELOVA, and L. I. KOROVINA

Moscow State University

Submitted to JETP editor November 4, 1960

J. Exptl. Theoret. Phys. (U.S.S.R.) 40, 1160-1165 (April, 1961)

The polarization of radiation following the capture of a relativistic electron into the K shell is considered. Partial elliptical polarization is shown to occur in this case. The expression for the intensity of the unpolarized part of the radiation is given. The electron-spin contribution is discussed. The calculations are performed to the lowest order in αZ.

1. The photoelectric effect and its inverse processes have recently, after a long lapse, again begun to attract attention. Special attention has been given to the study of the polarization phenomena which occur in these processes. Polarization phenomena in the photoelectric effect and also in the inverse process of single-photon positron annihilation have first been studied in detail by McVoy.[1] However, the results obtained were found to contradict the formula of Sauter-Sommerfeld, since McVoy, who used Born's method, limited himself to the zero Born approximation.

Recently, in a series of articles by Fano, McVoy, and Albers,[2] the earlier results of McVoy have been corrected.* The authors have abandoned Born's method, although there is no fundamental reason for doing so, and have used the Sauter approximation.

In the present paper, we shall discuss in detail the so-far untreated case of polarization effects in the inverse process of electron capture by an ionized atom. Such a process is determined by the first-order matrix element

$$S^{(1)}_{i\to f} = -\frac{e}{\hbar c} L^{-3/2} \sum_{\varkappa} \sqrt{\frac{2\pi c\hbar}{\varkappa}} \int \psi_f^+ (\boldsymbol{\alpha} \mathbf{a}^+) e^{-i(\varkappa x)} \psi_i d^4x. \quad (1)$$

Henceforth, we shall limit ourselves to the electron capture into the K shell by a nucleus with charge Ze and, assuming that $\alpha Z \ll 1$ (where $\alpha = e^2/\hbar c$), we shall carry out all calculations to the lowest order in αZ.

It is interesting to note that the matrix element (1), as has been shown by Fano, McVoy, and Albers,[2] can, in calculations to the lowest order in αZ, also be used to describe the short-wave bremsstrahlung, where almost all the initial kinetic electron energy is carried away by the radiated photon. In connection with the above, the results referring to the polarization properties of recombination radiation are equally applicable to bremsstrahlung near the upper limit of its spectrum.

2. We shall find the wavefunction of the initial state using Born's method. It has been shown by Gavrila,[3] who considered the relativistic photoeffect from the K shell, that, in order to obtain the correct result, it is necessary to take into account the first-order Born approximation even for the lowest order in αZ. In this approximation, we have

$$\psi_i = \left\{ 1 - \frac{k_0'}{2\pi^2 k_0} \int \frac{[K + \boldsymbol{\alpha}(\mathbf{k} - \boldsymbol{\varkappa}) + \rho_3 k_0] e^{-i\varkappa'\mathbf{r}}}{\varkappa'^2 [k^2 - (\mathbf{k} - \boldsymbol{\varkappa}')^2 + i\eta]} d^3x \right\} \psi, \quad (2)$$

where the wavefunction

$$\psi = L^{-3/2} \sum_{s=\pm 1} C_s b(s) e^{-icKt + i\mathbf{kr}} \quad (3)$$

describes the free electron with energy $\hbar cK$ with momentum $\hbar\mathbf{k}$. $b(s)$ is the spinor amplitude, and the coefficient C_s characterizes the initial electron polarization.[4,5] The real infinitesimal quantity η is chosen as positive so that, for larger r, the function ψ_i represents asymptotically the sum of a plane and of a diverging spherical wave.[6]

In the approximation under consideration, the finite wavefunction of the K state can be written as follows, neglecting the electron binding energy, which is small as compared with its rest energy:

$$\psi_f = \pi^{-1/2} k_0'^{3/2} \left\{ 1 + \tfrac{1}{2} i\alpha Z (\boldsymbol{\alpha}\mathbf{r}/r) \exp(-ick_0 t - k_0' r) \right\}, \quad (4)$$

where $\hbar ck_0$ is the electron rest energy, $k_0' = \alpha Z k_0$, and the row matrix b_0^+ is (1,0,0,0) and (0,-1,0,0) for the K state with magnetic quantum number $j_z = 1/2$ and $j_z = -1/2$ respectively.

From Eqs. (1) to (4) we find the following expression for the differential cross section for electron capture into the K shell of the nucleus with the charge Ze:

$$d\sigma = \frac{32 e^2 k_0'^5 \varkappa K d\Omega}{\hbar ck (\mathbf{k} - \boldsymbol{\varkappa})^8} \sum_{s,s'} R_{s'}^+ R_s, \quad (5)$$

---

*Correct results have also been obtained by Banerjee.[14]

$$R_s = C_s b\,(s)\,\{A\,(\boldsymbol{\varkappa}\mathbf{a}^+) - iB\,(\boldsymbol{\sigma}\,[\mathbf{a}^+\,(\mathbf{k}-\boldsymbol{\varkappa})])$$

$$+ C\,(\mathbf{a}^+\,(\mathbf{k}-\boldsymbol{\varkappa}))\};$$

$$A = 1 - \frac{K\,(\mathbf{k}-\boldsymbol{\varkappa})^2}{2k_0^2\varkappa}, \qquad B = \frac{1}{2k_0}\left(1 - \frac{(\mathbf{k}-\boldsymbol{\varkappa})^2}{2k_0\varkappa}\right),$$

$$C = \frac{1}{2k_0}\left(1 + \frac{(\mathbf{k}-\boldsymbol{\varkappa})^2}{2k_0\varkappa}\right), \tag{6}$$

where $\hbar c\kappa$ and $\hbar\kappa$ are the energy and momentum of the radiated photon. (See also reference 7, where a detailed derivation of an analogous formula for the photoeffect is given.)

3. As is well known,[8,9] the polarization properties of radiation may be described by calculating the intensity of the radiation in two linear W_λ ($\lambda = 2, 3$) and two circular W_l ($l = \pm 1$) polarization states. In calculating W_λ, the quantized photon amplitude should be resolved into two mutually perpendicular components

$$\mathbf{a} = \sum_\lambda g_\lambda \boldsymbol{\beta}_\lambda, \qquad [g_\lambda g^+_{\lambda'}]_- = \delta_{\lambda\lambda'}, \tag{7}$$

where β_2 and β_3 are arbitrary unit vectors satisfying the orthogonality condition

$$\boldsymbol{\beta}_\lambda \boldsymbol{\varkappa} = 0. \tag{8}$$

A different resolution of the photon amplitudes is necessary for the calculation of W_l:

$$\mathbf{a} = \sum_l g_l \boldsymbol{\beta}_l, \qquad [g_l g_{l'}]_- = \delta_{ll'}, \tag{9}$$

where β_l are related to β_λ by the equation

$$\boldsymbol{\beta}_l = 2^{-1/2}(\boldsymbol{\beta}_2 + il\boldsymbol{\beta}_3).$$

It should be noted that, in classical optics, the polarization of a radiation is characterized by the amplitudes of the oscillations of electrical vectors in two mutually perpendicular directions and by the phase difference δ between these vibrations. Both methods of describing the polarization properties of radiation are equivalent, and this equivalence is established by the formula relating the quantities W_λ and W_l with the quantity δ. Such a formula for the case of a totally polarized radiation has been derived by Sokolov and Ternov[8] [see also reference 9, Eq. (28.41)].

In the case where the radiation is only partially polarized, we should use a somewhat more general formula

$$\sin\delta = \tfrac{1}{2}\,(W_{-1} - W_1)\,[(W_2 - W_0/2)\,(W_3 - W_0/2)]^{-1/2} \tag{10}$$

where W_0 is the intensity of the unpolarized component of the radiation. The quantity W_0 may be found from the following considerations. In Eq. (10), only the quantities W_2 and W_3 depend on the actual resolution of the photon amplitude, i.e., on the choice of the vectors β_2 and β_3. We shall now choose these vectors in such a way that the quantities W_2 and W_3 reach their extremum values. In such a case, the polarization ellipse of the polarized component of the radiation will be brought to the main axes and, consequently, for such a choice of β_2 and β_3 we have $|\sin\delta| = 1$.

Taking this into account, we find from Eq. (10)

$$W_0/W = 1 - (P_\lambda^2 + P_l^2)^{1/2}, \tag{11}$$

where P_λ and P_l are the degrees of linear and circular polarization of the radiation respectively:

$$P_\lambda = (W_3 - W_2)/W, \qquad P_l = (W_1 - W_{-1})\,/\,W, \tag{12}$$

and W is the total radiation intensity. Moreover, in view of the above, in order to calculate P_λ the photon amplitude is divided so that P_λ will reach a maximum. It should be noted that an equation analogous to (11) is well known* in classical electrodynamics [see reference 10, Eq. (50.13)]. We shall now directly apply the results given above to the study of the polarization properties of recombination radiation.

4. We consider first the radiation accompanying the K capture of an unpolarized electron by a nucleus with charge Ze. For this case, we should, in Eqs. (5) and (6), set

$$C_1^+ C_1 = C_{-1}^+ C_{-1} = 1/2, \qquad C_1^+ C_{-1} = C_{-1}^+ C_1 = 0. \tag{13}$$

We furthermore choose the vector β_2 as perpendicular to the plane of the vectors $\mathbf{k}$ and $\boldsymbol{\kappa}$, and place the vector β_3 in this plane. It can easily be seen that such a resolution of the photon amplitude results in the extremum of W_λ. Omitting the rather trivial calculations, we present the final expressions for the degree of polarization

$$P_l = 0,$$

$$P_\lambda = [2 - \gamma\,(\gamma + 1)\,(1 - \beta\cos\theta)]\,/\,[2 + \gamma\,(\gamma^2 - 1)$$

$$\times (1 - \beta\cos\theta)]. \tag{14}$$

where $\gamma = \kappa/k_0$, $\beta = k/K$, and θ is the angle between the vectors $\mathbf{k}$ and $\boldsymbol{\kappa}$.

Thus, the recombination of the unpolarized electron is, according to Eqs. (11)–(13), accompanied by radiation which is partially linearly polarized. In the nonrelativistic limit, where $\gamma \ll 1$, the polarization of the radiation becomes total. In the ultrarelativistic case, the radiation is fully depolarized ($W_0 = W$). The variation of the degree of linear polarization with the photon energy for

---

*The relation between Eq. (11) and Eq. (50.13) of reference 10 can be established directly by taking into account that $|J_{yz}| = 1/2\,|W_1 - W_{-1}|$ if, for the direction of x, y, we take the direction of the principal axes of the polarization ellipse.

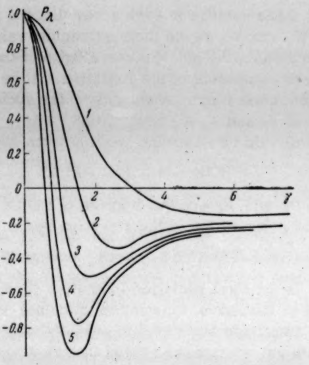

FIG. 1. Variations of the degree of linear polarization with energy. Curves 1–5 correspond to angles $\theta = 30, 60, 90, 120$, and 150° respectively.

the intermediate cases is shown in Fig. 1 for certain values of the angle θ.

5. We shall now study the capture of longitudinally polarized electrons. In such a case, $C_1 = 1$ and $C_{-1} = 0$, or $C_1 = 0$ and $C_{-1} = 1$. Choosing the vectors β_λ as in the previous case, we find that P_λ, as before, is given by Eq. (14), and the degree of circular polarization is equal to

$$P_l = \frac{s\gamma}{\sqrt{\gamma(\gamma+2)}}\,\frac{2+\gamma(\gamma+1)(\gamma^2-2)(1-\beta\cos\theta)}{2+\gamma(\gamma^2-1)(1-\beta\cos\theta)}, \qquad (15)$$

where $s = \pm 1$ for the electron polarized along the direction of motion or along the opposite direction respectively. Equation (15), with an accuracy limited by the substitution $s \rightarrow l$ (where l characterizes the circular photon polarization), coincides with the formula for the longitudinal polarization of electrons in the photoeffect from the K shell. The corresponding curves are given in reference 11.[*] In a nonrelativistic approximation ($\gamma \ll 1$), P_l vanishes, so that the radiation is, as before, fully linearly polarized in the plane of the vectors **k** and κ. In the case of high energies, the radiation becomes fully circularly polarized, and its helicity coincides with that of the incident electron. In the intermediate cases, $P_\lambda^2 + P_l^2 \neq 1$, and, according to Eq. (11), the recombination radiation is partially elliptically polarized.

The variation of the unpolarized-component intensity of the radiation with photon energy is shown in Fig. 2. As can be seen from the figure, the depolarization is greatest in the energy range $\gamma \sim 1$.

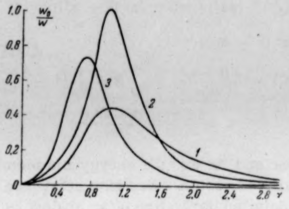

FIG. 2. Variation on the intensity of the unpolarized component of the radiation with energy. Curves 1–3 correspond to angles $\theta = 60, 90$, and 120° respectively.

Since the condition that P_λ be maximum is the same for any γ and θ, the orientation of the polarization ellipse is independent of γ and θ. (One of its axes always lies in the plane of the vectors **k** and κ).

6. We consider finally the case of transverse polarization of the incident electron. Without loss of generality, we can assume that the electron initially moves along the z axis. Furthermore, let the spin vector make an angle φ with the **k**, κ plane. In this case, the coefficient C_s should be chosen in the following manner:[12]

$$C_1 = 1/\sqrt{2}, \qquad C_{-1} = e^{i\varphi}/\sqrt{2}. \qquad (16)$$

In the calculation, we have to use the formula

$$b^+(s)\,\alpha'_\nu b_0 b_0^+ \alpha_\mu b\,(-s) = \tfrac{1}{8}\,\mathrm{Sp}\,\alpha'_\nu(1+\rho_3)\,\alpha_\mu(1+\rho_1 sk/K + \rho_3 k_0/K)(1+s\sigma_3)\,\rho_1\sigma_3, \qquad (17)$$

where α'_ν and α_μ are any of the sixteen Dirac matrices.[9,13]

Omitting the calculations, the final result is

$$P_l = 2\gamma\,[2+\gamma(\gamma^2-1)(1-\beta\cos\theta)]^{-1}\sin\theta\cos\varphi. \qquad (18)$$

P_λ is again given by Eq. (14). It follows from Eqs. (11), (14), and (18) that, for $\gamma \ll 1$ and for $\gamma \gg 1$, the polarization is the same as for the case of an unpolarized electron. For intermediate energies, we have partial elliptical polarization, the degree of which considerably depends on the angle φ.

7. The above discussion of the polarization properties of the radiation accompanying the electron capture into the K shell of a nucleus with charge Ze shows that, for the case of low energies, the radiation is fully linearly polarized in the plane of the vectors **k** and κ, irrespective of the initial polarization of the electron. With increasing energy, the linear polarization becomes elliptical on one hand, and, on the other, an unpolarized component appears, whose magnitude depends considerably on the initial polarization of the electron.

---

[*] It should be kept in mind that the final formula (35) for the degree of the longitudinal polarization given by Fano et al.[11] contains an error; the graphs are correct.

In conclusion, it is necessary to note that the results obtained are in need of a further increase of accuracy for angles θ close to zero. This is due to the fact that the quantities W_λ and W_l calculated by us to the lowest order in αZ contain a factor $\sin^2\theta$. Consequently, if by taking higher powers of αZ into account we obtain a cross section for the recombination process that does not vanish for $\theta = 0$, then this will considerably change the picture of the polarization properties of radiation for $\theta \sim 0$. Until now, this problem has not been solved. Thus, Gavrila,[3] who calculated the cross section for the photoeffect taking the second Born approximation into account, found that, for $\theta = 0$, the cross section does not vanish. On the other hand, Banerjee,[14] using the Sommerfeld approximation, found that it does vanish. Only recently, it has been possible to carry out an exact integration in the matrix element for the relativistic photoeffect from the K shell for $\theta = 0$.[15] A nonvanishing expression was obtained for the cross section.

The authors would like to thank Prof. A. A. Sokolov for his constant interest in the present work, and for his helpful advice.

---

[1] K. W. McVoy, Phys. Rev. **108**, 365 (1957).

[2] Fano, McVoy, and Albers, Phys. Rev. **116**, 1147 (1959); Fano, McVoy, and Albers, Phys. Rev. **116**, 1159 (1959); U. Fano, Phys. Rev. **116**, 1156 (1959); Fano, McVoy, and Kirk, Phys. Rev. **116**, 1168 (1959).

[3] M. Gavrila, Phys. Rev. **113**, 514 (1959).

[4] Sokolov, Ternov, and Loskutov, JETP **36**, 930 (1959), Soviet Phys. JETP **9**, 657 (1959).

[5] A. A. Sokolov and M. M. Kolesnikova, JETP **38**, 165 (1960), Soviet Phys. JETP **11**, 120 (1960).

[6] A. I. Akhiezer and V. B. Berestetskii Квантовая электродинамика (Quantum Electrodynamics) 2d ed., Fizmatgiz, 1959, Sec. 29.

[7] B. A. Lysov, Известия высших учебных заведений (News of Colleges, Physics) 1960, in press.

[8] A. A. Sokolov and I. M. Ternov, JETP **31**, 473 (1956), Soviet Phys. JETP **4**, 396 (1957).

[9] A. A. Sokolov, Введение в квантовую электродинамику (Introduction to Quantum Electrodynamics), Fizmatgiz, 1958, Sec. 28.

[10] L. D. Landau and E. M. Lifshitz, Теория поля (Field Theory), 2d ed., Fizmatgiz, 1960, Sec. 50.

[11] Fano, McVoy, and Albers, Phys. Rev. **116**, 1147 (1959).

[12] A. A. Sokolov and M. M. Kolesnikova, JETP **38**, 1778 (1960), Soviet Phys. JETP **11**, 1281 (1960).

[13] B. A. Lysov, JETP **37**, 571 (1959), Soviet Phys. JETP **10**, 404 (1960).

[14] H. Banerjee, Nuovo cimento **10**, Suppl., 863 (1958); **11**, 220 (1959).

[15] K. Mork and H. Olsen, Proc. Phys. Sem. in Trondheim, 5, 1960 (preprint).

Translated by H. Kasha
195

SOVIET PHYSICS JETP VOLUME 13, NUMBER 4 OCTOBER, 1961

CONTRIBUTION TO THE THEORY OF LOCALIZED PERTURBATIONS IN LARGE SYSTEMS

V. I. OSHEROV

The L. Ya. Karpov Physico-Chemical Institute

Submitted to JETP editor November 5, 1960

J. Exptl. Theoret. Phys. (U.S.S.R.) 40, 1166-1171 (April, 1961)

We evaluate the energy shift for the ground state of a large Fermi system when a localized perturbation is switched on, taking the interaction between the particles in the system into account. The energy levels of the localized states are then broadened into bands. We establish a condition for the applicability of single-particle approximations to the description of states of this kind.

THE theory of localized perturbations in large Fermi systems (in particular, the theory of defects in crystal lattices) has up to the present time been constructed in the framework of the independent-particle model. It is known, all the same, that the approximation involved in this model is insufficient for a number of problems. Recent progress in the physics of many-particle systems (see, for instance, reference 1 which lists an extensive bibliography) enables us now to approach anew also the problem of localized perturbations, using field-theory methods.

1. THE EVALUATION OF THE SHIFT IN THE GROUND STATE ENERGY

We consider here the problem of the shift in the ground state energy of a large system of interacting fermions when a localized perturbation is adiabatically switched on.

We can write the Hamiltonian of the system in the second quantization representation in the form

$$H = H_0 + \lambda\hat{V}, \tag{1.1}$$

$$\hat{V} = \int d\mathbf{x} V(\mathbf{x})\, \psi^+(\mathbf{x})\, \psi(\mathbf{x}); \tag{1.2}$$

H_0 contains the interaction between the fermions, and λ is the parameter which switches on the perturbation. The operators $\psi^+(\mathbf{x})$ and $\psi(\mathbf{x})$ satisfy the well-known commutation relations

$$[\psi(\mathbf{x}), \psi^+(\mathbf{x}')] = \delta(\mathbf{x} - \mathbf{x}'),$$

$$[\psi(\mathbf{x}), \psi(\mathbf{x}')] = [\psi^+(\mathbf{x}), \psi^+(\mathbf{x}')] = 0. \tag{1.3}$$

The energy of the perturbed ground state of the system can be written in the form

$$E = \langle\Psi| H_0 + \lambda\hat{V} |\Psi\rangle, \tag{1.4}$$

where Ψ is the actual state-vector of the system, or

$$E = \langle\Psi| H_0 |\Psi\rangle - i\lambda \int d\mathbf{x} V(\mathbf{x}) \lim_{\mathbf{x}'\to\mathbf{x};\, t'\to t+0} G_\lambda(\mathbf{x}, t; \mathbf{x}', t'). \tag{1.5}$$

We have introduced here a single-particle Green's function by the relation (reference 1 gives a bibliography on Green's functions)

$$G_\lambda(x, x') = i\langle\Psi(\lambda)| T(\psi(x)\psi^+(x')) |\Psi(\lambda)\rangle; \tag{1.6}$$

x, x′ are points in four-space and T indicates Wick's chronologically ordered product.

We use the obvious consequence of the fact that the ground state energy of the system is stationary with respect to a variation of the state vectors:

$$dE/d\lambda = \langle\Psi(\lambda)| \hat{V} |\Psi(\lambda)\rangle. \tag{1.7}$$

The expression ΔE in which we are interested can then be written as follows:

$$\Delta E = -i \int_0^\lambda d\lambda \int d\mathbf{x} V(\mathbf{x}) \lim_{t'\to t+0} G_\lambda(\mathbf{x}, t; \mathbf{x}, t'). \tag{1.8}$$

If we write the Green's function $G_\lambda(\mathbf{x}, t; \mathbf{x}, t')$ as a Fourier integral in the energy ϵ, we get

$$\Delta E = \frac{1}{2\pi i}\int_0^\lambda d\lambda \int d\mathbf{x} \lim_{t'\to t+0} \int_C d\varepsilon e^{i\varepsilon(t'-t)} V(\mathbf{x})\, G_\lambda(\mathbf{x}, \mathbf{x}; \varepsilon). \tag{1.9}$$

The choice of the contour C in this equation is connected with some general analytical properties of G_λ. The function G_λ is defined by the following formal operator relation[2]

$$G_\lambda = G\frac{1}{1 - \lambda VG}, \tag{1.10}$$

where G is the complete unperturbed fermion Green's function. Its Fourier transform can be written in the form

$$G(\mathbf{k}, \varepsilon) = [\varepsilon - \varepsilon(\mathbf{k}) - M(\mathbf{k}, \varepsilon)]^{-1}. \tag{1.11}$$

Here $M(\mathbf{k}, \epsilon)$ is the irreducible operator of the fermion self-energy. $M(\mathbf{k}, \epsilon)$ has a cut on the real axis for $-\infty < \epsilon < \epsilon_F$ and $\epsilon_F < \epsilon < \infty$. The branch point ϵ_F is the Fermi energy which is perturbed by the interaction.

The function G_λ has still poles corresponding to localized states with energies $\epsilon < 0$ which satisfy the equation

$$1 - \lambda V G(\varepsilon) = 0. \tag{1.12}$$

One sees easily that these poles lie indeed on the analytical continuation of G_λ in the upper half-plane of complex ϵ. It will, however, become clear in the following that they can be replaced in the discussion by some singular points on the real axis. The integration contour in (1.9) goes thus slightly below the real axis for $-\infty < \epsilon < \epsilon_F$ and slightly above it for $\epsilon_F < \epsilon < \infty$.

The exponential factor in (1.9) makes it possible to apply the residue theorem only in the upper half-plane and can formally be omitted. We have thus

$$\Delta E = \frac{1}{2\pi i}\int^{\lambda} d\lambda \int d\mathbf{x} \int_C d\varepsilon V(\mathbf{x})\, G(\mathbf{x}, \mathbf{x}'; \varepsilon) \frac{1}{1 - \lambda V(\mathbf{x}')\, G(\mathbf{x}', \mathbf{x}; \varepsilon)}. \tag{1.13}$$

Integrating over λ we have

$$\Delta E = -\frac{1}{2\pi i}\int_C d\varepsilon \operatorname{Sp} \ln (1 - \lambda V G(\varepsilon)). \tag{1.14}$$

This last equation can be written in the form[2]

$$\Delta E = -\frac{1}{2\pi i}\int_C d\varepsilon \ln \det (1 - \lambda V G(\varepsilon)). \tag{1.15}$$

We consider now the imaginary part of the integrand in (1.15). Under quite general assumptions[2] about the character of the perturbation we have

$$\operatorname{Im} \ln \det (1 - \lambda V G(\varepsilon)) = \operatorname{arc\,tg} \frac{-\lambda V \operatorname{Im} G(\varepsilon)}{1 - \lambda V \operatorname{Re} G(\varepsilon)}. \tag{1.16}^*$$

Here

$$\operatorname{Im} G(\mathbf{x}, \varepsilon) = (2\pi)^{-3}\int d\mathbf{k} e^{i\mathbf{k}\mathbf{x}} \frac{-\operatorname{Im} M(\mathbf{k}, \varepsilon)}{(\varepsilon - \varepsilon(\mathbf{k}) - \operatorname{Re} M(\mathbf{k}, \varepsilon))^2 + (\operatorname{Im} M(\mathbf{k}, \varepsilon))^2}$$
$$\times [\eta(\mathbf{k} - \mathbf{k}_F) - \eta(\mathbf{k}_F - \mathbf{k})], \tag{1.17a}$$

$$\operatorname{Re} G(\mathbf{x}, \varepsilon) = (2\pi)^{-3}\int d\mathbf{k} e^{i\mathbf{k}\mathbf{x}} \frac{\varepsilon - \varepsilon(\mathbf{k}) - \operatorname{Re} M(\mathbf{k}, \varepsilon)}{(\varepsilon - \varepsilon(\mathbf{k}) - \operatorname{Re} M(\mathbf{k}, \varepsilon))^2 + (\operatorname{Im} M(\mathbf{k}, \varepsilon))^2}. \tag{1.17b}$$

We shall see in the following that when $\epsilon < 0$, $\operatorname{Im} G(\epsilon)$ is small and decreases rather fast with increasing $|\epsilon|$. Neglecting therefore $(\operatorname{Im} G(\epsilon))'$ in comparison with $\operatorname{Im} G(\epsilon)$ we find

$$\frac{d}{d\varepsilon} \arg \det (1 - \lambda V G(\varepsilon)) = -\frac{\lambda V \operatorname{Im} G(\varepsilon)\,(d/d\varepsilon)\,[\lambda V \operatorname{Re} G(\varepsilon)]}{(1 - \lambda V \operatorname{Re} G(\varepsilon))^2 + (\lambda V \operatorname{Im} G(\varepsilon))^2} \equiv f(\varepsilon). \tag{1.18}$$

We go now over to the limit $\operatorname{Im} G(\epsilon) \to 0$:

$$\lim_{\operatorname{Im} G(\varepsilon)\to 0} \frac{d}{d\varepsilon} \arg \det (1 - \lambda V G(\varepsilon)) = \pi \sum_i \delta(\varepsilon - \varepsilon'_{0i}). \tag{1.19}$$

In this equation ϵ'_{0i} are the energies of the "physical" localized states which are determined from the equation

$$1 - \lambda V \operatorname{Re} G(\varepsilon'_{0i}) = 0 \qquad (\varepsilon'_{0i} < 0). \tag{1.20}$$

We have thus

$$\int_{-\infty}^{0} \lim_{\operatorname{Im} G(\varepsilon)\to 0} \frac{d}{d\varepsilon} \arg \det (1 - \lambda V G(\varepsilon))\, d\varepsilon = \nu\pi, \tag{1.21}$$

where ν is the total number of localized states.

In the case where $\operatorname{Im} G(\epsilon) \neq 0$, ν can be written in the form

$$\nu = \frac{1}{\pi}\int_{-\infty}^{0} f(\varepsilon)\, d\varepsilon. \tag{1.22}$$

In our discussion there enters thus naturally the energy distribution function $f(\epsilon)$ of the localized states which is given by (1.18). This function has a steep maximum near each of the roots of (1.20).

We turn now to the evaluation of ΔE and we take into account that we can assume $\ln \det (1 - \lambda V G(\epsilon))$ to be a regular function on its Riemann surface in the upper half-plane and it can then under well-known limitations imposed upon V (see references 2 and 3) on the real axis be expressed in terms of its imaginary part, as follows[3]

$$\ln \det (1 - \lambda V G(\varepsilon)) = \frac{1}{\pi}\int_{-\infty}^{\infty} \frac{\arg \det (1 - \lambda V G(\varepsilon'))}{\varepsilon - \varepsilon'}\, d\varepsilon'. \tag{1.23}$$

After taking residues in the expression for ΔE we integrate the contribution from the "discrete" states by parts which leads to

$$\Delta E = \frac{1}{\pi}\int_{-\infty}^{0} \varepsilon f(\varepsilon)\, d\varepsilon - \frac{1}{\pi}\int_{0}^{\varepsilon_F} \arg \det (1 - \lambda V G(\varepsilon))\, d\varepsilon. \tag{1.24}$$

This reminds us of the relation derived by I. M. Lifshitz,[4] but there is an essential difference in the first term which is connected with the localized states and this compels us to revise the concept itself of states of this kind. These are not ordinary discrete states but are wave packets where states with arbitrary ϵ from the interval $-\infty < \epsilon < 0$ are present with weights proportional to $f(\epsilon)$. Each ("physical") discrete level is broadened into a band. Different states in the band are occupied with a probability proportional to $f(\epsilon)$. One sees easily that the effective width of this band is given by the imaginary part of the root of Eq. (1.12) when it is analytically continued in the upper ϵ-half-plane.

---

*arctg = $\tan^{-1}$

2. THE WIDTH OF THE LEVELS OF THE LOCALIZED STATES

The analytical continuation mentioned a moment ago is easily obtained if we consider $G_+(\epsilon)$ and $G_-(\epsilon)$. The function $G_+(\epsilon)$ corresponds to $G(\epsilon)$ of section 1 while the integration contour for $G_-(\epsilon)$ is above the real axis for $e < e_F$ and below it for $\epsilon > \epsilon_F$. Because the Hamiltonian is Hermitian we have on the real axis $G_+(\epsilon) = \overline{G}_-(\epsilon)$.

We now expand $G_+(\epsilon)$ around $\epsilon'_{0i} - i\delta(\delta > 0)$. We get for the imaginary part of the root of (1.12)

$$\frac{1}{2}\Gamma(\varepsilon_0) = V \operatorname{Im} G(\varepsilon_0) \Big/ \left[\frac{d}{d\varepsilon} V \operatorname{Re} G(\varepsilon)\right]_{\varepsilon=\epsilon_0} \qquad (2.1)$$

For the sake of simplicity we write in the following ϵ_0 instead of ϵ'_{0i} and $G(\epsilon_0)$ instead of $G_+(\epsilon_0)$.

We now bear in mind that for $\epsilon < 0$ we have $\operatorname{Im} G_0(\epsilon) = 0$ and thus

$$\operatorname{Im} G(\varepsilon) = \operatorname{Re} G_0(\varepsilon) \operatorname{Im} \frac{1}{1 - MG_0(\varepsilon)}, \qquad (2.2)$$

where $G_0(\epsilon)$ is the Green's function when there are no interactions.

When we take into account that $\operatorname{Re} G_0(\epsilon)$ decreases when $|\epsilon|$ increases we can find for sufficiently large $|\epsilon_0|$

$$\Gamma(\varepsilon_0) = 2V \operatorname{Re} G_0(\varepsilon_0) \operatorname{Im} M \operatorname{Re} G_0(\varepsilon_0) \Big/ \left[\frac{d}{d\varepsilon} V \operatorname{Re} G_0(\varepsilon)\right]_{\varepsilon=\epsilon_0} \qquad (2.3)$$

This equation can be rewritten as follows (if we use the explicit form of $G_0(\epsilon)$ and assume that V does not introduce any analytical complications)

$$\Gamma(\varepsilon_0) = 2V \operatorname{Re} G_0(\varepsilon_0) \operatorname{Im} M \operatorname{Re} G_0(\varepsilon_0) / V (\operatorname{Re} G_0(\varepsilon_0))^2. \qquad (2.4)$$

We shall now consider the important case of a model with a δ-function perturbation when V = constant in the k-representation. In that case

$$\Gamma(\varepsilon_0) = 2\int \operatorname{Im} M(\mathbf{k}, \varepsilon_0) \times (\operatorname{Re} G_0(\mathbf{k}, \varepsilon_0))^2 d\mathbf{k} \Big/ \int (\operatorname{Re} G_0(\mathbf{k}, \varepsilon_0))^2 d\mathbf{k} \qquad (2.5)$$

and Γ depends thus on the perturbation only through ϵ_0.

For our further considerations we need to know the asymptotic behavior of $\operatorname{Im} M(k, \epsilon_0)$ for large negative ϵ_0. To get this we write down an explicit expression in the simplest approximation[5]

$$\operatorname{Im} M(\mathbf{k}, \varepsilon_0) = -\frac{\xi}{4\pi} \int \frac{d\mathbf{q}}{q^2} \frac{\operatorname{Im} P(\mathbf{q}, \Delta\varepsilon)}{|1 - P(\mathbf{q}, \Delta\varepsilon)|^2} \eta(|\mathbf{k} - \mathbf{q}| - 1), \qquad (2.6)$$

where

$$\Delta\varepsilon = \varepsilon(\mathbf{k} - \mathbf{q}) - \varepsilon_0, \qquad (2.7)$$

$P(\mathbf{q}, \Delta\epsilon)$ is the polarization operator and $\xi = e^2 k_F / \pi e_F$. In our case $\Delta\epsilon$ is large and as $P(\mathbf{q}, \Delta\epsilon)$ is then small we have

$$\operatorname{Im} M(\mathbf{k}, \varepsilon_0) = -\frac{\xi}{4\pi} \int \frac{d\mathbf{q}}{q^2} \operatorname{Im} P(\mathbf{q}, \Delta\varepsilon)\, \eta(|\mathbf{k} - \mathbf{q}| - 1). \qquad (2.8)$$

We restrict ourselves to the lowest order polarization operator $P_0(\mathbf{q}, \Delta\epsilon)$. The quantity $P_0(\mathbf{q}, \Delta\epsilon)$ is for sufficiently large $\Delta\epsilon$ different from zero only in the interval

$$-1 + \sqrt{1 + \Delta\varepsilon/\varepsilon_F} \leqslant q/q_F \leqslant 1 + \sqrt{1 + \Delta\varepsilon/\varepsilon_F} \qquad (2.9)$$

and can be written in dimensionless units ($y = \Delta\epsilon/\epsilon_F$, $x = q/q_F$) as follows[6]

$$\operatorname{Im} P_0(x, y) = -\frac{\pi\xi}{2x^3}\left[1 - \frac{1}{4}\left(\frac{y}{x} - x\right)^2\right]. \qquad (2.10)$$

This enables us to evaluate the average value of the integral in (2.8) by putting

$$\Delta x = 2, \qquad x = \sqrt{y}. \qquad (2.11)$$

We note now that by virtue of (2.7)

$$y = x^2 + \Delta - \mathbf{kq}/\varepsilon_F, \qquad \Delta = [\varepsilon(\mathbf{k}) - \varepsilon_0]/\varepsilon_F. \qquad (2.12)$$

The main contribution to (2.8) is thus provided by those values of q which satisfy the relation

$$\mathbf{kq}/\varepsilon_F = \Delta. \qquad (2.13)$$

This gives

$$\operatorname{Im} P_0(x, y) = -\frac{\pi\xi}{2x^3}. \qquad (2.14)$$

In this equation x is determined from (2.13).

The remaining integration over the angle (from 0 to $\pi/2$, as $\Delta > 0$) is trivial. If $|\epsilon_0| > e_F$ we get

$$\operatorname{Im} M(k, \varepsilon_0) = 4\pi\varepsilon_F \xi^2 (k/k^F)^3 \Delta^{-3}. \qquad (2.15)$$

We can now find $\Gamma(\epsilon_0)$ from (2.5):

$$\Gamma(\varepsilon_0) = \frac{\sqrt{2}}{3} \varepsilon_F \xi^2 \left(\frac{|\varepsilon_0|}{\varepsilon_F}\right)^{-3/2} \qquad (2.16)$$

The single-particle approximation gives only a real contribution to $M(k, \epsilon_0)$. It is thus possible for us to establish some criterion for the applicability of the independent particle model to a description of localized states. This can be written in the form

$$\xi^2 \left(\frac{|\varepsilon_0|}{\varepsilon_F}\right)^{-3/2} \ll 1. \qquad (2.17)$$

It follows from general considerations that contributions in higher order perturbation theory to $\Gamma(\epsilon_0)$ decrease faster than the term (2.16) and this determines how effective the criterion (2.17) will be. Condition (2.17) is for the case of lattice defects rather well satisfied and this justifies to a certain extent the application of single-electron theories to describe defects.

It is necessary to note in conclusion that we have practically made no use of perturbation theory as far as V is concerned. Such a theory must be constructed rather carefully to avoid divergences which are possible when localized states are formed. Schwinger[2,3] has considered a similar problem.

---

[1] The collection: Вопросы квантовой теории многих тел (Problems in the Quantum Theory of Many-Body Systems) IIL, 1959.

[2] J. Schwinger, Phys. Rev. 93, 615 (1954).

[3] J. Schwinger, Phys. Rev. 94, 1362 (1954).

[4] I. M. Lifshitz, Usp. Mat. Nauk 7, 171 (1952).

[5] D. F. Dubois, Doctoral Thesis, California Institute of Technology, 1959.

[6] J. Hubbard, Proc. Roy. Soc. (London) A243, 336 (1958).

Translated by D. ter Haar
196

SOVIET PHYSICS JETP VOLUME 13, NUMBER 4 OCTOBER, 1961

EQUATIONS FOR THE SPECTRAL FUNCTIONS OF CHARGED PIONS

Yu. A. SIMONOV and K. A. TER-MARTIROSYAN

Institute for Experimental and Theoretical Physics, Academy of Sciences, U.S.S.R.

Submitted to JETP editor November 5, 1960; resubmitted December 23, 1960

J. Exptl. Theoret. Phys. (U.S.S.R.) 40, 1172-1178 (April, 1960)

The amplitudes for the scattering of charged pions by charged pions are expressed by means of the Mandelstam representation in terms of the spectral functions. A set of equations is derived for the one-dimensional and two-dimensional spectral functions. One of the methods for obtaining an approximate solution is discussed.

1. INTRODUCTION

ONE of the authors (Ter-Martirosyan) has recently proposed a method for constructing a symmetric system of equations for the spectral functions for the two-particle transition amplitude. The method was based on Mandelstam's equations[1] for the two-dimensional spectral functions. The equations were given both in general form,[2] and for a number of simple cases[3] involving the interactions of neutral particles. The resultant system of equations involves only experimentally observable quantities (i.e., in the language of old theory, renormalized quantities) and the parameters that appear are the particle masses and the usual coupling constants (for example the constant g for the meson-nucleon interaction, the constant λ for the pion-pion interaction). The theory requires no other parameters and, furthermore, no divergences appear in this formulation.

When the two-particle transition amplitude (in all three channels) is expanded in Legendre polynomials the system of equations for the spectral functions is transformed into an infinite system of coupled equations[4] for partial amplitudes, of the same type as those considered by Chew and Mandelstam[5] and Cini and Fubini.[6] However, when this is done divergences appear (as noted by Efremov et al.[7]), whose degree increases with increasing number of partial waves taken into account in the equations. These divergences are a simple consequence of an illegitimate use of the Legendre expansion in a region (substantial in the equations) in which it fails to converge. In the original equations for the two-dimensional spectral functions these divergences do not appear. Therefore in the solution of our equations one should make use of some method other than the expansion in Legendre polynomials, for example the method of partial iteration of the equations for the spectral functions $A_{ij}(s)$ described previously,[2,3] provided of course that convergent results are obtained.

In this note we obtain equations for the one- and two-dimensional spectral functions for the interaction of charged pions with each other. We use throughout the same notation as was introduced previously (see Mandelstam[1] and Ter-Martirosyan[2]).

2. DERIVATION OF THE EQUATIONS

The amplitude describing the interaction of charged pions may be expressed as follows

$$A_{\alpha\beta\gamma\delta}(s_1, s_2, s_3) = \lambda(s_1, s_2; s_3)\delta_{\alpha\gamma}\delta_{\beta\delta} + \lambda(s_3, s_2; s_1)\delta_{\alpha\beta}\delta_{\gamma\delta} + \lambda(s_1, s_3; s_2)\delta_{\alpha\delta}\delta_{\beta\gamma}, \qquad (1)$$

where $\lambda(s_1, s_2; s_3) = \lambda(s_2, s_1; s_3)$ is a function of the invariants

$$s_1 = (p_1 + p_2)^2, \quad s_2 = (p_1 + p_4)^2,$$
$$s_3 = (p_1 + p_3)^2, \quad s_1 + s_2 + s_3 = 4\mu^2,$$

and $(p_1\alpha)$, $(p_2\beta)$, $(p_3\gamma)$ and $(p_4\delta)$ are the momenta and isospin indices of the four pions. (Fig. 1).

The Mandelstam representation for the function λ, when written with one subtraction, has the form [see Eq. (4) of Ter-Martirosyan[3]]

$$\lambda(s_1, s_2; s_3) = \lambda_0 + \frac{1}{\pi}\int_0^\infty \{\alpha(\sigma)[\varphi(\sigma, s_1) + \varphi(\sigma, s_2)] + \beta(\sigma)\varphi(\sigma, s_3)\}\,d\sigma + \frac{1}{\pi^2}\iint_0^\infty \{\rho_c(\sigma, \sigma')\varphi(\sigma, s_1)\varphi(\sigma', s_2) + \rho(\sigma, \sigma')[\varphi(\sigma', s_1) + \varphi(\sigma', s_2)]\,\varphi(\sigma, s_3)\}\,d\sigma\,d\sigma', \qquad (2)$$

where

$$\varphi(\sigma, s) = \frac{1}{\sigma - s} - \frac{1}{\sigma - s_0}, \quad s_0 = \frac{4\mu^2}{3}, \quad \lambda_0 = \lambda(s_0, s_0, s_0),$$
$$\rho_c(\sigma, \sigma') = \rho_c(\sigma', \sigma).$$

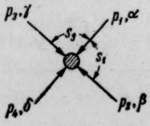

FIG. 1

The equations for the spectral functions $\alpha(\sigma)$, $\beta(\sigma)$ and ρ_C, ρ follow (see Ter-Martirosyan[2]) directly from Eq. (2) and the unitarity conditions, when the latter are written out for the invariant function λ. This can be done by, for example, making use of the relation determining the $\pi\pi$ scattering amplitude $\alpha^{(I)}$ in states with prescribed isospin I.

For transitions in the first channel we have

$$\begin{aligned} \alpha^{(0)} &= 3\lambda(s_3, s_2; s_1) + \lambda(s_1, s_2; s_3) + \lambda(s_1, s_3; s_2), \\ \alpha^{(1)} &= \lambda(s_1, s_2; s_3) - \lambda(s_1, s_3; s_2), \\ \alpha^{(2)} &= \lambda(s_1, s_2; s_3) + \lambda(s_1, s_3; s_2). \end{aligned} \tag{3}$$

From the three unitarity conditions for the amplitudes $\alpha^{(I)}$ it is easy to obtain two relations for the absorptive parts λ_1 and λ_3 of the amplitude λ in the first and third channel:

$$\begin{aligned} \lambda_1(s_1, s_2; s_3) &= \sqrt{\frac{s_1 - 4\mu^2}{s_1}} \int \{\lambda^*(s_1, s_2'; s_3')\, \lambda(s_1, s_2''; s_3'') \\ &\quad + \lambda^*(s_1, s_3'; s_2')\, \lambda(s_1, s_3''; s_2'')\} \frac{dn}{4\pi} + \Delta_1(s_1, s_2; s_3), \\ \lambda_3(s_3, s_2; s_1) &= \sqrt{\frac{s_1 - 4\mu^2}{s_1}} \int \{3\lambda^*(s_3', s_2'; s_1)\, \lambda(s_3'', s_2''; s_1) \\ &\quad + \lambda^*(s_3', s_2'; s_1)\, [\lambda(s_1, s_2''; s_3'') + \lambda(s_1, s_3''; s_2'')] \\ &\quad + \lambda(s_3'', s_2''; s_1)\, [\lambda^*(s_1, s_2'; s_3') + \lambda^*(s_1, s_3'; s_2')]\} \\ &\quad + \Delta_3(s_3, s_2; s_1). \end{aligned} \tag{4}$$

Here Δ_1 and Δ_3 refer to the contributions from states containing more than two mesons (i.e. from four-, six-, etc., meson states). The Δ_i are symmetric functions of their first two arguments, i.e. $\Delta_i(s_1, s_2; s_3) = \Delta_i(s_2, s_1; s_3)$. We use the normalization of Chew and Mandelstam,[5] so that $d\sigma/d\Omega = |4s_1^{-1/2}\lambda|^2$.

As far as its symmetry properties are concerned the amplitude λ is of precisely the type for which equations for the spectral functions were formulated by Ter-Martirosyan,[3] Sec. 2. We may therefore make direct use of those results.[3] At the same time we give, for convenience of the reader, a different derivation of these equations in Appendix 1, making use of the unitarity conditions and spectral representations directly for the functions $\alpha^{(I)}(s_1, s_2; s_3)$.

In this way one obtains from Eq. (2) of this work and Eqs. (10) and (11) of Ter-Martirosyan[3] the result

$$\begin{aligned} \rho(s', s) &= Q_1(s', s) + Q_3(s, s'), \\ \rho_c(s, s') &= Q_2(s, s') + Q_2(s', s), \end{aligned} \tag{5}$$

where

$$\begin{aligned} Q_1(s', s) &= \frac{2}{\pi^2} \iint \Gamma(\sigma', \sigma''; s', s)\, \{\lambda_2^*(\sigma')\, \lambda_2(\sigma'') \\ &\quad + \lambda_3^*(\sigma')\, \lambda_3(\sigma'')\}\, d\sigma'\, d\sigma'', \\ Q_2(s', s) &= \frac{2}{\pi^2} \iint \Gamma(\sigma', \sigma''; s', s)\, \{\lambda_2^*(\sigma')\, \lambda_3(\sigma'') \\ &\quad + \lambda_3^*(\sigma')\, \lambda_2(\sigma'')\}\, d\sigma'\, d\sigma'', \\ Q_3(s', s) &= \frac{2}{\pi^2} \iint \Gamma(\sigma', \sigma''; s', s)\, \{3\lambda_1^*(\sigma')\, \lambda_1(\sigma'') \\ &\quad + 2\operatorname{Re} \lambda_1^*(\sigma')\, [\lambda_2(\sigma'') + \lambda_3(\sigma'')]\}\, d\sigma'\, d\sigma''. \end{aligned} \tag{6}$$

The arguments of the absorptive parts have the following values

$$\begin{aligned} \lambda_1(\sigma) &= \lambda_1(\sigma, 4\mu^2 - s - \sigma; s), \\ \lambda_2(\sigma) &= \lambda_2(s, \sigma; 4\mu^2 - s - \sigma), \\ \lambda_3(\sigma) &= \lambda_3(s, 4\mu^2 - s - \sigma; \sigma), \end{aligned}$$

and the function Γ stands for the spectral function of the box diagram shown in Fig. 2 [see the equation following Eq. (18) of Ter-Martirosyan[3]]:

$$\begin{aligned} \Gamma(\sigma', \sigma''; s', s) &= 2\pi s^{-1/2} \{(s - 4\mu^2)\, s'^2 \\ &\quad - 2s'\, [(s - 4\mu^2)(\sigma' + \sigma'') + 2\sigma'\sigma''] \\ &\quad + (s - 4\mu^2)(\sigma' - \sigma'')^2\}^{-1/2}\, \theta(s' - s_c), \\ s_c &= \sigma' + \sigma'' + \frac{2\sigma'\sigma''}{s - 4\mu^2} \\ &\quad + \left\{\left(\sigma' + \sigma'' + \frac{2\sigma'\sigma''}{s - 4\mu^2}\right)^2 - (\sigma' - \sigma'')^2\right\}^{1/2}, \\ \theta(x) &= \begin{cases} 1, & x > 0 \\ 0, & x < 0 \end{cases}. \end{aligned} \tag{7}$$

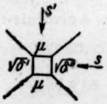

FIG. 2

With the help of Eq. (2) the functions $\lambda_i(\sigma)$ may be expressed in terms of α, β, ρ, ρ_C:

$$\begin{aligned} \lambda_1(\sigma) &= \alpha(\sigma) + \frac{1}{\pi} \int_0^\infty [\rho(\tau, \sigma)\, \varphi(\tau, s) \\ &\quad + \rho_c(\sigma, \tau)\, \varphi(\tau, 4\mu^2 - s - \sigma)]\, d\tau, \\ \lambda_2(\sigma) &= \alpha(\sigma) + \frac{1}{\pi} \int_0^\infty [\rho(\tau, \sigma)\, \varphi(\tau, 4\mu^2 - s - \sigma) \\ &\quad + \rho_c(\tau, \sigma)\, \varphi(\tau, s)]\, d\tau, \\ \lambda_3(\sigma) &= \beta(\sigma) + \frac{1}{\pi} \int_0^\infty \rho(\sigma, \tau)\, [\varphi(\tau, s) \\ &\quad + \varphi(\tau, 4\mu^2 - s - \sigma)]\, d\tau. \end{aligned} \tag{8}$$

Together, Eqs. (5), (6) and (8) relate ρ and ρ_c to α and β.

The remaining two equations [determining the functions $\alpha(\sigma)$ and $\beta(\sigma)$] are obtained by averaging Eq. (4) over the scattering angles. If we denote by $\langle\lambda(s)\rangle_1$ and $\langle\lambda(s)\rangle_3$ the amplitudes averaged over the scattering angles of the first and third channel respectively, then we obtain

$$\langle\lambda_1(s)\rangle_1 = 2\sqrt{(s-4\mu^2)/s}\,|\langle\lambda(s)\rangle_1|^2, \tag{9}$$

$$\langle\lambda_3(s)\rangle_3 = \sqrt{(s-4\mu^2)/s}\,\{3|\langle\lambda(s)\rangle_3|^2 + 4\,\mathrm{Re}\,\langle\lambda^*(s)\rangle_3\langle\lambda(s)\rangle_1\}. \tag{10}$$

Here the expressions appearing on the left sides of Eqs. (9) and (10) can be written as follows [see Eq. (9′) of Mandelstam[1]]:

$$\langle\lambda_1(s)\rangle_1 = \alpha(s) + \frac{1}{\pi}\int_0^\infty [Q_1(\sigma, s) + Q_2(\sigma, s)]\,l(\sigma, s)\,d\sigma, \tag{11}$$

$$\langle\lambda_3(s)\rangle_3 = \beta(s) + \frac{2}{\pi}\int_0^\infty Q_3(\sigma, s)\,l(\sigma, s)\,d\sigma. \tag{12}$$

The function $l(\sigma, s)$ has the form[2]

$$l(\sigma, s) = \frac{1}{s-4\mu^2}\ln\left(1+\frac{s-4\mu^2}{\sigma}\right) - \frac{1}{\sigma-s_0}.$$

In order to find $\langle\lambda(s)\rangle_{1,3}$ we make use of dispersion relations, following directly from Eq. (2):

$$\lambda(s_1, s_2; s_3) = \Phi(s_1) + \frac{1}{\pi}\int_0^\infty [\lambda_2(s_1, \sigma)\,\varphi(\sigma, s_2) + \lambda_3(s_1, \sigma)\,\varphi(\sigma, s_3)]\,d\sigma. \tag{13}$$

The functions $\lambda_2(\sigma)$ and $\lambda_3(\sigma)$ are given by Eq. (8) and stand for the imaginary parts of the amplitude in the second and third channel respectively:

$$\Phi(s_1) = \lambda_0 + \frac{1}{\pi}\int_0^\infty \varphi(\sigma, s_1)\,\alpha(\sigma)\,d\sigma + \frac{1}{\pi^2}\iint_0^\infty \frac{\rho(\sigma, \sigma')(s_0-s_1)\,d\sigma\,d\sigma'}{(\sigma+\sigma'+s_1-4\mu^2)(\sigma-s_0)(\sigma'-s_0)}. \tag{14}$$

Therefore

$$\langle\lambda(s)\rangle_1 = \Phi(s) + \frac{1}{\pi}\int_0^\infty l(\sigma, s)\,[\lambda_2(s, \sigma) + \lambda_3(s, \sigma)]\,d\sigma. \tag{15}$$

Similarly

$$\lambda(s_1, s_2; s_3) = F(s_3) + \frac{1}{\pi}\int_0^\infty \lambda_1(s_3, \sigma)\,[\varphi(\sigma, s_1) + \varphi(\sigma, s_2)]\,d\sigma; \tag{16}$$

here λ_1 is determined by Eq. (8) and

$$F(s) = \lambda_0 + \frac{1}{\pi}\int_0^\infty \beta(\sigma)\,\varphi(\sigma, s)\,d\sigma + \frac{1}{\pi^2}\iint_0^\infty \frac{\rho_c(\sigma, \sigma')(s_0-s)\,d\sigma\,d\sigma'}{(\sigma+\sigma'+s_1-4\mu^2)(\sigma-s_0)(\sigma'-s_0)}. \tag{17}$$

Hence

$$\langle\lambda(s)\rangle_3 = F(s) + \frac{2}{\pi}\int_0^\infty \lambda_1(s, \sigma)\,l(\sigma, s)\,d\sigma. \tag{18}$$

3. DISCUSSION

Together, the four equations (5), (6), (9) and (10) determine the four functions α, β, ρ and ρ_c. It is natural to try to solve the system of equations approximately, ignoring in the first approximation the contributions due to the functions ρ and ρ_c in comparison with the contributions due to α and β. Instead of α and β one may introduce the S wave scattering amplitudes $\alpha_0^{(0)}$ and $\alpha_0^{(2)}$ in the isospin $I = 0$ and 2 states respectively.

A first approximation for ρ and ρ_c then follows from Eqs. (9) and (10) (with only α and β on their right hand sides). The expressions for ρ and ρ_c obtained in this manner are given in Appendix 2. Given ρ and ρ_c we can obtain corrections to the S wave amplitudes, as well as P, D, etc., wave amplitudes. The S wave dominant solution found by Chew, Mandelstam and Noyes[8] is precisely characterized by the property that the P and higher waves are very small in comparison with the S wave. It is therefore clear that the above described procedure will lead in essence to the Chew, Mandelstam and Noyes solution and will differ from it only by corrections from higher order approximations. Should it turn out that it is the P wave (or any other wave with $l > 0$) that is large then the functions ρ and ρ_c cannot be ignored in our equations and it is necessary to solve the four equations with ρ and ρ_c taken into account.

APPENDIX 1

We present here a derivation of the equations for the spectral functions that is different from that given by Ter-Martirosyan.[3] Let us write

$$\alpha_1^{(l)}(s_1, s_2, s_3) = \sqrt{\frac{s_1-4\mu^2}{s_1}}\int \alpha^{(l)*}(s_1, s_2', s_3')\,\alpha^{(l)}(s_1, s_2'', s_3'')\,\frac{dn_1}{4\pi} + \Delta^{(l)}(s_1, s_2, s_3). \tag{A.1}$$

The first term on the right hand side of Eq. (A.1) may be expressed in the form

$$\frac{1}{\pi}\int_0^\infty Q_l(\sigma, s_1)\,\varphi(\sigma, s_3)\,d\sigma + \frac{1}{\pi}\int_0^\infty P_l(\sigma, s_1)\,\varphi(\sigma, s_2)\,d\sigma, \tag{A.2}$$

where

$$Q_l(\sigma, s_1) = \frac{1}{\pi^2}\iint_0^\infty \Gamma(\tau, \tau'; \sigma, s_1)\,[\alpha_2^{(l)*}(\tau)\,\alpha_2^{(l)}(\tau') + \alpha_3^{(l)*}(\tau)\,\alpha_3^{(l)}(\tau')]\,d\tau\,d\tau',$$

$$P_l(\sigma, s_1) = \frac{1}{\pi^2}\iint_0^\infty \Gamma(\tau, \tau'; \sigma, s_1)\,[\alpha_2^{(l)*}(\tau)\,\alpha_3^{(l)}(\tau') + \alpha_3^{(l)*}(\tau)\,\alpha_2^{(l)}(\tau')]\,d\tau\,d\tau' \tag{A.3}$$

and $\alpha_2^{(\mathrm{I})}$ denotes the jump in s_2 of the function $\alpha^{(\mathrm{I})}(s_1, s_2, s_3)$. The arguments of the functions $\alpha_2^{(\mathrm{I})}$ and $\alpha_3^{(\mathrm{I})}$ are as follows:

$$\alpha_2^{(I)} = \alpha_2^{(I)}(s_1,\ \tau,\ 4\mu^2 - s_1 - \tau),$$

$$\alpha_3^{(I)} = \alpha_3^{(I)}(s_1,\ 4\mu^2 - s_1 - \tau,\ \tau).$$

Evaluating on both sides of Eq. (A.1) the jump in s_2 we obtain

$$\alpha_{12}^{(I)}(s_1, s_2, s_3) = P_I(s_2, s_1) + v_I(s_2, s_1); \qquad \text{(A.4)}$$

$v_\mathrm{I}(s_2, s_1) = 0$ for $s_1 \leq 16\mu^2$. With the help of Eqs. (2) and (3) the functions $\alpha_{12}^{(\mathrm{I})}$, $\alpha_2^{(\mathrm{I})}$ and $\alpha_3^{(\mathrm{I})}$ are easily expressed in terms of ρ and ρ_C. Then Eq. (A.4) for $\mathrm{I} = 0, 1, 2$ takes on the form

$$3\rho(s_1, s_2) + \rho(s_2, s_1) + \rho_c(s_1, s_2) = L_0, \qquad \text{(A.5)}$$

$$-\rho_c(s_1, s_2) + \rho(s_2, s_1) = L_1, \qquad \text{(A.6)}$$

$$\rho(s_2, s_1) + \rho_c(s_1, s_2) = L_2, \qquad \text{(A.7)}$$

where we have introduced the notation

$$L_i = \frac{2}{\pi^2}\iint_0^\infty \Gamma(\tau, \tau';\ s_2,\ s_1)\, A_i(\tau)\, A_i(\tau')\, d\tau\, d\tau'$$
$$+ v_i(s_2,\ s_1) \quad (i = 1, 2, 3);$$

$$A_0(\sigma) \equiv \alpha_2^{(0)}(s_1, \sigma, 4\mu^2 - s_1 - \sigma) = 4\alpha(\sigma) + \beta(\sigma)$$
$$+ \frac{1}{\pi}\int_0^\infty [3\rho(\sigma', \sigma) + \rho(\sigma, \sigma') + \rho_c(\sigma, \sigma')]\varphi(\sigma', s_1)\, d\sigma'$$
$$+ \frac{1}{\pi}\int_0^\infty [3\rho_c(\sigma, \sigma') + \rho(\sigma', \sigma)$$
$$+ \rho(\sigma, \sigma')]\, \varphi(\sigma', 4\mu^2 - s_1 - \sigma)\, d\sigma', \qquad \text{(A.8)}$$

$$A_1(\sigma) \equiv \alpha_2^{(1)}(s_1, \sigma) = \alpha(\sigma) - \beta(\sigma)$$
$$+ \frac{1}{\pi}\int_0^\infty [\rho_c(\sigma', \sigma) - \rho(\sigma, \sigma')]\, \varphi(\sigma', s_1)\, d\sigma'$$
$$+ \frac{1}{\pi}\int_0^\infty [\rho(\sigma', \sigma) - \rho(\sigma, \sigma')]\, \varphi(\sigma', 4\mu^2 - s_1 - \sigma)\, d\sigma', \qquad \text{(A.9)}$$

$$A_2(\sigma) \equiv \alpha_2^{(2)}(s_1, \sigma) = \alpha(\sigma) + \beta(\sigma)$$
$$+ \frac{1}{\pi}\int_0^\infty [\rho(\sigma, \sigma') + \rho_c(\sigma, \sigma')]\, \varphi(\sigma', s_1)\, d\sigma'$$
$$+ \frac{1}{\pi}\int_0^\infty [\rho(\sigma, \sigma') + \rho(\sigma', \sigma)]\, \varphi(\sigma', 4\mu^2 - s_1 - \sigma)\, d\sigma'. \qquad \text{(A.10)}$$

Subtracting Eq. (A.6) from Eq. (A.7) and making use of the symmetry of $\rho_\mathrm{C}(s_1, s_2)$ we find for $\rho_\mathrm{C}(s_1, s_2)$ an expression which coincides exactly with Eq. (5). Adding Eqs. (A.6) and (A.7) we get $\rho(s_2, s_1)$ in the region $s_1 \geq 16\mu^2$, $s_2 < 16\mu^2$, whereas by subtracting Eq. (A.7) from Eq. (A.5) we obtain $\rho(s_1, s_2)$ in the same region. From this point on it is easy to get the expression for $\rho(s_1, s_2)$ which coincides with Eq. (5).

APPENDIX 2

Let us find the first approximation for ρ and ρ_C. We make use of Eqs. (5) and (6), with λ_1, λ_2, λ_3 determined with the help of Eq. (8). Leaving in λ_1, λ_2 and λ_3 only $\alpha(\sigma)$ and $\beta(\sigma)$ we get

$$\rho(s', s) = \frac{2}{\pi^2}\iint_0^\infty \Gamma(\tau, \tau';\ s', s)\, \{\alpha(\tau)\, \alpha(\tau')$$
$$+ \beta(\tau)\, \beta(\tau')\}\, d\tau\, d\tau' + \frac{2}{\pi^2}\iint_0^\infty \Gamma(\tau, \tau';\ s, s')$$
$$\times \{3\alpha(\tau)\, \alpha(\tau') + 2\alpha(\tau)\, [\alpha(\tau') + \beta(\tau')]\}\, d\tau\, d\tau', \qquad \text{(A.11)}$$

$$\rho_c(s, s') = \frac{4}{\pi^2}\iint_0^\infty \{\Gamma(\tau, \tau';\ s,\ s')$$
$$+ \Gamma(\tau, \tau';\ s',\ s)\}\, \alpha(\tau)\, \beta(\tau')\, d\tau\, d\tau'. \qquad \text{(A.12)}$$

---

[1] S. Mandelstam, Phys. Rev. **112**, 1344 (1958).

[2] K. A. Ter-Martirosyan, JETP **39**, 827 (1960), Soviet Phys. JETP **12**, 575 (1960).

[3] K. A. Ter-Martirosyan, Nuclear Phys. (in press).

[4] Yu. A. Simonov, JETP **40**, 626 (1961), Soviet Phys. JETP **13**, 436 (1961).

[5] G. Chew and S. Mandelstam, Phys. Rev. **119**, 467 (1960).

[6] M. Cini and S. Fubini, Ann. of Phys. **10**, 352 (1960).

[7] Efremov, Meshcheryakov, Shirkov, and Tzu, Nuclear Phys. **22**, 202 (1961).

[8] Chew, Mandelstam, and Noyes, Phys. Rev. **119**, 478 (1960).

Translated by A. M. Bincer
197

SOVIET PHYSICS JETP VOLUME 13, NUMBER 4 OCTOBER, 1961

A DRESSED PARTICLE ANALYSIS OF THE π + d ⇄ 2N *REACTION*

M. A. BRAUN

Leningrad State University

Submitted to JETP editor November 10, 1960

J. Exptl. Theoret. Phys. (U.S.S.R.) 40, 1179-1184 (April, 1961)

The π + d ⇄ 2N reaction is treated by a nonrelativistic meson theory of the πN interaction in the P state. Dressed particle techniques are used to express the amplitude for this process in terms of the coupling constant and the P-wave phase shifts for πN scattering. The energy and angle dependence of the calculated cross sections are in qualitative agreement with experiment. The maximum difference between the theoretical and observed cross sections for angles far from 90° and energies that are not too high is 30%. For angles close to 90° and energies much higher than resonant the calculated cross section becomes as much as two times as large as the experimentally observed one. Improvement of the results requires including the S state in the πN interaction, as well as high nucleon velocities.

1. INTRODUCTION

THERE is much experimental material on the + d ⇄ 2N reaction.[1] Progress in the theoretical explanation of this reaction, on the other hand, is quite modest in scope. The best results are obtained with the phenomenological theory of Mandelstam.[2] He guesses the form of the resonance factor and uses three adjustable parameters, and in this way is able to give a relatively good explanation of the experimental data for incident pion energies from 0 to roughly 300 Mev. Investigations based on meson theory consider the reaction cross section close to threshold.[3,4] The agreement with experiment obtained in this way is satisfactory.[4] From the theoretical point of view, however, these investigations are not very systematic, since the two-nucleon problem is treated in them phenomenologically, rather than in terms of the meson field. Furthermore, in the most interesting region, that of resonance, the cross section is yet to be studied.

In the present paper the π + d ⇄ 2N interaction is treated by the dressed-particle method, by means of which the two-nucleon problem is reduced to a calculation involving only single-nucleon matrix elements.[5,6]

As with other authors, our description of the nucleon is not relativistic, and the Hamiltonian we choose is

$$H = H_{N_1} + H_{N_2} + H_\pi + \sum_k \{c_k(G_k^{(1)} + G_k^{(2)}) + \text{Herm. adj.}\},$$

$$G_k^{(s)} = \frac{i\sqrt{4\pi}\, f_0\, v(k)}{2\sqrt{2k_0}}\, \tau_k^{(s)} \left[\left(\sigma^{(s)}, \mathbf{k} + i\frac{k_0}{M}\nabla_s\right), e^{i\mathbf{k}\mathbf{r}_s}\right]_+,$$

$$s = 1, 2. \qquad (1)$$

Here H_{N_1}, H_{N_2}, and H_π are the kinetic energies, respectively, of the first and second nucleon and the meson field. The index k includes the meson three-momentum K and its isotopic spin coordinate. We use the system of coordinates in which $\hbar = c = \mu = 1$ (where μ is the pion mass). The rest of the notation is quite common and need not be explained. We remark that the Hamiltonian of (1) describes correctly the resonance interaction of π mesons with nonrelativistic nucleons in the P state. As is known, there is no successful theory of the πN interaction in the S state, and we therefore must neglect this interaction.

The following approximations are made in the calculation.

1. Terms describing two-meson and higher exchange between the nucleons are dropped. Effects related to such terms increase rapidly with increasing distance r between the nucleons (as fast as and faster than e^{-2r}), and therefore for a system as weakly bound as the deuteron one may reliably treat them as small.*

2. In calculating the single-nucleon matrix elements, we drop terms that depend on the square and higher powers of the nucleon velocities and terms linear in the velocities of the nucleon in the deuteron. This latter approximation is probably justified because the nucleons move relatively slowly inside the deuteron. As for neglecting the square of the nucleon velocities in the final state (in the π + d → 2N reaction), it cannot be justified by simply pointing to low velocities, for they are of the order of 0.3 to 0.5. Essentially one

---

*Clearly this is not equivalent to perturbation theory.

must assume that the matrix elements depend only weakly on these velocities.

3. We neglect all πN scattering phase shifts other than that for resonance (namely δ_{33}), since there is no reliable way to deal with small phase shifts in the presently existing theory.

4. From similar considerations, the outgoing nucleons are described by plane waves. The error involved is probably not large, because the nucleon energies are so high.

2. TRANSITION AMPLITUDE

In this section we shall briefly describe the derivation of the formulas for the transition amplitude. The technical details are available in other works[5-7] discussing the calculation.

For the process we are dealing with, the transition amplitude is of the form

$$T = \langle \Psi_\alpha^{(-)} | (H - E) c_q^+ | \Psi_{d,P} \rangle,$$

where $\Psi_\alpha^{(-)}$ is the incoming two-nucleon state with spins and momenta indicated by α, $\Psi_{d,\,P}$ is the deuteron state with momentum $\mathbf{P}$, q is the π-meson momentum and spin, and E is the energy of the system. By using dressed particle techniques one can reduce the calculation of T to one involving single-nucleon matrix elements.[6] The final result, which is all we shall present here, is

$$T = \sum_{\beta,\gamma} f_\alpha^{(-)*}(\beta)\, K_{\beta\gamma}\, f_{d,P}(\gamma), \qquad K_{\beta\gamma} = \sum_{s=0}^{4} K_{\beta\gamma}^{(s)},$$

$$K_{\beta\gamma}^{(0)} = \langle \beta | G_q^{(1)} + G_q^{(2)} | \gamma \rangle, \qquad K_{\beta\gamma}^{(1)} = \langle \beta | N (G_q^{(1)} + G_q^{(2)}) | \gamma \rangle,$$

$$K_{\beta\gamma}^{(2)} = -\tfrac{1}{2} \sum_\delta \{ \langle \beta | G_q^{(1)} + G_q^{(2)} | \delta \rangle N_{\delta\gamma} + N_{\beta\delta} \langle \delta | G_q^{(1)} + G_q^{(2)} | \gamma \rangle \},$$

$$K_{\beta\gamma}^{(3)} = -\left\langle \beta \left| (G_q^{(1)} + G_q^{(2)}) \frac{1 - P_{00}}{H_1 + H_2 - E_\gamma + i0} U_{12} \right| \gamma \right\rangle,$$

$$K_{\beta\gamma}^{(4)} = -\left\langle \beta \left| U_{12}^+ \frac{1 - P_{00}}{H_1 + H_2 - E_\beta - i0} (G_q^{(1)} + G_q^{(2)}) \right| \gamma \right\rangle. \quad (2)$$

Here $f_\alpha^{(-)}(\beta)$ is the wave function of the incoming unbound nucleons, and $f_{d,\,P}(\gamma)$ is the deuteron wave function. The variables β and γ include the nucleon momenta ($\mathbf{p}_1'\mathbf{p}_2'$ and $\mathbf{p}_1$, $\mathbf{p}_2$, respectively) and spins. The remaining notation is the same as is usually used in the dressed-particle method.[5,6] The first term in (2) gives the impulse approximation, and the remaining terms arise from single-meson exchange.

The calculation of the single-nucleon matrix elements in (2) is not particularly difficult, (see, for instance, Novozhilov and Terent'ev[7]). Some peculiarities arise in calculating $K_{\beta\gamma}^{(4)}$. This is because the denominator $H_1 + H_2 - E_\beta$ may vanish, and therefore standard methods would lead to difficult singular integrals over the πN scattering cross section. A typical term in $K_{\beta\gamma}^{(4)}$ may be of the form

$$\sum_k \left\langle \beta \left| G_k^{(1)+} c_k^{(2)} \frac{1 - P_{00}}{H_1 + H_2 - E_\beta - i0} G_q^{(1)} \right| \gamma \right\rangle$$

$$= \sum_k \left\langle \beta_1 \left| G_k^{(1)+} \frac{1 - P_0}{H_1 + E_{\gamma_2} - E_\beta - i0} G_q^{(1)} \right| \gamma_1 \right\rangle \langle \beta_2 | c_k^{(2)+} | \gamma_2 \rangle$$

(where β_1 is the spin and momentum of the first nucleon in the β state, and E_{β_1} is its energy, etc.) The second term is calculated in the usual way. The first one is subjected to the unitary transformation $|\gamma_1\rangle = \exp[i(\mathbf{s} - \mathbf{u})\mathbf{r}_1]|\gamma_1)$ (where $\mathbf{s}$ is the total momentum and $\mathbf{u}$ is the momentum of the meson field), which transforms into

$$\delta(\mathbf{p}_1' + \mathbf{k} - \mathbf{q} - \mathbf{p}_1) \left(\beta_1 \left| \widetilde{G}_k^{(1)+} \frac{1 - \widetilde{P}_0}{\widetilde{H}_1 + E_{\gamma_2} - E_\beta - i0} \widetilde{G}_q^{(1)} \right| \gamma_1 \right),$$

where we have used the notation

$$\widetilde{A} \equiv \exp[-i(\mathbf{s} - \mathbf{u})\mathbf{r}_1]\, A \exp[i(\mathbf{s} - \mathbf{u})\mathbf{r}_1].$$

The matrix element here depends only quadratically on the nucleon velocities in the β_1 and γ_1 states. Then according to our approximations, we may replace the β_1 state by some other state $\widetilde{\beta}_1$ with the same spin, but with another momentum which we shall choose later. We note now that in our approximation we may write

$$E_{\gamma_2} - E_\beta \approx E_{\gamma_2} - E \approx E_{\gamma_2} - (q_0 + E_\gamma) = -q_0 - E_{\gamma_1}$$

and that

$$\frac{1}{\widetilde{H}_1 - q_0 - E_{\gamma_1} - i0} \widetilde{G}_q^{(1)} | \gamma_1) = c_q^{(1)+} | \gamma_1) - | q\gamma_1)^{(+)},$$

where $|q\gamma_1)^{(+)}$ is an outgoing state containing a single nucleon (spin and momentum γ_1) and a single meson (spin and momentum q). Of the two matrix elements obtained, the first, which contains no singular denominators, is calculated in the usual way, while the second gives the T matrix for πN scattering, but with neither energy nor momentum conservation. We now use the arbitrariness in the choice of $\widetilde{\beta}_1$ and the explicit form of the T matrix for the P-wave πN interaction to achieve conservation, and thus the matrix element can be written in terms of the πN scattering phase shifts.

The final expression for $K_{\beta\gamma}$ is then

$$K_{\beta\gamma} = i\delta(\mathbf{p}_1' + \mathbf{p}_2' - \mathbf{q} - \mathbf{P}) \left(1 - \frac{q_0}{2M}\right) \Big\{ \delta(\mathbf{p}_1' - \mathbf{p}_1) \times \frac{f v(q)}{2\pi \sqrt{q_0}} \left(\sigma^{(2)}, \mathbf{q} + \frac{q_0}{M}\mathbf{p}_1'\right) + F(q_0) \int d^3k \frac{v^2(k)}{k_0^2} \delta(\mathbf{k} - \mathbf{p}_2' + \mathbf{p}_2) \times \boldsymbol{\sigma}^{(2)}\mathbf{k}\, [3\mathbf{kq} - (\boldsymbol{\sigma}^{(1)}\mathbf{k})(\boldsymbol{\sigma}^{(1)}\mathbf{q})] - (1 \rightleftarrows 2) \Big\}. \quad (3)$$

The resonance factor $F(q_0)$ is given by

$$F(q_0) = \frac{8}{3}\frac{fv(q)}{(2\pi)^3\sqrt{q_0}}\left[\frac{e^{i\delta_{33}(\bar{q}_0)}\sin\delta_{33}(\bar{q}_0)}{\bar{q}^2 q v^2(q)} - \frac{3}{2}\frac{f^2}{q_0}\right]. \quad (4)$$

Here $\bar{q}_0$ and $\bar{q}$ are the energy and the magnitude of the momentum in the π-nucleon center-of-mass system.

3. NUMERICAL RESULTS AND DISCUSSION

We now take the absolute square of the amplitude T of Eq. (2) (dropping the δ function, which gives total momentum conservation), sum over final spins, and average over initial. If we denote by Z the expression obtained in the laboratory system ($\mathbf{P} = 0$), the differential cross section obtained in the center-of-mass system for the $\pi + d \rightleftarrows 2N$ reaction is

$$\frac{d\sigma(\pi + d \to 2N)}{d\Omega} = \frac{8\pi^4 q_0 l}{q}\sqrt{M^2 + l^2 Z}$$

$$\frac{d\sigma(2N \to \pi + d)}{d\Omega} = \frac{3}{2}\frac{\eta^2}{l^2}\frac{d\sigma(\pi + d \to 2N)}{d\Omega}. \quad (5)$$

Here l^2 and η^2 are the squares of the nucleon and π momenta in the center-of-mass system for this reaction.

As was mentioned in the introduction, the $f_\alpha(\beta)$ we use are free-particle functions. For the deuteron function we take the expression given by Hulthén and Sugawara,[8] which gives the probability $p_D = 4\%$ for the D wave, and a hard-core radius $r_c = 0.306$. The cutoff factor is chosen as $v(k) = a^2/(a^2 + k^2)$ with $a = 7$. The cross section depends weakly on a.

We have tabulated our theoretical results alongside the experimental[1] ones for the $2p \to \pi^+ + d$ reaction for several values of η and scattering angle θ in the center-of-mass system. It should be emphasized that it is not possible for us to calculate in any reliable way the contribution to the cross section from the triplet state of the nucleons. This is because the most important part of this contribution comes from the S-state part of the πN interaction, and we do not include this. For this reason we tabulate the results both with and without the triplet-state contribution.

As is seen from the table, the energy and angle dependence of the calculated cross section agree qualitatively with experiment. The total cross section exhibits a resonant behavior with a maximum for η in the region of 1.5 to 1.8, which is supported by the experimental data.

As for a quantitative comparison with experiment, we must emphasize that in view of the third of the approximations we make (see Introduction) the calculated cross section can be considered reliable (assuming the other approximations valid) only where the resonant terms with the δ_{33} phase shift are large compared to the small-phase shift terms we have not included. This is true only for angles far from 90° and energies below the resonance in the πN scattering. Therefore it is only in these regions that our theory may attempt to reproduce the experimental results.

Then excluding angles close to 90° and the point $\eta = 2.05$, we find that the theory deviates from experiment by at most about 30%. In our

Differential and total cross sections for the $2p \to \pi^+ + d$ reaction

$\eta/\mu c$	θ, deg	Differential cross sections (10^{-28} cm^2/sr)			Total cross sections (10^{-27} cm^2)		
		theory			theory		
		including $d\sigma_t$	not including $d\sigma_t$	experiment	including σ_t	not including σ_t	experiment
0.54	0	0.256	0.239	0.312±0.031	0.151	0.116	0.156±0.016
	45	0.153	0.123	0.145±0.018			
	90	0.054	0.027	0.028±0.011			
1.15	0	1.72	1.70	2,85±0,32	1.32	0.92	1,53±0.23
	45	1.17	0.87	1.70±0.22			
	90	0.77	0.40	0.55±0,12			
1.55	0	5.11	5.07	5.55±0.52	3.80	2.71	3.15±0.25
	45	3.40	2.63	3,26±0.32			
	90	2.17	1.04	0.99±0.13			
1.74	0	6.68	6.55	5,05±0,42	4.63	3.44	3.06±0.31
	30	5.28	4.76	4,05±0,35			
	45	4.15	3.35	3.09±0.30			
	60	3.22	2.22	2.14±0.24			
	90	2.54	1.25	1,18±0.18			
2.05	0	5.41	5.03	2.73±0,22	3.14	2.44	1.89±0.17
	45	3.03	2.57	1,81±0.17			
	90	1.30	0.59	0,86±0.11			

opinion this is quite satisfactory when one recalls the approximations made.

If all angles and energies are included, the theoretical differential cross section differs from experiment by at most 100%. For the total cross section this figure is about 50%. Better results are obtained if one neglects the triplet state of the nucleons. Then, as the table shows, the total cross section differs from experiment by no more than 30% for all energies, and 10% at resonance.

We note also that around 90° the cross section depends strongly on the choice of p_D and r_c. We have chosen the values generally used, but they are almost definitely not the best ones from the point of view of obtaining agreement with experiment for our calculation. A final choice, however, can be made only after one takes account of other factors influencing the cross section, especially the S-state πN interaction and the low phase shifts in the πN scattering. For this reason we do not vary p_D and r_c in our calculation.

In conclusion we wish to emphasize that our calculation is necessarily a first approximation, presenting only the roughest outlines of the mechanism by which the $\pi + d \rightleftarrows 2N$ reaction takes place. A real improvement of the calculations will become possible only when we learn to include the high nucleon velocities characteristic of this reaction, i.e., when there exists a relativistic theory of strong interactions.

The author expresses his sincere gratitude to Yu. V. Novozhilov for advice and discussion, and to R. Boĭkova and G. Dmitrieva for aid in the numerical calculations.

---

[1] A. Rosenfeld, Phys. Rev. **96**, 139 (1954); C. Cohn, Phys. Rev. **105**, 1582 (1957); B. S. Neganov and L. B. Parfenov, JETP **34**, 767 (1958), Soviet Phys. JETP **7**, 512 (1959).

[2] S. Mandelstam, Proc. Roy. Soc. (London) **244**, 491 (1958).

[3] D. B. Lichtenberg, Phys. Rev. **100**, 303 (1955); **105**, 1084 (1957).

[4] A. Woodruff, Phys. Rev. **117**, 1113 (1960).

[5] Yu. V. Novozhilov, JETP **35**, 742 (1958), Soviet Phys. JETP **8**, 515 (1959); Nuclear Phys. **15**, 469 (1960).

[6] M. A. Braun, Vestnik Leningrad State Univ. **4**, 26 (1960).

[7] Yu. V. Novozhilov and I. A. Terent'ev, JETP **36**, 129 (1959), Soviet Phys. JETP **9**, 89 (1959).

[8] Handbuch d. Physik **39** (1957).

Translated by E. J. Saletan
198

SOVIET PHYSICS JETP VOLUME 13, NUMBER 4 OCTOBER, 1961

THE DYNAMIC EFFECT OF THE NUCLEAR VOLUME IN CONVERSION M1 TRANSITIONS IN EVEN-EVEN NUCLEI FOR THE NONAXIAL ROTATOR MODEL AND FOR THE VIBRATIONAL MODEL OF THE NUCLEUS

D. P. GRECHUKHIN

Submitted to JETP editor November 16, 1960

J. Exptl. Theoret. Phys. (U.S.S.R.) **40**, 1185-1189 (April, 1961)

The corrections to the internal conversion coefficient for a M1 nuclear transition arising when the potential produced by the intranuclear electron transition current is taken into account are estimated for the transitions of K, LI, and LII electrons to the $s_{1/2}$ and $p_{1/2}$ states of the continuous spectrum. The calculations are carried out according to the harmonic vibrational model and the nonaxial rotator model (Davydov-Filippov model) of the nucleus.

1. INTRODUCTION

In the internal conversion of orbital electrons, the vector potential due to the electron current $\mathbf{j}_e$ of the transition

$$\mathbf{A}(\mathbf{r}) = \int \mathbf{j}_e(\mathbf{r}') \frac{\exp\{i\omega|\mathbf{r}-\mathbf{r}'|\}}{|\mathbf{r}-\mathbf{r}'|}(d\mathbf{r}') \qquad (1)$$

is composed of the potential $\mathbf{A}_{in}(\mathbf{r})$, which is due only to the electron current $\mathbf{j}_e(\mathbf{r}')$ (where $r' \leq R_0$) distributed over the volume of the nucleus, and of $\mathbf{A}_{ex}(\mathbf{r})$ due mainly to the extranuclear electron current $\mathbf{j}_e(\mathbf{r}')$ (where $r' \geq R_0$):

$$\mathbf{A}(\mathbf{r}) = \mathbf{A}_{in}(\mathbf{r}) + \mathbf{A}_{ex}(\mathbf{r}). \qquad (2)$$

Since the nuclear volume is small as compared with the volume of the atomic shell, we have $|\mathbf{A}_{in}| \ll |\mathbf{A}_{ex}|$. Since the quantity $\mathbf{A}_{in}$ is determined by the probability of penetration of the conversion electron into the nuclear volume, the maximum potential $\mathbf{A}_{in}$ is produced in M1 transitions of an electron of the type $s_{1/2} \to s_{1/2}$ and $p_{1/2} \to p_{1/2}$ (e.g., $K \to s_{1/2}$, $LI \to s_{1/2}$, and $LII \to p_{1/2}$), while in these transitions the internal potential has the order of magnitude

$$\mathbf{A}_{in} \sim \frac{Z}{137}\left[R_0 Z \frac{m_e e^2}{\hbar^2}\right]^{2\gamma-1}\mathbf{A}_{ex}, \qquad \gamma = \left[1-\left(\frac{Z}{137}\right)^2\right]^{1/2}.$$

In other M1 transitions of orbital electrons, $\mathbf{A}_{in}$ is considerably less than the estimate given above, and its contribution to the conversion probability may be neglected.

Usually, in the theory of internal conversion, $\mathbf{A}_{in}$ is not considered, and the conversion transition probability is calculated taking only the potential $\mathbf{A}_{ex}$ into account. In that case, the probability of the γ transition in a nucleus, as well as the probability of the conversion transition, is determined by the same nuclear matrix element, which drops out from the internal conversion coefficient, the latter consequently becoming independent of the nuclear structure.

However, the potentials $\mathbf{A}_{in}(\mathbf{r})$ and $\mathbf{A}_{ex}(\mathbf{r})$ have a qualitatively different radial dependence, and the corresponding nuclear matrix elements of the operators of the interaction of the nuclear current $\mathbf{j}_N$ with this potential ($\mathbf{j}_N\mathbf{A}_{in}$ and $\mathbf{j}_N\mathbf{A}_{ex}$) are, in general, subject to different selection rules determined by the given structure of the excited states of the nucleus. Therefore, in separate transitions, the contribution of $\mathbf{A}_{in}$ may be comparable to that of $\mathbf{A}_{ex}$ irrespective of the fact that $\mathbf{A}_{in} \ll \mathbf{A}_{ex}$. In such cases, we are dealing with forbidden transitions inside the nucleus; the conversion probability is determined by several matrix elements, and the internal conversion coefficient depends on the ratio of the contributions of the operators $\mathbf{j}_N\mathbf{A}_{in}$ and $\mathbf{j}_N\mathbf{A}_{ex}$, i.e., on the nuclear structure.

This effect of the contribution of $\mathbf{A}_{in}$ has been called the dynamic effect of the nuclear volume, and the corresponding changes in the internal conversion coefficient are called "anomalies."

It should be mentioned that an anomaly may also arise in the case of a strongly forbidden nuclear transition due to the potential $\mathbf{A}_{ex}$ only, i.e., where the matrix element of the operator $\mathbf{j}_N\mathbf{A}_{ex}$ is small as compared with its usual value for allowed transitions, while the matrix element of the operator $\mathbf{j}_N\mathbf{A}_{in}$ has a usual order of magnitude. However, another type of forbidden M1 transitions is possible if the matrix elements of the operators $\mathbf{j}_N\mathbf{A}_{ex}$ and $\mathbf{j}_N\mathbf{A}_{in}$ are small as compared with their values in allowed transitions. In forbidden M1 transitions of such a type, the internal conversion coefficient has its normal listed value, and is practically independent of the nuclear structure.

Thus, the fact that an M1 transition is forbidden is a necessary but not sufficient condition for an anomaly in the internal conversion coefficient.

The dynamic effect of the nuclear volume has first been studied for the independent-particle model by the author.[1] Church and Weneser[2] have, in a more general form, considered the corrections to the internal conversion coefficient in M1 transitions and, in particular, have drawn attention to the forbidden collective M1 transitions in even-even nuclei where one can expect an anomaly in the internal conversion coefficient.

The vibrational nuclear model[3] and the rotator model[3,4] have recently been developed to describe the structure of collective excited states of even-even nuclei. The purpose of the present paper is to estimate the contribution of $\mathbf{A}_{in}(\mathbf{r})$ to the internal conversion coefficient within the framework of these collective nuclear models, and to compare these estimates for nuclei where both the rotator model[4] and the vibrational model are applicable.

Henceforth, all quantities are expressed in relativistic units $\hbar = m_e = c = 1$, $e^2 = 1/137$; the nuclear transition energy ω and the energy of electronic states ϵ_i are expressed in units of $m_e c^2$; and the nuclear radius $R_0 = 0.43\, e^2 A^{1/3}$ corresponds to $R_0 = 1.2 \times 10^{-13} A^{1/3}$ cm in the usual units.

In calculating the electron potentials, the formalism of spherical vector functions[5] is used. In the wave functions of an orbital electron and of an electron in the continuous energy spectrum, the effect of finite dimensions of the nucleus is taken into account assuming, moreover, that the nucleon represents a uniformly charged sphere with radius R_0. The functions of the continuous-spectrum electrons are normalized to the energy interval.

2. POTENTIALS OF THE M1 TRANSITIONS OF K, LI, AND LII ELECTRONS

In the transition of an electron from an orbital state with energy ϵ_1, total momentum j_1, and total orbital momentum $l_1 = j_1 + \lambda_1$ to a continuous-spectrum state $(\epsilon_2, j_2, \lambda_2)$, the potentials of the M1 transitions are found to be

$$\mathbf{A}_{ex}(\mathbf{r}) = ie\left(\sum_M \sqrt{4\pi} C^{j_1\mu_1}_{j_2\mu_2 1M} \mathbf{Y}^0_{1M}(\mathbf{r})\right) f_1(\omega r)\, \mathfrak{M}, \qquad (3)$$

where

$$\mathfrak{M} = i\omega\beta\left\{\int_0^{R_0} dr\, r^2 h_1^{(1)}(\omega r)\,[G_{j_2\lambda_2}F_{j_1\lambda_1} + G_{j_1\lambda_1}F_{j_2\lambda_2}] + \int_{R_0}^{\infty} dr\, r^2 h_1^{(1)}(\omega r)\,[g_{j_2\lambda_2}f_{j_1\lambda_1} + g_{j_1\lambda_1}f_{j_2\lambda_2}]\right\}. \qquad (4)$$

In the above, the contribution of the intranuclear electron current is taken into account in $\mathbf{A}_{ex}(\mathbf{r})$. For a field **A**, this is identical to the contribution of the extranuclear transition electron current. $G_{ji\lambda i}$ and $F_{ji\lambda i}$ are the large and small radial components of the electron wavefunction in the range $r' \le R_0$, $g_{ji\lambda i}$ and $f_{ji\lambda i}$ are those for the range $r' \gg R_0$; $f_1(\omega r)$ and $h_1^{(1)}(\omega r)$ are spherical Bessel and Hankel functions; $C^{a\alpha}_{b\beta c\gamma}$ is the Clebsch-Gordan coefficient. The coefficient β for transitions $s_{1/2} \to s_{1/2}$ equals $\beta = -\sqrt{2}$, while, for transitions $p_{1/2} \to p_{1/2}$ of an electron, $\beta = +\sqrt{2}$.

The internal potential of an M1 electron transition may be represented by the series

$$\mathbf{A}_{in}(\mathbf{r}) = ie\left(\sum_M \sqrt{4\pi} C^{j_1\mu_1}_{j_2\mu_2 1M} \mathbf{Y}^0_{1M}(\mathbf{r})\right) \sum_{\varkappa=1} B_{2\varkappa+1}\left(\frac{r}{R_0}\right)^{2\varkappa+1}, \qquad (5)$$

where all coefficients $B_{2\kappa+1}$ are real.

The series in κ converges rapidly, so that, for the estimate of the potentials, it is sufficient to limit ourselves to one term with $\kappa = 1$. For the transitions $K \to s_{1/2}$, $LI \to s_{1/2}$, and $LII \to p_{1/2}$, the required coefficients B_3 are given by the equations

$$\begin{aligned}
B_3(K \to s_{1/2}) &= -\frac{\sqrt{2}}{30}\,[3Ze^2 + (\varepsilon_1 + \varepsilon_2 - 2)\,R_0]\,A(K)\,A(s_{1/2})\,R_0^2,\\
B_3(LI \to s_{1/2}) &= -\frac{\sqrt{2}}{30}\,[3Ze^2 + (\varepsilon_1 + \varepsilon_2 - 2)\,R_0]\,A(LI)\,A(s_{1/2})\,R_0^2,\\
B_3(LII \to p_{1/2}) &= -\frac{\sqrt{2}}{30}\,[3Ze^2 + (\varepsilon_1 + \varepsilon_2 + 2)\,R_0]\,A(LII)\,A(p_{1/2})\,R_0^2.
\end{aligned} \qquad (6)$$

Neglecting the screening effect, we find the amplitudes of electrons in the K, LI, LII, $s_{1/2}$, and $p_{1/2}$ states to be

$$\begin{aligned}
A(K) &= -\left[\frac{(1+\varepsilon_1)}{2\Gamma(2\gamma+1)}\right]^{1/2} (2Ze^2)^{\gamma+1/2} R_0^{\gamma-1} \exp(-Ze^2R_0),\\
A(LI) &= -\left[\frac{(1+\varepsilon_1)(2\gamma+1)}{N(N+1)\Gamma(2\gamma+1)}\right]^{1/2} \left(\frac{2Ze^2}{N}\right)^{\gamma+1/2} R_0^{\gamma-1} \exp\left(-\frac{Ze^2R_0}{N}\right),\\
A(LII) &= -\left[\frac{(1-\varepsilon_1)(2\gamma+1)}{N(N-1)\Gamma(2\gamma+1)}\right]^{1/2} \left(\frac{2Ze^2}{N}\right)^{\gamma+1/2} R_0^{\gamma-1} \exp\left(-\frac{Ze^2R_0}{N}\right),\\
A(s_{1/2}) &= -\left[\frac{\varepsilon_2+1}{\pi p}\right]^{1/2} \frac{(2p)^\gamma\,|\Gamma(\gamma + iZe^2\varepsilon_2/p)|}{\Gamma(2\gamma+1)} R_0^{\gamma-1} \exp\left(\frac{\pi Ze^2\varepsilon_2}{2p}\right),\\
A(p_{1/2}) &= -\left[\frac{\varepsilon_2-1}{\pi p}\right]^{1/2} \frac{(2p)^\gamma\,|\Gamma(\gamma + iZe^2\varepsilon_2/p)|}{\Gamma(2\gamma+1)} R_0^{\gamma-1} \exp\left(\frac{\pi Ze^2\varepsilon_2}{2p}\right).
\end{aligned} \qquad (7)$$

where

$$\gamma = \sqrt{1 - Ze^2}, \qquad N = \sqrt{2 + 2\gamma}, \qquad p = \sqrt{\varepsilon_2^2 - 1},$$

and p is the electron momentum.

3. GENERAL FORMULA FOR THE INTERNAL CONVERSION COEFFICIENT IN M1 TRANSITIONS OF THE NUCLEUS, TAKING THE DYNAMIC EFFECT OF THE NUCLEAR VOLUME INTO ACCOUNT

Using Eqs. (3) and (5) for the potentials $\mathbf{A}_{\text{ex}}$ and $\mathbf{A}_{\text{in}}$ and the normalized potential of the M1 quantum, we obtain a general formula for the internal conversion coefficient (ICC), valid for nuclear transitions $I_1M_1 \rightarrow I_2M_2$ with an arbitrary transition energy ω and an arbitrary selection rule

$$\text{ICC} = \frac{\pi e^2}{3\omega} |\mathfrak{M}|^2 \Bigg| 1 + \sum_{\varkappa=1}^{\infty} \frac{B_{2\varkappa+1}}{\mathfrak{M}} \frac{\langle I_2M_2 | (r/R_0)^{2\varkappa+1} (\mathbf{j}_N \mathbf{Y}^0_{1M}) | I_1M_1 \rangle}{\langle I_2M_2 | j_1(\omega r) (\mathbf{j}_N \mathbf{Y}^0_{1M}) | I_1M_1 \rangle} \Bigg|^2 . \tag{8}$$

Neglecting the contribution of $\mathbf{A}_{\text{in}}(\mathbf{r})$, we find the usual value of the internal conversion coefficient, as listed, for example, by Sliv[6]

$$(\text{ICC})_0 = \pi e^2 |\mathfrak{M}|^2 / 3\omega, \tag{9}$$

and hence we determine the absolute value of the integral $\mathfrak{M}$ expressed in terms of the listed quantity $(\text{ICC})_0$

$$|\mathfrak{M}| = \sqrt{3\omega (\text{ICC})_0 / \pi e^2}. \tag{10}$$

It is important to note that the integral $\mathfrak{M}$ is a complex quantity, and Eq. (10) only enables us to find its absolute value, leaving the phase φ undetermined. Only in the case $\omega \ll Ze^2$, where we can limit ourselves to the approximation $h_1'(\omega r) \approx 1/i(\omega r)^2$, is the integral $\mathfrak{M}$ real. In the general formula for the internal conversion coefficient obtained by Church and Weneser[2] and afterwards used by Reiner[7] in the analysis of the anomalies of the internal conversion coefficient in M1 transitions of odd deformed nuclei, the phase φ of the integral $\mathfrak{M}$ has been neglected. In transitions $I_1 \rightarrow I_2$ of even-even nuclei, we have as a rule $\omega \approx Ze^2$ or $\omega > Ze^2$, so that, in the analysis of the internal conversion coefficient in these transitions, it is necessary to take the phase φ into account.

Taking into account that, in the usual nuclear transitions, the condition $\omega R_0 \ll 1$ is always satisfied, and limiting ourselves to the first term of the series in κ, we obtain a more convenient formula for the internal conversion coefficient in M1 nuclear transitions:

$$\text{ICC} = (\text{ICC})_0 \left| 1 + \frac{B_3}{\omega R_0} \sqrt{\frac{3\pi e^2}{\omega (\text{ICC})_0}} e^{-i\varphi} X \right|^2, \tag{11}$$

where

$$X = \frac{\langle I_2M_2 | (r/R_0)^3 (\mathbf{j}_N \mathbf{Y}^0_{1M}) | I_1M_1 \rangle}{\langle I_2M_2 | (r/R_0) (\mathbf{j}_N \mathbf{Y}^0_{1M}) | I_1M_1 \rangle} . \tag{12}$$

The quantities B_3 are determined by Eqs. (6) and (7).

4. ESTIMATE OF X FOR M1 TRANSITIONS OF EVEN-EVEN NUCLEI IN MODELS WITH COLLECTIVE QUADRUPOLE EXCITATION

Both in the vibrational nuclear model[3] and in the rotator model,[3,8] the transition current in the nucleus $\mathbf{j}_N$ is determined in the hydrodynamical approximation by the flow velocity of the nuclear liquid

$$\mathbf{V} = \frac{1}{2} \sum_m \dot{\alpha}_{2m} \nabla (r^2 Y_{2m}), \tag{13}$$

where α_{2m} are the parameters of nuclear deformations in the laboratory coordinate system:

$$R(\vartheta, \varphi) = R_0 \left[1 + \alpha_0 + \sum_m \alpha_{2m} Y_{2m} \right].$$

In this approximation for the ratio X, we have

$$X = \frac{\langle I_2M_2 | \hat{J}^{(3)}_{1M} | I_1M_1 \rangle}{\langle I_2M_2 | \hat{J}^{(1)}_{1M} | I_1M_1 \rangle}, \tag{14}$$

where

$$J^{(\varkappa)}_{1M} = \int d\Omega \int_0^{R(\vartheta,\varphi)} dr r^2 \left(\frac{r}{R_0} \right)^{\varkappa} \sum_m \dot{\alpha}_{2m} (\mathbf{Y}^0_{1M} \nabla r^2 Y_{2m}). \tag{15}$$

Integrating Eq. (15) and retaining only the first term in $\alpha_{2\mu}$ which gives a nonvanishing matrix element of the M1 transition, we obtain for the operator $\hat{J}^{(\kappa)}_{1M}$ the equation

$$\hat{J}^{(\varkappa)}_{1M} = (\varkappa + 3) \frac{3\sqrt{5}}{8\pi} R_0^4 C^{20}_{20\,20} \sum_{m\nu\mu_1\mu_2} C^{2\nu}_{2m1M} C^{2\nu}_{2\mu_1 2\mu_2} \dot{\alpha}_{2m} \alpha^*_{2\mu_1} \alpha^*_{2\mu_2}. \tag{16}$$

Equation (16) is valid for any model with a collective quadrupole excitation, and is valid as long as the current $\mathbf{j}_N$ is determined by the velocity (13). In the rotator model, the operators $\dot{\alpha}_{2m}$ and $\alpha_{2\mu}$ are acting on the angles of orientation of the deformed nucleus in space, while, in the vibrational model (harmonic or anharmonic), $\dot{\alpha}_{2m}$ and $\alpha_{2\mu}$ are expressed in terms of phonon creation and destruction operators. However, independent of the actual choice of the operators $\dot{\alpha}_{2m}$ and $\alpha_{2\mu}$, we find the ratio X for the collective models to be $X = 3/2$.

5. CONCLUSIONS

1. For collective M1 transitions in even-even nuclei, the ratio of the matrix elements of M1 transitions is $X = 3/2$, independent of the actual model used.

2. Since $\mathbf{A}_{\text{in}} \approx Ze^2 (R_0 Ze^2)^{2\gamma - 1} \mathbf{A}_{\text{ex}}$ and

$X = {}^3/_2$, the correction to the internal conversion coefficient in collective M1 transitions of even nuclei has an order of magnitude of $Ze^2(R_0Ze^2)^{2\gamma-1}$, i.e., ~ 1%, and consequently no anomaly, as compared with the listed values of $(ICC)_0$, should be observed in the internal conversion coefficient of collective M1 transitions.

---

[1] D. P. Grechukhin, JETP **33**, 183 (1957), Soviet Phys. JETP **6**, 144 (1958).

[2] E. L. Church and J. Weneser, Phys. Rev. **104**, 1382 (1956).

[3] Alder, Bohr, Huus, Mottelson, and Winter, Revs. Modern Phys. **28**, 432 (1956).

[4] A. S. Davydov and G. F. Filippov, JETP **35**, 440 (1958), Soviet Phys. JETP **8**, 309 (1959).

[5] Berestetskii, Dolzhnov, and Ter-Martirosyan, JETP **20**, 527 (1950).

[6] L. A. Sliv and I. M. Band, Коэффициенты внутренней конверсии γ-излучения (Internal Conversion Coefficients of γ Radiation), U.S.S.R. Academy of Sciences, 1956.

[7] A. S. Reiner, Nucl. Phys. **5**, 544 (1958).

[8] A. S. Davydov and G. F. Filippov, JETP **35**, 703 (1958), Soviet Phys. JETP **8**, 488 (1959).

Translated by H. Kasha
199

SOVIET PHYSICS JETP VOLUME 13, NUMBER 4 OCTOBER, 1961

THE MAXIMUM CHARGE FOR GIVEN MASS OF A BOUND STATE

V. N. GRIBOV, Ya. B. ZEL'DOVICH and A. M. PERELOMOV

Submitted to JETP editor November 16, 1960

J. Exptl. Theoret. Phys (U.S.S.R.) 40, 1190-1198 (April, 1961)

Using dispersion relations, we give an elementary derivation of the inequality restricting the charge, which was found by Ruderman and Gasiorowicz.[2] The maximum charge corresponds to our notion of a composite particle. A field-theoretic nonrelativistic model is treated; it is shown that the physical (renormalized) charge tends to its maximum value when the bare charge increases without limit (for a fixed mass of the particle). The scattering then corresponds to the theory of the deuteron. In this same model, with an unstable particle, as the charge increases without limit the scattering tends toward zero.

1. INTRODUCTION

If a system of two particles A and B is capable of transforming into a stable particle D, the interaction A + B ⇄ D is characterized by a "charge" g. The mass of D determines the position of the pole in the amplitude for scattering of A by B.

From the definition of the physical charge g, the pole term is

$$A = -\frac{mg^2}{2\pi(E_{AB} - m_D c^2)} = -\frac{g^2}{E'_{AB} + Q}\,\frac{m_A m_B}{2\pi(m_A + m_B)}, \quad (1.1)$$

where E'_{AB} is the energy omitting the rest mass, and Q is the binding energy of D. On the other hand, as was first shown by Heisenberg,[1] the residue at the pole of a bound state can be expressed in terms of the constant in the asymptotic form of the normalized wave function:

$$\psi(r) \to Ce^{-\varkappa r}/2\pi\sqrt{2}\,r \quad (1.2)$$

for $r \to \infty$, where $\kappa = \sqrt{2mQ}$,

$$\operatorname{Res} A = -|C|^2/4\pi m. \quad (1.3)$$

This relation holds also when the state of the physical particle D is a superposition of the "bare" particle D_0 and the "cloud" A + B, which for the case of an S state is described by the function $\psi(r)$.

If the interaction is local, expression (1.1) holds for any r > 0, and the normalization condition (including the amplitude for the bare particle D_0) gives:

$$\int|\psi|^2 dv = |C|^2/4\pi\varkappa \leqslant 1. \quad (1.4)$$

By using (1.3) and (1.1), Ruderman and Gasiorowicz[2] then obtained the inequalities

$$-\operatorname{Res} A \leqslant \varkappa/m = \sqrt{2Q/m},$$

$$g^2 \leqslant 2\pi\varkappa/m^2 = 2\pi\sqrt{2Q/m^3} \quad (1.5)$$

(we give their formulas for the simplest case of an S wave and zero range of interaction).

Exact equality in (1.5), upon which Landau[3] insists, corresponds to the case where the particle D consists entirely of A + B (so that $\int|\psi|^2 dv = 1$), i.e., D is a composite particle with local interaction of A and B. There do exist in nature weak interactions, whose charge is several orders of magnitude less than its maximum value. At the present time, theory is not in a position to predict the fact that there exists no interaction intermediate in charge value between the weak and the electromagnetic interactions, on the one hand, and the strong interactions (π- and K-mesonic interactions) on the other. Thus Landau's statement should be regarded not as a theoretical derivation, but rather as a hypothesis.

The inequalities (1.5) can be derived by means of dispersion relations, without using any pictorial representations of the cloud A + B (cf. reference 1 and the second section of the present paper).

In Sec. 3 we treat the properties of a system with the maximum residue. In the real case of two particles whose interaction is described by an attractive potential U(r), the inequality (1.5) is violated. The residue A is greater than κ/m, for example in the case of the deuteron the residue is 1.5 times greater than κ/m.

A proof of this and an explanation of the violation in the language of dispersion relations is given in Sec. 4.

Finally, in Sec. 5 we give the results of a computation of a nonrelativistic field model with three elementary particles A, B and D; for a given physical (renormalized) mass of D, we give the expression for the physical renormalized charge g, satisfying the inequality (1.5). For the case of a single channel $D \rightleftarrows A + B$, and for increase to infinity of the bare (unrenormalized) charge, g^2 tends to its upper limit. The presence of several channels does not change this conclusion.

In Appendix I we present the computations whose results are given in Sec. 5. In Appendix II we consider the case of an unstable particle D; in this case, when the bare charge goes to infinity, the pole (which is on the second sheet of the complex energy plane) goes out to infinity, and the scattering amplitude tends to zero; in the limit of strong interaction, unstable particles do not have to be considered.

2. DISPERSION RELATIONS

Let us consider the elastic S-scattering of spinless particles A and B; in order to fix the notation, we write some familiar formulas:

$$\psi_S \to \frac{1}{2ikr}\left(-e^{-ikr} + S(k)\,e^{ikr}\right) \quad \text{as} \quad r \to \infty;$$

$$A = (S-1)/2ik, \qquad h = -1/A. \qquad (2.1)$$

If we assume that A is an analytic function in the complex E plane, with a cut along the positive real axis $E > 0$, with poles for $E < 0$, and with no singular points at infinity, then from the unitarity condition $\mathrm{Im}\,A = k\,|A|^2$ it follows that h is an R-function[4] and has the form

$$h(E) = \alpha + i\sqrt{2mE} + \beta E - \sum \frac{R_n}{T_n + E}, \qquad (2.2)$$

since it is easily shown that, for example, the functions E^n, $1/(T_n + E)^n$ where $n \neq 1$, and $\ln(E - E_0)$ are not R-functions. In Eq. (2.2), α, β, R_n and T_n are real and, in addition, β, R_n and T_n are positive.

On the negative real axis

$$h(E) = \alpha - \sqrt{2m\,|E|} + \beta E - \sum \frac{R_n}{T_n + E}. \qquad (2.3)$$

If $h(E_0) = 0$, where E_0 is real and negative ($E_0 = -Q$), then to this E_0 there corresponds a pole of A:

$$A = -\left(\frac{dh}{dE}\right)^{-1}_{E=-Q} \frac{1}{E+Q}. \qquad (2.4)$$

It is obvious that

$$\left.\frac{dh}{dE}\right|_{E=-Q} = \sqrt{\frac{m}{2Q}} + \beta + \sum \frac{R_n}{(T_n - E)^2} \geqslant \sqrt{\frac{m}{2Q}}, \qquad (2.5)$$

and consequently the residue of A at this pole is

$$|\mathrm{Res}\,A|_{E=-Q} \leqslant \sqrt{2Q/m} = \varkappa/m. \qquad (2.6)$$

Thus the residue of A at the pole corresponding to the bound state is negative, and its absolute value is below an upper limit which depends only on the position of the pole.

From Eq. (1.1) we see that the dispersion relations give a definite upper limit for the interaction constant,

$$g^2 \leqslant 2\pi\varkappa/m^2. \qquad (2.7)$$

This upper limit depends only on the masses of the particles A, B, and D. It is easily shown that the presence of inelastic processes only lowers this upper limit.

3. PROPERTIES OF A SYSTEM AT THE MAXIMUM OF THE RESIDUE

For a given location of the pole, i.e., for a fixed value of Q, the maximum value of the residue is reached for $\beta = R_n = 0$. Consequently, at the maximum of the residue, using the fact that $h(-Q) = 0$, the expression for h reduces to

$$h = \alpha + i\sqrt{2mE} = \sqrt{2mQ} + i\sqrt{2mE} = \varkappa + ik,$$

$$k = \sqrt{2mE}. \qquad (3.1)$$

This expression for h corresponds to the classical theory of Bethe and Peierls for the neutron-proton triplet scattering, in which the whole scattering is determined by the binding energy of the deuteron. In other words, at the maximum of the residue we get an expression which corresponds to the scattering by a singular potential well of small radius and large depth, at whose boundary, for $r = r_0$, $r_0 \to 0$, we get the condition

$$d \ln r\psi / dr = -\varkappa \qquad (3.2)$$

for the wave function.

Actually, we have from (2.1):

$$A = -\frac{1}{\varkappa + ik} = -\frac{\sqrt{2mQ} - i\sqrt{2mE}}{2m(E+Q)},$$

$$\sigma = 4\pi\,|A|^2 = 4\pi\,\frac{1}{k^2 + \varkappa^2}. \qquad (3.3)$$

According to the expression (3.3) for $A(E)$, the residue at the pole $E = -Q$ is

$$\mathrm{Res}\,A = -\sqrt{2Q/m} = -\varkappa/m. \qquad (3.4)$$

From (1.3) it follows that

$$|C|^2_{max} = 4\pi\varkappa. \qquad (3.5)$$

This value of $|C|^2$ is distinguished by the fact that if we substitute it into the asymptotic expression for $|\psi|^2$ and integrate over all space we get unity:

$$\int |\psi|^2 dv = 1. \qquad (3.6)$$

It is obvious that for a local interaction $|C|^2$ cannot in actuality exceed the limit corresponding to (3.5). It is however not a trivial point that this assertion is already contained implicitly in the arguments leading to (1.5) and (3.4).

4. POTENTIAL SCATTERING AND DISPERSION RELATIONS

In the preceding section it was shown that the maximum possible value of the residue of A corresponds to scattering by a singular (i.e., essentially local) potential with a bound level at a given energy $E = -Q$. Let us now consider a potential well of finite extension r_0, which has a bound level with this same energy $E = -Q$. Outside the well, where $r > r_0$, the wave function can be written in the form of (1.2). But inside the well it is obvious that

$$\psi < Ce^{-\varkappa r} / 2\pi \sqrt{2}\, r. \qquad (4.1)$$

Consequently, normalizing the function, we get

$$1 = \int |\psi|^2 dv < |C|^2 / 4\pi\varkappa, \qquad |C|^2 > 4\pi\varkappa. \qquad (4.2)$$

Thus, for scattering by an extended potential well, the result (2.7) which is a consequence of the dispersion relations, is violated.

From this it is clear that in the preceding arguments, which led to (1.5) and (2.7), the assumption of analyticity (absence of singular points at infinity) implied locality of the interaction. Nonlocal interaction necessarily results in such behavior of the functions A and h at infinity which violates the relations of Sec. 1 and 2. We note that in a relativistic theory the scattering amplitude is given on a plane with two cuts; on the right cut the sign of the imaginary part of the function coincides with the sign of the imaginary part of the argument, while on the left cut the sign of the imaginary part of the function is not determined. As a result the scattering amplitude cannot be an R-function, and inequality (1.4) may be violated. In particular, this inequality is violated for the deuteron.

5. INTERACTION WITH AN INTERMEDIATE PARTICLE

Let us consider in more detail a model of scattering according to the scheme $A + B \rightarrow D \rightarrow A' + B'$, with a given mass of the particle D. Basically such a model is close to the familiar Lee model.[5] The only difference is that, since we are not considering antiparticles, we must require a consistent nonrelativistic treatment of the problem.[6,7] One then introduces into the theory the mass μ and charge f (interaction constant) of the "bare" particle D_0, and the concept of the wave function α of the bare particle D_0. In such a model the only divergent quantity is the bare mass μ, and one can in an elementary fashion carry out the renormalization of the charge and mass, and compute the scattering $A + B \rightarrow A' + B'$ as a second-order process.

The computation is presented in Appendix I; here we give only the results.* We fix the renormalized mass of the physical particle D according to (1.1), so that the position of the pole in the scattering amplitude as a function of the energy E of the particles A + B is fixed. The result expressed in terms of the bare charge f is

$$h = \varkappa + (2\pi / mf^2)\, Q + i\sqrt{2mE} + (2\pi / mf^2)\, E. \qquad (5.1)$$

This form of h agrees with the general formula (2.2).

We get the corresponding A(E) by separating out the pole at $E = -Q$:

$$A = -\frac{mf^2/2\pi}{1 + m^2f^2/\pi\,(\sqrt{2mQ} - i\sqrt{2mE})}\,\frac{1}{E+Q}. \qquad (5.2)$$

We obtain the residue by making the substitution

$$\sqrt{2mE} \rightarrow i\sqrt{2mQ} = i\varkappa \quad \text{for} \quad E \rightarrow -Q \qquad (5.3)$$

in the denominator. We have

$$\operatorname{Res} A = -mf^2/2\pi\,(1 + m^2f^2/2\pi\varkappa^2). \qquad (5.4)$$

We then see that the model with the D particle actually leads, in agreement with (1.5), to

$$|\operatorname{Res} A| \rightarrow \varkappa/m = |\operatorname{Res} A|_{max} \quad \text{as} \quad f^2 \rightarrow \infty. \qquad (5.5)$$

(To save space we write f^2 in place of $|f|^2$.)

The scattering amplitude A as a function of the complex variable $k = \sqrt{2mE}$ in formula (4.3) has another pole in the lower k halfplane at

$$k = -i\,(\varkappa + m^2f^2/\pi). \qquad (5.6)$$

This second pole does not fall on the sheet in the complex E plane which we are considering.

The wave function of the physical particle D can be written as a superposition of the bare particle D_0 and the cloud A + B. The normalized function has the form

---

*In Appendix II we give the formulas for the case of an unstable particle (cf. reference 7). In that case A has two complex conjugate poles on the second energy sheet, and no pole at all on the sheet considered here. There is then no limit in which the formulas go over into the familiar expressions for the singular scattering from a virtual level (i.e., into formulas like those for the singlet n–p scattering).

$$D^+|0\rangle = \left\{ D_0^+|0\rangle - \frac{mf}{2\pi}\frac{e^{-\varkappa r}}{r} A^+B^+|0\rangle \right\}\left[1 + \frac{m^2f^2}{2\pi\varkappa}\right]^{-1/2}, \quad (5.7)$$

so that the constant C, which characterizes the asymptotic behavior of the wave functions, is

$$C = -\frac{mf\sqrt{2}}{\sqrt{1 + m^2f^2/2\pi\varkappa}},$$

$$|C|^2 = \frac{2m^2f^2}{1 + m^2f^2/2\pi\varkappa} = -4\pi m \operatorname{Res} A, \quad (5.8)$$

in agreement with (1.3).

The renormalized coupling constant (charge) g characterizes the interaction of A + B with the physical particle D, unlike the bare charge f which characterizes the interaction of A + B with the bare particle D_0. We find for g:

$$g = f/\sqrt{1 + m^2f^2/2\pi\varkappa} \leqslant \sqrt{2\pi\varkappa}/m, \quad (5.9)$$

where equality is reached for f → ∞. In a local Hermitian theory, $|f|^2 > 0$ and this limit for g cannot be exceeded.

Formulas (5.5) – (5.9) make clear the physical meaning of the maximum value of |Res A| and the coupling constant g, which we obtained earlier from the dispersion relations. These limiting values are attained when the bare constant f increases without limit. Then the fraction of bare particle D_0 in the physical particle D tends to zero, and in the limit the physical particle D "consists" entirely of A + B. Thus the limiting value of Res A corresponds to the transition to a composite model for the particle D, consisting of locally coupled particles A and B.

As we see in particular from (5.1) and (5.2), in the limit as $f^2 \to \infty$, the theory of the scattering as a second order process $A + B \to D \to A' + B'$ gives results which are identical with those for potential scattering by a singular potential with a fixed position of the discrete level at E = – Q. A measure of how close one is to the limit is the closeness to unity of the fraction of A + B in the amplitude for the physical particle D; at the same time the fraction of D_0 in D tends to zero. Essentially the particle D_0 as such drops out, and only plays the role of a carrier of the local interaction coupling A and B into the physical particle D.

The condition for being close to the limit can be expressed as

$$f^2 \gg 2\pi\varkappa/m^2 = 2\pi\sqrt{2Q/m^3}. \quad (5.10)$$

Thus we see that the closer the pole (i.e., the smaller the value of Q), the sooner (i.e., the smaller the value of f) we get the limiting relations characteristic of the composite model.

APPENDIX I

SOLUTION OF THE EQUATIONS FOR THE CASE OF A STABLE INTERMEDIATE PARTICLE

We try to find a wave function of the form

$$\Phi = \alpha D_0^+|0\rangle + \psi(r) A^+B^+|0\rangle. \quad (I.1)$$

We choose as the zero of energy the rest energy of the particles A and B: $(m_A + m_B)c^2$. The Schroedinger equation for a stationary state with energy E has the form

$$E\alpha = \mu\alpha + f\psi(\rho), \quad (I.2)$$

$$E\psi(r) = -(1/2m)\,\Delta\psi(r) + f\alpha\delta(\mathbf{r}). \quad (I.3)$$

The quantity ρ is introduced in (I.2) as a cutoff radius; after mass renormalization, we let $\rho \to 0$.

We find a solution corresponding to a bound state with energy $E = -Q = -\kappa^2/2m$:

$$\psi(r) = Ce^{-\varkappa r}/2\pi\sqrt{2}r,$$

$$\Delta\psi = \varkappa^2\psi - (4\pi/2\pi\sqrt{2})\,C\delta(\mathbf{r}). \quad (I.4)$$

Substituting in (I.3), we obtain

$$C = -fm\sqrt{2}\alpha. \quad (I.5)$$

Strictly speaking, if we take $\psi(\rho)$ in (I.2) to be completely general, so that

$$\int\psi(r)\,K(r)\,dv, \qquad \int K(r)\,dv = 1, \qquad \int\frac{K(r)}{r}\,dv = \frac{1}{\rho}$$

we should accordingly change the form of the source term in (I.3), replacing $\delta(\mathbf{r})$ by $\delta_1(r - \rho)/4\pi\rho^2$ or by $K(r)[\delta_1(r - \rho)$ is the one dimensional Dirac function, and not the three-dimensional $\delta(\mathbf{r})$ for which $\int\delta(\mathbf{r})\,dv = 1$]. However it is easy to see that these corrections are of higher order in ρ than those retained in (I.2) since, for example, when we replace $\delta(\mathbf{r})$ by $\delta_1(r - \rho)/4\pi\rho^2$ the solution has the form

$$\psi(r) = Ce^{-\varkappa r}/2\pi\sqrt{2}r, \qquad r > \rho,$$
$$\psi(r) = F(e^{+\varkappa r} - e^{-\varkappa r})/2\pi\sqrt{2}r, \qquad r < \rho.$$

We substitute this solution in (I.3), in which $\delta(\mathbf{r})$ has been replaced by $\delta_1/4\pi\rho^2$ and use $\psi(\rho - 0) = \psi(\rho + 0)$. We find

$$\Delta\psi|_{r=\rho} = [(d\psi/dr)_{\rho+0} - (d\psi/dr)_{\rho-0}]\,\delta_1(r - \rho).$$

Expanding in powers of the small quantity $\kappa\rho$, we find that there are no corrections of order $\kappa\rho$, while we neglect the correction of order $(\kappa\rho)^2$. This gives the result (I.4) and (I.5), which is the solution of (I.3) with $\delta(\mathbf{r})$.

We expand $\psi(\mathbf{r})$ in powers of ρ and drop terms

$\sim \rho$. Substituting in (I.2), we find

$$-Q\alpha = -(\varkappa^2/2m)\alpha = \mu\alpha - (f^2 m\alpha/2\pi)(1/\rho - \varkappa), \qquad (I.6)$$

$$\mu = f^2 m/2\pi\rho - f^2 m\varkappa/2\pi - \varkappa^2/2m. \qquad (I.7)$$

Normalization of the bound state, $\alpha^2 + \int |\psi|^2 dv = 1$, gives the value of α_b (where the subscript b denotes a bound state):

$$\alpha_b = 1/\sqrt{1 + m^2 f^2/2\pi\varkappa}. \qquad (I.8)$$

The complete expression for the wave function is given in (5.7).

We now go on to the scattering problem. We look for a solution of Eqs. (I.2) and (I.3), with $E = k^2/2m$, in the form

$$\Phi = \alpha \overset{+}{D_0} |0\rangle + \frac{1}{2ikr}(-e^{-ikr} + Se^{ikr}) A^+ B^+ |0\rangle. \qquad (I.9)$$

Substituting such a ψ [cf. Eq. (I.1)] in (I.2), we get

$$\frac{k^2}{2m}\alpha = \mu\alpha + \frac{f}{2ik}\frac{S-1}{\rho} + \frac{f}{2}(S+1). \qquad (I.10)$$

Equation (I.3) gives*

$$0 = (\pi/mik)(-1 + S)\,\delta(\mathbf{r}) + f\alpha\delta(\mathbf{r}),$$

$$\alpha = -(\pi/fmik)(S-1). \qquad (I.11)$$

We substitute the value of α from (I.11) and the value of μ from (I.7) into (I.10). Then the terms in ρ^{-1} cancel, which means a renormalization of the theory for $\rho \rightarrow 0$, $\mu \rightarrow \infty$, but the results concerning scattering tend to a limit which is independent of the cutoff radius as $\rho \rightarrow 0$. At the same time the bare mass μ of the bare particle D_0 is eliminated from the equations, and the result contains the quantity κ which depends on the energy (mass) of the physical particle D.

After an elementary computation we find

$$\frac{1+S}{1-S} = \frac{\varkappa}{ik} + \frac{1}{ik}\frac{\pi}{m^2 f^2}(k^2 + \varkappa^2), \qquad (I.12)$$

from which we get the limiting formulas (5.1) and (5.2).

We determine the coupling constant g of the particles A and B to form the physical particle D by taking the product of the coupling constant f to the bare particle D_0 and the amplitude α of the bare particle D_0 in the physical particle D. Using (I.8), we get (5.9).

APPENDIX II

SOLUTION OF THE EQUATIONS WITH AN UNSTABLE INTERMEDIATE PARTICLE AND COMPARISON OF THE SOLUTIONS WITH THE CASE OF SINGULAR SCATTERING.

We shall assume that the nonstationary Schrödinger equation has a solution which has an exponential time dependence, i.e., $\sim e^{-iE_0 t}$ with a complex E_0, characterizing the fact that the spatial part of the solution describing the particles A and B contains only an outgoing wave, i.e. $\psi \sim r^{-1} e^{ik_0 r}$. Then k_0 also turns out to be complex. For such an exponential solution, even though it is not stationary, we can again use Eqs. (I.2) and (I.3).

The general behavior of the solution is the same as for the case of a stable D. We assume that the properties of the physical unstable state and E_0 and k_0 are known ($E_0 = k_0^2/2m$), and by using the equations we express the nonphysical value of the bare mass μ in terms of the physical complex E_0, the charge f and the cutoff radius ρ. We then go on to the scattering problem, i.e. to the problem with arbitrary real positive k, with incoming and outgoing waves, and find the scattering amplitude. We use the value of μ expressed in terms of E_0, f, and ρ; as before, the terms in $1/\rho$ vanish, the computation gives a definite limit as $\rho \rightarrow 0$ and $\mu \rightarrow \infty$.

However we must make two remarks. The result for our case cannot be obtained by formally replacing κ by $-ik_0$ in the corresponding formula for a stable particle, since the bare mass μ, even though it is an unphysical quantity, contains a term in $1/\rho$, so that $\mu \rightarrow \infty$ when $\rho \rightarrow 0$; on the other hand, μ must be real in order for the Hamiltonian to be Hermitian and to guarantee unitarity; the formal replacement of κ by $-ik_0$ in (1.7) violates the reality of μ.

The second remark is purely methodological. It is simply that it is convenient to choose $k_0 = v - iw$ as the starting quantity, and express the answer in terms of the positive real quantities v and w.

So for an unstable state,

$$\psi(r) = Ce^{ivr + wr}/2\pi\sqrt{2}\,r, \quad E_0 = (v^2 - w^2)/2m - vwi/m. \qquad (II.1)$$

We substitute (II.1) in (I.3), after which the terms $E_0\psi$ and $-(\Delta/2m)\psi$ again cancel and we once more obtain the relation (I.5) between C and α.

In analogy to (I.6), we have

$$\psi(\rho) = -(fm\alpha/2\pi)(1/\rho + w + iv). \qquad (II.2)$$

Substituting (II.2) in (I.2), we obtain

$$\mu = E_0 + (f^2 m/2\pi)(1/\rho + w + iv)$$
$$= (v^2 - w^2)/2m - vwi/m + (f^2 m/2\pi)(1/\rho + w + iv). \qquad (II.3)$$

In contrast to (I.7), this equation is complex. Since μ is real, by treating the imaginary part of (II.3) we immediately get

---

*The argument for the use of (I.3) with $\delta(\mathbf{r})$ is also valid for this case; we drop corrections of order $k^2\rho^2$.

$$w = f^2 m^2 / 2\pi. \qquad \text{(II.4)}$$

The problem with a stable particle D was characterized by two parameters Q (or κ) and f. At first glance, it seems that the problem with an unstable particle is characterized by three quantities: v, w and f; but the relation (II.4) leaves us with two parameters. To shorten the formulas we shall express f in terms of w in all succeeding work. In particular

$$\mu = \frac{v^2 - w^2}{2m} + \frac{f^2 m}{2\pi}\frac{1}{\rho} + \frac{f^2 m}{2\pi}\, w = \frac{v^2 + w^2}{2m} + \frac{w}{m}\frac{1}{\rho}. \qquad \text{(II.5)}$$

Now let us turn to the scattering problem. Equations (I.10) and (I.11) are still valid, the only change being that we use (II.5) for μ and express f in the answer in terms of w according to (II.4).

Elementary computations give

$$ik(1+S)/(1-S) = (k^2 - v^2 - w^2)/2w, \qquad \text{(II.6)}$$

$$S = (k - v - iw)(k + v - iw)/(k - v + iw)(k + v + iw). \qquad \text{(II.7)}$$

The function S, and consequently the scattering amplitude also, has two poles in the k plane, below the real axis at k = ± v − iw. There are no poles in the upper half of the k plane and on the first sheet for E. We also give the function

$$\begin{aligned} h &= ik + k^2/2w - (v^2 + w^2)/2w \\ &= i\sqrt{2mE} + 2\pi E / mf^2 - \pi v^2 / m^2 f^2 - m^2 f^2 / 4\pi. \qquad \text{(II.8)} \end{aligned}$$

For $E < 0$, all the terms in (II.8) are negative, and h has no zeros. It is curious that the model gives no pole terms in h.

It is obvious that for a ψ of the form of (2.1),

$$d \ln r\psi / dr = ik(S+1)/(S-1). \qquad \text{(II.9)}$$

Consequently the expression (I.12), which refers to a stable particle in the limit as $f^2 \to \infty$, gives

$$d \ln r\psi / dr = -\varkappa, \qquad \text{(II.10)}$$

in accordance with the classical Bethe-Peierls theory. In the case of an unstable D, the expression (II.6) gives

$$d \ln r\psi / dr = v^2/2w + w/2 - k^2/2w, \qquad \text{(II.11)}$$

which, for real v and w and positive w, cannot be transformed to the form

$$d \ln r\psi / dr = \varkappa_1, \qquad \varkappa_1 > 0, \qquad \text{(II.12)}$$

which would correspond to scattering by a singular potential with a virtual level (like the singlet neutron-proton interaction). In other words, for the case of an unstable particle the computation gives two poles in the k plane which are located symmetrically with respect to the imaginary axis, and below the real axis.

A singular potential with a virtual level corresponds to a single pole on the imaginary axis and below the real axis, at $k = -i\kappa_1$ [cf. Eq. (II.12)]. Even if we could make the two poles for the unstable particle fuse and appear at the same point $k = -i\kappa$, there would be a second order pole at this point, and the formulas would still not coincide with those for the singular potential, where the pole is of first order.

In the case of a stable particle, both poles lie on the imaginary axis and do not coincide, so that one of the poles can be moved to infinity while the other remains fixed; in the case of an unstable particle this cannot be done because of the condition of symmetry of the poles with respect to the imaginary axis. As we see from (II.4), $w \to \infty$ in the limit as $f^2 \to \infty$; substituting in (II.7), we get S = 1 for any finite k and v. Thus the theory with an unstable particle has no reasonable strong coupling limit. This constitutes the difference between it and the theory with a stable particle, which in the strong-coupling limit goes over into the theory of the deuteron.

In the present work the relation of the limiting value of g to the particle mass and to the concept of a composite particle has been investigated on an elementary nonrelativistic example. The secret hope of one of the authors is that perhaps, by using the dispersion relations, it may be possible in the future to succeed in giving a sensible formulation of the theory of composite particles (of the Fermi-Yang type[8]) in the relativistic case.

---

[1] Ning Hu, Phys. Rev. **74**, 131 (1948).

[2] M. A. Ruderman and S. Gasiorowicz, Nuovo cimento **8**, 861 (1958).

[3] L. D. Landau, JETP **39**, 1856 (1960), Soviet Phys. JETP **12**, 1294 (1961).

[4] Castillejo, Dalitz, and Dyson, Phys. Rev. **101**, 453 (1956).

[5] T. D. Lee, Phys. Rev. **95**, 1329 (1954).

[6] Ya. B. Zel'dovich, JETP **33**, 1488 (1957), Soviet Phys. JETP **6**, 1148 (1958).

[7] Ya. B. Zel'dovich, JETP **39**, 776 (1960), Soviet Phys. JETP **12**, 542 (1961).

[8] E. Fermi and C. N. Yang, Phys. Rev. **76**, 1739 (1949).

Translated by M. Hamermesh
200

SOVIET PHYSICS JETP VOLUME 13, NUMBER 4 OCTOBER, 1961

CALCULATION OF THE ELASTIC SCATTERING CROSS SECTIONS FOR 5.45 Mev PROTONS ACCORDING TO THE OPTICAL MODEL OF THE NUCLEUS

R. A. VANETSIAN, A. P. KLYUCHAREV, G. F. TIMOSHEVSKII, and E. D. FEDCHENKO

Submitted to JETP editor November 22, 1960

J. Exptl. Theoret. Phys. (U.S.S.R.) **40**, 1199-1202 (April, 1961)

The differential cross sections for the elastic scattering of 5.45 Mev protons from the separated isotopes $Cr^{52,53}$, Co^{59}, $Ni^{58,60,62,64}$, $Zn^{64,68}$, and Cu^{65} have been calculated with the help of the complex optical model potential. The real part of the potential was chosen in the Saxon form and the imaginary part in the Gaussian form. Satisfactory agreement with the experimental data has been achieved for isotopes whose (p, n) threshold is below the energy of the scattered protons. It has been impossible to make the optical model calculations consistent with the experimental data for isotopes whose cross sections increase at large angles.

THE purpose of the investigation of the elastic scattering of nucleons from nuclei with the help of the optical model is the determination of the parameters of the nuclear potential. Such investigations have been carried out by many authors;[1-3] they have led to an explanation of the basic regularities in the behavior of the angular distribution of the elastic scattering as a function of the optical model parameters. However, the calculations that have been carried out so far have mainly been concerned with the analysis of the experimental data on the elastic scattering of nucleons from targets which contain a natural mixture of isotopes.

In the present paper we report an analysis of the experimental data on the elastic scattering of 5.45-Mev protons obtained by Klyucharev and Rutkevich.[4] Analogous calculations by the authors for the proton energy 6.8 Mev have been reported earlier.[5] The difference between the present calculations and the earlier ones consists in the fact that we did not include the spin-orbit interaction for the energy 5.45 Mev.

The potential used in the calculation was chosen in the form

$$V(r) = V_{\text{coul}}(r) + V_0 f(r) + iW_0 g(r), \qquad (1)$$

where $V_{\text{Coul}}(r)$ is the potential of the Coulomb field of the nucleus; V_0 and W_0 are the real and imaginary parts of the nuclear potential, respectively; f(r) and g(r) are the form factors of the real and imaginary parts of the nuclear potential:

$$f(r) = \left[1 + \exp\left(\frac{r-k_0}{a}\right)\right]^{-1}, \qquad g(r) = \exp\left[-\left(\frac{r-k_0}{b}\right)^2\right]. \qquad (2)$$

In accordance with the results of a number of investigations,[6,7] we assume that, for a given proton energy, the Gaussian form is more reasonable physically for the imaginary part of the potential than the Saxon form. This is why we have chosen the form (2) for g(r) in the calculations.

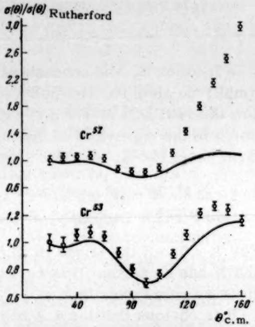

FIG. 1. Results of the calculation for $Cr^{52,53}$ at E_p = 5.4 Mev. The points indicate the experimental data with account of the statistical errors.

In the determination of the optical model parameters, one usually attempts to obtain the same set of parameters for several neighboring nuclei if the energy of the scattered nucleon is given. In the present paper, we choose as the basic criterion for the comparison of the calculated curves with the experimental ones the coincidence of the position and the depth of the minimum of the curve representing the ratio of the differential elastic cross section over the Coulomb cross section. The results of the calculations are shown in Figs. 1 – 3, where we also indicate the experimental data of Klyucharev and Rutkevich.[4] In the table we give the parameters for the calculated curves. These sets of optical model parameters for the elastic scattering at 5.45 Mev were obtained by

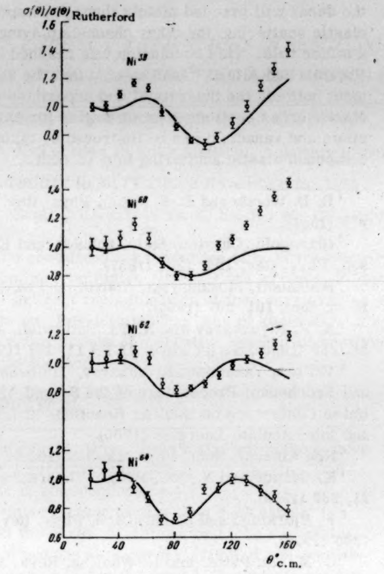

FIG. 2. Results of the calculation for $Ni^{58,60,62,64}$ at $E_p = 5.4$ Mev. The points indicate the experimental data.

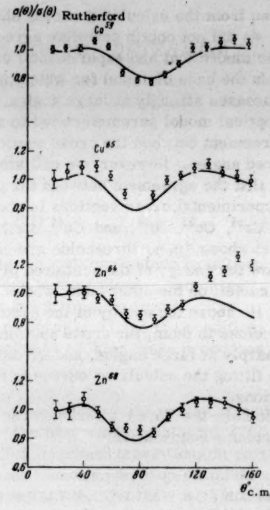

FIG. 3. Results of the calculation for Co^{59}, Cu^{65}, and $Zn^{64,68}$ at $E_p = 5.4$ Mev. The points indicate the experimental data.

the method of least squares and also by empirical methods.

It follows from previous calculations,[2,6] that the form of the differential elastic cross section curve depends practically only on the product $V_0 r_0^2$. The position and the depth of the minimum of the curve depend not only on the values of the parameters V_0 and r_0, but also on the values of the parameters a, b, and W_0. However, it was not possible to make the minima of the calculated curves agree with those of the experimental curves for different nuclei by varying only the parameters a, b, and W_0. We therefore also had to vary somewhat the value of r_0 or V_0. In particular, if we fix the value of r_0 for all nuclei, we must vary the parameter V_0. It is seen from the table that the variation of the value of V_0 reaches 5% even for the isotopes of one and the same element (for example, Ni or Zn).

We may conclude from our earlier calculations[6] that the character of the dependence of the angular distribution on the parameter b is similar to that of the dependence on the parameter W_0.

In order to minimize the ambiguities in the choice of the parameters, we have fixed the value of b at b = 1.2. With this value of b the values of W_0 that we obtained were close to the values obtained by an analysis of the elastic scattering of neutrons.[8]

We did not include the spin-orbit interaction in the present calculations, because in the absence of polarization data it was not possible to get any idea of the magnitude of the spin-orbit potential.

Element	r_0*	a	b	V_0	W_0	Element	r_0*	a	b	V_0	W_0
Cr^{52}	1.23	0.40	1.2	−60	−11.5	Ni^{62}	1.23	0.36	1,2	−60.5	−7.0
Cr^{53}	1.23	0.36	1.2	−60	−7.5	Ni^{64}	1.23	0.40	1.2	−58.5	−5.5
Co^{59}	1.23	0.35	1.2	−58	−8.5	Cu^{65}	1.23	0.36	1,2	−60.5	−6.0
Ni^{58}	1.23	0.35	1.2	−57	−3.5	Zn^{64}	1,23	0.40	1,2	−60	−5.5
Ni^{60}	1,23	0.36	1.2	−57	−8.5	Zn^{68}	1.23	0.40	1.2	−59.5	−5.5

*The potentials are given in Mev and the linear dimensions in 10^{-13} cm.

It is seen from the calculated curves shown above that we did not obtain complete agreement between the theoretical and experimental cross sections. In the case of nuclei for which the cross section increases strongly at large angles, no choice of optical model parameters led to a satisfactory agreement between the cross sections for all measured angles. However, we call attention to the fact that the agreement between the theoretical and experimental cross sections is good for the nuclei Cr^{53}, Co^{59}, Ni^{64}, and Cu^{65}, i.e., for those nuclei whose (p, n) thresholds are considerably below the energy of the scattered protons. For those nuclei, on the other hand, whose (p, n) thresholds lie above the energy of the scattered protons or close to them, the cross section increases sharply at large angles, and we did not succeed in fitting the calculated curves to these cross sections.

We quote here the (p, n) thresholds for the elements under consideration:[9]

	Cr^{52}	Cr^{53}	Co^{59}	Ni^{60}	Ni^{62}	Ni^{64}	Cu^{65}	Zn^{64}	Zn^{68}
$E_{\text{threshold}}$, Mev	5.52	1.41	1.87	6.72	4.69	2.50	2.18	8.12	3.45

Since the optical model does not take into account the compound elastic scattering (which cannot be distinguished experimentally from the "pure elastic" scattering), one may assume that the disagreement is due to a large contribution from this type of scattering. Considering the (p, n) thresholds for the above-mentioned nuclei, we may assume that, as long as the (p, n) reaction channel for the decay of the compound nucleus is closed, the decay will proceed mainly through compound elastic scattering, the other channels playing only a minor role. This conclusion was reached by Preskitt and Alford,[10] who showed that the agreement between the theoretical and experimental elastic cross sections at large angles for chromium and vanadium can be improved by taking the compound elastic scattering into account.

---

[1] R. D. Woods and D. S. Saxon, Phys. Rev. **95**, 577 (1954).

[2] Glassgold, Cheston, Stein, Schuldt, and Erickson, Phys. Rev. **106**, 1207 (1957).

[3] Melkanoff, Moszkowski, Nodvik, and Saxon, Phys. Rev. **101**, 507 (1956).

[4] A. P. Klyucharev and N. Ya. Rutkevich, JETP **38**, 285 (1960), Soviet Phys. JETP **11**, 307 (1960).

[5] Val'ter, Vanetsian, Klyucharev, Timoshevskii, and Fedchenko, Proceedings of the Second All-Union Conference on Nuclear Reactions at Low and Intermediate Energies (1960).

[6] Ken Kikuchi, Nucl. Phys. **12**, 305 (1959).

[7] K. Harada and N. Odo, Progr. Theoret. Phys. **21**, 260 (1959).

[8] F. Bjorklund and S. Fernbach, Phys. Rev. **109**, 1295 (1958).

[9] D. M. van Patter and N. Whaling, Revs. Modern Phys. **29**, 757 (1957).

[10] C. A. Preskitt and W. P. Alford, Phys. Rev. **115**. 389 (1959).

Translated by R. Lipperheide
201

SOVIET PHYSICS JETP VOLUME 13, NUMBER 4 OCTOBER, 1961

USE OF INDIRECT TRANSITIONS IN SEMICONDUCTORS FOR THE DETERMINATION OF STATES WITH NEGATIVE ABSORPTION COEFFICIENTS

N. G. BASOV, O. N. KROKHIN, and Yu. M. POPOV

P. N. Lebedev Physics Institute, Academy of Sciences, U.S.S.R.

Submitted to JETP editor November 25, 1960

J. Exptl. Theoret. Phys. (U.S.S.R.) **40**, 1203-1209 (April, 1961)

The conditions for formation of negative temperature states in semiconductors have been obtained for indirect transitions of non-equilibrium carriers in the following two cases: a) indirect recombination of free carriers and b) indirect recombination from exciton states. Possible mechanisms of absorption of radiation are considered and the conditions for appearance of a negative absorption coefficient are derived by taking these processes into account.

INTRODUCTION

At the present time, three different methods have been suggested to obtain states with negative temperature in semiconductors.[1-3]

The pulse method of obtaining such states[1] is based on the essential difference in the recombination time and the slowing-down time of non-equilibrium carriers inside the band.[4] The conditions for the appearance of states with negative temperature in this method are: a long lifetime of non-equilibrium carriers, high densities of excitation, and low temperature of the specimen.[5] All this strongly limits the selection of superconducting materials and produces a series of technical difficulties.

A method was suggested by Lax[2] of obtaining states with negative temperature in superconductors, based on the non-equidistance of the Landau levels in strong magnetic fields. The comparatively short relaxation times of the non-equilibrium carriers for these levels makes difficult the production of states with negative temperature by this method.

In the present paper a method of producing states with negative temperature in semiconductors, which was earlier suggested by the authors,[3] is investigated in detail. To accomplish this method, as will be shown, comparatively low excitation densities are required.

1. CONDITIONS FOR ESTABLISHING NEGATIVE TEMPERATURES FOR INDIRECT TRANSITIONS

Indirect transitions in semiconductors represent a recombination process or the formation of current carriers — electrons and holes — with simultaneous emission or absorption of a photon and phonons. The long wavelength edge of the absorption band for interband transitions in certain semiconductors (for example, in germanium and silicon) corresponds to precisely such processes, owing to the structure of the fundamental bands.[6,7] In these semiconductors, the minimum energy in the conduction band and the maximum energy in the valence band correspond to different values of the quasimomentum of the electron. It is obvious that the longest wavelength radiation corresponds to a transition of the electron from the minimum of the conduction band to the maximum of the valence band with the emission of a phonon.* The simultaneous absorption of a photon and a phonon is opposite in behavior to the process mentioned above.

If the temperature of the specimen is sufficiently low, and the phonons necessary for the inverse transition are absent, then the absorption of the long wavelength radiation under consideration will be small. Therefore, one can expect in this case that for comparatively small increase in the carrier concentration (in comparison with the equilibrium value) the occurrence of a state with negative temperature relative to the given transition is possible.

We shall consider this process in more detail. The number of transitions per unit time with simultaneous emission of a photon and a phonon is equal to

$$I^+ = W(n_r + 1)(\varphi + 1) f_e(\varepsilon_e) f_h(\varepsilon_h), \qquad (1)$$

---

*We shall not consider many-phonon processes since their relative probability is small.

where W is the transition probability, n_r and φ are, respectively, the number of photons and phonons in the given state, $f_e(\epsilon_e)$ and $f_h(\epsilon_h)$ are distribution functions of the electrons in the conduction band and of the holes in the valence band. The number of transitions with absorption of a photon and a phonon is equal to

$$I^- = W n_r \varphi\, [1 - f_h(\varepsilon_h)]\, [1 - f_e(\varepsilon_e)]. \tag{2}$$

The energy of the electron ϵ_e and of the hole ϵ_h are connected by the law of conservation of energy with that of the photon $\hbar\omega_r$ and of the phonon $\hbar\omega_f$ through the equation

$$\varepsilon_e + \varepsilon_h + \Delta - \hbar\omega_r - \hbar\,\omega_f = 0, \tag{3}$$

where Δ is the minimum width of the forbidden band. In the state of thermodynamic equilibrium, $I^+ - I^- = 0$, which holds if we insert the corresponding thermodynamic equilibrium distributions for n_r, φ, f_e and f_h in (1) and (2).

In order that the system be in a state with negative temperature, it is necessary to disrupt the thermodynamic equilibrium so that the induced emission exceeds the absorption, which leads to the condition

$$(\varphi + 1) f_e(\varepsilon_e) f_h(\varepsilon_h) - \varphi\, [1 - f_h(\varepsilon_h)]\, [1 - f_e(\varepsilon_e)] > 0. \tag{4}$$

Taking the temperature of the lattice equal to T° K, we get from (4)

$$f_e(\varepsilon_e) f_h(\varepsilon_h) [1 - f_h(\varepsilon_h)]^{-1} [1 - f_e(\varepsilon_e)]^{-1} > e^{-\hbar\omega_f/kT} \tag{5}$$

In the case in which there is no degeneracy of the free carriers, Eq. (5) is simplified:

$$f_e(\varepsilon_e) f_h(\varepsilon_h) > e^{-\hbar\omega_f/kT} \tag{6}$$

The electron and hole distribution functions which enter on the left side of Eq. (6) can be found by solution of the kinetic equation with account of the production of carriers by an external source, by the process of their slowing down, and by recombination. The slowing down of non-equilibrium carriers has been investigated previously,[4] where it was shown that the time for establishing thermal equilibrium between the lattice and the non-equilibrium carriers is small and, for germanium and silicon, has a magnitude of the order of 10^{-10} sec, which is significantly less than the lifetimes of the non-equilibrium carriers in these materials. Therefore, it can be assumed that the electrons and holes inside the corresponding bands have a Boltzmann distribution (no degeneracy) with a crystal temperature T. Carrying out integration on the left side of (6) over the range ~ kT of energies of electrons and holes, we get the following inequality for the concentration of electrons n and of holes p:

$$np > n_{\text{eff}}\, p_{\text{eff}}\, e^{-\hbar\omega_f/kT}, \tag{7}$$

where

$$n_{\text{eff}} = 2\left(\frac{m_e kT}{2\pi\hbar^2}\right)^{3/2} \approx 4.8\cdot 10^{15}\left(\frac{m_e}{m}T\right)^{3/2}, \quad p_{\text{eff}} = 2\left(\frac{m_h kT}{2\pi\hbar^2}\right)^{3/2}.$$

(We note that we have $n_0 p_0 = n_{\text{eff}} p_{\text{eff}} e^{-\Delta/kT}$ for the equilibrium values $n = n_0$, $p = p_0$). The conditions (7) are easily established in germanium and silicon at a temperature of T ~ 10° K, since they require that $np > 10^{22}$ ($\hbar\omega_f \sim 0.03$ ev).

We now consider the conditions for the generation of a negative temperature for indirect transitions from exciton states. The density of electrons ν_0 in the state of thermodynamic equilibrium can be determined from the condition[8] $\mu_\nu = \mu_e + \mu_h = 0$ (μ_ν, μ_e, μ_h are the chemical potentials of excitons, electrons and holes, respectively), which leads to the expression

$$\nu_0 = \nu_{\text{eff}} \exp\left\{-\frac{\Delta - U_\nu}{kT}\right\}, \tag{8}$$

or, if there is no degeneracy of free carriers,

$$\nu_0 / n_0 p_0 = \tfrac{1}{4}(m_\nu / m_e m_h)^{3/2}\, (2\pi\hbar^2/kT)^{3/2} e^{U_\nu/kT},$$

where U_ν is the binding energy of the exciton ($U_\nu > 0$), m_ν is the effective mass of the exciton, and $\nu_{\text{eff}} = (m_\nu kT/2\pi\hbar^2)^{3/2}$. The conditions for the production of a negative temperature for the indirect transition from the exciton state leads to the inequality

$$\nu > \nu_{\text{eff}}\, e^{-\hbar\omega_f/kT}. \tag{9}$$

Assuming that the additional carriers formed by the external source are in thermal equilibrium with the crystal lattice and with the exciton states of electrons and holes (which is valid, inasmuch as the probability of formation of an exciton is large in comparison with the probability of its recombination), we get for the non-equilibrium concentration of excitons

$$\nu = \nu_{\text{eff}}\, (pn / p_{\text{eff}} n_{\text{eff}})\, e^{U_\nu/kT}. \tag{10}$$

In this case, the condition for formation of a negative temperature takes the form

$$pn > p_{\text{eff}} n_{\text{eff}} \exp\left\{-\frac{\hbar\omega_f + U_\nu}{kT}\right\}, \tag{11}$$

which practically coincides with (7).

2. INDIRECT INTERBAND TRANSITIONS AND ABSORPTION OF RADIATION BY FREE CARRIERS

As was noted earlier,[5] the condition for formation of a negative absorption coefficient in a medium which is in a state with negative temperature relative to the transition under consideration is that the radiation induced by a light quantum propagating in the medium exceed the absorption of this quantum by the other levels of the system which are in a state with positive temperature.

The probability W_{ij} of indirect recombination of an electron in the state i with a hole in the state j with radiation of a photon was considered by Dumke.[9] This probability takes into account both the absorption of the phonon and its emission; however, it is evident that at the lattice temperature for which $kT \ll \hbar\omega_f$ the probability of transition with absorption of the phonon $\hbar\omega_f$ is small.

The total number of radiative transitions in a unit volume of a crystal with emission of a light quantum of frequency ω_r per unit time is equal to

$$dn/dt = \sum_{ij} W_{ij} f_e(\varepsilon_i) f_h(\varepsilon_j). \tag{12}$$

Summation in (12) should be carried out only over such values of i and j which are consistent with the conservation of energy:

$$\varepsilon_i + \varepsilon_j + \Delta = \hbar\omega_r + \hbar\omega_f. \tag{13}$$

Proceeding to a continuous spectrum, and taking into account radiation in this case for the range of frequencies from ω_r to $\omega_r + \Delta\omega$ we get the following expression for the number of quanta N radiated as a result of induced transitions per unit time in a unit volume of the specimen:

$$\left(\frac{dN}{dt}\right)^+ = n_r \hbar \Delta\omega \int W_{ij}(\varepsilon_i, \varepsilon_j)\, f_e(\varepsilon_i)\, f_h(\varepsilon_j)\, \rho(\varepsilon_i)\, \rho(\varepsilon_j)\, d\varepsilon_i, \tag{14}$$

where $\rho(\epsilon)$ is the density of states per unit energy interval, n_r the average number of quanta per radiation oscillator with frequency ω_r, and

$$N = \int_{\omega}^{\omega+\Delta\omega} n_r\, \rho(\omega)\, d\omega \approx n_r\, \rho(\omega)\, \Delta\omega.$$

In Eq. (14), ϵ_j takes on the values determined by Eq. (13). In the absence of degeneracy, and if the electrons and holes inside the corresponding bands are in thermal equilibrium with the lattice, but have non-equilibrium concentrations n and p, integration in (14) gives

$$\left(\frac{dN}{dt}\right)^+ = n_r \overline{W}_{ij} \frac{4np}{\pi kT} e^{-y} y^2 \frac{\Gamma^2(^3/_2)}{\Gamma(3)} \hbar\Delta\omega, \tag{15}$$

where $\overline{W}_{ij}$ is the mean value of the transition probability and

$$y = (\hbar\omega_f + \hbar\omega_r - \Delta)/kT.$$

The question of the line shape of spontaneous emission of a system which has the form

$$J(\omega) \sim \left(\frac{\hbar\omega_r + \hbar\omega_f - \Delta}{kT}\right)^2 \exp\left\{-\frac{\hbar\omega_r + \hbar\omega_f - \Delta}{kT}\right\} \tag{16}$$

is solved by Eq. (15).

Thus the maximum intensity of spontaneous radiation corresponds to the frequency determined by the condition

$$\hbar\omega_r = \Delta + 2kT - \hbar\omega_f,$$

and the width of the spontaneous radiation line is ~ kT.

Absorption of radiation in the case that we have considered will be principally determined by the absorption by free current carriers, whose investigation has been treated in a number of works.[10-12] The change in the number of quanta per unit volume as a result of absorption by the free carriers is determined by the equation

$$(dN/dt)^- = -\varkappa c N, \tag{17}$$

where c is the velocity of light in the material, and the absorption coefficient κ is equal to $\kappa = n\sigma_e + p\sigma_h$ (σ_e and σ_h are cross sections for the absorption of the photon by the electron and hole).

The condition for the formation of a negative coefficient of absorption gives

$$(dN/dt)^+ > (dN/dt)^-. \tag{18}$$

If we substitute here value $(dN/dt)^\pm$ from Eqs. (15) and (17), the condition for the appearance of a negative absorption coefficient takes on the form

$$\overline{W}_{ij} \hbar \lambda^2 np e^{-y} y^2 / 8kTD\, (n\sigma_e + p\sigma_h) > 1, \tag{19}$$

where λ is the wavelength of the radiation in vacuum, and D the dielectric constant of the material. One can express the averaged probability $\overline{W}_{ij}$ in terms of the spontaneous radiation lifetime τ_R relative to the indirect transition at the temperature of interest to us:

$$\tau_R^{-1} = \overline{W}_{ij}(n_0 + p_0). \tag{20}$$

In the case in which $n\sigma_e > p\sigma_h$, the condition (19) gives

$$p > 8kTD\sigma_e / \hbar\lambda^2 e^{-y} y^2 \overline{W}_{ij}. \tag{21}$$

For $n\sigma_e < p\sigma_h$, we must make the substitution $p \to n$, $\sigma_e \to \sigma_h$ in (21). An estimate made by Eq. (21) for germanium at $\lambda \sim 10^{-4}$ cm, $D \sim 10$, $T \sim 4°$K, $\tau_R \sim 0.75$ sec[9]* (for $n \sim 2.4 \times 10^{13}$ cm^{-3}), $\sigma_e \sim 10^{-19}$ cm^2,[11] gives the condition $p > 5 \times 10^{15}$ cm^{-3} for the concentration of non-equilibrium carriers. If it is assumed that the absorption coefficient of the generated light is ~ 10^3 cm^{-1} and the lifetime of the non-equilibrium carriers is $\sim 10^{-4}$ sec, the inequality given above will be satisfied for an excitation density $i > 5 \times 10^{16}$ quanta/cm^2-sec, which is practically attainable. However, the lifetime for such high excitation densities will be much less than 10^{-4} sec, which requires high excitation density, and consequently, difficulties of cooling the specimen arise. Therefore, from our point of view, a more appropriate method of obtaining the negative absorption coefficient lies in processes connected with indirect transitions from exciton states.

---

*The quantity τ_R was given in reference 9 for $T \sim 300°$K; it is more correct to take τ_R at 4°K.

3. INDIRECT TRANSITIONS FROM EXCITON STATES

We now consider the condition of formation of a negative absorption coefficient in the case of indirect transitions from exciton states, when the criteria for generation of a negative temperature (9) are satisfied. In this case, the absorption of radiation takes place as a result of ionization of the exciton by the photon into an electron and hole (absorption by impurities and by the lattice will be considered later).

Let the lifetime of the exciton relative to radiation decay in the range of radiation frequencies from ω_r to $\omega_r + \Delta\omega$ be equal to τ. Then the number of quanta N produced by induced radiation per unit volume is determined by the equation

$$(dN/dt)^{+} = n_{\omega}\nu/\tau. \qquad (22)$$

On the other hand, the number of quanta absorbed per unit volume of the specimen is equal to

$$(dN/dt)^{-} = -c\sigma_i\nu N, \qquad (23)$$

where σ_i is the cross section for ionization of an exciton by the photon. The conditions for production of a negative absorption coefficient lead to the inequality

$$\sigma_i < \lambda^2/4D\Delta\omega\tau. \qquad (24)$$

Numerical estimates for this case in silicon[13] at $\lambda \sim 10^{-4}$ cm, $D \sim 10$, $\Delta\omega \sim 10^{12}$ sec^{-1} and $\tau \sim 10^{-5}$ sec give

$$\sigma_i < 0.25 \cdot 10^{-16}\ \text{cm}^2. \qquad (25)$$

The photo-ionization cross section of the exciton* is evidently less than the quantity on the right side of the inequality (25), so that the conditions for producing a negative absorption coefficient in transitions from exciton states are satisfied in this case.

It is easy to estimate the role of absorption of radiation by impurities and by the lattice. Actually, the number of quanta absorbed per unit time per unit volume is equal to

$$(dN/dt)^{-} = -c\varkappa_c N, \qquad (26)$$

where κ_c is the coefficient of absorption of radiation by the lattice and by impurities for wavelengths corresponding to the indirect transition. To obtain a negative absorption coefficient from (22) and (26), we shall determine the condition for the concentration of excitons:

$$\nu > 4D\Delta\omega\tau\lambda^{-2}\varkappa_c. \qquad (27)$$

A numerical estimate by means of the values of parameters used in (25) gives

$$\nu > 4 \cdot 10^{16}\varkappa_c. \qquad (28)$$

The width of the radiation line of the exciton, $\Delta\omega$, which enters into the expressions (24) and (27), is determined by the temperature of the specimen and is of the order kT. Upon lowering the temperature, $\Delta\omega$ is decreased, which improves the condition for obtaining a negative absorption coefficient.

CONCLUSION

The investigation carried out above shows that the methods considered in the present research for obtaining states with negative temperature arise in the case of comparatively low concentrations of non-equilibrium current carriers, which is connected with a significant decrease in the probability of absorption at low temperature in indirect transitions. The concentrations of carriers necessary for the production of the negative temperature can be obtained relatively easily by experiment. The low concentrations of carriers make it possible to expect the possibility of obtaining negative temperatures in semiconducting specimens not only under pulse conditions but also in continuous operation.

The production of states with negative temperature can evidently also be observed in the absence of amplification of the light passing through the specimen (when the probability of absorption of quanta by free carriers exceeds the probability of induced radiation) by the narrowing of the width of the spectral line as a consequence of regeneration. The total amplification of radiation of quanta passing through the specimen can in principle always be obtained for certain concentrations of carriers, inasmuch as absorption by free carriers increases linearly with concentration, while radiation is proportional to the square of the concentration. However, the concentrations of free carriers necessary to obtain amplification of radiation appreciably exceed the concentrations necessary for formation of negative temperature. Therefore the creation of such concentrations requires additional investigation of the problem connected with the cooling of the specimen at high intensity of exciting radiation, although this difficulty is not one of principle, inasmuch as a changeover to pulse excitation with sufficiently short pulses is always possible.

---

*The exciton photo-ionization cross section can be estimated from the formula for ordinary photoeffect in the atom.[14] In this case, the inequality (25) is satisfied by a wide margin. Evidently, the more probable process is the photo-ionization of the exciton with emission of a phonon, a process whose cross section is equal in order of magnitude to the cross section of absorption by free carriers.

To obtain amplification of radiation for exciton transitions, lower densities of excitation are required because of the significant increase in the radiation probability which removes the difficulties associated with heating of the specimen.

The shape of the line obtained in Sec. 2 shows that its figure of merit is of the order of $\hbar\omega_r/kT$ and has a value of $\sim 10^3$ for a temperature of T $\sim 10°$K. Using a magnetic field, one can change the frequency of radiation by an amount of order $\Delta\omega \approx eH/mc$,[15] which, for example, at fields of $H \sim 10^4$ oe amounts to 10 percent of the frequency of radiation for germanium. Thus, a change in the magnetic field can be a very useful method for changing the frequency of quantum generators and amplifiers using indirect transitions in semiconductors.

[1] Basov, Vul, and Popov, JETP **37**, 587 (1959), Soviet Phys. JETP **10**, 416 (1960).

[2] B. Lax, Quantum Electronics, (Columbia University Press, New York, 1960).

[3] Basov, Krokhin, and Popov, JETP **39**, 1486 (1960), Soviet Phys. JETP **12**, 1033 (1961).

[4] O. N. Krokhin and Yu. M. Popov, JETP **38**, 1589 (1960), Soviet Phys. JETP **11**, 1144 (1960).

[5] Basov, Krokhin, and Popov, Usp. Fiz. Nauk **72**, 161 (1960), Soviet Phys. Uspekhi **3**, 702 (1961).

[6] F. Herman, Phys. Rev. **88**, 1210 (1952).

[7] Dresselhaus, Kip, and Kittel, Phys. Rev. **92**, 827 (1953).

[8] L. D. Landau and E. M. Lifshitz, Statistical Physics, Addison Wesley, 1958.

[9] W. P. Dumke, Phys. Rev. **105**, 139 (1957).

[10] Fan, Spitzer and Collins, Phys. Rev. **101**, 566 (1956).

[11] H. J. G. Meyer, Phys. Rev. **112**, 298 (1958).

[12] V. S. Vavilov, Физика твердого тела **2**, 374 (1960), Soviet Phys. Solid State **2**, 346 (1960).

[13] Haynes, Lax, and Flood, Report on International Conference on Semiconductor Physics, Prague, 1960.

[14] W. Heitler, Quantum Theory of Radiation (Oxford, 1954).

[15] Zwerdling, Lax, Roth, and Button, Phys. Rev. **114**, 80 (1959).

Translated by R. T. Beyer
202

SOVIET PHYSICS JETP VOLUME 13, NUMBER 4 OCTOBER, 1961

THE MOMENTUM DISTRIBUTION OF PARTICLES IN A DILUTE FERMI GAS

V. A. BELYAKOV

Moscow Engineering Physics Institute

Submitted to JETP editor November 26, 1960

J. Exptl. Theoret. Phys. (U.S.S.R.) 40, 1210-1212 (April, 1961)

The first two terms of the expansion in powers of the gas parameter of the momentum distribution of particles in a non-ideal Fermi gas are obtained, using a perturbation method.

A number of authors[1-4] have calculated the energy spectrum and the ground state energy of a dilute Fermi gas to second order in $an^{1/3}$, where n is the number of particles in unit volume, and a is the S-wave scattering amplitude. (The condition $an^{1/3} \sim a/\lambda \ll 1$, where λ is the de Broglie wavelength, allows one to include S scattering only.)

The momentum distribution function of particles is also of interest. It can be determined from the mean value of the operator giving the number of particles

$$n(p) = \langle \psi^* | a_{ps}^+ a_{ps} | \psi \rangle, \tag{1}$$

where ψ is the wave function of the system of interacting particles, while a_{ps}^+ and a_{ps} are the creation and annihilation operators of particles with momentum **p** and spin s.

We calculate n(p) to the second order of perturbation theory in the small parameter $an^{1/3}$. We write the particle interaction Hamiltonian in the form

$$V = U \Sigma a_{p_4 1/2}^+ a_{p_3, -1/2}^+ a_{p_2 1/2} a_{p_1, -1/2}. \tag{2}$$

(The summation is made with account of momentum conservation). The constant U is related to the scattering amplitude by

$$U = 4\pi a\hbar^2/m. \tag{3}$$

We write down ψ from perturbation theory, up to second order terms:[5]

$$\psi = \psi_0 + \sum_i \frac{V_{i0}}{E_0 - E_i}\psi_i + \sum_i\sum_k \frac{V_{ik}V_{k0}}{(E_0 - E_k)(E_0 - E_i)}\psi_i$$
$$- \sum_i \frac{V_{00}V_{i0}}{(E_0 - E_i)^2}\psi_i - \frac{1}{2}\psi_0 \sum_i \frac{|V_{i0}|^2}{(E_0 - E_i)^2}, \tag{4}$$

where ψ_0, and ψ_i are, respectively, the wave functions for the ground and excited states of an ideal gas.

The substitution of (4) into (1) gives for n(p)

$$n(p) = 1 - \frac{4U^2m^2}{(2\pi\hbar)^6} \int\limits_{p_1<p_0} d\mathbf{p}_1 \int\limits_{p_2>p_0} d\mathbf{p}_2$$
$$\times \int\limits_{p_3>p_0} d\mathbf{p}_3 \frac{\delta(\mathbf{p}_1 + \mathbf{p} - \mathbf{p}_2 - \mathbf{p}_3)}{(p_1^2 + p^2 - p_2^2 - p_2^2)^2}, \quad |\mathbf{p}| < p_0;$$

$$n(p) = \frac{4U^2m^2}{(2\pi\hbar)^6} \int\limits_{p_1<p_0} d\mathbf{p}_1 \int\limits_{p_2<p_0} d\mathbf{p}_2$$
$$\times \int\limits_{p_3>p_0} d\mathbf{p}_3 \frac{\delta(\mathbf{p}_1 + \mathbf{p}_2 - \mathbf{p} - \mathbf{p}_3)}{(p_1^2 + p_2^2 - p^2 - p_3^2)^2}, \quad |\mathbf{p}| > p_0,$$

where p_0 is the limiting Fermi momentum.

We consider the case $p < p_0$. Integration with respect to $\mathbf{p}_3$ and the substitution $\mathbf{s} = \mathbf{p}_1 + \mathbf{p} = \mathbf{p}_2 + \mathbf{p}_3$, $\mathbf{q} = \mathbf{p}_2 - \mathbf{p}_3$ gives

$$1 - \frac{2U^2m^2}{(2\pi\hbar)^6} \int ds \int dq\, [(s - 2p)^2 - q^2]^{-2},$$

where the integration range with respect to **s** is given by the conditions $|\mathbf{s} - \mathbf{p}| < p_0$, $\mathbf{s} < 2p_0$, and the integration range for **q** by the conditions $|\mathbf{s} - \mathbf{q}| > 2p_0$, $|\mathbf{s} + \mathbf{q}| > 2p_0$. Since the final result depends only on p, we can average our expression over the directions **p**. This greatly simplifies the further integration over **s** and **q**.

Finally, for $p < p_0$ we obtain

$$n(p) = 1 - \frac{1}{3x}\left(\frac{3na^3}{\pi}\right)^{2/3}\Big[(7\ln 2 - 8)x^3 + (10 - 3\ln 2)x$$
$$+ 2\ln\frac{1+x}{1-x} - 2(2 - x^2)^{3/2}\ln\frac{(2 - x^2)^{1/2} + x}{(2 - x^2)^{1/2} - x}\Big], \qquad x < 1,$$

where $x = p/p_0$, $n = \pi p_0^3/3(\pi\hbar)^3$.

Similar calculations for $p > p_0$ lead to the expressions*

$$\frac{1}{6x}\left(\frac{3na^3}{\pi}\right)^{2/3}\Big[(7x^3 - 3x - 6)\ln\frac{x-1}{x+1} + (7x^3 - 3x + 2)\ln 2$$
$$- 10x^3 + 30x^2 - 24 + 2(2 - x^2)^{3/2}\Big(\ln\frac{(2 - x^2)^{1/2} + 2 + x}{(2 - x^2)^{1/2} - 2 - x}$$
$$+ \ln\frac{1 + (2 - x^2)^{1/2}}{1 - (2 - x^2)^{1/2}} - 2\ln\frac{x + (2 - x^2)^{1/2}}{x - (2 - x^2)^{1/2}}\Big)\Big], \quad 1 < x < \sqrt{2};$$

---

*arctg = $\tan^{-1}$

$$\frac{1}{6x}\left(\frac{3na^3}{\pi}\right)^{2/3}\left[(7x^3-3x-6)\ln\frac{x-1}{x+1}+(7x^3-3x+2)\ln 2\right.$$

$$-10x^3+30x^2-24-4(2-x^2)^{3/2}\left(\operatorname{arctg}\frac{2+x}{(x^2-2)^{1/2}}\right.$$

$$\left.\left.+\operatorname{arctg}\frac{1}{(x^2-2)^{1/2}}-2\operatorname{arctg}\frac{x}{(x^2-2)^{1/2}}\right)\right],\quad \sqrt{2}<x<\sqrt{3};$$

$$\frac{2}{3x}\left(\frac{3na^3}{\pi}\right)^{2/3}\left[2\ln\frac{x+1}{x-1}-2x+(x^2-2)^{3/2}\left(2\operatorname{arctg}\frac{x}{(x^2-2)^{1/2}}\right.\right.$$

$$\left.\left.-\operatorname{arctg}\frac{x-2}{(x^2-2)^{1/2}}-\operatorname{arctg}\frac{x+2}{(x^2-2)^{1/2}}\right)\right],\quad x>3.$$

We quote the values of the function n (p) at several points:

$$n(0)=1-2(3na^3/\pi)^{2/3}\left(1-\tfrac{1}{2}\ln 2\right),$$

$$n(p_0-0)=1-2(3na^3/\pi)^{2/3}\left(\tfrac{1}{3}+\ln 2\right),$$

$$n(p_0+0)=2(3na^3/\pi)^{2/3}\left(\ln 2-\tfrac{1}{3}\right),$$

$$n(p)=(4/9x^4)(3na^3/\pi)^{2/3}\quad\text{as } p\to\infty.$$

In agreement with Migdal,[6] we find that the distribution function undergoes a discontinuity at p = p_0. The size of the jump at this discontinuity

$$n(p_0-0)-n(p_0+0)=1-4(3na^3/\pi)^{2/3}\ln 2$$

agrees with calculations made by Galitskii[4] by another method.

In conclusion, the author expresses his sincere gratitude to A. A. Abrikosov for suggesting the problem and for interest in the work.

---

[1] A. A. Abrikosov and I. M. Khalatnikov, JETP 33, 1154 (1957), Soviet Phys. JETP 6, 888 (1958).

[2] K. Huang and C. N. Jang, Phys. Rev. 105, 767 (1957).

[3] T. D. Lee and C. N. Yang, Phys. Rev. 105, 1119 (1957).

[4] V. M. Galitskii, JETP 34, 151 (1958), Soviet Phys. JETP 7, 104 (1958).

[5] L. D. Landau and E. M. Lifshitz, Quantum Mechanics, Pergamon, 1958.

[6] A. B. Migdal, JETP 32, 399 (1957), Soviet Phys. JETP 5, 333 (1957).

Translated by K. F. Hulme
203

SOVIET PHYSICS JETP VOLUME 13, NUMBER 4 OCTOBER, 1961

MAGNETOHYDRODYNAMICS FOR NONISOTHERMAL PLASMA WITHOUT COLLISIONS

Yu. L. KLIMONTOVICH and V. P. SILIN

Moscow State University

P. N. Lebedev Physics Institute, Academy of Sciences U.S.S.R.

Submitted to JETP editor November 28, 1960

J. Exptl. Theoret. Phys. (U.S.S.R.) 40, 1213-1223 (April, 1961)

The magnetohydrodynamic equations are considered for a plasma without collisions. Dissipation due to the absorption of magnetohydrodynamic and magneto-acoustic waves by electrons is taken into account. The resultant equations are applied in the analysis of the smearing out of a packet in the plasma. It is shown that under the conditions assumed, when the spatial dimensions considerably exceed the Debye and Larmor ranges, stationary shock waves with a width much smaller than the mean free path cannot exist.

INTRODUCTION

IN the description of processes in rarefied plasma, when the mean free path is large in comparison with all characteristic dimensions, frequent use is made of the equations of magnetohydrodynamics. It can be shown that such a mode of description of the plasma without collisions, as was shown, for example, in the work of Ginzburg,[1] can be completely justified for problems in which the thermal motions of the particles of the plasma is unimportant. Under conditions in which the thermal motion becomes important, the kinetic approach is usually employed, which is based on the utilization of the kinetic equation and self-consistent interaction.[2] Such an approach is obviously incomparably more difficult than the hydrodynamic one. Therefore, in a number of researches,[3,4] attempts were made, on the basis of kinetic considerations, to develop the possibilities of application of magnetohydrodynamics to a plasma without collisions. In this case, it was shown that the hydrodynamic description is not possible in the general case; therefore, use of the kinetic consideration is necessary. On the other hand, the possibility of application of magnetohydrodynamics to the special problem of plasma remains, and, for example, in the work of Chew, Goldberger and Low (CGL),[3] hydrodynamics is considered for the case in which the dissipation effects can be entirely neglected.

The value of the absorption of sound or magneto-acoustic and magnetohydrodynamic waves in the plasma can serve as a measure of the dissipation processes. In an isothermal plasma, sound waves cannot propagate.[7] Accordingly, weakly attenuated magnetohydrodynamic waves can exist in an isothermal plasma only for rather large fields, when the role of thermal motion of the particles reduces to a small correction.[8] On the contrary, in the case of a non-isothermal plasma, when the temperature of the electrons is significantly greater than the temperature of the ions, the acoustic vibrations are shown to be weakly damped.[9] In such an isothermal plasma there are in the corresponding case weakly damped magneto-acoustic waves even in the case of fields for which the magnetic pressure is comparable with the pressure brought about by the thermal motion of the particles of the plasma [see references 10 — 12, and especially reference 13].

In the present article we consider the magnetohydrodynamic approximation for a plasma without collisions under the condition that the temperature of the electrons is much greater than the temperature of the ions. In the first section, a derivation is given in the linear approximation of the equations of magnetohydrodynamics for such a nonisothermal plasma, with account of dissipative processes. Dissipation in a plasma without collisions is caused by absorption of waves originating in the plasma by the charged particles.[14] Because of the fact that the thermal velocity of the electrons in our problem is large in comparison with the velocity of the magneto-acoustic waves, the dissipative terms in the hydrodynamic equations that we have obtained are non-localized in space.

In the second section, the system of hydrodynamic equations that has been derived is used for the investigation of the law of spreading out of the wave packet (discontinuity of small intensity) in a plasma without collisions. In this case, in contrast with the usual hydrodynamics where the width of such a discontinuity increases as the square root of the time, the width in a plasma without collisions is shown to be proportional to the time. The third section is devoted to the problem of the possibility of existence of stationary discontinuities (shock waves) in a plasma without collisions. Since the dissipative effects are taken into account only in the linear approximation, the problem, strictly speaking, is one of shock waves of low intensity. The nondissipative terms of the equations of magnetohydrodynamics are obtained in the nonlinear approximation.

1. THE EQUATIONS OF MAGNETOHYDRODYNAMICS FOR A NONISOTHERMAL PLASMA WITHOUT COLLISIONS, WITH ACCOUNT OF THE THERMAL MOTION OF THE ELECTRONS

In the frequently encountered case of nonisothermal plasma of electron temperature much higher than the ion temperature, one can neglect the thermal motion of the ions in a wide range of problems. Furthermore, neglecting collisions, we can use for description of the ions the equation of continuity

$$\partial\rho/\partial t + \operatorname{div}\rho\mathbf{V} = 0 \qquad (1.1)$$

as well as Newton's equation

$$\rho\frac{d\mathbf{V}}{dt} = \rho\frac{\partial\mathbf{V}}{\partial t} + \rho\left(\mathbf{V}\frac{\partial}{\partial\mathbf{r}}\right)\mathbf{V} = q_i\left\{\mathbf{E} + \frac{1}{c}[\mathbf{VB}]\right\}. \qquad (1.2)^*$$

Here ρ = mass density, q_i = charge density of the ions, $\mathbf{V}(r, t)$ determines the distribution of velocity of the ions; finally, **E** and **B** are the intensities of the electric and magnetic fields.

The thermal velocities of the electrons are not small. Therefore it is necessary to make use of the kinetic equation for the electrons. For electrons of a plasma without collisions, we have the following kinetic equation with self-consistent field:

$$\frac{\partial f}{\partial t} + \mathbf{v}\frac{\partial f}{\partial\mathbf{r}} + e\left\{\mathbf{E} + \frac{1}{c}[\mathbf{vB}]\right\}\frac{\partial f}{\partial\mathbf{p}} = 0. \qquad (1.3)$$

Magnetohydrodynamics holds only for low frequencies in comparison with the Larmor frequency of the ions. In this case, the question is one of the frequencies in a system of coordinates connected with the ions. Then, rewriting Eq. (1.2) in the form

$$\mathbf{E} = -\frac{1}{c}[\mathbf{VB}] + \frac{M}{e_i}\frac{d\mathbf{V}}{dt},$$

where M = mass and e_i = charge of the ions, we can show that the last term of the right side is of the order of the ratio of the change of the characteristic frequency to the Larmor frequency of the ions in comparison with the first term. If we neglect terms of such an order of smallness, we have

$$\mathbf{E} = -[\mathbf{VB}]/c. \qquad (1.4)$$

Substituting such an expression for the field in the equation c curl **E** = − ∂**B**/∂t, we get

$$\partial\mathbf{B}/\partial t = \operatorname{rot}[\mathbf{VB}]. \qquad (\mathrm{I})^*$$

Equation (I) corresponds to that usually employed in the magnetohydrodynamics of an ideal liquid. Neglect of collisions makes the conductivity actually infinite in our case. The second equation of magnetohydrodynamics is not needed in the derivation: this is

$$\operatorname{div}\mathbf{B} = 0. \qquad (\mathrm{II})$$

Furthermore, assuming the plasma to be sufficiently dense, so that the Langmuir frequency can be taken to be many times the frequencies considered, we can neglect the displacement current in the field equations, which then take the form

$$\mathbf{j} = (c/4\pi)\operatorname{rot}\mathbf{B}, \qquad q = 0. \qquad (1.5)$$

Here **j** = current density and **q** = charge density of the plasma:

$$\mathbf{j} = q_i\mathbf{V} + e\int\mathbf{v}f\,d\mathbf{p}, \qquad q = q_i + e\int f\,d\mathbf{p}. \qquad (1.6)$$

We note that when we neglect the thermal motion of the electrons, we can use for their description an equation which is similar to (1.2). In this case, the equation of motion of the liquid can immediately be obtained in the form

$$\rho\,d\mathbf{V}/dt = -(4\pi)^{-1}[\mathbf{B}, \operatorname{rot}\mathbf{B}]. \qquad (1.7)$$

For the problem in which we are interested — namely, of obtaining a magnetohydrodynamic theory that takes into account the thermal motion of the electrons, it is necessary to determine the electric field by means of Eqs. (1.3) and (1.5), and to eliminate it from Eq. (1.2). We thereby obtain for the liquid (plasma) an equation of motion which takes into account the effects produced by the thermal motion of the electrons, and therefore generalizes Eq. (1.7).

We note that the desired equation for the electric field should really be computed with account of terms of the next order of smallness in comparison with those kept in Eq. (1.4). Below, we shall limit ourselves to obtaining an equation of motion of the liquid only for the case of plasma states which are slightly different from the ground state.

---

*$[\mathbf{VB}] = \mathbf{v}\times\mathbf{B}$.

*rot = curl

In the system of reference in which there is no constant drift of the electrons, we shall take for the distribution function of the ground state the Maxwellian distribution:*

$$f_0(p) = N_e (2\pi m \varkappa T)^{-3/2} \exp\{-p^2/2m\varkappa T\}. \qquad (1.8)$$

We can then write the equation for the non-equilibrium contribution δf to the electron distribution function:

$$\frac{\partial \delta f}{\partial t} + \mathbf{v}\frac{\partial \delta f}{\partial \mathbf{r}} + \frac{e}{c}[\mathbf{v}\mathbf{B}_0]\frac{\partial \delta f}{\partial \mathbf{p}} = -e\mathbf{E}\frac{\partial f_0}{\partial \mathbf{p}}, \qquad (1.9)$$

The solution of this equation has the form

$$\delta f(\mathbf{p}, \mathbf{r}, t) = \int_{-\infty}^{t} dt' \int d\mathbf{r}' \mathbf{E}(\mathbf{r}'\, t')\, \Phi(\mathbf{r}-\mathbf{r}', t-t', \mathbf{p}), \qquad (1.10)$$

where

$$\Phi(\mathbf{r}, t, \mathbf{p}) = f_0(p)\frac{e}{m\varkappa T}\frac{1}{(2\pi)^3}\int d\mathbf{k}e^{i\mathbf{k}\mathbf{r}}\left\{\frac{\mathbf{B}_0(\mathbf{p}\mathbf{B}_0)}{B_0^2} - \frac{[\mathbf{p}\mathbf{B}_0]}{B_0}\sin\Omega_e t - \frac{[\mathbf{B}_0[\mathbf{p}\mathbf{B}_0]]}{B_0^2}\cos\Omega_e t\right\}\exp\left\{i\mathbf{k}, \frac{[\mathbf{p}\mathbf{B}_0]}{m\Omega_e B_0}[1-\cos\Omega_e t] - \frac{\mathbf{B}_0(\mathbf{p}\mathbf{B}_0)}{mB_0^2}t - \frac{[\mathbf{B}_0[\mathbf{p}\mathbf{B}_0]]}{m\Omega_e B_0^2}\sin\Omega_e t\right\}. \qquad (1.11)$$

Here $\Omega_e = eB_0/mc$ is the Larmor frequency of the electrons. Under the assumption that ω is small in comparison with the Larmor frequency and ω/k is small in comparison with the thermal velocity of the electrons, we have the following expression for the Fourier components of the current density of the electrons:

$$\mathbf{j}^e(\omega, \mathbf{k}) = -i\frac{\omega_{0i}^2}{4\pi}\frac{\omega}{v_s^2}\frac{\mathbf{B}_0(\mathbf{B}_0\mathbf{E})}{(\mathbf{k}\mathbf{B}_0)^2} - \frac{\omega_{0i}^2}{4\pi}\frac{\mathbf{B}_0}{\Omega_i}\frac{[\mathbf{E}\mathbf{k}]}{(\mathbf{k}\mathbf{B}_0)} + \tau\frac{\omega_{0i}^2}{4\pi}\left\{\frac{\omega^2}{v_s^2}\frac{\mathbf{B}_0(\mathbf{B}_0\mathbf{E})}{(\mathbf{k}\mathbf{B}_0)^2} + i\omega\frac{\mathbf{B}_0([\mathbf{B}_0\mathbf{k}]\mathbf{E})}{\Omega_i(\mathbf{k}\mathbf{B}_0)B_0} - i\omega\frac{[\mathbf{B}_0\mathbf{k}](\mathbf{B}_0\mathbf{E})}{\Omega_i(\mathbf{k}\mathbf{B}_0)B_0} + 2\frac{v_s^2}{\Omega_i^2}\frac{[\mathbf{k}\mathbf{B}_0]([\mathbf{k}\mathbf{B}_0]\mathbf{E})}{B_0^2}\right\}. \qquad (1.12)$$

Here $\Omega_i = e_i B_0/Mc$ is the Larmor frequency of the ions, $\omega_{0i} = \sqrt{4\pi e_i^2 N_i/M}$ is the Langmuir frequency of the ions, $v_s = \sqrt{|e_i/e|(\kappa T/M)}$ and, finally,

$$\tau(\mathbf{k}) = \int_0^\infty dt \exp\left\{-\frac{\varkappa T}{2m}\left(\frac{\mathbf{k}\mathbf{B}_0}{B_0}\right)^2 t^2 - i\omega t\right\} \approx \sqrt{\frac{\pi}{2}\frac{m}{\varkappa T}}\frac{B_0}{|\mathbf{k}\mathbf{B}_0|}. \qquad (1.13)$$

To obtain the relation (1.12), account was taken of the fact that the total charge of the plasma vanishes: $e_i N_i + eN_e = 0$. We note that because of the assumptions we have made, the component of the right side of (1.12), which is proportional to $\tau(\mathbf{k})$, is shown to be small.

With the aid of Eq. (1.12), and also by bearing in mind Eq. (1.5), we find the following expression for the electric field:

$$e_i N_i \mathbf{E}(\mathbf{r}, t) = \frac{1}{c}[\mathbf{j}^{(e)}\mathbf{B}_0] - v_s^2\frac{\partial \delta\rho}{\partial \mathbf{r}} + \mathbf{F}^{(\mathrm{diss})}, \qquad (1.14)$$

where $\delta\rho$ is the non-equilibrium contribution to the mass density and

$$F_\alpha^{(\mathrm{diss})} = \frac{\rho_0 v_s^2}{B_0^2}\left\{\left[B_{0\alpha}\left(\mathbf{B}_0\frac{\partial}{\partial \mathbf{r}}\right) + \left[\mathbf{B}_0\left[\mathbf{B}_0\frac{\partial}{\partial \mathbf{r}}\right]\right]_\alpha\right]\frac{1}{B_0^2}\left(\mathbf{B}_0\frac{\partial}{\partial \mathbf{r}}\right)B_{0\beta} - \left[\mathbf{B}_0\left[\mathbf{B}_0\frac{\partial}{\partial \mathbf{r}}\right]\right]_\alpha\frac{\partial}{\partial r_\beta}\right\}\int d\mathbf{r}' Q(\mathbf{r}-\mathbf{r}')V_\beta(\mathbf{r}', t). \qquad (1.15)$$

Here

$$Q(\mathbf{r}) = \frac{1}{(2\pi)^3}\int e^{i\mathbf{k}\mathbf{r}}d\mathbf{k}\,\tau(\mathbf{k}). \qquad (1.16)$$

Substituting (1.13) in (1.2), and taking into consideration the first of Eqs. (1.5), we get the desired equation of motion of the material:

$$\frac{d\mathbf{V}}{dt} = \frac{1}{4\pi\rho_0}[\mathrm{rot}\,\mathbf{B}, \mathbf{B}_0] - v_s^2\frac{\partial}{\partial \mathbf{r}}\frac{\delta\rho}{\rho_0} + \frac{1}{\rho_0}F^{(\mathrm{diss})} \qquad \text{(III)}$$

Without account of the dissipative force $F^{(\mathrm{diss})}$, Eq. (III) corresponds to the equation of motion of an ideal liquid in magnetohydrodynamics with an isotropic pressure tensor (see reference 3).

The dissipative force in Eq. (III) has essentially a nonhydrodynamic form. Actually, the presence of $F^{(\mathrm{diss})}$ makes (III) an integral equation. The situation here is quite similar to that which takes place in an analysis of sound absorption in metals when the electronic mean free path is much greater than the acoustic wavelength and the spatial dispersion of the tensor of the elastic moduli becomes appreciable.[16] Such a peculiarity of the dissipative force is brought about by the fact that the processes of absorption in the plasma which is under analysis are brought about not by the collisions of particles with one another, but by radiation (Cerenkov or bremsstrahlung) and absorption of waves in the plasma by electrons.

In the case in which the gradients are parallel to the constant magnetic field $\mathbf{B}_0$, Eq. (III) goes over into the equation of motion of the material in the absence of a field:

$$\frac{d\mathbf{V}}{dt} = -\frac{v_s^2}{\rho_0}\frac{\partial \delta\rho}{\partial \mathbf{r}} + v_s^2\frac{\partial}{\partial \mathbf{r}}\int d\mathbf{r}' Q_0(\mathbf{r}-\mathbf{r}')\,\mathrm{div}\,\mathbf{V}(\mathbf{r}', t). \qquad (1.17)$$

Here Q_0 is determined by Eq. (1.16) with replacement of the quantity $|\mathbf{k}\cdot\mathbf{B}_0|/B_0$ by $|\mathbf{k}|$ in $\tau(\mathbf{k})$.

The kernel $Q(\mathbf{r})$, or $Q_0(\mathbf{r})$ in the absence of a magnetic field, decreases slowly with increase in r. This is associated with the fact that $\tau(\mathbf{k})$ has a singularity at $k = 0$. The appearance of this singularity is connected with the fact that in our consideration the characteristic dimensions of the spatial inhomogeneities of the particle distribution are taken to be small in comparison with the mean free path. In particular, this applies fully to the kernels Q and Q_0.

---

*Frequently, distributions with different temperatures are taken parallel to and transverse to the constant magnetic field. In this case, such a state can generally be unstable.[6,15] We take this opportunity to thank Kitsenko and Stepanov for making their work[15] available to us before publication.

If we were interested in values of r comparable with or larger than the mean free path, then we could use the expression

$$\tau_1(\mathbf{k}) = \int_0^\infty dt \exp\left\{-\frac{\varkappa T}{2m}\left(\frac{\mathbf{k}\mathbf{B}_0}{B_0}\right)^2 t^2 - \nu t\right\} \qquad (1.18)$$

for estimates in this case, in place of (1.13). Here ν is the electron collision frequency (variation in the frequency ω is neglected). In contrast to $\tau(\mathbf{k})$, which increases without limit as $\mathbf{k} \to 0$, the expression for $\tau_1(\mathbf{k})$ increases only to such a point that $kl > 1$, where $l = \nu^{-1}\sqrt{\kappa T/m}$ is the mean free path. In the case in which $kl \ll 1$, the function τ_1 becomes constant and is equal to $1/\nu$. Therefore, we can use the following simple formula [which approximates $\tau_1(k)$] for an estimate of the role of collisions:

$$\left[\left(\frac{\mathbf{k}\mathbf{B}_0}{B_0}\right)^2 \frac{\varkappa T}{m}\frac{2}{\pi} + \nu^2\right]^{-1/2}. \qquad (1.19)$$

Such an expression can also serve, if the necessity arises, for the analysis of the singularity of the function τ at $k = 0$.

Such a simple approximation for Eq. (1.17) leads to the following expression for the kernel:

$$Q_0(r) = \frac{1}{(2\pi)^{3/2}}\sqrt{\frac{m}{\varkappa T}}\frac{d}{dr}K_0(r/\bar{l}), \qquad (1.20)$$

where $\bar{l} = l\sqrt{2/\pi}$ and K_0 is the MacDonald function. For the one-dimensional case, in which v does not depend on the coordinates y and z, but only on x and t, it is necessary to integrate the kernel (1.16) over y and z. In this case, we get

$$\overline{Q}(x) = \sqrt{\frac{m}{2\pi\varkappa T}}\frac{B_0}{|B_{0x}|}K_0\left(\frac{x}{\bar{l}}\frac{B_0}{|B_{0x}|}\right). \qquad (1.21)$$

2. SPREADING OUT OF THE WAVE PACKET

We shall use the equations of magnetohydrodynamics which were obtained in the previous section for the analysis of the problem of the spreading out of the wave packet, with the purpose of applying these results to the dissipation of low-intensity shocks in a plasma.

We begin our consideration with the case of a plasma without a constant magnetic field. We then have, by Eqs. (1.1) and (1.17):

$$\frac{\partial^2\delta\rho}{\partial t^2} = v_s^2\,\Delta\delta\rho + v_s^2\,\Delta\int dr'\,Q_0(\mathbf{r}-\mathbf{r}')\frac{\partial\delta\rho(\mathbf{r}')}{\partial t}. \qquad (2.1)$$

Assuming that the values of $\delta\rho$ and its time derivative are given at the time $t = 0$, we get, in the one-dimensional case,

$$\delta\rho(t, x) = \frac{1}{2\pi}\int dx'\left\{\left(\frac{\partial\delta\rho(t, x')}{\partial t}\right)_0 \frac{1}{v_s}[A(x'-x) + A(x-x')]\right.$$
$$+ \delta\rho(0, x')\left[\frac{2v_st + x' - x}{(v_swt)^2 + (v_st + x' - x)^2}\right.$$
$$\left.\left.+ \frac{2v_st - x' + x}{(v_swt)^2 + (v_st - x' + x)^2}\right]\right\},$$

$$A(u) \equiv \operatorname{arctg}\frac{v_st + u}{v_swt}, \quad w = \sqrt{\frac{\pi Zm}{8M}}, \quad Z = |e_i/e|. \qquad (2.2)^*$$

Let $\partial\delta\rho/\partial t = 0$ at the initial instant of time, and let $\delta\rho$ be different from zero and constant in $x_1 < x < x_2$. Then

$$\delta\rho(t, x) = \frac{\delta\rho(0)}{2\pi}\left\{A(x_2 - x) - A(x_1 - x)\right.$$
$$+ A(x - x_2) - A(x - x_1)$$
$$\left.+ \frac{w}{2}\ln\frac{[(v_swt)^2 + (v_st + x_2 - x)^2]\,[(v_swt)^2 + (v_st - x_1 + x)^2]}{[(v_swt)^2 + (v_st - x_2 + x)^2]\,[(v_swt)^2 + (v_st + x_1 - x)^2]}\right\}. \qquad (2.3)$$

It is then clear that the packet spreads out according to a linear law. That is, the width of the packet is proportional to the time. The spreading rate is equal to wv_s. The latter quantity is none other than the ratio of the damping decrement of a sound wave in a plasma without collisions to the wave vector. Neglecting the small term proportional to w in (2.3), we can show that the shape of the packet is determined by a combination of arctangents of the form $A(\Delta x)$.

The same analysis for the case of a plasma in a constant magnetic field (without account of small terms ~ w) leads to a similar shape for the spreading packets, with only this difference that the velocity of magnetohydrodynamic waves

$$v_\pm^2 = \frac{1}{2}\{(v_s^2 + v_A^2) \pm [(v_s^2 + v_A^2)^2 - 4v_A^2v_s^2\cos^2\alpha]^{1/2}\} \qquad (2.4)$$

replaces v_s (here, $v_A^2 = B_0^2/4\pi\rho_0$ is the Alfvén velocity and α is the angle between the constant magnetic field and the x axis), and also

$$w_\pm = \frac{w}{2}\left\{1 \pm \frac{(\cos 2\alpha - y)\cos 2\alpha}{\sqrt{1 + y^2 - 2y\cos 2\alpha}}\right\}\frac{1}{|\cos\alpha|}, \quad y = \left(\frac{v_A}{v_s}\right)^2 \qquad (2.5)$$

appears in place of w.

The quantity $w_\pm$ is the ratio of the damping decrement of the magnetoacoustic wave to the frequency (see reference 13). Knowledge of the decay law of the packet in ordinary magnetohydrodynamics of liquids makes it possible to determine the width of the weak shock wave (see reference 17).† In this situation, a stationary discontinuity can arise only when the rate of spreading out of the jump is comparable with the rate of overflow. The latter does not depend on the width of the jump and is determined by the properties of the medium before and after the discontinuity. On the other hand, the rate of smearing out in ordinary hydrodynamics is determined by the width of the discontinuity (it is inversely proportional to the width), which allows us to find the value of the stationary width. In our case of magnetohydrodynamics of a plasma without collisions, the rate of spreading out does not depend on the width of the packet (at least, from the point where it is small in comparison with the mean free path). Therefore, the equality of the rate of overflow with the rate of spreading out, on the one hand, does not determine the width of the shock and, on the other hand, it is possible only for a single, completely determined rate of overflow. Consequently, if the stationary shock wave is possible, it is only in the case in which the rate of overflow is equal to $w_\pm v_\pm$. The possibility of the existence of a stationary discontinuity in this case is doubtful, inasmuch as an arbitrary shock width remains. However, for sufficiently long development, the discontinuity becomes wider than the mean free path. In this case, as is shown in ordinary hydrodynamics, conditions arise under which the discontinuity can become stationary. The next section is devoted to the problem of the possibility of existence of stationary discontinuities with a width less than the mean free path.

---

*$\operatorname{arctg} = \tan^{-1}$.

†We take this opportunity to thank E. P. Sirotina and S. I. Syrovatskii who acquainted us with their research prior to its publication.

3. SHOCK WAVES IN A PLASMA

For the investigation of shock waves in a plasma, one must start from equations which take nonlinear effects into account. Therefore, the problem arises of the derivation of the nonlinear equations of magnetohydrodynamics. We shall find such equations for the conditions in which the dissipation terms can be considered small. Such a situation essentially obtains in ordinary hydrodynamics as well. As in the previous section, we first consider the case of no external magnetic field.

The equations of magnetohydrodynamics obtained in Sec. 1 hold under the conditions that the phase velocity of the wave processes in the plasma is much less than the thermal velocity of the electrons ($\omega/k \ll \sqrt{\kappa T/m}$). By ω we mean here the frequency in the system of coordinates attached to the ions. As a result, in the derivation of the equations of hydrodynamics for a plasma without account of dissipative processes, we can neglect $\partial f/\partial t$ in the kinetic equation for the electrons. Thus, for $B_0 = 0$, the initial kinetic equation for the electrons is written in the form

$$\mathbf{v}\,\partial f/\partial \mathbf{r} + e\mathbf{E}\,\partial f/\partial \mathbf{p} = 0. \qquad (3.1)$$

Denoting the electric potential by $\varphi(\mathbf{r}, t)$ and the drift velocity of the electrons by $\mathbf{V}_e(\mathbf{r}, t) = \mathbf{j}_e/q_e$, we attempt to satisfy Eq. (3.1) by a solution of the form

$$f = F\left(e\varphi(r, t) + m(\mathbf{v} - \mathbf{V}_e)^2/2\right).$$

Here F is an arbitrary function. In a special case, for example, the function f is the Maxwell-Boltzmann distribution.

We now find the connection between $\mathbf{E} = -\nabla\varphi$ and the density ρ, for which such a solution satisfies Eq. (3.1). For this purpose, we multiply Eq. (3.1) by $\mathbf{v}$ and integrate over $\mathbf{p}$. As a result, we get the equation for the transfer of momentum of the electrons

$$\frac{\partial}{\partial r_l}\int v_k v_l f\,d\mathbf{p} = q_e E_k. \qquad (3.2)$$

Making use of the given expression for the solution of Eq. (3.1), we get

$$\int v_k v_l f\,d\mathbf{p} = \frac{q_e}{e}\left\{\delta_{kl}\frac{\varkappa T}{m} + V_{ek}V_{el}\right\},$$

where

$$q_e = e\int f\,d\mathbf{p}, \qquad \frac{q_e}{e}\frac{\varkappa T}{m} = \int(\mathbf{v} - \mathbf{V}_e)^2 f\,d\mathbf{p}. \qquad (3.3)$$

Substituting Eq. (3.3) in (3.2) and using the equation of continuity, we obtain

$$mq_e V_{el}\frac{\partial V_{ek}}{\partial r_l} + \frac{\partial}{\partial r_k}(\varkappa T q_e) = eq_e E_k. \qquad (3.4)$$

By a comparison of Eq. (3.4) with Eq. (1.2), we see that in the computation of the intensity of the electric field, we can neglect the first term on the left side of Eq. (3.4) because of the smallness of the ratio m/M. As a result, when the velocity V_e is much smaller than the thermal velocity of the electrons, we obtain the following expression for **E**:

$$\mathbf{E} = \frac{1}{eq_e}\frac{\partial}{\partial \mathbf{r}}(\varkappa T q_e).$$

This relation also determines the desired connection among E, ρ, T, for which the solution selected above satisfies Eq. (3.1). Therefore, such a relation, consistent with the definition of T, is an equation of state.

If the characteristic dimension of the inhomogeneity is much larger than the Debye radius, then $\rho = |e_i/e|\,q_e$. As a result, we get the following set of hydrodynamic equations without account of dissipative processes (see reference 18):

$$\frac{\partial \rho}{\partial t} + \frac{\partial}{\partial \mathbf{r}}(\rho\mathbf{V}) = 0, \qquad \frac{\partial \mathbf{V}}{\partial t} + \left(\mathbf{V}\frac{\partial}{\partial \mathbf{r}}\right)\mathbf{V} = -\frac{|e_i/e|}{M\rho}\frac{\partial}{\partial \mathbf{r}}(\varkappa T\rho).$$

This set of equations is closed if the temperature of the electrons is given. With account of dissipative terms in the case of a constant temperature, the set of hydrodynamic equations takes the form

$$\frac{\partial\rho}{\partial t}+\frac{\partial}{\partial \mathbf{r}}(\rho\mathbf{V})=0,$$

$$\frac{\partial \mathbf{V}}{\partial t}+\left(\mathbf{V}\frac{\partial}{\partial \mathbf{r}}\right)\mathbf{V}=-\frac{v_s^2}{\rho}\frac{\partial\rho}{\partial \mathbf{r}}$$

$$+v_s^2\frac{\partial}{\partial \mathbf{r}}\int d\mathbf{r}'\,Q_0(\mathbf{r}-\mathbf{r}')\operatorname{div}\mathbf{V}(\mathbf{r}',t). \tag{3.5}$$

Here v_s is the sound velocity. The expression for the kernel Q_0 with account of the finite size of the mean free path is determined by Eq. (1.20).

To study the possibility of existence of shock waves in the plasma, it suffices to consider Eqs. (3.5) in the one-dimensional case. We introduce a set of coordinates connected with the surface of discontinuity, and direct the x axis perpendicular to this surface. Making use of Eq. (3.5), we write down the equations of continuity of matter flux and momentum flux on the surface of discontinuity:

$$\{\rho V\}=0, \tag{3.6}$$

$$\left\{\rho V^2+\rho v_s^2-\frac{a}{\pi}v_s\rho_0\int\limits_{-\infty}^{+\infty}K_0\left(\frac{|x-x'|}{l}\right)\frac{dV(x')}{dx'}dx'\right\}=0, \tag{3.7}$$

where $a=\sqrt{\pi m v_s^2/2\kappa T}$. Further, taking $\rho V=j_0=\text{const}$, and eliminating ρ from (3.7), we write the condition for the discontinuity of the momentum density in the form of an integral equation

$$\left(V+\frac{v_s^2}{V}\right)j_0-\frac{a}{\pi}v_s\rho_0\int\limits_{-\infty}^{+\infty}K_0\left(\frac{|x-x'|}{l}\right)\frac{dV(x')}{dx'}dx'=C. \tag{3.8}$$

Now we introduce a new constant V^- and write C in the form $V^-+v_s^2/V^-$. In this case, the integral equation (3.8) takes the form

$$(V-V^-)+v_s^2\left(\frac{1}{V}-\frac{1}{V^-}\right)=\frac{a}{\pi}v_s\rho_0\int\limits_{-\infty}^{+\infty}K_0\left(\frac{|x-x'|}{l}\right)\frac{dV(x')}{dx'}dx'. \tag{3.9}$$

The integral equation (3.9) is satisfied by definite constant values of the velocity V. In this case we get from Eq. (3.9)

$$(V-V^-)+v_s^2(1/V-1/V^-)=0, \tag{3.10}$$

whence follow the two constant values

$$V=V^-,\qquad V=V_s^2/V^-\equiv V^+. \tag{3.11}$$

Both values are the same only if $V^-=v_s$.

For an answer to the question of the existence of shock waves in the plasma, we must consider the possibility of such a solution of Eq. (3.9) which takes on the values V^+, V^- for $V^+\neq V^-$, as $x\to\pm\infty$. It follows from Eq. (3.9) that such a solution exists if a transition from V^- to V^+ takes place such that V(x) changes little over distances of the order of the mean free path. Actually, we can take dV/dx out from under the integral sign in Eq. (3.9) in this case, and the integral equation reduces in first approximation to the differential equation

$$V-V^-+v_s^2\left(\frac{1}{V}-\frac{1}{V^-}\right)=al\frac{V_s\rho_0}{j_0}\frac{dV}{dx}. \tag{3.12}$$

It is well known that Eq. (3.12) has a solution which takes on the values V^+, V^- as $x\to\pm\infty$. For the solution to be stable here, the conditions $V^->V_s$ and $V^+<V_s$ must be satisfied. The width of the transition region is determined by the mean free path. Thus, this case is analogous to that considered in ordinary gas dynamics (for the approximation that we have employed).

It follows from Eq. (3.9) that a stationary shock wave cannot exist in a plasma in which the transition from V^- to V^+ takes place at distances much less than the wavelength. Actually, in this case, if we assume that the transition from V^- to V^+ takes place near x_0, the equation can be written approximately in the form

$$V-V^-+v_s^2\left(\frac{1}{V}-\frac{1}{V^-}\right)=(V^--V^+)\frac{av_s\rho_0}{\pi j}K\left(\left|\frac{x-x_0}{l}\right|\right). \tag{3.13}$$

Since the correct form of Eq. (3.13) differs from zero when $x-x_0\sim l$, it then follows that the assumption made in obtaining Eq. (3.13) is not validated. Thus, stationary shock waves cannot exist in a plasma of width much less than the mean free path. Of course, it does not follow from this that no shock waves can in general exist in a plasma with a width less than the mean free path. Such shock waves can exist in the plasma, but they are not stationary.

We now consider the case in which the plasma is located in an external magnetic field. Here again the problem arises of obtaining the nonlinear equations under the condition that the dissipation be small. Since the expressions for the dissipative terms in the linear approximation are already known, it remains only to establish the form of the equations of magnetohydrodynamics without account of dissipative processes. In place of Eq. (3.1), we now have the equation

$$\mathbf{v}\frac{\partial f}{\partial \mathbf{r}}+e\left(\mathbf{E}+\frac{1}{c}[\mathbf{vB}]\right)\frac{\partial f}{\partial \mathbf{p}}=0. \tag{3.14}$$

Limiting ourselves here to the case of an isotropic velocity distribution, we seek a solution of Eq. (3.14) also in the form of (3.2). In order to find an expression for E, we proceed as in the case

$V = 0$. In place of Eq. (3.4), we now have the equation

$$m\left(\mathbf{V}_e \frac{\partial}{\partial \mathbf{r}}\right)\mathbf{V}_e = e\mathbf{E} + \frac{1}{q_e}\frac{\partial}{\partial \mathbf{r}}(q_e \varkappa T) + \frac{e}{c}[\mathbf{V}_e \mathbf{B}], \quad (3.15)$$

whence we find

$$e\mathbf{E} \approx -\frac{1}{q_e}\frac{\partial}{\partial \mathbf{r}}(q_e \varkappa T) - \frac{e}{c}[\mathbf{V}_e \mathbf{B}]. \quad (3.16)$$

Substituting this expression in Eq. (1.2), and taking it into account that $j_e = q_e V_e$ and $q_e = |e/e_i|\rho$, we obtain the equation of motion in the nonlinear approximation, but without account of dissipative terms. If we add the expression for $F^{(diss)}$ to this equation (which is computed in the linear approximation), we get the desired set of equations for $T = \text{const}$:

$$\frac{\partial \rho}{\partial t} + \operatorname{div} \rho\mathbf{V} = 0,$$

$$\frac{\partial \mathbf{V}}{\partial t} + \left(\mathbf{V}\frac{\partial}{\partial \mathbf{r}}\right)\mathbf{V} = -\frac{v_s^2}{\rho}\frac{\partial \rho}{\partial \mathbf{r}} + \frac{1}{4\pi\rho}[\operatorname{rot}\mathbf{B}, \mathbf{B}] + \frac{F^{(\text{diss})}}{\rho} \quad (3.17)$$

The value of $F^{(diss)}$ is determined by Eq. (1.15). Without the term $F^{(diss)}$, Eq. (3.17) is identical with the equation of magnetohydrodynamics for an ideal liquid, if we take the equation of state to be $p = v_s^2\rho$. We now proceed to the problem of the possibility of existence of shock waves in the plasma in the presence of a magnetic field. As above in the study of shock waves, the unit vector **n** is perpendicular to the surface of discontinuity. We consider the continuity condition on the discontinuity surface. In order to write down the continuity relation for the momentum flux vector, we write out the expression for $F^{(diss)}$ in the form of the divergence of the tensor $\mathcal{F}_{\alpha\beta}^{(diss)}$. Employing Eq. (1.14), we obtain the following expression for $\mathcal{F}_{\alpha\beta}^{(diss)}$:

$$\mathcal{F}_{\alpha\beta}^{(\text{diss})} = a v_s \rho_0$$
$$\left\{2b_\alpha b_\beta\left(\mathbf{b}\frac{\partial}{\partial \mathbf{r}}\right)(\mathbf{bL}) - b_\beta\frac{\partial}{\partial r_\alpha}(\mathbf{bL}) - b_\alpha b_\beta\left(\frac{\partial}{\partial \mathbf{r}}\mathbf{L}\right) + \frac{\partial}{\partial r_\alpha}L_\beta\right\}, \quad (3.18)$$

where

$$\mathbf{L} = \int Q(\mathbf{r} - \mathbf{r}')\,\mathbf{V}(\mathbf{r}')\,d\mathbf{r}', \qquad b_\alpha = B_{0\alpha}/B_0.$$

The expression for the momentum flux vector has the form

$$\pi_\alpha = (\rho V_\alpha V_\beta + p\delta_{\alpha\beta})n_\beta - \frac{1}{4\pi}\left[B_\alpha B_\beta - \frac{1}{2}B^2\delta_{\alpha\beta}\right]n_\beta - \mathcal{F}_{\alpha\beta}n_\beta. \quad (3.19)$$

It follows from Eq. (3.19) that the continuity condition for the components of the momentum flux vector on the surface of discontinuity, and the corresponding integral equations, will contain integral terms of the same type as in Eq. (3.10). Therefore, solutions here which describe stationary shock waves in a plasma, with a width much less than the mean free path, are shown to be impossible.

The conditions should again be noted for which the results given in the present paper are valid.

a) Conditions are considered for which the collisions are unimportant. The mean free path is assumed to be infinitely large.

b) The plasma is assumed to be strongly nonisothermal, which gives grounds for neglecting the thermal motion of the ions. Account of the thermal motion of the ions does not change the essentials of the results.

c) Significant changes in the functions ρ, **V**, **B** take place over distances much greater than the Debye radius, the Larmor radius and c/ω_L.

To conclude the paper, we make a brief comparison of the equations of magnetohydrodynamics obtained here for a plasma with the results of CGL[3]; these latter results were established on the basis of many investigations devoted to the magnetohydrodynamic theory of plasma. It should be noted here that the chief assumption of this work on the perpendicularity of the electric field and the magnetic induction in a plasma without collisions is actually not satisfied [as is seen from Eq. (1.14), and also (3.16)]. In particular, this leads to a violation of the adiabatic equations of CGL. Moreover, it must be noted that only the correct account of the longitudinal field arising in the plasma (a field which violates the basic assumption of CGL) leads to the true spectrum of magnetohydrodynamic waves (2.4) (see also reference 13).

Finally, we note that in a comparison of the present work with the results of CGL, it must be kept in mind that we have limited ourselves to a consideration of a strongly nonisothermal plasma, in which the temperature of the ions can be set equal to zero.

---

[1] V. L. Ginzburg, JETP **21**, 788 (1951).

[2] A. A. Vlasov, JETP **8**, 291 (1938).

[3] Chew, Goldberger, and Low, Proc. Roy. Soc. (London) **A236**, 112 (1956).

[4] Chandrasekhar, Kaufman, and Watson, Ann. of Phys. **2**, 433 (1957).

[5] B. B. Kadomtsev, Физика плазмы и проблема управляемых термоядерных реакций (Plasma Physics and Problems of Controlled Thermonuclear Reactions) **3** (Academy of Sciences Press, 1958), p. 24.

[6] L. I. Rudakov and R. Z. Sagdeev, ibid. p. 268.

[7] V. P. Silin, JETP 23, 649 (1952).

[8] B. N. Gershman, JETP 24, 453 (1953); also JETP 31, 707 (1956) and 37, 695 (1959), [Soviet Phys. JETP 4, 582 (1957) and 10, 497 (1960) Изв. Вузов. Радиофизика (News of the Universities, Radiophysics) 1, 3 (1958).

[9] G. V. Gordeev, JETP 27, 19 (1954).

[10] K. N. Stepanov, JETP 34, 1292 (1958) and 35, 1155 (1958), Soviet Phys. JETP 7, 892 (1958) and 8, 808 (1959).

[11] S. I. Braginskii and A. P. Kazantsev, op. cit. ref. 5 4, p. 24.

[12] I. B. Bernstein, Phys. Rev. 109, 10 (1958).

[13] K. N. Stepanov, Ukr. Phys. J. 4, 678 (1959).

[14] V. L. Ginzburg, Usp. Fiz. Nauk 69, 537 (1959) Soviet Phys.-Uspekhi 2, 874 (1960); V. L. Ginzburg and V. V. Zheleznyakov, Астрономический журнал 35, 694 (1958) Soviet Astronomy 2, 653 (1959); V. V. Zheleznyakov, Изв. Вузов. Радиофизика (News of the Universities-Radiophysics) 2, 14 (1959).

[15] A. B. Kitsenko and K. N. Stepanov, JETP 38, 1840 (1960), Soviet Phys. JETP 11, 1323 (1960).

[16] V. P. Silin, JETP 38, 977 (1960), Soviet Phys. JETP 11, 703 (1960).

[17] E. P. Sirotina and S. I. Syrovat-skii, JETP 39, 746 (1960), Soviet Phys. JETP 12, 521 (1961).

[18] L. Tonks and I. Langmuir, Phys. Rev. 33, 195 (1929).

Translated by R. T. Beyer
204

SOVIET PHYSICS JETP VOLUME 13, NUMBER 4 OCTOBER, 1961

POLARIZATION RESULTING FROM SCATTERING OF NEUTRONS BY FERROMAGNETIC SUBSTANCES

S. V. MALEEV

Leningrad Physico-Technical Institute, Academy of Sciences, U.S.S.R.

Submitted to JETP editor November 30, 1960

J. Exptl. Theoret. Phys. (U.S.S.R.) **40**, 1224-1227 (April, 1961)

An expression is obtained for the polarization of slow neutrons scattered by a ferromagnet. It is shown that the polarization vector consists of two mutually perpendicular components, one of which is due to the interference of nuclear and magnetic scattering, and the other to inelastic magnetic scattering with spin flip of the neutron.

In the present paper it is shown that an experimental study of the polarization resulting from the scattering of unpolarized slow neutrons in ferromagnets can, in certain cases, enable one to determine the fraction of those neutrons scattered in a given direction which are magnetically scattered.

As was shown by Halpern and Johnson,[1] the amplitude for scattering of a neutron by a system of N magnetic atoms has the form

$$f = \frac{1}{\sqrt{N}} \sum_l e^{i\mathbf{q}\mathbf{R}_l} \left\{ A_l + \frac{1}{2} B_l \mathbf{J}_l \boldsymbol{\sigma} - \gamma r_0 F(q) \left(\mathbf{S}_l, \boldsymbol{\sigma} - (\mathbf{e}\boldsymbol{\sigma})\, \mathbf{e} \right) \right\}. \quad (1)$$

Here $\mathbf{p}$ and $\mathbf{p}'$ are the neutron momentum before and after the scattering, $\mathbf{q} = \mathbf{p} - \mathbf{p}'$; $\mathbf{R}_l$ and $\mathbf{S}_l$ are the coordinates and spin of the l-th atom; $A_l + \frac{1}{2} B_l \mathbf{J}_l \cdot \boldsymbol{\sigma}$ is the amplitude for scattering of the neutron by the nucleus, where $\mathbf{J}_l$ is the spin of the nucleus and $\boldsymbol{\sigma}/2$ is the neutron spin. γ is the absolute value of the magnetic moment of the neutron in nuclear magnetons; $r_0 = e^2/mc^2$ is the classical radius of the electron; $F(q)$ is the magnetic form factor of the atom; $\mathbf{e} = \mathbf{q}q^{-1}$.

From (1) we see that the magnetic scattering amplitude is proportional to the matrix elements of the vector

$$\mathbf{K} = \sum_l \exp(i\mathbf{q}\mathbf{R}_l)\, \mathbf{S}_l.$$

The vector $\mathbf{K}$ consists of two parts: a longitudinal component K_z along the magnetization vector of the system, and two perpendicular components $K^{\pm} = K_x \pm iK_y$. As shown by Holstein and Primakoff,[2] the component K_z is responsible for transitions in which the total number of spin waves is unchanged (in our case, for elastic scattering and for scattering with absorption of one spin wave and emission of another), or is changed by two (simultaneous emission or absorption of two spin waves by the neutron). The components $K^{\pm}$ are responsible for transitions with a change of of the total number of spin waves by unity.*

Thus for scattering processes for which the matrix elements of the operator K_z are different from zero, the polarization of the scattered neutrons can arise only from interference with that part of the nuclear scattering which is independent of the nuclear spins (where we assume that the nuclei are unpolarized). Such interference is obviously possible only for elastic and for magnetovibrational scattering.

Now let us consider those scattering processes in which the matrix elements of the operators $K^{\pm}$ are different from zero. We shall neglect the small relativistic corrections to the interaction of the atomic spins (dipole-dipole interaction and anisotropy energy). Then the matrix elements of K^{+} (K^{-}) are different from zero only for transitions in which the total number of spin waves increases (decreases) by unity. Using this fact and the well known formula for the polarization in the scattering of an unpolarized beam

$$\mathbf{P} = \tfrac{1}{2}\, \mathrm{Sp} \langle f^{+} \boldsymbol{\sigma} f \rangle / \sigma(\mathbf{n}) \quad (2)$$

(where Sp is the trace over the spin indices of the neutron, and $\langle \ldots \rangle$ denotes an average over the initial state of the scatterer and an integration over all energies of the neutrons scattered in the direction $\mathbf{n}$; $\sigma(\mathbf{n})$ is the total cross section for scattering in the direction $\mathbf{n}$), we get the expression for the polarization:

---

*If we neglect relativistic corrections to the interaction of the atomic spins, we may say that the matrix elements of K_z are different from zero only for transitions in which the total spin of the system is unchanged, and $K^{\pm}$ for transitions with a change of the spin of the system by ± 1.

$$\mathbf{P} = \sigma^{-1}(\mathbf{n})\{-2\,\mathrm{Re}\,\overline{A}Sr_0\gamma F(q)(1-G(T))$$
$$+\ \sigma_{\mathrm{coh}}(\mathbf{n})\,|A|^{2}(\mathbf{m}-(\mathbf{em})\mathbf{e})$$
$$+\ 2(\mathbf{em})\mathbf{e}\,[1+(\mathbf{em})^2]^{-1}[\sigma_-(\mathbf{n})-\sigma_+(\mathbf{n})]\}. \qquad (3)$$

Here $\mathbf{m}$ is a unit vector along the direction of magnetization; $\overline{A}$ is the average of the amplitude A over the distribution of isotopes in the lattice; S is the spin of the atom; G(T) is the percentage deviation of the spontaneous magnetization at temperature T from its value at T = 0; $\sigma_{\mathrm{coh}}(\mathbf{n})$ is the cross section for coherent scattering by the crystal into the direction $\mathbf{n}$; $\sigma_+(\mathbf{n})$ and $\sigma_-(\mathbf{n})$ are the respective cross sections for magnetic scattering with increase or decrease by unity in the number of spin waves.

Strictly speaking, in Eq. (3) we should include the dependence of the vector $\mathbf{e}$ on the energy of the scattered neutrons, write the expression $\mathbf{P}$ for a given energy of scattering of the neutron and then integrate over all energies. But usually the intensity of the scattered neutrons is significantly differently from zero only when $\mathbf{q} \approx \boldsymbol{\tau}$, where $\boldsymbol{\tau}$ is a vector of the reciprocal lattice multiplied by 2κ, and consequently the veotor $\mathbf{e} \approx \boldsymbol{\tau}\tau^{-1}$ can be regarded as independent of energy to a high degree of accuracy.

The most interesting consequence of formula (3) is that the polarization vector consists of two mutually perpendicular components. One of them, directed along the vector $\mathbf{m} - \mathbf{e}(\mathbf{e}\cdot\mathbf{m})$, is the result of interference between nuclear and magnetic scattering. As we have already remarked, this interference occurs for elastic and magneto-vibrational scattering. The other component, which is along the vector $\mathbf{e}$, is proportional to the difference of the cross sections $\sigma_-(\mathbf{n}) - \sigma_+(\mathbf{n})$. By separately studying these two components of the polarization vector, one can draw various conclusions concerning elastic magnetic and magneto-vibrational scattering one the one hand, and concerning inelastic magnetic scattering with emission and absorption of spin waves on the other. Since the scatterer is magnetized, the polarization vector will rotate around the field. As a result of such rotation, at sufficiently large distances from the scatterer the component of $\mathbf{P}$ which is perpendicular to the field will effectively be averaged to zero (since the neutrons arriving at the detector will have traversed different paths in the magnetic field). Thus we practically observe only the component of $\mathbf{P}$ which is parallel to the field.

Having magnetized the crystal perpendicular to the vector $\mathbf{e}$ (where $\mathbf{e} \approx \boldsymbol{\tau}/\tau$, with $\boldsymbol{\tau}$ a vector of the reciprocal lattice, in whose neighborhood we are studying the scattering), we separate out the part of the polarization vector which is due to interference of magnetic and nuclear scattering:

$$\mathbf{P}_{\mathrm{int}} = -\frac{2\,\mathrm{Re}\,\overline{A}Sr_0\gamma F(q)(1-G(T))\,\sigma_{\mathrm{coh}}(\mathbf{n})\,|\overline{A}|^{-2}}{\sigma(\mathbf{n})}\,\mathbf{m}. \qquad (4)$$

This part of the polarization vector was studied experimentally by Nathans, Shull et al.[3] If we magnetize the scatterer along $\mathbf{e}$, we get the part of the vector $\mathbf{P}$ due to inelastic magnetic scattering:

$$\mathbf{P}_{\mathrm{mag}} = [(\sigma_-(\mathbf{n}) - \sigma_+(\mathbf{n}))/\sigma(\mathbf{n})]\,\mathbf{e}. \qquad (5)$$

The numerator of (5) contains the difference $\sigma_-(\mathbf{n}) - \sigma_+(\mathbf{n})$. It is known[4,5] that at low temperatures (when one can speak of spin waves*) the main scattering processes are those with absorption or emission of one spin wave. The kinematics of these scattering processes are such that there are cases where there is a considerable intensity of inelastic magnetic scattering and, at the same time, there is scattering accompanied only by emission or only by absorption of a spin wave. Then Eq. (5) becomes

$$\mathbf{P}_{\mathrm{mag}} = \mp(\sigma_\pm(\mathbf{n})/\sigma(\mathbf{n}))\,\mathbf{e}, \qquad \mathbf{m} \parallel \mathbf{e}. \qquad (6)$$

From (6) it follows that if we know $\mathbf{P}_{\mathrm{mag}}$ and the total scattered intensity we can easily determine $\sigma_+(\mathbf{n})$.

Let us consider the two most important cases.

1. Scattering when the Bragg condition $|\mathbf{p} + \boldsymbol{\tau}| \approx \mathrm{p}$ is almost satisfied. If $\Delta > (2\alpha)^{-1}$, then only scattering with absorption of a spin wave can occur; but if $\Delta < (2\alpha)^{-1}$, then one can have only emission of a spin wave. Here Δ is defined by the formula

$$\Delta = (|\mathbf{p} + \boldsymbol{\tau}| - p)/p \approx 2\sin 2\psi_B\,\delta\psi$$

(where ψ_B is the angle between $\mathbf{p}$ and $\boldsymbol{\tau}$ satisfying the Bragg condition:

$$|\mathbf{p} + \boldsymbol{\tau}| = p \qquad (\cos\psi_B = -\tau/2p),$$

$\delta\psi$ is the deviation of the angle ψ between $\mathbf{p}$ and $\boldsymbol{\tau}$ from the angle ψ_B), and

$$\alpha = 2JMS\gamma_0\delta^2/3\hbar^2 \gg 1$$

(J is the exchange integral, γ_0 the number of nearest neighbors, δ the distance between them, and M the mass of the neutron).

2. Scattering of slow neutrons, $p < (\tau_{\min}/2)\times(1 - 1/4\alpha)$. In this case scattering at large angles

---

*Recently Engert[6] and Ginzburg and Faǐn[7] have attempted to extend the spin wave picture to the whole range of temperature below the Curie point. In this note we shall not discuss the consequences of their theory for the scattering of neutrons.

can occur only with absorption of a spin wave. A detailed discussion of the kinematics of the scattering as well as formulas for the cross section for these cases can be found in reference 4.

We note that for both cases the wave vector of the spin wave cannot be very small. But we know[2] that relativistic corrections to the interaction of the atomic spins affect the dispersion law only for very long spin waves. Thus they need not be included in the cases considered here.

In conclusion the author expresses his gratitude to G. M. Drabkin for a discussion of various questions concerning magnetic scattering of neutrons, which stimulated the writing of this note.

---

[1] O. Halpern and M. H. Johnson, Phys. Rev. 55, 898 (1939).

[2] T. Holstein and H. Primakoff, Phys. Rev. 58, 1098 (1940).

[3] Nathans, Shull, Shirane and Andresen, J. Phys. Chem. Solids 10, 138 (1959).

[4] S. V. Maleev, JETP 33, 1010 (1957), Soviet Phys. JETP 6, 776 (1958).

[5] S. V. Maleev JETP 34, 1518 (1958), Soviet Phys. JETP 7, 1048 (1958).

[6] F. Englert, Phys. Rev. Letters 5, 102 (1960).

[7] V. L. Ginzburg and V. M. Faĭn, JETP 39, 1323 (1960), Soviet Phys. JETP 12, 923 (1961).

Translated by M. Hamermesh
205

SOVIET PHYSICS JETP VOLUME 13, NUMBER 4 OCTOBER, 1961

Letters to the Editor

SPONTANEOUS MAGNETIZATION OF THIN FERROMAGNETIC FILMS

V. A. IGNATCHENKO

Institute of Physics, Siberian Branch,
Academy of Sciences, U.S.S.R.

Submitted to JETP editor December 21, 1960

J. Exptl. Theoret. Phys. (U.S.S.R.) **40**, 1228-1229 (April, 1961)

IT is known that when thin ferromagnetic films are deposited on an isotropic substrate, they acquire a uniaxial anisotropy, even in the case of perpendicular incidence of the metal ions (the anisotropy that occurs with angle of incidence less than 90° will not concern us here). Málek, Schüppel, et al.[1,2] conducted elegant experiments that demonstrated that this anisotropy occurs spontaneously, together with the appearance of ferromagnetism, at a certain film thickness, independently of whether or not an external magnetic field was applied to the film at the time of deposition. They studied certain properties of the spontaneous anisotropy, and they presented a hypothesis that attributes the occurrence of the anisotropy to a definite orientation of interacting pairs, formed by atoms of the ferromagnet and by defects.

In a thin film, in contrast to bulk polycrystals, the vector $\mathbf{I}_s$ upon appearance of ferromagnetism orients itself along a single direction throughout the whole film (the film either is magnetized to saturation or breaks up into domains with oppositely directed magnetizations). This direction is random when the film is deposited in the absence of an external field; when the deposition occurs in a magnetic field, the selected direction coincides with the direction of the field (or is close to it). Therefore the pairs of ferromagnet atoms and defects in any case are oriented by the internal field (from the requirement of minimum energy of the demagnetizing field) along a direction that is common to the whole polycrystalline film.

Another mechanism capable of leading to the occurrence of spontaneous anisotropy is proposed here; it is connected with magnetostriction. Upon appearance of spontaneous magnetization, magnetostrictive deformations of the film material occur. A circular region on the film surface elongates under the influence of magnetostriction (for $\lambda > 0$) to an ellipse in the direction of $\mathbf{J}_s$. It is such a deformed film that will adhere to the substrate. Magnetizing the film in the perpendicular direction entails doing work against the forces of adhesion of the film to the substrate (and of the individual "crystallites" to one another). The difference in magnetoelastic energy between the original and the perpendicular magnetizations of the film is

$$\Delta f_{\mathrm{me}} = {}^3/_2\,\lambda\sigma, \tag{1}$$

where σ is the stress produced by the magnetostrictive deformations. From the known relation of the stresses to the deformations, in the case of isotropic magnetostriction, we get

$$\sigma = E\lambda/(1+\nu)$$

(E = Young's modulus, ν = Poisson's ratio). Consequently the difference in magnetoelastic energy density, or the effective constant of spontaneous anisotropy, is

$$K_1' = 3E\lambda^2/2(1+\nu). \tag{2}$$

The values of E and ν for different materials do not differ greatly; and it may be assumed that the values measured on bulk specimens can be used for thin films. For the magnetostriction constant, such an assumption is appreciably further from correctness. But since the magnetostriction of thin films is not known, we shall use the bulk values for preliminary estimation. On taking[3] $\lambda = -7 \times 10^{-6}$ for iron and -34×10^{-6} for nickel, we get for the effective anisotropy constants 1.1×10^2 and 2.34×10^3 erg/cm^3, respectively.

Verification of this hypothesis can be accomplished either by direct measurement of the quantities that appear in formula (2) or by an indirect method. For example, the spontaneous anisotropy should diminish on separation of the film from the substrate; stronger adhesion of the film to the substrate should be associated with greater stability of the position of the anisotropy axis; etc.

The hypothesis presented here and the hypothesis advanced in references 1 and 2 appear not to be mutually exclusive.

---

[1] Z. Málek and W. Schüppel, Ann. Physik **6**, 252 (1960).

[2] Z. Málek, W. Schüppel, O. Stemme, and W. Andrä, Ann. Physik **5**, 211 (1960).

[3] C. Kittel, Revs. Modern Phys. **21**, 541 (1949).

Translated by W. F. Brown, Jr.
206

THE DEPENDENCE OF THE HALL CONSTANT OF p-TYPE GERMANIUM ON THE MAGNETIC FIELD STRENGTH

É. A. ZAVADSKII, Yu. T. KOVRIZHNYKH and I. G. FAKIDOV

Institute for the Physics of Metals, Academy of Sciences, U.S.S.R.

Submitted to JETP editor January 18, 1961

J. Exptl. Theoret. Phys. (U.S.S.R.) **40**, 1229-1231 (April, 1961)

THE dependence of the Hall constant of hole type semiconductors on the strength of the magnetic field has been studied several times. The experimental investigations of the field dependence of the Hall constant in p-type InSb[1,2] showed good qualitative agreement between the results of measurements and the deductions from classical theory.[3] This agreement consists in the change of sign of the Hall constant with increasing magnetic field in the temperature region where the Hall effect has the electronic sign. However, the Hall constant of p-type germanium in weak fields changes sign from positive to negative. Willardson, Harman, and Beer[4] used a model with three types of current carriers (electrons, ordinary holes and "light" holes) to explain the field dependence of the Hall constant in p-type germanium, and obtained good agreement between the deductions from the theory and the experimental results in weak fields up to 8 koe. Measurements of the Hall effect in p-type germanium by Stafeev and Tuchkevich in fields up to 20 koe[5] did not show a second change in sign of the Hall constant, which they interpreted as a disagreement between the results and the deductions from the theory. In addition, Orlova and Tuchkevich[6] suggested that the disagreement between the theoretical and experimental values of the Hall constant lies in the incorrectness of the energy model of germanium. It is thus of great interest to measure the Hall effect in p-type germanium specimens in the region of stronger magnetic fields and to compare the results obtained with the theoretical predictions.

The aim of the present work is to measure the Hall effect in p-type germanium over a wide range of magnetic fields. The measurements were made on a p-type specimen with room temperature resistivity 25 ohm-cm (specimen No. 1) in pulsed magnetic fields up to 200 koe, and also on a specimen with room temperature resistivity 58 ohm-cm (specimen No. 2) in fields up to 300 koe).

The high pulsed magnetic field generator described earlier[7] was used in the measurements. The specimens had dimensions 8 × 2.5 × 0.8 mm and were placed in the uniform field region of the solenoid with the help of a special holder. The ohmic contacts were fixed with indium, followed by heating in vacuum. The temperature was regulated by a thermostat and was controlled by a copper-constantan thermocouple. The measuring system made it possible to obtain the field dependence of the Hall voltage directly on the oscilloscope screen.

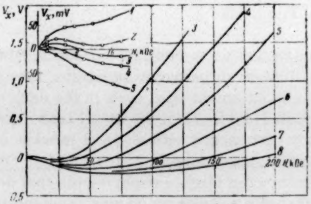

Field dependence of the Hall voltage for specimen No. 1. Curve 1 corresponds to a temperature of 50°C; 2 – 53.5°C; 3 – 55°C; 4 – 58.5°C; 5 – 62.5°C; 6 – 68.5°C. 7 – 76°C; 8 – 85°C.

The figure shows the results for specimen No. 1. The curves, obtained in pulsed field, were not plotted point by point, as they are enlarged oscillograms. The initial part of the dependence $V_X(H)$ (up to 20 koe) was measured in the constant field of an electromagnet.

The results can be explained by a model in which the resultant Hall field is made up of components produced by separate types of current carriers. The relation between the separate components of the Hall effect changes with changing temperature and field strength.

In specimen 1, the ratio of mobilities and concentrations of the separate types of current carriers is such that for $t < 60°C$ the Hall constant in weak fields becomes positive. On increasing the magnetic field, the ratio of the components changes, owing to the bending of the lines of current flow. Since the bending of the lines is determined by the parameter uH (where u is the mobility of the current carriers and H is the field strength), an increase in the field decreases first the contribution of the most mobile fast holes and then that of the electrons. This leads to a double change in sign of the Hall constant with a change in field strength in the temperature interval between 56 and 60° C. The first time that $V_X(H)$ passes through zero is connected with the reduction in the contribution of fast holes, and the second with that of electrons.

The form of the $V_X(H)$ dependence also changes with changing temperature. On increasing the temperature, the field corresponding to the first change decreases, while the field corresponding to the second increases. There is thus no first passing of the Hall constant through zero for $t > 60°$ C (curve 5). A decrease in the temperature leads to a reduction in the number of free electrons and to an increase in the mobility of the current carriers. As a result, the role of electrons in the Hall effect decreases, and the field range in which the influence of fast holes becomes appreciable narrows. Our results agree with the deductions from classical theory of galvanomagnetic phenomena not only qualitatively but quantitatively. In fact, if we take the concentration of light holes to be 5% of that of heavy holes, and the ratio of their mobilities to be 8.0, then the experimental field dependence of the Hall constant agrees well with theory. Numerical comparison was made for specimen No. 1 at 55, 62.5, and 76° C. The experiments show that in the temperature range studied the ratio of mobilities of "light" and "heavy" holes does not change, while the ratio of their concentrations is, to a first approximation, proportional to the absolute temperature.

---

[1] D. N. Nasledov and A. Yu. Khalilov, J. Tech. Phys. (U.S.S.R.) **26**, 6 (1956), Soviet Phys.-Tech. Phys. **1**, 3 (1956).

[2] H. Weiss, Z. Naturforschg. **8a**, 463 (1953).

[3] O. Madelung, Z. Naturforschg. **8a**, 791 (1953).

[4] Willardson, Harman and Beer, Phys. Rev. **96**, 1512 (1954).

[5] V. I. Stafeev and V. M. Tuchkevich, J. Tech. Phys. (U.S.S.R.) **28**, 1642 (1958); Soviet Phys.–Tech. Phys. **3**, 1513 (1958).

[6] N. S. Orlova and V. M. Tuchkevich, Физика твердого тела **1**, 1631 (1959), Soviet Phys. Solid State 1, 1491 (1960).

[7] I. G. Fakidov and É. A. Zavadskii, Физика металлов и металловедение **8**, 562 (1959), The Physics of Metals, Vol. 8, No. 4, 81 (1960).

Translated by R. Berman
207

THE WEIZSÄCKER-WILLIAMS RELATION FOR MATRIX ELEMENTS

A. M. BADALYAN and Ya. A. SMORODINSKII

Submitted to JETP editor February 8, 1961

J. Exptl. Theoret. Phys. (U.S.S.R.) **40**, 1231-1233 (April, 1961)

FERMI[1] was evidently the first to use the analogy between the electromagnetic field of a moving charge and a radiation field. This method was developed by Weizsäcker[2] and Williams,[3] who obtained the spectrum of photons equivalent to the field of a charge. Recently there have been a number of papers in which authors have used this method (cf. Low,[4] and especially Pomeranchuk and Shmushkevich[5]).

In these papers, however, the method is applied only to cross sections averaged over polarizations. We shall show how a virtual quantum can be replaced by a real one directly in the matrix element.

Let us consider a diagram describing some process that occurs in the field of another particle (and with the diagram connected with the source of the field by one photon line). The momentum of the virtual photon is $q = P_1 - P_2$ (the difference of the four-momenta of the heavy particle before and after the collision). The Fourier components of such a field are given by

$$A(q) = -2\pi Zeq^{-2}P\delta(qP), \tag{1}$$

where $P = P_1 + P_2$, and the δ function expresses the obvious relation $(P_1 - P_2)(P_1 + P_2) = 0$; we use throughout $ab = \mathbf{a}\cdot\mathbf{b} - a_0b_0$. In the system in which $\mathbf{P} = 0$, Eq. (1) goes over into the Fourier component of index 4 for the static Coulomb field.

We call one of the external lines of the diagram the incident particle [momentum $p(p_0, \mathbf{p})$, mass m]. In order for the expression (1) to go over into a free field, we must choose a new gauge. In the calculation of formulas with a free photon one usually chooses the gauge so that the photon will have no scalar component in some chosen coordinate system (usually in the system $\mathbf{p} = 0$). This condition can be written in the form $ep = 0$. Therefore let us choose a new polarization vector $\tilde{e}$ by the formula

$$\tilde{e} = [P - q(qp)^{-1}(pP)]f^{-1}, \quad f^2 = P^2 + q^2(qp)^{-2}(pP)^2, \tag{2}$$

so that $\tilde{e}p = 0$. Then the field (1) is replaced by

$$A(q) = -2\pi Zeq^{-2}\delta(qP)f\tilde{e}. \tag{3}$$

This formula gives the field of equivalent photons (amplitude and polarization).

It is not hard to get from it also the spectrum of equivalent photons. Let us determine the number of equivalent photons in the invariant interval d^4q:

$$I(\varkappa, q^2)d^4q = -\varkappa^{-1} m^{-2} \int T_{ik} p_i p_k \, dV d^4q, \qquad (4)$$

where T_{ik} is the energy-momentum tensor of the field (3), and $-\kappa = m^{-1}(pq)$ is a variable that plays the part of the energy of the quantum. The integration is over a spacelike hypersurface orthogonal to p. It is not hard to see that in the system $\mathbf{p} = 0$ this expression goes over into the ratio of the energy T_{00} of the field to the energy q_0 of one quantum, and consequently Eq. (4) gives an invariant definition of the number of equivalent photons. It is important to note that only with the gauge (2) is the number of photons proportional to the square of the amplitude of the field (as in the usual gauge for free photons). The calculations give

$$I(\varkappa, q^2) = \frac{Z^2\alpha}{2\pi^2}\frac{(q_1p)}{(pP)} f^2 \left[1 + \frac{m^2}{2(q_1p)^2} q_1^2\right] \frac{\delta(qP)}{q^4}. \qquad (5)$$

Here we have introduced q_1, which is the component of q orthogonal to $\tilde{e}$ and plays the part of the wave vector of the quantum:

$$q_1\tilde{e} = 0, \quad q_1 = q - \tilde{e}(\tilde{e}q), \quad qp = q_1p.$$

If the condition $q_1^2 \ll (q_1p)^2m^{-2}$ is satisfied, we can neglect the second term in the square brackets in Eq. (5). In the system $\mathbf{p} = 0$ this condition requires that the four-length of the "wave vector" be small in comparison with its energy. When this condition holds the spectrum can be written in the form

$$I(\varkappa, q^2) = \frac{Z^2\alpha}{2\pi^2}\frac{(pP)}{(q_1p)}\left(q^2 + P^2\frac{(qp)^2}{(pP)^2}\right)\frac{\delta(qP)}{q^4}. \qquad (6)$$

The spectrum can also be written in an invariant three-dimensional form.

To get rid of the δ function, we introduce

$$P = P_{\mathrm{I}} + P_{\mathrm{II}}, \; P_{\mathrm{I}} = -m^{-2}(pP)p, \; P_{\mathrm{II}}p = 0.$$

Then

$$\delta(pP) = \delta[-m^{-2}(pP)(qp) + qP_{\mathrm{II}}].$$

We can integrate over the component of q parallel to p [integral over d(qp)]. After this there remains the integration over the three-dimensional space orthogonal to p, under the supplementary condition

$$m^{-1}(qp) = m(qP_{\mathrm{II}})(pP)^{-1} = -(qv),$$

where the vector $\mathbf{v} = -m(pP)^{-1}P_{\mathrm{II}}$ has three independent components (because of the condition $vp = 0$) and goes over into the ordinary velocity vector in the reference system in which $\mathbf{p} = 0$. The spectrum is finally written in the form

$$I(\varkappa, q^2)d^3q = \frac{Z^2\alpha}{2\pi^2}\frac{m}{(qv)}[q - (qv)v - m^{-1}(qv)p]^2\frac{d^3q}{q^4}$$

$$\text{with } qp = 0. \qquad (7)$$

It is not hard to see that for $\mathbf{p} = 0$ this expression agrees with the usual one (for $|\mathbf{v}| \sim 1$). The square-bracket expression in this case goes over into $\mathbf{q}_\perp^2$, where $\mathbf{q}_\perp$ is the three-dimensional vector orthogonal to $\mathbf{v}$.

---

[1] E. Fermi, Z. Physik **29**, 315 (1924).

[2] C. Weizsäcker, Z. Physik **88**, 612 (1934).

[3] E. J. Williams, Phys. Rev. **45**, 729 (1934); Proc. Roy. Soc. **A139**, 163 (1933); Kgl. Danske Videnskab. Selskab, Mat.-fys. Medd. **13**, No. 4 (1935).

[4] F. E. Low, Phys. Rev. **120**, 582 (1960).

[5] I. Ya. Pomeranchuk and I. M. Shmushkevich, Nuclear Phys. **23**, 452 (1961).

Translated by W. H. Furry
208

ON THE PARTICIPATION OF π^0 MESONS IN ELECTROMAGNETIC PROCESSES

V. N. BAĬER and V. V. SOKOLOV

J. Exptl. Theoret. Phys. (U.S.S.R.) **40**, 1233-1234 (April, 1961)

Submitted to JETP editor February 8, 1961

THE direct interaction of π^0 mesons with the electromagnetic field can be written in the form[1]

$$H_{int} = \frac{1}{\mu}\sqrt{\frac{8\pi}{\mu\tau}}\,\psi(x)\varepsilon_{\alpha\beta\gamma\delta}\frac{\partial A^\alpha(x)}{\partial x_\beta}\frac{\partial A^\gamma(x)}{\partial x_\delta} \qquad (1)$$

where τ is the mean life of the π^0 meson and μ its mass. From this follows that π^0 mesons can be produced in electromagnetic processes:

1) $e + e \rightarrow e + e + \pi^0$[2]; 2) $\gamma + e \rightarrow \pi^0 + \gamma + e$;

3) $e^+ + e^- \rightarrow \pi^0 + \gamma$; 4) $e^+ + e^- \rightarrow \pi^0$;

5) γ + nucleus $\rightarrow \pi^0$ + nucleus;

6) e + nucleus $\rightarrow \pi^0 + e$ + nucleus.

The last two processes are meant to take place in the Coulomb field of the nucleus. The cross sections of these processes are generally small because the mean life of the π^0 meson is large compared with the characteristic time of the electromagnetic interaction. So the cross section of process 1) (see reference 2) at an electron energy of 300 Mev equals roughly 10^{-6} of the elastic scattering cross section.

However, if a π^0 propagator is contained in the amplitude for another process, poles will appear, of which some may lie in the physical region. Then the diagrams containing these singularities can dominate in the expression for the cross sections of that particular process. All such diagrams characteristically contain a part that corresponds to photon-photon scattering via a π^0 meson. Such a part will be contained in the diagrams of the following processes:

a) $e^+ + e^- \rightarrow 3\gamma$; b) $e + \gamma \rightarrow e + 2\gamma$; c) $e^+ + e^- \rightarrow 2\gamma$;

d) $e + e \rightarrow e + e$; e) $\gamma + e \rightarrow \gamma + e$; f) $e + e \rightarrow e + e + 2\gamma$.

The photon-photon scattering was investigated by Oraevskii,[3] who showed that there exists a sharp maximum in the cross section for this process at a photon energy $\omega = \mu/2$. Analogous maxima will exist also in the cross sections of processes c) and d) (in the latter case — in the annihilation diagram of electron-positron scattering). However, due to the small probability of a decay of the π^0 meson into two electrons the contribution of the π^0 intermediate state to these processes is smaller than the purely electrodynamic part even at its peak. We assume here and later that the "widths" of the π^0 "level" are determined by its experimental mean life.

The situation is completely different for the processes a) and b). Here the cross section of the process going via the π^0 meson contains just the additional factor $e^2 = 1/137$ as compared to the case of photon-photon scattering. As a result of this the contribution of the diagrams going via a π^0 meson will dominate the cross sections in the vicinity of the pole of the π^0 propagator. For example, the cross section for the three photon annihilation of a pair at an energy of the positron or electron in the center-of-mass system (c.m.s.) of 140 Mev has the order of magnitude of 10^{-29} — 10^{-30} cm^2/sr. This is 5 — 6 orders of magnitude larger than the corresponding electrodynamic cross section and has the same order of magnitude as the two-photon annihilation cross section. As collision processes which have three particles in the final state are characterized by five parameters the maximum of the scattering amplitude for process a) will lie on the line $\omega = \epsilon - \mu^2/4\epsilon$ (ω — energy of one of the final photons, ϵ — energy of the electron or positron in the c.m.s.) and for process b) on the line $\epsilon_2 = \omega - \mu^2/4\omega$ (ω — energy of the incoming photon in the c.m.s., ϵ — energy of the final electron).

In processes which do not have an annihilation character, and also in the process e), the pole of the π^0 propagator lies in the unphysical region. For example, for process e) it lies at c.m.s. scattering angle with $\cos\vartheta = 1 + \mu^2/2\omega^2$.

Amongst the possible π^0 production processes the process 3) is of particular interest. It is not masked by photonuclear production processes like the processes 5) and 6); it has a larger cross section than processes 1) and 4), and it is easier to observe than process 2). Its cross section in the c.m.s. is given by

$$\sigma(\vartheta) = (e^2/4\tau\mu^3)(q/\varepsilon)^3(1 + \cos^2\vartheta)f^2(\varepsilon^2), \qquad (2)$$

where q — momentum of the π^0 meson, ϑ — angle between the momenta of the initial and the final particles, $f(\epsilon^2)$ — form factor of the π^0 meson. The latter makes its appearance because the interaction (1) is not a "fundamental" interaction and, generally speaking, has to be chosen in a nonlocal form. At an energy of 130 Mev the process has a cross section of the order of 10^{-36} cm^2.

Recently the possibility of the existence of a neutral vector meson of mass $M \sim 3\mu$ has been widely discussed. It has been proposed by Nambu[4] to explain the isoscalar part of Hofstadters charge distributions. In this connection we would like to remark that the existence of such a meson could be checked by means of the reaction $e^+ + e^- \rightarrow \pi^0 + \gamma$. In this case in the reaction cross section there would appear a resonance denominator of the form $[(2\epsilon - M)^2 + \Gamma^2/4]$ (Γ — "width of the level"). If the mean life of that meson with respect to the decay into $\pi^0 + \gamma$ would be 10^{-20} — 10^{-21} sec then the reaction cross section averaged over an interval of 5 Mev at the energy containing the resonance would be of order 10^{-27} to 10^{-28} cm^2 which is considerably larger than all electrodynamic cross sections at such an energy.

In conclusion the authors thank I. B. Khriplovich for discussions.

---

[1] R. H. Dalitz, Proc. Phys. Soc. London **A64**, 667 (1951); A. D. Galanin and V. G. Solov'ev, JETP **27**, 112 (1954).

[2] F. Low, Phys. Rev. **120**, 582 (1960).

[3] V. N. Oraevskii, JETP **39**, 1049 (1960), Soviet Phys. JETP **12**, 730 (1961).

[4] Y. Nambu, Phys. Rev. **106**, 1366 (1957).

Translated by M. Danos

QUANTIZED CYCLOTRON RESONANCE IN METALS

I. M. LIFSHITZ

Khar'kov State University

Submitted to JETP editor March 4, 1961

J. Exptl. Theoret. Phys. (U.S.S.R.) 40, 1235-1236 (April, 1961)

IN metals with a complicated dispersion law for the conduction electrons there is a continuous spectrum of values for the effective masses and, consequently, a whole range of natural frequencies of rotation of the electrons in a magnetic field $H_z = H$ ($\omega_H = \mu H$; $\mu = e/mc$; $2\pi m = \partial S/\partial\epsilon$, where $S = S(\epsilon, p_z)$ is the cross-section area of the isoenergetic surface by the plane $p_z = \text{const}$).[1]

Under the conditions for cyclotron resonance (i.e., in a magnetic field parallel to the surface of the metal and in a high-frequency electric field of frequency ω),[2] electrons of mass m contribute to all the high frequency characteristics of the metal a term with a "resonance" denominator $\omega - \mu H + i/\tau$ (τ is the relaxation time). This means that the corresponding characteristics (such as the conductivity of surface impedance) are of the form, for $\omega\tau \gg 1$

$$M = \int \frac{\chi(\mu)\,d\mu}{\omega - \mu H + i/\tau} \approx -i\frac{\pi}{H}\chi\left(\frac{\omega}{H}\right) + \mathop{\int\!\!\!\!\!\!-}\frac{\chi(\mu)\,d\mu}{\omega - \mu H}, \quad (1)$$

where $\chi(\mu)$ is a smooth function of μ over the whole range of variation of effective masses, except for points where the density of states has a singularity or a discontinuity; in particular near the extremal values $\mu = \mu_g$: $\chi(\mu) \sim (\mu - \mu_g)^{-1/2}$. As can be seen from (1) it is just these singularities $\omega_g = \mu H$ which are also resonances for M, and for all other natural frequencies M is a smooth function of ω.

At low temperatures ($kT \ll \mu\hbar H \ll \epsilon_0$) when the integration in (1) is only carried out for electrons at the Fermi surface $\epsilon = \epsilon_0$, quantization of p_z in a magnetic field leads to discrete values of the effective mass and, as a result, to the replacement of (1) by a sum of the form

$$M' = \sum_n \frac{\chi(\mu_n)\,\delta\mu_n}{\omega - \mu_n H + i/\tau}. \quad (2)$$

By considering the cross section area of the Fermi surface as a function of μ ($S = S(\mu)$), we can express the condition for quasi-classical quantization as

$$S(\mu_n) = ehnH/c.$$

From this $\delta\mu = ehH/c\,(\partial S/\partial\mu)$, and near the point $\mu H = \omega$

$$\delta\mu/\mu = h\omega/(\partial S/\partial m). \quad (3)$$

If the relative distance between the levels $\delta\mu/\mu$ is of the same order as or larger than the attenuation constant $1/\omega\tau$, i.e.,

$$h\omega/(\partial S/\partial m) \lesssim 1/\omega\tau, \quad (4)$$

then the separate frequencies $\mu_n H$ in the sum (3) are split and M' is no longer a smooth function of ω/H. A simple calculation gives*

$$M' = \frac{\pi}{H}\chi(\mu)\operatorname{ctg}\pi\left\{\frac{cS(\mu)}{ehH} + i\frac{\mu}{\omega\tau\delta\mu}\right\}\Big|_{\mu=\omega/H} + \mathop{\int\!\!\!\!\!\!-}\frac{\chi(\mu)\,d\mu}{\omega - \mu H}. \quad (5)^*$$

For $\mu/\omega\tau\delta\mu \gg 1$, $\cot\pi\{\ldots\} \to -i$ and (5) goes over into (1). On the other hand, for $\mu/\omega\tau\delta\mu \lesssim 1$, M' has oscillations of large amplitude $\Delta M'/M' \sim (\delta\mu/\mu)\,\omega\tau$ which correspond to resonance at each of the discrete frequencies $\omega_n = \mu_n H$. The periods of these oscillations, in the inverse of the magnetic field Δ are

$$\Delta = \frac{eh}{c} \Big/ \left(S + \mu\frac{\partial S}{\partial\mu}\right)\Big|_{\mu=\omega/H}. \quad (6)$$

The period Δ is thus a function of the magnetic field.

By measuring the $\Delta(\omega/H)$ dependence we can obtain a variety of information about the Fermi surface, in particular we can find the area of any cross-section as a function of the inverse of the mass μ:

$$\mu S(\mu) = \frac{eh}{c}\int_{\mu_0}^{\mu}\frac{d\mu}{\Delta(\mu)}, \qquad S(\mu_0) = 0.$$

Condition (4) is most easily fulfilled for the "anomalous" electron groups with long period oscillations in the de Haas-van Alphen effect (in this case it is apparently fully realized for frequencies $\omega \sim 10^{11}\ \text{sec}^{-1}$). It is still not quite clear for which cases it can be realized for the normal electron groups.

We should remark that the expression $\partial S/\partial m$ appearing in the denominators of (3) and (4) can, in general, change sign and be zero at certain points ($\partial S/\partial m = v_z^0/(\partial \ln m/\partial p_z)$; $v_z^0(p_z)$ is the mean value of v_z along the contour $p_z = \text{const}$). Near points where $v_z^0 = 0$, $\partial m/\partial p_z \neq 0$, $\partial S/\partial m$

---

*If the $S(\mu)$ dependence has several branches, then the sum in (5) must be taken over all these branches.

*ctg = cot.

will be $\sim m - m_0$, and the relative distance between levels will be $\delta\mu/\mu \sim \sqrt{\hbar\omega/\epsilon_0}$. Near the critical points p_z^k, corresponding to self-intersecting trajectories (of the figure-of-eight type), $m \sim -\ln|p_z - p_z^k|$ (see reference (1)), and a simple calculation gives $\delta\mu/\mu \sim 1/\ln(\epsilon_0/\hbar\omega)$. In these cases the condition (4) goes over to a considerably weaker condition $\omega\tau \gtrsim \ln(\epsilon_0/\hbar\omega)$, which is almost always realized.

The oscillations connected with the splitting of the resonance frequencies differ considerably from the usual quantum oscillations of the de Haas–van Alphen and Shubnikov–de Haas effect, and also from the high frequency conductivity oscillations considered by Azbel'. All these oscillations have a universal period, independent of magnetic field, $\Delta = eh/cS_{\text{extr}}$, determined by the extremal Fermi surface cross-section; the form of these oscillations is also described by a single universal function.[3] In calculating the sum in (2), these oscillations arise from terms lying in the region of singular points in the density of states $\nu(p_z)\,dp_z = \nu(p_z)(dp_z/d\mu)\,d\mu$, i.e., singular points of the function $\chi(\mu)$. These points, naturally, are independent of H and ω and correspond to extremal cross-sections S_{extr}. The oscillations determined by them have very small amplitude and can be neglected if condition (4) holds, as has been done in (5). On the other hand, for the opposite limiting case $\delta\mu/\mu \ll 1/\omega\tau$, when there is no splitting of the resonance frequencies, quantum effects enter only into these small oscillations.

---

[1] I. M. Lifshitz and M. I. Kaganov, Usp. Fiz. Nauk **69**, 419 (1959), Soviet Phys.-Uspekhi **2**, 831 (1960).

[2] M. Ya. Azbel' and É. A. Kaner, JETP **30**, 811 (1956) and **32**, 896 (1957), Soviet Phys. JETP **3**, 772 (1956) and **5**, 730 (1957).

[3] I. M. Lifshitz and A. M. Kosevich, JETP **29**, 730 (1955), Soviet Phys. JETP **2**, 636 (1956); Izv. Akad. Nauk SSSR, Ser. Fiz. **19**, 395 (1955), Columbia Tech. Transl. p. 353; I. M. Lifshitz, JETP **32**, 1507 (1957), Soviet Phys. JETP **5**, 1227 (1957); M. Ya. Azbel', JETP **34**, 969 (1958), Soviet Phys. JETP **7**, 669 (1958).

Translated by R. Berman
210

SOVIET PHYSICS JOURNALS

Translations of the 1961 Originals—*Published in English by the American Institute of Physics with the cooperation of the National Science Foundation.*

Publication year July, 1961—June, 1962.

Soviet Physics—**JETP**

A translation, beginning with 1955 issues of *Zhurnal Eksperimental'noi i Teoreticheskoi Fiziki* of the USSR Academy of Sciences. Leading physics journal of Soviet Union. Similar to "The Physical Review" in quality and range of topics. Outstanding new work is most likely to appear in this journal.

Vols. 13 and 14 comprising twelve issues, approx. 4000 pp.
$75 domestic, $79 foreign
Libraries $50 domestic, $54 foreign. Single copies, $8*

Soviet Physics—**SOLID STATE**

A translation, beginning with 1959 issues of *Fizika Tverdogo Tela* of the USSR Academy of Sciences. Offers results of theoretical and experimental investigations in the physics of semiconductors, dielectrics, and on applied physics associated with these problems. Also publishes papers on electronic processes taking place in the interior and on the surface of solids.

Vol. 3 comprising twelve issues, approx. 3800 pp.
$70 domestic, $74 foreign
Libraries $45 domestic, $49 foreign. Single copies, $8*

Soviet Physics—**TECHNICAL PHYSICS**

A translation, beginning with 1956 issues of *Zhurnal Tekhnicheskoi Fiziki* of the USSR Academy of Sciences. Contains work on plasma physics and magnetohydrodynamics, aerodynamics, ion and electron optics, and radio physics. Also publishes articles in mathematical physics, the physics of accelerators, and molecular physics.

Vol. 6 comprising twelve issues, approx. 2000 pp.
$55 domestic, $59 foreign
Libraries $35 domestic, $39 foreign. Single copies, $8*

Soviet Physics—**ACOUSTICS**

A translation, beginning with 1955 issues of *Akusticheskii Zhurnal* of the USSR Academy of Sciences. Devoted principally to physical acoustics but includes electro-, bio-, and psychoacoustics. Mathematical and experimental work with emphasis on pure research.

Vol. 7 comprising four issues, approx. 500 pp.
$12 domestic, $14 foreign
(No library discounts.) Single copies, $4

Soviet Physics—**DOKLADY**

A translation, beginning with 1956 issues of the physics sections of *Doklady Akademii Nauk SSSR*, the proceedings of the USSR Academy of Sciences. All-science journal offering four-page reports of recent research in physics and borderline subjects.

Vol. 6 comprising twelve issues, approx. 1500 pp.
$35 domestic, $38 foreign
Libraries $25 domestic, $28 foreign*
Single copies Vols. 1 and 2, $5;
Vol. 3 and later issues, $7

Soviet Physics—**CRYSTALLOGRAPHY**

A translation, beginning with 1957 issues of the journal *Kristallografiya* of the USSR Academy of Sciences. Experimental and theoretical papers on crystal structure, lattice theory, diffraction studies, and other topics of interest to crystallographers, mineralogists, and metallurgists.

Vol. 6 comprising six issues, approx. 1000 pp.
$25 domestic, $27 foreign
Libraries $15 domestic, $17 foreign. Single copies, $5*

SOVIET ASTRONOMY—AJ

A translation, beginning with 1957 issues of *Astronomicheskii Zhurnal* of the USSR Academy of Sciences. Covers various problems of interest to astronomers and astrophysicists including solar activity, stellar studies, spectroscopic investigations of radio astronomy.

Vol. 5 comprising six issues, approx. 1100 pp.
$25 domestic, $27 foreign
Libraries $15 domestic, $17 foreign. Single copies, $5*

Soviet Physics—**USPEKHI**

A translation, beginning with September, 1958, issue of *Uspekhi Fizicheskikh Nauk* of the USSR Academy of Sciences. Offers reviews of recent developments comparable in scope and treatment to those carried in *Reviews of Modern Physics.* Also contains reports on scientific meetings within the Soviet Union, book reviews, and personalia.

Vol. 4 comprising six issues, approx. 1700 pp.
(Contents limited to material from Soviet sources)
$45 domestic, $48 foreign
Libraries $30 domestic, $33 foreign. Single copies, $9*

**For libraries of nonprofit academic institutions.*

CONTENTS—continued

Page — Russian Reference

Excitation Spectrum of a Particle System in an External Field . . . . V. M. Eleonskii 804 40, 1143
Scattering of Low-Energy Photons on a System with Spin $1/2$ . . . . V. A. Petrun'kin 808 40, 1148
Unstable Particle in the Lee Model . . . . Ya. B. Zel'dovich 813 40, 1155
On the Polarization of Recombination Radiation . . . . B. A. Lysov, L. P. Belova, and L. I. Korovina 816 40, 1160
Contribution to the Theory of Localized Perturbations in Large Systems . . . . V. I. Osherov 820 40, 1166
Equations for the Spectral Functions of Charged Pions . . . . Yu. A. Simonov and K. A. Ter-Martirosyan 824 40, 1172
A Dressed-Particle Analysis of the $\pi + d \rightleftarrows 2N$ Reaction . . . . M. A. Braun 828 40, 1179
The Dynamic Effect of the Nuclear Volume in Conversion Ml Transitions in Even-Even Nuclei for the Nonaxial Rotator Model and for the Vibrational Model of the Nucleus . . . . D. P. Grechukhin 832 40, 1185
The Maximum Charge for Given Mass of a Bound State . . . . V. N. Gribov, Ya. B. Zel'dovich, and A. M. Perelomov 836 40, 1190
Calculation of the Elastic Scattering Cross Sections for 5.45 Mev Protons According to the Optical Model of the Nucleus . . . . R. A. Vanetsian, A. P. Klyucharev, G. F. Timoshevskii, and E. D. Fedchenko 842 40, 1199
Use of Indirect Transitions in Semiconductors for the Determination of States with Negative Absorption Coefficients . . . . . . N. G. Basov, O. N. Krokhin, and Yu. M. Popov 845 40, 1203
The Momentum Distribution of Particles in a Dilute Fermi Gas . . . . . V. A. Belyakov 850 40, 1210
Magnetohydrodynamics for Nonisothermal Plasma without Collisions . . . . Yu. L. Klimontovich and V. P. Silin 852 40, 1213
Polarization Resulting from Scattering of Neutrons by Ferromagnetic Substances . . . . S. V. Maleev 860 40, 1224

LETTERS TO THE EDITOR

Spontaneous Magnetization of Thin Ferromagnetic Films . . . . V. A. Ignatchenko 863 40, 1228
The Dependence of the Hall Constant of p-Type Germanium on the Magnetic Field Strength . . . . É. A. Zavadskii, Yu. T. Kovrizhnykh, and I. G. Fakidov 864 40, 1229
The Weizsäcker-Williams Relation for Matrix Elements . . . . A. M. Badalyan and Ya. A. Smorodinskii 865 40, 1231
On the Participation of π^0 Mesons in Electromagnetic Processes . . . . V. N. Baĭer and V. V. Sokolov 866 40, 1233
Quantized Cyclotron Resonance in Metals . . . . I. M. Lifshitz 868 40, 1235

SOVIET PHYSICS JETP VOLUME 13, NUMBER 4 OCTOBER, 1961

CONTENTS

	Page	Russian Reference
Experimental Investigation of Electron Capture by Multiply Charged Ions. . . . . V. S. Nikolaev, I. S. Dmitriev, L. N. Fateeva, and Ya. A. Teplova	695	40, 989
Positron Annihilation in Sulphur, Selenium, and Silicon. . . . . K. A. Baskova, B. S. Dzhelepov, and Z. A. Komissarova	703	40, 1001
Neutron Emission from Strongly Excited Nuclei. . . . . A. S. Karamyan, G. A. Dorofeev, and D. S. Klochkov	705	40, 1004
Alpha Decay of the Bi^{210m} Isomer. . . . . L. I. Rusinov, Yu. N. Andreev, S. V. Golenetskii, M. I. Kislov, and Yu. I. Filimonov	707	40, 1007
Electronic Paramagnetic Resonance in the V^{3+} Ion in Corundum . . . . G. M. Zverev and A. M. Prokhorov	714	40, 1016
Stripping Reactions on the Zr^{90} and Zr^{91} Nuclei . . . . N. I. Zaika and O. F. Nemets	716	40, 1019
Neutron Diffraction Study of the Crystalline Structure of Solid Hydrogen and Deuterium . . . . V. S. Kogan, V. G. Lazarev, R. P. Ozerov and G. S. Zhdanov	718	40, 1022
Estimate of the Upper Limit of the Charge-Exchange Cross Section for the pn Interaction at 8.5 Bev. . . . . V. A. Nikitin and É. N. Tsyganov	722	40, 1027
Resonance Scattering of Gamma Rays by Te^{124} Nuclei. . . . . A. F. Akkerman, D. K. Kaĭpov and Yu. K. Shubnyĭ	725	40, 1031
Mass of the Pu^{240} Isotope . . . . R. A. Demirkhanov and V. V. Dorokhov	727	40, 1033
Magnetoelectric Effect in Chromium Oxide. . . . . D. N. Astrov	729	40, 1035
Investigation of the Spectrum and Asymmetry of Electrons from the $\pi - \mu - e$ Decay in Nuclear Emulsion. . . . . A. O. Vaĭsenberg, V. A. Smirnit-skii, and E. D. Kolganova	734	40, 1042
On the Kinetic Theory of Shock Waves . . . . G. Ya. Lyubarskii	740	40, 1050
Structure of the Transition Layer Between a Plasma and a Magnetic Field. . . . . V. P. Shabanskii	746	40, 1058
Quantum Theory of the Spectrum of Excitations of an Electron Gas in a Magnetic Field . . . . P. S. Zyryanov	751	40, 1065
Commutation Function of a Nonlinear Meson Field. . . . . D. Ivanenko and D. F. Kurdgelaidze	756	40, 1072
On the Use of an Arbitrary Gauge of the Electromagnetic Potentials in the Dispersion Method. . . . . V. D. Mur and V. D. Skarzhinskii	759	40, 1076
Resonance Charge Exchange in Hydrogen and Sodium . . . . Yu. E. Murakhver	762	40, 1080
Double Dispersion Relations and Photoproduction of Pions. . . . . N. F. Nelipa	766	40, 1085
Nucleon-Nucleon Interaction at an Energy of 9 Bev. . . . . I. M. Gramenitskii, I. M. Dremin, V. M. Maksimenko, and D. S. Chernavskii	771	40, 1093
Effect of Unresolved Structures on the Line Width in Electronic Paramagnetic Resonance. . . . . R. Kh. Timerov	777	40, 1101
Phase Shift Analysis of pp Scattering at 95 Mev . . . . V. A. Borovikov, I. M. Gel'fand, A. F. Grashin, and I. Ya. Pomeranchuk	780	40, 1106
Reconstruction of the Energy Gap in a Superconductor by Measurement of Sound Attenuation. . . . . V. L. Pokrovskii and V. A. Toponogov	785	40, 1112
Stability of a Plasma Pinch with Anisotropic Particle Velocity Distribution and Arbitrary Current Distribution. . . . . V. F. Aleksin and V. I. Yashin	787	40, 1115
Losses of Electrons in Synchrotrons Due to the Quantum Character of the Radiation . . . . P. S. Landa	789	40, 1119
Superfluidity in a Fermi System in the Presence of Pairs with Nonzero Angular Momentum . . . . L. P. Gor'kov and V. M. Galitskii	792	40, 1124
Dispersion Relations for Vertex Parts. . . . . Yu. M. Malyuta	795	40, 1128
The Equation of State of Partially Ionized Hydrogen . . . . L. P. Kudrin	798	40, 1134
Some Isotopic Relations for Reactions of the Type $\pi n \to \pi\pi n$ . . . . V. N. Strel'tsov	802	40, 1140

(Contents continued on inside back cover)